GUEST EDITORIAL

National Science Review
8: nwab201, 2021
https://doi.org/10.1093/nsr/nwab201
Advance access publication 12 November 2021

Special Topic: Physics of the BESIII Experiment

Preface: special topic on physics of the BESIII experiment

Yifang Wang

The Beijing electron positron collider (BEPC) was constructed in the 1980s and its upgraded version (BEPCII) with a center-of-mass energy region of 2–5 GeV and a maximum luminosity of $1 \times 10^{33}\,\mathrm{cm}^{-2}\,\mathrm{s}^{-1}$ started operation in 2008. The colliding events are recorded by a newly designed detector, called the Beijing spectrometer (BESIII), based on state-of-the-art technologies. Physicists working at the BESIII experiment formed the BESIII Collaboration in 2005, which is a large international collaboration consisting of more than 500 physicists from 80 institutions in 17 countries. Over the course of more than ten years, about 400 physics papers have been published in internationally renowned journals covering a large variety of physics topics and notable achievements, including the following.

- Discovery of the 'four-quark matter' $Z_c(3900)$, $Z_c(4020)$ and $Z_{cs}(3985)$, the fine structure of $Y(4260)$ and a new production mode for $X(3872)$.
- Precision measurements of the standard model (SM) parameters, the τ-lepton mass and $|V_{cd}|$ and $|V_{cs}|$ CKM matrix elements.
- A huge sample of J/ψ decays have provided a deeper understanding of the glueballs, the resonant structures at the proton-antiproton mass threshold, as well as possibilities of searching for other light exotic hadrons.
- Precision measurements of low-energy e^+e^- annihilation cross sections and complex phases in D-meson decays provide important input for experiments at other energies, and measurements of the purely leptonic and semileptonic decay rates of D and D_s mesons provide sensitive tests of lattice QCD calculations.
- The discovery of the polarization of hyperons produced in J/ψ decays provides new and unique opportunities for high-sensitivity searches for non-SM sources of CP violation.
- Investigations of time-like electromagnetic form factors of nucleons, Λ, and Λ_c baryons revealed unexpected threshold behaviors and motivated measurements for other stable baryons.

A collection of review articles in this issue of the journal will cover some of the most important results and future prospects for the next ten years, including charm physics, charmonium and charmonium-like exotic states, light hadron spectroscopy, QCD studies with light meson decays, properties of baryons and new physics searches. These represent the advancement of our understanding on tau-charm physics in the last decades. An interview with Luciano Maiani, who proposed the existence of the charm quark and was the Director General of CERN from 1999 to 2003, is also included in this Special Topic.

BEPCII was originally intended to operate at a variety of energy points in accordance with the physics plan that was articulated in its 2009 yellow book [1]. To date, BESIII has accumulated 10 billion J/ψ events, 3 billion $\psi(2S)$ events, an integrated luminosity of 3 fb^{-1} at the $\psi(3770)$ resonance and about 25 fb^{-1} at energies above $\psi(3770)$, as was collected in the BESIII physics book in 2020 [2]. An upgrade that would increase the center-of-mass energy from 5 to 5.6 GeV and dramatically increase the luminosity at higher energies was requested by BESIII/BEPCII as part of their proposed program for the next decade [2] and was approved recently by the Chinese Academy of Sciences (CAS). With data from the next three years and more data after the upgrade, BESIII is able to measure charm decays with a three-fold improvement in the precision and to investigate the 4.7–5.6 GeV energy region that has been barely touched previously. The latter opens a window for new exotic hadrons with charm quarks.

BESIII as the world's premier experiment for physics in the charm and tau energy region is an exemplary, large-scale and ever-expanding international collaboration that is paving the way for Chinese physicists to take a world-leading role in the pursuit of a basic understanding of nature.

We thank the BESIII Collaboration, the BEPCII and the IHEP supporting staff, as well as funding agencies including MOST, NSFC, and CAS in China, and those of foreign countries in the BESIII Collaboration.

Yifang Wang
Institute of High Energy Physics, Chinese Academy of Sciences, China
Guest Editor of Special Topic
Editorial Board Member of NSR
E-mail: yfwang@ihep.ac.cn

REFERENCES

1. Asner DM, Barnes T and Bian JM *et al. Int J Mod Phys A* 2009; **24**: S1.
2. Ablikim M, Achasov MN and Adlarson P *et al. Chin Phys C* 2020; **44**: 040001.

REVIEW

National Science Review
8: nwab198, 2021
https://doi.org/10.1093/nsr/nwab198
Advance access publication 2 November 2021

PHYSICS

Special Topic: Physics of the BESIII Experiment

Highlights of light meson spectroscopy at the BESIII experiment

Shan Jin[1,*] and Xiaoyan Shen[2,3,*]

ABSTRACT

Hadron spectroscopy provides a way to understand the dynamics of the strong interaction. For light hadron systems, only phenomenological models or lattice quantum chromodynamics (QCD) are applicable, because of the failure of perturbation expansions for QCD at low energy. Experimental data on light hadron spectroscopy are therefore crucial to provide necessary constraints on various theoretical models. Light meson spectroscopy has been studied using charmonium decays with the Beijing Spectrometer Experiment (BES) at the Beijing Electron-Positron Collider, operating at 2.0–4.6 GeV center-of-mass energy, for nearly three decades. Charmonium data with unprecedented statistics and well-defined initial and final states provide BESIII with unique opportunities to search for glueballs, hybrids and multi-quark states, as well as perform systematic studies of the properties of conventional light mesons. In this article, we review BESIII results that address these issues.

Keywords: hadron, spectroscopy, charmonium, meson, glueball, hybrid, multi-quark state

[1]School of Physics, Nanjing University, Nanjing 210008, China; [2]Institute of High Energy Physics, Chinese Academy of Sciences, Beijing 100049, China and [3]University of Chinese Academy of Sciences, Beijing 100049, China

*__Corresponding authors__. E-mails: jins@ihep.ac.cn; shenxy@ihep.ac.cn

Received 30 April 2021; **Revised** 20 October 2021; **Accepted** 20 October 2021

INTRODUCTION

Our knowledge of mesons and, in parallel, our understanding of the strong interactions have undergone several major revisions. Mesons were first introduced when Yukawa [1] predicted the existence of pions as the exchange boson responsible for the strong interaction between nucleons. Later, more and more mesons and baryons showed up in cosmic ray and high-energy accelerator experiments. It was eventually realized that light hadrons, mesons and baryons of a given J^{PC} are arranged in representations of the SU(3) group, and this led to the quark model by Gell-Man and Zweig [2,3]. In the quark model, hadrons are, in fact, objects that are comprised of constituent spin-$\frac{1}{2}$ fermions, called quarks. Constituent quarks are valence quarks for which the correlations for the description of hadrons by means of gluons and sea quarks are put into effective quark masses of these valence quarks. Mesons are made of quark-antiquark ($q\bar{q}$) pairs and baryons are made of three quark (qqq) combinations. With this simple quark scheme, the qualitative properties of hadrons were explained quite well. However, serious problems with the Pauli exclusion principle occurred for some of the quark wavefunctions. This problem was solved when Greenberg [4] pointed out that quarks had another quantum number that was subsequently named 'color'. But still, considerable skepticism about the quark model persisted, primarily due to the fact that isolated quarks were never observed. This situation changed when the results from deep inelastic scattering of electrons on protons and bound neutrons [5] came out in 1968, indicating the presence of hard and point-like components in neucleons, and the discovery of J/ψ was reported in 1974 [6,7], which was interpreted as the bound state of a new heavy quark 'charm' and its antiquark, as proposed by Glashow *et al.* [8]. Subsequent experimental and theoretical developments proved to be convincing evidence that quarks were real objects and the fundamental building blocks of hadronic matter.

The constituent quark model (CQM) proposed by Gell-Mann and Zweig was able to reproduce the charmonium spectrum and describe the phenomenology of meson and baryon spectroscopy

rather well. However, problems remained. The well-accepted theory of the strong interaction is quantum chromodynamics (QCD) [9,10], a non-Abelian gauge-field theory that describes the interactions of quarks and gluons and has the features of asymptotic freedom and confinement of quarks. For the light scalars, such as $f_0(500)$, the dispersive formalisms, which are shown to follow from first principles, determine the mass and width of $f_0(500)$ within small uncertainties [11,12]. For the mesons containing at least one heavy (c or b) quark, the simulations using non-relativistic QCD or heavy quark effective theory, which expanses the QCD Lagrangian in powers of the heavy quark velocity, or the heavy quark mass, have become a high-precision task [13–15]. However, first-principle computations, directly from the QCD Lagrangian, of hadron properties for light hadrons are difficult, due to the failure of perturbation expansions for QCD at low energies. As a result, our knowledge of light hadrons mainly relies on either QCD-based phenomenological approaches or lattice QCD (LQCD) calculations. Lattice calculations of QCD are a major source of information about QCD masses and matrix elements. A review of the hadron spectrum from lattice QCD can be found in the review of the quark model in Particle Data Group 2020 (PDG 2020) [16] and in [17]. Aside from the conventional $q\bar{q}$ mesons and qqq baryons in the CQM, QCD-based models also allow the possible existence of bound states that are made of only gluons, i.e. so-called 'glueballs'. Furthermore, it is also possible to form multi-quark hadrons, with the number of quarks larger than three, and 'hybrids' that contain both $q\bar{q}/qqq$ and at least one gluon (g) as its constituents, $q\bar{q}g/qqqg$. All of these unconventional states, so-called new forms of hadrons, if they exist, will greatly enrich the spectra of mesons and baryons, and shed light on the dynamics of long-distance QCD. In the past decades, despite the fact that LQCD has experienced dramatic improvements together with rapid developments in computing resources, there still remain many technical difficulties in the extraction of precise properties of glueballs, hybrids and multi-quark states in LQCD calculations. Moreover, these new forms of hadrons may have J^{PC} that are the same as those of CQM states and thus mix with conventional hadrons, which makes their identification more complicated. Still, searching for unconventional hadrons, such as glueballs, hybrids and multi-quark states, as well as investigating their spectra in experiments have been important subjects of modern (intermediate) high-energy physics for many decades. In particular, the observations of new hadron candidates, XYZ states with heavy quarks in the past decade, have drawn further attention in this field.

Many experiments have been dedicated to studies of light hadron spectroscopy. In recent years, charmonium data samples with unprecedent statistics were accumulated by the Beijing Spectrometer (BESIII) at the Beijing Electro-Positron Collider (BEPCII), and these provide numerous opportunities for investigating light hadrons produced in charmonium decays. In this article, the highlights on studies of glueball and hybrid candidates, and searches for the multi-quark states from J/ψ decays by the BESIII experiment are reviewed.

STUDY OF THE GLUEBALL CANDIDATES

The CQM has had considerable success in predicting the spectrum of hadrons and their decay properties. However, CQM is only a phenomenological model, and it is not derived from the underlying QCD theory of the strong interaction. Therefore, the CQM spectrum is not necessarily the same as the physical spectrum in the QCD theory. QCD-based phenomenological models, such as bag models [18–21], flux-tube models [22,23], QCD sum rules [24–27] and LQCD [28–31] can make predictions of the masses and other properties of glueballs. Of them, the only first-principle calculations of spectroscopy from QCD is LQCD.

In the early years, most of the LQCD calculations of the glueball spectrum were confined to the quenched approximation in which internal quark loops are neglected. Figure 1(a) shows the results of the glueball spectrum for the lightest glueballs from quenched calculations [31]. The lowest glueball is a $J^{PC} = 0^{++}$ scalar state with mass in the range 1.5–1.7 GeV/c^2; the next lightest glueball is a $J^{PC} = 2^{++}$ tensor state with mass around 2.4 GeV/c^2. For the lightest $J^{PC} = 0^{-+}$ pseudoscalar glueball, the LQCD calculated mass is above 2.3 GeV/c^2. In recent years, the lattice calculations of the glueball spectrum with dynamical light quarks and high statistics appeared [32,33]. Figure 1(b) shows the unquenched results for the glueball spectrum from [32], along with comparisons to the quenched lattice calculation of [30] and to experimental isosinglet mesons. The effects of quenching seem to be small, and the quenched and unquenched predicted masses for the lightest glueballs are close to each other.

As for glueball couplings and decay rates, we still lack first-principle theoretical predictions, although some expectations [34] from phenomenological models for a glueball with conventional quantum numbers can provide useful guidance for distinguishing a glueball candidate from a

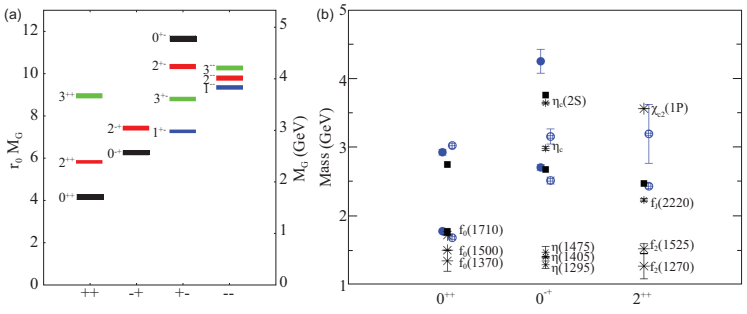

Figure 1. (a) The mass spectrum of the lightest glueball states predicted from quenched LQCD calculations [31]. (b) The mass spectrum of glueball states predicted from unquenched LQCD [32]. The open and filled circles are the full QCD calculation of glueball masses, with larger and smaller lattice spacing, respectively. Squares are the quenched calculations for glueball masses of [30]. The bursts labeled by particle names are experimental states.

conventional hadron, such as

- well-established states that lack a close correspondence or a clear assignment to quark model nonets;
- enhanced production in gluon-rich processes, such as J/ψ radiative decays, pp central productions and $p\bar{p}$ annihilations;
- flavor blindness of glueball decays—since glueballs are SU(3) flavor singlets, they are expected to couple equally to u, d and s quarks;
- the production of glueballs in two-photon collisions and the decay of glueballs into two-photon final states are expected to be suppressed, since gluons are electrically neutral.

On the other hand, the properties of glueballs are not expected to be significantly different from those of conventional hadrons. These make the identification of a glueball more complicated and difficult.

The scalar and tensor glueball candidates

The scalar and tensor meson spectra have been studied in many reactions, including pion induced reactions $\pi^- p$ [35], $p\bar{p}$ annihilations [36–39], central pp collisions [40–42] and the decays of $\psi(2S)$ [43], J/ψ [44–52], B [53], D [54], ϕ [55] and K [56] mesons, as well as two-photon processes [57]. An attractive and important feature in the study of two-pseudoscalar systems, such as $\pi\pi$, $K\bar{K}$ and $\eta\eta$, in radiative J/ψ decays is the simplicity in the partial wave analysis (PWA), a generally accepted method of amplitude analysis to determine the spin parities of intermediate states in decay processes. Conservation of parity in strong and electromagnetic interactions, as well as the conservation of angular momentum, restrict the quantum numbers of the pseudoscalar-pseudoscalar pairs. Thus, for pseudoscalar pairs produced in J/ψ radiative decays, only amplitudes with even angular momentum and positive parity and charge conjugation quantum numbers are accessible ($J^{PC} = 0^{++}, 2^{++}, 4^{++}$, etc.). While in the two-vector systems ($\phi\phi$, $\omega\omega$, etc.) in J/ψ radiative decays, pseudoscalar, scalar and tensor mesons with the masses higher than 2 GeV/c^2 can be accessed.

The scalar resonances $f_0(1500)$ and $f_0(1710)$ are main competitors for the lightest 0^{++} glueball candidates, since they are copiously produced in gluon-rich processes and both have masses that are near the LQCD predicted values. The inclusion of data from radiative J/ψ decays provides a source that is complementary to hadronic production experiments.

Radiative J/ψ decays to $\pi^+\pi^-$ and $\pi^0\pi^0$ have been studied by the MARKIII [44], DM2 [45], Crystal Ball [46] and BES [58,59] experiments. Based on a sample of 1.3×10^9 J/ψ events accumulated with the BESIII detector [60], $J/\psi \to \gamma\pi^0\pi^0$ decays [58] were used to study $f_0(1500)$ and $f_0(1710)$. The $\pi^0\pi^0$ invariant mass spectrum for the selected $J/\psi \to \gamma\pi^0\pi^0$ events is shown in Fig. 2(a) as the black dots with error bars. A strong well-known $f_2(1270)$ signal, a shoulder on the high mass side of $f_2(1270)$, an enhancement at $\sim$1.7 GeV/c^2 and a peak at $\sim$ 2.1 GeV/c^2 are evident. A mass-independent PWA was performed, where the amplitudes for radiative J/ψ decays to $\pi^0\pi^0$ are constructed in the radiative multipole basis, as described in detail in Appendix A of [58]. The components of the $\pi\pi$ amplitude were measured independently for many $\pi\pi$ invariant mass intervals. This provides a piecewise complex function that describes the $\pi\pi$ dynamics with minimal assumptions. Figure 2(b) shows the intensities for the 0^{++} amplitudes as a function of $M_{\pi^0\pi^0}$ that are determined by the mass-independent PWA, where there are significant 0^{++} structures just below 1.5 GeV/c^2 and near 1.7 GeV/c^2. In the mass-dependent PWA, the s dependence of the $\pi\pi$ interaction (where s is the invariant mass squared of the two pions) is parameterized as a coherent sum of resonances, each described by a Breit–Wigner line shape with resonance properties, e.g. the mass, width and branching fraction, that are extracted from the fit. The preceding BESII experiment [61] performed a mass-dependent PWA in $J/\psi \to \gamma\pi^+\pi^-$ and $\gamma\pi^0\pi^0$, using relativistic covariant tensor amplitudes constructed from Lorentz-invariant combinations of the polarization and four-momentum vectors of the initial- and final-state particles, with helicity ± 1 J/ψ initial states [62]. The PWA results [59] show similar features as those extracted from the BESIII mass-independent PWA [58]. The measured product branching fractions for

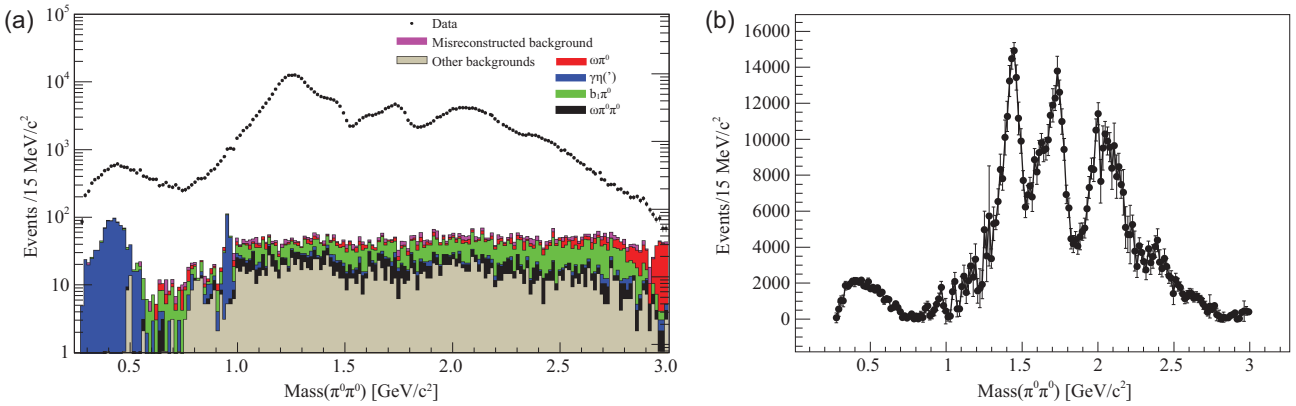

Figure 2. (a) The $M_{\pi^0\pi^0}$ invariant mass spectrum after all selection criteria have been applied. The black markers represent the data, while the histograms are the backgrounds from Monte Carlo simulations. (b) The PWA-determined intensities for the 0^{++} as a function of $M_{\pi^0\pi^0}$ (only statistical errors are presented).

Table 1. The product branching fractions for $\mathcal{B}(J/\psi \to \gamma X) \times \mathcal{B}(X \to M_1 M_2)$ in different decay channels.

	$f_0(1500)$ (10^{-5})	$f_0(1710)$ (10^{-5})	$f_2(2340)$ (10^{-5})
$\pi\pi$	1.01 ± 0.30	4.00 ± 1.00	
$K\bar{K}$	$6.36 \pm 0.64^{+0.72}_{-2.24}$	$80.00^{+1.20}_{-0.80}{}^{+1.20}_{-4.00}$	$5.54^{+0.34}_{-0.40}{}^{+3.82}_{-1.49}$
$\eta\eta$	$1.65^{+0.26}_{-0.31}{}^{+0.51}_{-1.40}$	$23.50^{+1.30}_{-1.10}{}^{+12.40}_{-7.40}$	$5.60^{+0.62}_{-0.65}{}^{+2.37}_{-2.07}$
$\phi\phi$			$1.91 \pm 0.14^{+0.72}_{-0.73}$

$f_0(1500)$ and $f_0(1710)$ decaying to $\pi\pi$ are listed in Table 1.

Scalar and tensor glueball candidates were also studied with J/ψ radiative decays to $\eta\eta$ and $K\bar{K}$. Using 2.25×10^8 J/ψ events collected with the BESIII detector, the decays of $J/\psi \to \gamma\eta\eta$ were investigated [63]. The black points with error bars in Fig. 3(a) show the invariant mass distributions of $\eta\eta$ for the selected $\gamma\eta\eta$ candidates, where peaks around 1.5, 1.7 and 2.1 GeV/c^2 are apparent. A mass-dependent PWA was carried out, and the results indicate that the peak at around 1.5 GeV/c^2 is mainly from the well-established tensor state $f_2'(1525)$ with some contribution from $f_0(1500)$. The statistical significance of the $f_0(1500)$ signal is 8σ. The peaks around 1.7 and 2.1 GeV/c^2 are dominated by $f_0(1710)$ and $f_0(2100)$, respectively, and the significance for the presence of a tensor $f_2(2340)$ state is $7.6\,\sigma$. The red histogram in Fig. 3(a) shows the PWA fit projection with all of the components included, which agrees well with data. The green and blue histograms in Fig. 3(a) represent the contributions from 0^{++} and 2^{++} components, respectively.

A study of the K_SK_S system produced in radiative J/ψ decays was performed [64] using 1.3×10^9 J/ψ decays collected by the BESIII detector. The black dots with error bars in Fig. 3(b) show the invariant mass spectrum of K_SK_S for the selected γK_SK_S events. Three significant peaks in the K_SK_S mass spectrum around 1.5, 1.7 and 2.2 GeV/c^2 are observed. A mass-dependent amplitude analysis was applied to extract the parameters and product branching fractions of the resonances that parameterized the K_SK_S invariant mass spectrum as a sum of Breit–Wigner line shapes. In addition, a mass-independent analysis was performed to obtain the

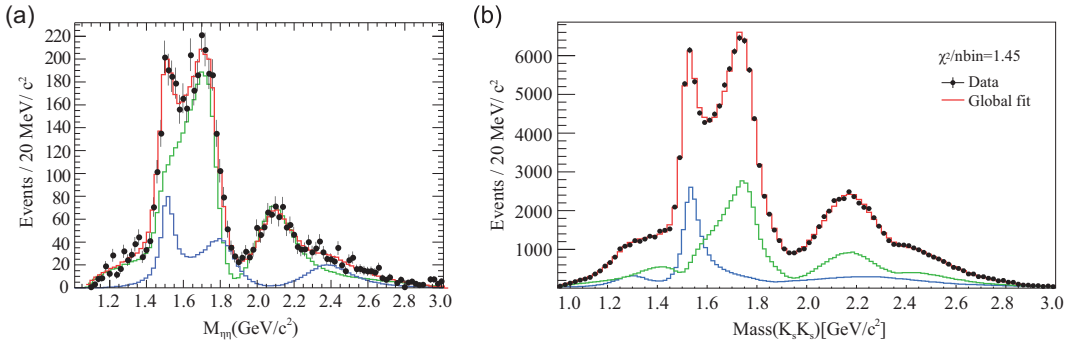

Figure 3. (a) The $\eta\eta$ invariant mass distributions for the selected $\gamma\eta\eta$ candidates. (b) The K_SK_S invariant mass distributions for the selected γK_SK_S candidates. In both plots, the black points with error bars are data, the green and blue histograms are contributions from the 0^{++} and 2^{++}, respectively, and the red histogram is the PWA fit projection of all contributions.

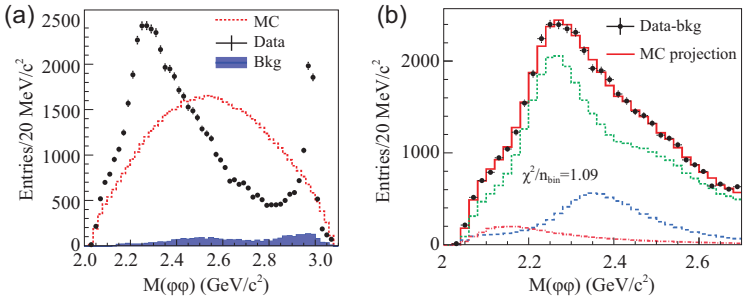

Figure 4. (a) and (b) The $\phi\phi$ invariant mass distributions for the selected $\gamma\phi\phi$ candidates. The black points with error bars are data. The red short-dashed histogram in (a) shows the phase space shape from a Monte Carlo (MC) simulation. The green short-dashed, the red dash–dot and the blue long-dashed histograms in (b) are the coherent superpositions of the Breit-Wigner (BW) resonances with $J^{PC} = 0^{-+}$, 0^{++} and 2^{++}, respectively, and the red solid histogram in (b) shows the total contribution from all components.

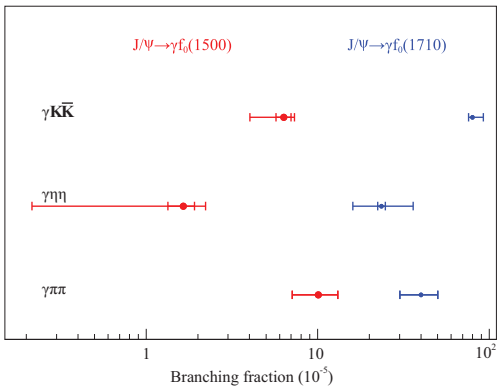

Figure 5. The comparison of the product branching fractions in different processes.

Table 2. The production rates of $f_0(1500)$ and $f_0(1710)$ in J/ψ radiative decays from experiments and LQCD calculations [66].

$\mathcal{B}(J/\psi \to \gamma f_0(1500))$ (10^{-3})	$\mathcal{B}(J/\psi \to \gamma f_0(1710))$ (10^{-3})	$\mathcal{B}(J/\psi \to \gamma$ scalar glueball) (LQCD calculation) (10^{-3})
~0.29	~2.2	3.8 (8)

function that describes the dynamics of the K_SK_S system while making minimal assumptions about the properties and number of poles in the amplitudes. The two approaches give consistent results. The red histogram in Fig. 3(b) shows the PWA fit projection for all components, which agrees well with data. The green and blue histograms represent the contributions from the 0^{++} and 2^{++} components, respectively. The dominant scalar contributions come from $f_0(1500)$, $f_0(1710)$, and $f_0(2200)$. The tensor spectrum in $J/\psi \to \gamma K_SK_S$ is dominated by the well-known $f_2'(1525)$. However, an additional $f_2(2340)$ is needed in the fit.

The measured product branching fractions for the $f_0(1500)$ and $f_0(1710)$ scalars and the $f_2(2340)$ tensor in $J/\psi \to \gamma\eta\eta$ and γK_SK_S are listed in Table 1. In both decay modes, the product branching fractions for $f_0(1710)$ are about an order of magnitude larger than that for $f_0(1500)$. A contribution from $f_2(2340)$ is needed in both the $J/\psi \to \gamma\eta\eta$ and $J/\psi \to \gamma K_SK_S$ channels. The mass of the tensor state $f_2(2340)$ is consistent with the LQCD prediction for a pure tensor glueball.

The $\phi\phi$ invariant mass distribution for selected radiative $J/\psi \to \gamma\phi\phi$ decay events [65], from the same 1.3×10^9 J/ψ data sample, is shown as black dots with error bars in Fig. 4(a). A distinct η_c signal and clear structures at lower $\phi\phi$ invariant masses are observed. Both mass-dependent and mass-independent PWA were performed for the $M(\phi\phi) < 2.7$ GeV/c^2 region with results that are consistent. In addition to three dominant 0^{-+} pseudoscalar states $\eta(2225)$, $\eta(2100)$ and $X(2500)$, three tensors, $f_2(2010)$, $f_2(2300)$ and $f_2(2340)$, and one scalar $f_0(2100)$ contribute significantly in the PWA fit. The green short-dashed, the red dash–dot and the blue long-dashed histograms in Fig. 4(b) show the coherent superpositions of the Breit–Wigner resonances with $J^{PC} = 0^{-+}$, 0^{++} and 2^{++}, respectively from the model-dependent PWA fit, and the red solid histogram shows the total contribution from all components, which is in good agreement with data. The statistical significance of $f_2(2340) \to \phi\phi$ is 11σ.

We show a comparison between the product branching fractions for the scalar glueball candidates $f_0(1500)$ and $f_0(1710)$ in different decay modes in Fig. 5.

By taking $\mathcal{B}(f_0(1500) \to \pi\pi) = (34.9 \pm 2.3)\%$ and $\mathcal{B}(f_0(1710) \to K\bar{K}) = (36.0 \pm 12.0)\%$ from the PDG tables, together with BES product branching fraction results, we determine the $f_0(1500)$ and $f_0(1710)$ production rates in J/ψ radiative decays. A comparison of the measured production rates with those obtained from LQCD calculations for a scalar glueball is given in Table 2.

The production rate for $f_0(1710)$ in gluon-rich J/ψ radiative decays is close to LQCD calculations for a scalar glueball and is about an order of magnitude larger than that for $f_0(1500)$. This might suggest that $f_0(1710)$ has a larger gluonic component than $f_0(1500)$. Studies of $f_0(1500)$ and $f_0(1710)$ production in other gluon-favored and gluon-disfavored processes will be crucial to conclusively establish the scalar glueball. For the $f_2(2340)$ tensor state,

the LQCD prediction for the production rate of a pure-gauge tensor glueball in radiative J/ψ decays [67] is $\Gamma_{TensorGlueball}/\Gamma_{total} = 1.1(2) \times 10^{-2}$. The presence of $f_2(2340)$ in the $\eta\eta$ [63], K_SK_S [64] and $\phi\phi$ [65] final states suggests that $f_2(2340)$ might be a candidate for the tensor glueball. However, the current measured production rate for $f_2(2340)$, based on the observed $\eta\eta$, $K\bar{K}$ and $\phi\phi$ modes alone, appears to be substantially lower than that obtained in the LQCD calculation. Searches for additional decay modes of $f_2(2340)$ are needed.

Pseudoscalar states

The ground states of the $I = 0, J^{PC} = 0^{-+}$ pseudoscalars are the η and η'. The small number of expected radial excitations for 0^{-+} states in the quark model provides a clean and promising environment for the search of pseudoscalar glueballs.

$\eta(1405/1475)$

A pseudoscalar state around 1440 MeV/c^2, $\eta(1440)$, was first observed in $p\bar{p}$ annihilation at rest into $\eta(1440)\pi^+\pi^-$ with $\eta(1440) \to \eta\pi^+\pi^-$ and $K\bar{K}\pi$ [68], and further observed in the π^-p process [69,70] and J/ψ radiative decays [71,72]. Considerable theoretical and experimental efforts have been made to try to understand its nature. It was proposed as a candidate for a pseudoscalar glueball [73,74], due to its copious production in gluon-rich processes. However, the measured mass is much lower than that obtained from lattice QCD calculations, which is above 2.3 GeV/c^2 [31]. Subsequent experiments produced evidence that this state was really two different pseudoscalar states, $\eta(1405)$ and $\eta(1475)$. The former has large couplings to $a_0(980)\pi$ or direct $K\bar{K}\pi$, while the latter decays mainly to $K^*(892)\bar{K}$. A detailed review of the experimental situation can be found in the review by PDG2020 for pseudoscalar and pseudovector mesons in the 1400 MeV region [16] or in [75]. However, it remains controversial whether one or two pseudoscalar mesons exist in this mass region. Klempt *et al.* [76] claimed that the splitting of a single state could be due to nodes in the decay amplitudes that differ for the $\eta\pi\pi$ and $K^*(892)\bar{K}$ channels.

With 2.25×10^8 J/ψ events collected with the BESIII detector, the decays of $J/\psi \to \gamma\pi^+\pi^-\pi^0$ and $\gamma 3\pi^0$ were studied [77]. The isospin-violating decay $\eta(1405) \to f_0(980)\pi^0$ was observed for the first time with a statistical significance larger than 10σ in both the charged ($f_0(980) \to \pi^+\pi^-$, Fig. 6(a)) and neutral ($f_0(980) \to \pi^0\pi^0$, Fig. 6(b)) modes. The isospin violating ratio $\mathcal{B}(\eta(1405) \to f_0(980)\pi^0 \to \pi^+\pi^-\pi^0)$ to $\mathcal{B}(\eta(1405) \to a_0(980)\pi^0 \to \eta\pi^+\pi^-)$ is $(17.9 \pm 4.2)\%$ [16,77,78], which is an order of magnitude larger than the $a_0^0(980) - f_0(980)$ mixing intensity (less than 1%) that was measured by BESIII [79].

The anomalous large isospin violations in $J/\psi \to \gamma\eta(1405/1475) \to \gamma\pi^0 f_0(980) \to \gamma 3\pi$ stimulated many theoretical efforts to understand the nature of $\eta(1405/1475)$. With the assumption that only one 0^{-+} exists around 1.4 GeV/c^2, the triangle singularity mechanism was found to play a more dominant role than $a_0(980) - f_0(980)$ mixing, and it can produce the anomalously large isospin violations in $\eta(1405) \to \pi^+\pi^-\pi^0$, according to [80,81].

The $\eta(1405/1475)$ state was also observed in J/ψ decays to $\gamma\eta(1405/1475)$ and $\eta(1405/1475) \to \gamma\phi$, with 1.3×10^9 J/ψ events at BESIII [82]. The observation of $\eta(1405/1475) \to \gamma\phi$ indicates that $\eta(1405/1475)$ contains a sizable $s\bar{s}$ component and this does not match very well to the expectations for a pseudoscalar glueball.

$X(2370)$

The mass for the lightest pseudoscalar glueball is expected to be higher than 2.3 GeV/c^2 from LQCD calculations, while the existence of any pseudoscalar states above 2.0 GeV/c^2 is not well established experimentally. In $J/\psi \to \gamma\eta'\pi^+\pi^-$ decays at BESIII [83], the observation of $X(1835)$ by BESII [84] was confirmed, as is shown in Fig. 7(a) (to be discussed in detail in the next section) in the $\eta'\pi^+\pi^-$ invariant mass distribution. In addition, two additional states, $X(2120)$ and $X(2370)$, are observed with statistical significances larger than 7.2σ and 6.4σ, respectively. The mass of the $X(2370)$ state is measured to be $M = 2376.3 \pm 8.7^{+3.2}_{-4.3}$ MeV/c^2 from a one-dimensional fit. The $X(2370)$ state has been further confirmed in the $\eta' K\bar{K}$ invariant mass distribution in J/ψ radiative decays (shown in Fig. 7 (b)) [85] with a statistical significance of 8.3σ. The fitted masses of $X(2370)$ in the two decay modes agree with each other, and coincide with the mass of the lightest pseudoscalar glueball from LQCD calculations, which makes $X(2370)$ a candidate for the lightest pseudoscalar glueball. However, it is crucial to determine its spin parity and observe it in more decay modes before this conclusion can be firmly established.

SEARCH FOR HYBRID STATES WITH EXOTIC QUANTUM NUMBERS

Hybrid states are color-singlet combinations of constituent quarks and gluons, such as a $q\bar{q}g$ state. Evidence for the existence of hybrid states would

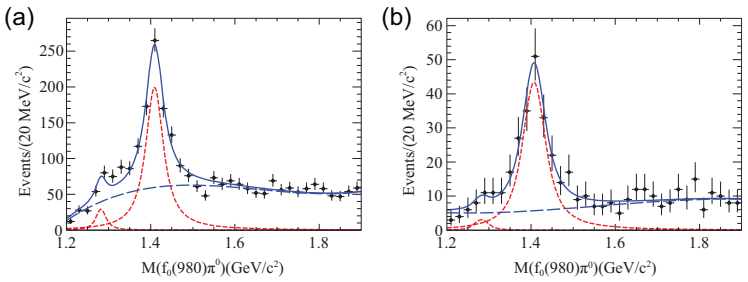

Figure 6. Results of the fit to (a) the $f_0(980)(\pi^+\pi^-)\pi^0$ and (b) $f_0(980)(\pi^0\pi^0)\pi^0$ invariant mass spectra.

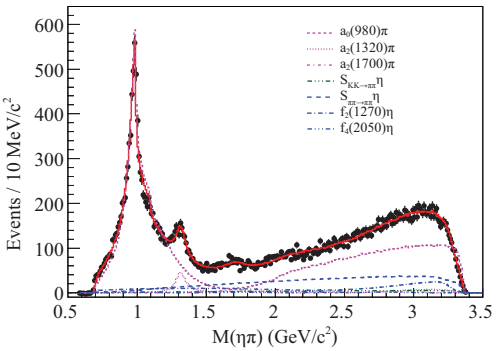

Figure 8. The $\eta\pi$ invariant mass, compared with amplitude analysis fit (solid curve) with corresponding amplitudes (various dashed and dotted lines).

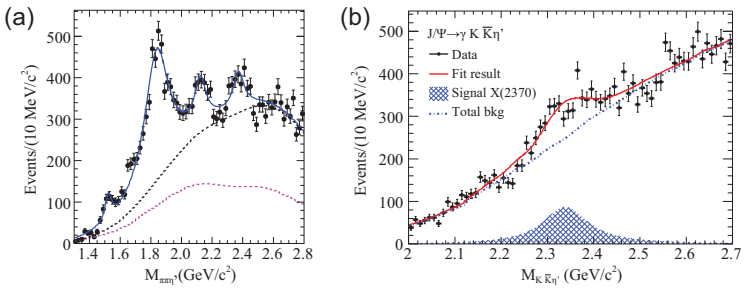

Figure 7. Results of the fit to (a) the $\eta'\pi^+\pi^-$ and (b) $\eta' K \bar{K}$ invariant mass spectra.

be direct proof of the existence of gluonic degrees of freedom in hadrons. Low mass hybrids have the additional attraction that, unlike low-lying glueballs, they could have exotic J^{PC} quantum numbers, in which case they would not mix with conventional $q\bar{q}$ states. This exotic quantum number signature for hybrid states allows for the unambiguous identification of hybrids.

The observation of isovector 1^{-+} exotic hybrid candidates, i.e. $\pi_1(1400)$ and $\pi_1(1600)$, which decay into different final states, such as $\eta\pi$, $\eta'\pi$, $f_1(1285)\pi$, $b_1(1235)\pi$ and $\rho\pi$, were reported in different reactions. The evidence for $\pi_1(2015)$ has also been reported. Reviews of the experimental status on these isovector 1^{-+} exotic states can be found in [16,76,86–88]. With 4.48×10^8 $\psi(3686)$ events collected with BESIII, an amplitude analysis is applied to $\psi(3686) \to \gamma\chi_{c1}$, $\chi_{c1} \to \eta\pi^+\pi^-$ to search for $\pi_1(1400)$, $\pi_1(1600)$ and $\pi_1(2015)$ [89]. Figure 8 shows the $\eta\pi$ invariant mass, compared with results of an amplitude analysis fit (solid curve) with various corresponding amplitudes (dashed and dotted lines). There is no significant 1^{-+} state in the $\eta\pi$ invariant mass spectrum, and upper limits for the branching fractions $\chi_{c1} \to \pi_1(1400)^{\pm}\pi^{\mp}$, $\chi_{c1} \to \pi_1(1600)^{\pm}\pi^{\mp}$ and $\chi_{c1} \to \pi_1(2015)^{\pm}\pi^{\mp}$, with subsequent $\pi_1(X)^{\pm} \to \eta\pi^{\pm}$ decay, are established. BESIII searches for isovector exotic states in $\eta'\pi$ invariant mass spectra are ongoing.

There is no evidence for the existence of isosinglet 1^{-+} states. The theoretical predictions for their main decay modes are $f_1(1285)\eta$, $a_1\pi$ and $\eta\eta'$, etc. [90–93]. The 10 billion J/ψ events that were recently accumulated by BESIII provide an ideal laboratory for the search for such states.

NEW HADRONS NEAR THE PROTON-ANTIPROTON MASS THRESHOLD

An anomalously proton-antiproton $(p\bar{p})$ mass threshold enhancement, $X(p\bar{p})$, was first observed by BESII in $J/\psi \to \gamma p\bar{p}$ decays [94] (Fig. 9) and later confirmed by BESIII [95] and CLEO [96]. This strong enhancement was subsequently determined to have spin parity $J^P = 0^-$ by BESIII [97], with a mass of $M = 1832\,^{+19}_{-5}$ (stat.) $^{+18}_{-17}$ (syst.)$\pm$19 (model) MeV/c^2 and width of $\Gamma < 76$ MeV/c^2 at the 90% C.L. The non-observation of $X(p\bar{p})$ in $J/\psi \to \omega p\bar{p}$ indicates that the pure final-state interaction (FSI) interpretation is disfavored for this structure [98]; however, FSI effects should be included in the fit of the $p\bar{p}$ mass spectrum near threshold and they have significant impact on the parameters of the $X(p\bar{p})$ resonance [97].

The $X(1835)$ state was first observed by the BESII experiment as a peak in the $\eta'\pi^+\pi^-$ invariant mass distribution in $J/\psi \to \gamma\eta'\pi^+\pi^-$ decays [84] (Fig. 10). It was later confirmed by BESIII studies of the same process [83] (Fig. 7) with mass and width measured to be $M = 1836.5 \pm 3\,^{+5.6}_{-2.1}$ MeV/c^2 and $\Gamma = 190 \pm 9\,^{+38}_{-36}$ MeV/c^2; the $X(1835)$ state was also observed in the $K^0_S K^0_S \eta$ invariant mass spectrum in $J/\psi \to \gamma K^0_S K^0_S \eta$ decays (Fig. 11), where its spin parity was determined to be $J^P = 0^-$ by a model-dependent PWA [99]. A new decay mode of $X(1835)$ decaying into $\gamma\phi$ was recently observed in $J/\psi \to \gamma\gamma\phi$ [82].

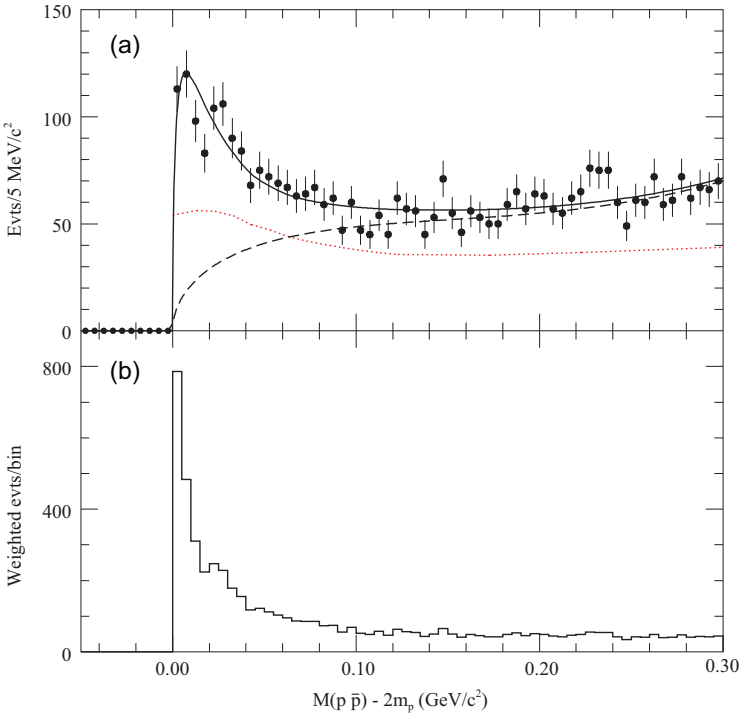

Figure 9. (a) The near threshold $M_{p\bar{p}} - 2m_p$ distribution. The solid curve is the result of the fit; the dashed curve shows the fitted background function. The dotted curve indicates how the acceptance varies with $p\bar{p}$ invariant mass. (b) The $M_{p\bar{p}} - 2m_p$ distribution with phase space correction.

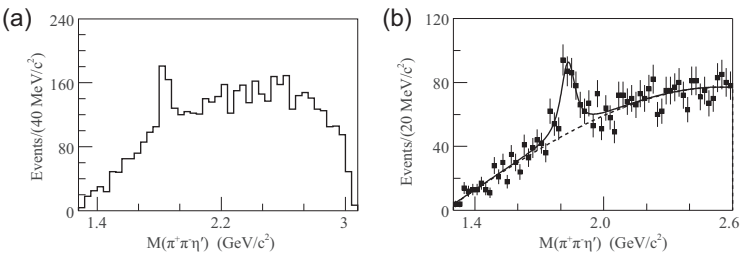

Figure 10. (a) and (b) The $\eta'\pi^+\pi^-$ invariant mass distribution. The figure (b) shows the fit (solid curve) to the data (points with error bars); the dashed curve indicates the background function.

One of the theoretical interpretations of the natures of $X(1835)$ and $X(p\bar{p})$ [100–105] suggests that the two structures originate from a $p\bar{p}$ bound state [106–110]. If $X(1835)$ is really a $p\bar{p}$ bound state, it should have a strong coupling to $0^- p\bar{p}$ systems, in which case the line shape of $X(1835)$ at the $p\bar{p}$ mass threshold would not be described as a simple BW line shape. A study of the $\eta'\pi^+\pi^-$ line shape of $X(1835)$ with high statistical precision therefore provides valuable information that helps clarify the natures of $X(1835)$ and $X(p\bar{p})$.

With 1.09×10^9 J/ψ events accumulated at the BESIII experiment, we studied the $J/\psi \to \gamma\eta'\pi^+\pi^-$ process and observed a significant abrupt change in the slope of the $\eta'\pi^+\pi^-$ invariant mass

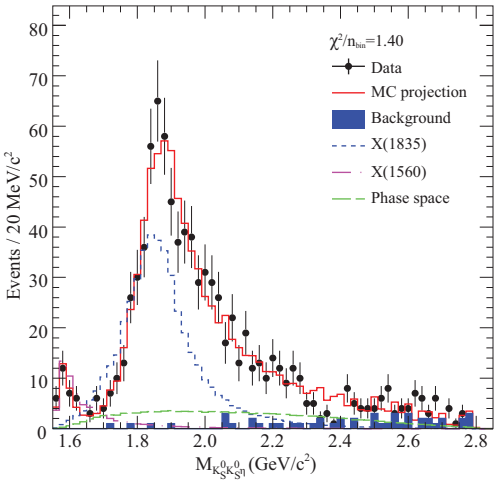

Figure 11. Invariant mass distribution of $K^0_S K^0_S \eta$. The black dots with error bars represent data, the red histograms are the PWA projections and the blue shaded histograms show backgrounds estimated by the η sideband. The contribution of $X(1835)$ is shown by the blue short-dashed histograms.

distribution at the proton-antiproton $(p\bar{p})$ mass threshold. Two models were used to characterize the $\eta'\pi^+\pi^-$ line shape around 1.85 GeV/c^2: one explicitly incorporates the opening of a decay threshold in the mass spectrum (Flatté formula), and another is the coherent sum of two resonant amplitudes.

In the first model, we assume that state $X(1835)$ couples to $p\bar{p}$. The line shape of $\eta'\pi^+\pi^-$ above the $p\bar{p}$ threshold is therefore affected by the opening of the $X(1835) \to p\bar{p}$ decay channel, similar to the distortion of the $f_0(980) \to \pi^+\pi^-$ line shape at the $K\bar{K}$ threshold. To study this, the Flatté formula [111], defined below, is used to describe the $X(1835)$ line shape:

$$T = \frac{\sqrt{\rho_{\rm out}}}{\mathcal{M}^2 - s - i\sum_k g_k^2 \rho_k}. \qquad (1)$$

Here, T is the decay amplitude, $\rho_{\rm out}$ is the phase space for $J/\psi \to \gamma\eta'\pi^+\pi^-$, $\mathcal{M}$ is a parameter with the dimension of mass, s is the square of the $\eta'\pi^+\pi^-$ system mass, ρ_k is the phase space for decay mode k and g_k^2 is the corresponding coupling strength. The term $\sum_k g_k^2 \rho_k$ describes how the decay width varies with s:

$$\sum_k g_k^2 \rho_k \approx g_0^2 \left(\rho_0 + \frac{g_{p\bar{p}}^2}{g_0^2} \rho_{p\bar{p}} \right). \qquad (2)$$

Here, g_0^2 is the sum of g^2 of all decay modes other than $X(1835) \to p\bar{p}$, ρ_0 is the maximum two-body decay phase space volume [16] and $g_{p\bar{p}}^2/g_0^2$ is the ratio between the coupling strength to the $p\bar{p}$ channel and the sum of all other channels.

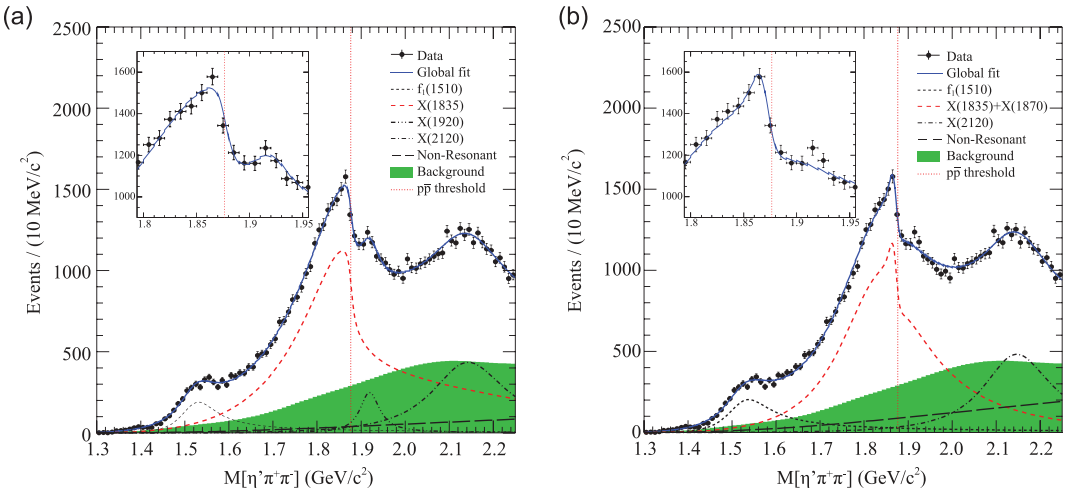

Figure 12. (a) Fit results using the Flatté formula. (b) Fit results based on a coherent sum of two Breit–Wigner amplitudes. The dash–dot vertical lines show the position of the $p\bar{p}$ mass threshold, the black dots with error bars represent data, the solid curves are total fit results, the red dashed curve in (a) shows the state around 1.85 GeV/c^2 and the red dashed curve in (b) is the sum of $X(1835)$ and $X(1870)$. The insets show the data and global fit between 1.8 and 1.95 GeV/c^2.

The fit results for this model are shown in Fig. 12(a). The fit yields $g^2_{p\bar{p}}/g^2_0 = 2.31 \pm 0.37^{+0.83}_{-0.60}$ with a statistical significance of $g^2_{p\bar{p}}/g^2_0$ being non-zero larger than 7σ. The value of $g^2_{p\bar{p}}/g^2_0$ implies that the couplings between the $X(1835)$ and $X(p\bar{p})$ final states is very large. According to the definitions given in [112], the pole position is determined by requiring that the denominator in Equation (1) be zero. The pole that is nearest to the $p\bar{p}$ mass threshold is found to be $M_{\rm pole} = 1909.5 \pm 15.9\,({\rm stat.})\,^{+9.4}_{-27.5}({\rm syst.})\,{\rm MeV/c^2}$ and $\Gamma_{\rm pole} = 273.5 \pm 21.4\,({\rm stat.})\,^{+6.1}_{-64.0}\,({\rm syst.})\,{\rm MeV/c^2}$.

In the second model, we assume that the distortion comes from the interference between $X(1835)$ and another resonance with mass close to the $p\bar{p}$ mass threshold. A fit with a coherent sum of two interfering Breit–Wigner amplitudes to describe the $\eta'\pi^+\pi^-$ mass spectrum around 1.85 GeV/c^2 is performed. This fit yields a narrow resonance below the $p\bar{p}$ mass threshold with $M = 1870.2 \pm 2.2({\rm stat.})^{+2.3}_{-0.7}({\rm syst.})\,{\rm MeV/c^2}$ and $\Gamma = 13.0 \pm 6.1({\rm stat.})^{+2.1}_{-3.8}({\rm syst.})\,{\rm MeV/c^2}$, with a statistical significance larger than 7σ. The fit results for the second model are shown in Fig. 12(b).

Based on current data samples, two models fit the data with similar fit qualities. Both fits suggest the existence of either a broad state with strong couplings to $p\bar{p}$, or a narrow state just below the $p\bar{p}$ mass threshold. For the former case, its strong coupling to $p\bar{p}$ suggests the existence of a $p\bar{p}$ molecule-like state. For the latter case, the narrow state just below the $p\bar{p}$ mass threshold suggests that it is an unconventional meson, possibly a $p\bar{p}$ bound state. So both fits support the existence of a $p\bar{p}$ molecule-like or bound state. However, more sophisticated models such as a mixture of the above two models cannot be ruled out.

SUMMARY AND PERSPECTIVES

Continuous experimental efforts are being made to search for and study glueballs, hybrids and multiquark states from charmonium decays, supported by the huge statistics data samples accumulated at BESIII.

We have found that the production rate for $f_0(1710)$ in gluon-rich J/ψ radiative decays is about an order of magnitude higher than that for $f_0(1500)$ and is close to LQCD calculations for the production rate of a scalar glueball, under current circumstance. This suggests that $f_0(1710)$ can have a larger gluonic component than $f_0(1500)$. Studies of $f_0(1500)$ and $f_0(1710)$ in other gluon-favored and gluon-disfavored processes with improved analysis techniques will be crucial to further refine this conclusion. The mass of the $f_2(2340)$ tensor state matches the LQCD expectation for a pure tensor glueball. This, and its copious production in J/ψ radiative decays to $\eta\eta$, K_SK_S and $\phi\phi$, might suggest that $f_2(2340)$ is a candidate of the tensor glueball. However, the current measured production rates for $f_2(2340)$ appear to be substantially lower than LQCD expectations. Since no dominant glueball decay mode can be expected, due to the flavor blindness of glueball decays, searches for additional $f_2(2340)$ decay modes are necessary. In light of the observation of $X(2370)$ in $J/\psi \to \gamma\eta'\pi^+\pi^-$ and $\gamma\eta' K\bar{K}$, the identification of the lowest-pseudoscalar glueball has become a recent major focus of BESIII. In particular, the 10 billion

J/ψ event sample and the clean environment in $J/\psi \to \gamma\eta' K_S K_S$ decays will make an amplitude analysis and the determination of the spin parity of $X(2370)$ possible.

In searching for hybrid states with exotic quantum numbers, no significant signals for the isovector 1^{-+} exotic hybrid candidates $\pi_1(1400)$, $\pi_1(1600)$ and $\pi_1(2015)$ were seen in the $\psi(3686) \to \gamma\chi_{c1}$, $\chi_{c1} \to \eta\pi^+\pi^-$ decay process with 4.48×10^8 $\psi(3686)$ events collected with BESIII. As of yet, no evidence for an isoscalar 1^{-+} exotic hybrid has been found. The 10 billion J/ψ event sample will provide an ideal laboratory for the search of isoscalar 1^{-+} exotic hybrids in $f_1(1285)\eta$, $a_1\pi$ and $\eta\eta'$, etc. decay channels.

In order to elucidate further the nature of the states around $1.85\,\mathrm{GeV/c^2}$, more data are needed to further study the $J/\psi \to \gamma\eta'\pi^+\pi^-$ process. Also, line shapes for other radiative decay channels should be studied near the $p\bar{p}$ mass threshold, along with further studies of $J/\psi \to \gamma p\bar{p}$ and $J/\psi \to \gamma\eta K_S^0 K_S^0$.

FUNDING

This work was supported in part by the National Natural Science Foundation of China (NSFC) (11935016), the Chinese Academy of Sciences (CAS) Center for Excellence in Particle Physics (CCEPP), the CAS Large-Scale Scientific Facility Program and the CAS Key Research Program of Frontier Sciences (QYZDJ-SSW-SLH040).

Conflict of interest statement. None declared.

REFERENCES

1. Yukawa H. On the interaction of elementary particles I. *Proc Phys Math Soc Japan* 1935; **17**: 48–57.
2. Zweig G. An SU(3) model for strong interaction symmetry and its breaking. In: Lichtenberg DB and Rosen SP (eds). *Developments in the Quark Theory of Hadrons*. Vol. 1, Nonantum, MA: Hadronic Press, 1980, 22–101.
3. Gell-Mann M. A schematic model of baryons and mesons. *Phys Lett* 1964; **8**: 214–5.
4. Greenberg OW. Spin and unitary spin independence in a paraquark model of baryons and mesons. *Phys Rev Lett* 1964; **13**: 598–602.
5. Coward DH, DeStaebler HC and Early RA *et al.* Electron-proton elastic scattering at high momentum transfers. *Phys Rev Lett* 1968; **20**: 292–5.
6. Aubert JJ, Becker U and Biggs PJ *et al.* Experimental observation of a heavy particle *J*. *Phys Rev Lett* 1974; **33**: 1404–6.
7. Augustin JE, Boyarski A and Breidenbach M *et al.* Discovery of a narrow resonance in e^+e^- annihilation. *Phys Rev Lett* 1974; **33**: 1406–8.
8. Glashow SL, Iliopoulos J and Maiani L. Weak interactions with lepton-hadron symmetry. *Phys Rev D* 1970; **2**: 1285–92.
9. Fritzsch H, Gell-Mann M and Leutwyler H. Advantages of the color octet gluon picture. *Phys Lett B* 1973; **47**: 365–8.
10. Weinberg S. Nonabelian gauge theories of the strong interactions. *Phys Rev Lett* 1973; **31**: 494–7.
11. Caprini I, Colangelo G and Leutwyler H. Mass and width of the lowest resonance in QCD. *Phys Rev Lett* 2006; **96**: 132001.
12. Pelaéz JR. From controversy to precision on the sigma meson: a review on the status of the non-ordinary $f_0(500)$ resonance. *Phys Rep* 2016; **658**: 1.
13. Dowdall RJ, Davies CTH and Hammant TC *et al.* Precise heavy-light meson masses and hyperfine splittings from lattice QCD including charm quarks in the sea. *Phys Rev D* 2012; **86**: 094510.
14. Daldrop JO, Davies CTH and Dowdall RJ. Prediction of the bottomonium D-wave spectrum from full lattice QCD. *Phys Rev Lett* 2012; **108**: 102003.
15. Donald GC, Davies CTH and Dowdall RJ *et al.* Precision tests of the J/ψ from full lattice QCD: mass, leptonic width and radiative decay rate to η_c. *Phys Rev D* 2012; **86**: 094501.
16. Zyla PA, Barnett RM and Beringer J *et al.* Review of particle physics. *Prog Theor Exp Phys* 2020; **2020**: 083C01.
17. Kronfeld AS. Twenty-first century lattice gauge theory: results from the QCD lagrangian. *Annu Rev Nucl Part Sci* 2012; **62**: 265–84.
18. Barnes T, Close FE and de Viron F. QQG hermaphrodite mesons in the MIT bag model. *Nucl Phys B* 1983; **224**: 241–64.
19. Carlson CE, Hansson TH and Peterson C. The glueball spectrum in the bag model and in lattice gauge theories. *Phys Rev D* 1984; **30**: 1594.
20. Donoghue JF, Johnson K and Li BA. Low mass glueballs in the meson spectrum. *Phys Lett B* 1981; **99**: 416–20.
21. Chanowitz MS and Sharpe SR. Hybrids: mixed states of quarks and gluons. *Nucl Phys B* 1983; **222**: 211–44. Erratum: 1983; **228**: 588.
22. Isgur N and Paton JE. A flux tube model for hadrons. *Phys Lett B* 1983; **124**: 247–51.
23. Isgur N and Paton JE. A flux tube model for hadrons in QCD. *Phys Rev D* 1985; **31**: 2910.
24. Latorre JI, Narison S and Pascual P *et al.* Hermaphrodite mesons and QCD sum rules. *Phys Lett B* 1984; **147**: 169–74.
25. Huang T, Jin HY and Zhang AL. Determination of the scalar glueball mass in QCD sum rules. *Phys Rev D* 1999; **59**: 034026.
26. Kisslinger LS, Gardner J and Vanderstraeten C. Mixed scalar glueballs and mesons. *Phys Lett B* 1997; **410**: 1–5.
27. Narison S. Masses, decays and mixings of gluonia in QCD. *Nucl Phys B* 1998; **509**: 312–56.
28. Michael C and Teper M. The glueball spectrum in SU(3). *Nucl Phys B* 1989; **314**: 347–62.
29. Bali GS, Schilling K and Hulsebos A *et al.* A comprehensive lattice study of SU(3) glueballs. *Phys Lett B* 1993; **309**: 378–84.
30. Morningstar CJ and Peardon MJ. The glueball spectrum from an anisotropic lattice study. *Phys Rev D* 1999; **60**: 034509.
31. Chen Y, Alexandru A and Dong SJ *et al.* Glueball spectrum and matrix elements on anisotropic lattices. *Phys Rev D* 2006; **73**: 014516.

32. Richards CM, Irving AC and Gregory EB *et al.* Glueball mass measurements from improved staggered fermion simulations. *Phys Rev D* 2010; **82**: 034501.
33. Gregory E, Irving A and Lucini B *et al.* Towards the glueball spectrum from unquenched lattice QCD. *J High Energy Phys* 2012; **10**: 170.
34. Close FE and Tornqvist NA. Scalar mesons above and below 1 GeV. *J Phys G* 2002; **28**: R249–67.
35. Gunter J, Dzierba AR and Lindenbusch R *et al.* Partial wave analysis of the $\pi^0\pi^0$ system produced in $\pi^- p$ charge exchange collisions. *Phys Rev D* 2001; **64**: 072003.
36. Amsler C, Armstrong DS and Baker CA *et al.* Coupled channel analysis of pp annihilation into $\pi^0\pi^0\pi^0$, $\pi^0\eta\eta$ and $\pi^0\pi^0\eta$. *Phys Lett B* 1995; **355**: 425–32.
37. Abele A, Adomeit J and Amsler C *et al.* A study of $f_0(1500)$ decays into $4\pi^0$ in $\bar{p}p \to 5\pi^0$ at rest. *Phys Lett B* 1996; **380**: 453–60.
38. Abele A, Adomeit J and Amsler C *et al.* Observation of $f_0(1500)$ decay into $K_L K_L$. *Phys Lett B* 1996; **385**: 425–32.
39. Abele A, Adomeit J and Armstrong DS *et al.* Further analysis of $\bar{p}p \to 3\pi^0$, $\eta\eta\pi^0$ and $\eta\pi^0\pi^0$ at rest. *Nucl Phys A* 1996; **609**: 562–84. Erratum: 1997; **625**: 899–900.
40. Antinori F, Barberis D and Bayes A *et al.* A further study of the centrally produced $\pi^+\pi^-$ and $\pi^+\pi^-\pi^+\pi^-$ channels in pp interactions at 300-GeV/c and 450-GeV/c. *Phys Lett B* 1995; **353**: 589–94.
41. Barberis D, Beusch W and Binon FG *et al.* A study of the centrally produced $\pi^+\pi^-\pi^+\pi^-$ channel in pp interactions at 450-GeV/c. *Phys Lett B* 1997; **413**: 217–24.
42. Bellazzini R, Binon FG and Boutemeur M *et al.* A partial wave analysis of the centrally produced $\pi^0\pi^0$ system in pp interactions at 450 GeV/c. *Phys Lett B* 1999; **467**: 296–302.
43. Ablikim M, Bai JZ and Ban Y *et al.* Production of σ in $\psi(2S) \to \pi^+\pi^- J/\psi$. *Phys Lett B* 2007; **645**: 19–25.
44. Becker J, Blaylock G and Bolton T *et al.* Radiative decays of the J/ψ into $\gamma\pi^+\pi^-$ and γK^+K^-. *Phys Rev D* 1987; **35**: 2077.
45. Augustin JE, Cosme G and Couchot F *et al.* Radiative decay of J/ψ Into $\gamma\pi^+\pi^-$. *Z Phys C* 1987; **36**: 369–76.
46. Kopke L and Wermes N. J/ψ decays. *Phys Rep* 1989; **174**: 67.
47. Bai JZ, Chen GP and Chen HF *et al.* Studies of $\xi(2230)$ in J/ψ radiative decays. *Phys Rev Lett* 1996; **76**: 3502–5.
48. Bai JZ, Bian JG and Blum IK *et al.* Study of the P-wave charmonium state χ_{cJ} in $\psi(2S)$ decays. *Phys Rev Lett* 1998; **81**: 3091–5.
49. Bugg DV, Scott I and Zou BS *et al.* Further amplitude analysis of $J/\psi \to \gamma(\pi^+\pi^-\pi^+\pi^-)$. *Phys Lett B* 1995; **353**: 378–84.
50. Ablikim M, Bai JZ and Ban Y *et al.* The σ pole in $J/\psi \to \omega\pi^+\pi^-$. *Phys Lett B* 2004; **598**: 149–58.
51. Ablikim M, Bai JZ and Ban Y *et al.* Study of $J/\psi \to \omega K^+K^-$. *Phys Lett B* 2004; **603**: 138–45.
52. Ablikim M, Bai JZ and Ban Y *et al.* Resonances in $J/\psi \to \phi\pi^+\pi^-$ and ϕK^+K^-. *Phys Lett B* 2005; **607**: 243–53.
53. Lees JP, Poireau V and Tisserand V *et al.* Study of CP violation in Dalitz-plot analyses of $B^0 \to K^+K^-K^0_S$, $B^+ \to K^+K^-K^+$, and $B^+ \to K^0_S K^0_S K^+$. *Phys Rev D* 2012; **85**: 112010.
54. Bonvicini G, Cinabro D and Dubrovin M *et al.* Dalitz plot analysis of the $D^+ \to \pi^-\pi^+\pi^+$ decay. *Phys Rev D* 2007; **76**: 012001.
55. Aloisio A, Ambrosino F and Antonelli A *et al.* Study of the decay $\phi \to \pi^0\pi^0\gamma$ with the KLOE detector. *Phys Lett B* 2002; **537**: 21–7.
56. Batley JR, Culling AJ and Kalmus G *et al.* New high statistics measurement of K_{e4} decay form factors and $\pi\pi$ scattering phase shifts. *Eur Phys J C* 2008; **54**: 411–23.
57. Mori T, Uehara S and Watanabe Y *et al.* High statistics study of $f_0(980)$ resonance in $\gamma\gamma \to \pi^+\pi^-$ production. *Phys Rev D* 2007; **75**: 051101.
58. Ablikim M, Achasov MN and Ai XC *et al.* Amplitude analysis of the $\pi^0\pi^0$ system produced in radiative J/ψ decays. *Phys Rev D* 2015; **92**: 052003. Erratum: 2016; **93**: 039906.
59. Ablikim M, Bai JZ and Ban Y *et al.* Partial wave analyses of $J/\psi \to \gamma\pi^+\pi^-$ and $\gamma\pi^0\pi^0$. *Phys Lett B* 2006; **642**: 441–8.
60. Ablikim M, An ZH and Bai JZ *et al.* Design and construction of the BESIII detector. *Nucl Instrum Methods Phys A* 2010; **614**: 345–99.
61. Bai JZ, Bao HC and Blum IK *et al.* The BES upgrade. *Nucl Instrum Meth A* 2001; **458**: 627–37.
62. Zou BS and Bugg DV. Covariant tensor formalism for partial wave analyses of ψ decay to mesons. *Eur Phys J A* 2003; **16**: 537–47.
63. Ablikim M, Achasov MN and Albayrak O *et al.* Partial wave analysis of $J/\psi \to \gamma\eta\eta$. *Phys Rev D* 2013; **87**: 092009. Erratum: 2013; **87**: 119901.
64. Ablikim M, Achasov MN and Ahmed S *et al.* Amplitude analysis of the $K_S K_S$ system produced in radiative J/ψ decays. *Phys Rev D* 2018; **98**: 072003.
65. Ablikim M, Achasov MN and Ai XC *et al.* Observation of pseudoscalar and tensor resonances in $J/\psi \to \gamma\phi\phi$. *Phys Rev D* 2016; **93**: 112011.
66. Gui LC, Chen Y and Li G *et al.* Scalar glueball in radiative J/ψ decay on the lattice. *Phys Rev Lett* 2013; **110**: 021601.
67. Yang YB, Gui LC and Chen Y *et al.* Lattice study of radiative J/ψ decay to a tensor glueball. *Phys Rev Lett* 2013; **111**: 091601.
68. Baillon PH, Edwards D and Marechal B *et al.* Further study of the e-meson in antiproton-proton annihilations at rest. *Nuovo Cim A* 1967; **50**: 393–421.
69. Rath MG, Cason NM and Bensinger JR *et al.* The $K^0_s K^0_s \pi^0$ system produced in $\pi^- p$ interactions at 21.4 GeV/*c*. *Phys Rev D* 1989; **40**: 693.
70. Adams GS, Adams T and Bar-Yam Z *et al.* Observation of pseudoscalar and axial vector resonances in $\pi^- p \to K^+K^-\pi^0 n$ at 18 GeV. *Phys Lett B* 2001; **516**: 264–72.
71. Bai Z, Blaylock G and Bolton T *et al.* Partial wave analysis of $J/\psi \to \gamma K^0_s K^\pm \pi^\pm$. *Phys Rev Lett* 1990; **65**: 2507–10.
72. Augustin JE, Cosme G and Couchot F *et al.* Partial wave analysis of DM2 data in the $\eta(1430)$ energy range. *Phys Rev D* 1992; **46**: 1951–8.
73. Acciarri M, Achard P and Adriani O *et al.* Light resonances in $K^0_S K^\pm \pi^\mp$ and $\eta\pi^+\pi^-$ final states in $\gamma\gamma$ collisions at LEP. *Phys Lett B* 2001; **501**: 1–11.
74. Faddeev L, Niemi AJ and Wiedner U. Glueballs, closed flux tubes and $\eta(1440)$. *Phys Rev D* 2004; **70**: 114033.
75. Masoni A, Cicalo C and Usai GL. The case of the pseudoscalar glueball. *J Phys G* 2006; **32**: R293–335.
76. Klempt E and Zaitsev A. Glueballs, hybrids, multiquarks: experimental facts versus QCD inspired concepts. *Phys Rep* 2007; **454**: 1–202.
77. Ablikim M, Achasov MN and Alberto D *et al.* First observation of $\eta(1405)$ decays into $f_0(980)\pi^0$. *Phys Rev Lett* 2012; **108**: 182001.
78. Amsler C, Armstrong DS and Baker CA *et al.* E decay to $\eta\pi\pi$ in pp annihilation at rest. *Phys Lett B* 1995; **358**: 389–98.
79. Ablikim M, Achasov MN and An L *et al.* Study of $a_0^0(980) - f_0(980)$ mixing. *Phys Rev D* 2011; **83**: 032003.
80. Wu JJ, Liu XH and Zhao Q *et al.* The puzzle of anomalously large isospin violations in $\eta(1405/1475) \to 3\pi$. *Phys Rev Lett* 2012; **108**: 081803.
81. Wu XG, Wu JJ and Zhao Q *et al.* Understanding the property of $\eta(1405/1475)$ in the J/ψ radiative decay. *Phys Rev D* 2013; **87**: 014023.
82. Ablikim M, Achasov MN and Ahmed S *et al.* Study of $\eta(1475)$ and $X(1835)$ in radiative J/ψ decays to $\gamma\phi$. *Phys Rev D* 2018; **97**: 051101.

83. Ablikim M, Achasov MN and An L *et al.* Confirmation of the *X*(1835) and observation of the resonances *X*(2120) and *X*(2370) in $J/\psi \to \gamma\pi^+\pi^-\eta'$. *Phys Rev Lett* 2011; **106**: 072002.
84. Ablikim M, Bai JZ and Ban Y *et al.* Observation of a resonance *X*(1835) in $J/\psi \to \gamma\pi^+\pi^-\eta'$. *Phys Rev Lett* 2005; **95**: 262001.
85. Ablikim M, Achasov MN and Adlarson P *et al.* Observation of *X*(2370) and search for X(2120) in $J/\psi \to \gamma K\bar{K}\eta'$. *Eur Phys J C* 2020; **80**: 746.
86. Meyer CA and Van Haarlem Y. The status of exotic-quantum-number mesons. *Phys Rev C* 2010; **82**: 025208.
87. Meyer CA and Swanson ES. Hybrid mesons. *Prog Part Nucl Phys* 2015; **82**: 21–58.
88. Ketzer B, Grube B and Ryabchikov D. Light-meson spectroscopy with COMPASS. *Prog Part Nucl Phys* 2020; **113**: 103755.
89. Ablikim M, Achasov MN and Ahmed S *et al.* Amplitude analysis of the $\chi_{c1} \to \eta\pi^+\pi^-$ decays. *Phys Rev D* 2017; **95**: 032002.
90. Isgur N, Kokoski R and Paton J. Gluonic excitations of mesons: why they are missing and where to find them. *Phys Rev Lett* 1985; **54**: 869.
91. Page PR, Swanson ES and Szczepaniak AP. Hybrid meson decay phenomenology. *Phys Rev D* 1999; **59**: 034016.
92. Huang PZ, Chen HX and Zhu SL. The strong decay patterns of the 1^{-+} exotic hybrid mesons. *Phys Rev D* 2011; **83**: 014021.
93. Chen HX, Cai ZX and Huang PZ *et al.* The decay properties of the 1^{-+} hybrid state. *Phys Rev D* 2011; **83**: 014006.
94. Bai JZ, Ban Y and Bian JG *et al.* Observation of a near-threshold enhancement in the $p\bar{p}$ mass spectrum from radiative $J/\psi \to \gamma p\bar{p}$ decays. *Phys Rev Lett* 2003; **91**: 022001.
95. Ablikim M, Achasov MN and An L *et al.* Observation of a $p\bar{p}$ mass threshold enhancement in $\psi' \to \pi^+\pi^- J/\psi (J/\psi \to \gamma p\bar{p})$ decay. *Chin Phys C* 2010; **34**: 421.
96. Alexander JP, Cassel DG and Das S *et al.* Study of $\psi(2S)$ decays to $\gamma p\bar{p}$, $\pi^0 p\bar{p}$ and $\eta p\bar{p}$ and search for $p\bar{p}$ threshold enhancements. *Phys Rev D* 2010; **82**: 092002.
97. Ablikim M, Achasov MN and Alberto D *et al.* Spin-parity analysis of $p\bar{p}$ mass threshold structure in j/ψ and ψ' radiative decays. *Phys Rev Lett* 2012; **108**: 112003.
98. Ablikim M, Achasov MN and Albayrak O *et al.* Study of $J/\psi \to \omega p\overline{p}$ at BESIII. *Phys Rev D* 2013; **87**: 112004.
99. Ablikim M, Achasov MN and Ai XC *et al.* Observation and spin-parity determination of the *X*(1835) in $J/\psi \to \gamma K_S^0 K_S^0 \eta$. *Phys Rev Lett* 2015; **115**: 091803.
100. Huang T and Zhu SL. X(1835): natural candidate of η''s second radial excitation. *Phys Rev D* 2006; **73**: 014023.
101. Kochelev N and Min DP. X(1835) as the lowest mass pseudoscalar glueball and proton spin problem. *Phys Lett B* 2006; **633**: 283–8.
102. Hao G, Qiao CF and Zhang AL. 0^{-+} trigluon glueball and its implication for a recent BES observation. *Phys Lett B* 2006; **642**: 53–61.
103. Li BA. Possible 0^{-+} glueball candidate *X*(1835). *Phys Rev D* 2006; **74**: 034019.
104. Liu XH, Zhang YJ and Zhao Q. Possible mechanism for producing the threshold enhancement in $J/\psi \to \gamma p\bar{p}$. *Phys Rev D* 2009; **80**: 034032.
105. Kang XW, Haidenbauer J and Meißner UG. Near-threshold $\bar{p}p$ invariant mass spectrum measured in J/ψ and ψ' decays. *Phys Rev D* 2015; **91**: 074003.
106. Zhu SL and Gao CS. X(1835): a possible baryonium? *Commun Theor Phys* 2006; **46**: 291.
107. Dedonder JP, Loiseau B and El-Bennich B *et al.* On the structure of the *X*(1835) baryonium. *Phys Rev C* 2009; **80**: 045207.
108. Ding GJ and Yan ML. Productions of X(1835) as baryonium with sizable gluon content. *Eur Phys J A* 2006; **28**: 351–60.
109. Liu C. Baryonium, tetra-quark state and glue-ball in large-N_c QCD. *Eur Phys J C* 2008; **53**: 413–9.
110. Wang ZG and Wan SL. X(1835) as a baryonium state with QCD sum rules. *J Phys G* 2007; **34**: 505–11.
111. Flatte SM. Coupled-channel analysis of the $\pi\eta$ and $K\bar{K}$ systems near $K\bar{K}$ threshold. *Phys Lett B* 1976; **63**: 224–7.
112. Zou BS and Bugg DV. Is $f_0(975)$ a narrow resonance? *Phys Rev D* 1993; **48**: R3948–52.

REVIEW

National Science Review
8: nwab052, 2021
https://doi.org/10.1093/nsr/nwab052
Advance access publication 31 March 2021

PHYSICS

Special Topic: Physics of the BESIII Experiment

Light meson physics at BESIII

Shuang-shi Fang [1,2]

ABSTRACT

Studies of light meson decays are important tools to perform precision tests of the effective field theories, determine transition form factors and test fundamental symmetries. With very high statistics data samples, the Beijing Spectrometer III (BESIII) experiment provides a unique laboratory for light meson studies and is contributing significantly to a variety of these investigations. A brief review of recent progress in light meson decay studied at the BESIII experiment, including detailed studies of common decay dynamics, searches for rare/forbidden decays and new particles, is presented. Finally, together with descriptions of different experimental techniques, prospects for future studies of light mesons are discussed in some detail.

Keywords: light meson decays, charmonium decays, e^+e^- annihilation, BESIII detector

INTRODUCTION

The discovery of light mesons and detailed studies of their decays have played crucial roles in the development of our understanding of elementary particle physics. In the case of weak interactions, important insights were gained from kaon and pion decays, such as the observation of *CP* violation and validation of the V-A structure of the theory. In addition, the discovery of strangeness inspired the SU(3) flavor symmetry, which, in turn, gave the birth to the quark model picture of the underlying structure of observed particles. To date, about seven decades since the discovery of the first light mesons (the pion and kaon), studies of light meson decays continue to provide opportunities for a variety of physics at low-energy scales, including precision tests of effective field theories, investigations of the quark structure of the light mesons, tests of the fundamental symmetries and searches for new particles.

The Beijing Spectrometer III (BESIII) experiment [1] collected the world's largest samples of 1.3×10^9 J/ψ events [2] and 4.5×10^8 $\psi(3686)$ events [3] produced directly from e^+e annihilation in 2009 and 2012. Because of the high production rates of light mesons in the charmonium decays, these data, in combination with the excellent performance of the detector, offer unprecedented opportunities to explore the light meson decays. Moreover, the BESIII data sample of e^+e^- annihilation events at energies between 2.0 and 3.08 GeV with an integrated luminosity of 650 pb^{-1} allows for explorations of properties of the light vector mesons, in particular the vector strangeonium states.

PRECISION TESTS OF QCD AT LOW ENERGIES

At high energies, QCD serves as a reliable and useful theory, whereas at low energies non–perturbative QCD calculations are usually performed by an effective field theory called chiral perturbation theory (ChPT). High-quality and precise measurements of low-energy hadronic processes are necessary in order to verify the systematic ChPT expansion. Thus, studies of light meson decays are important guides to our understanding of how QCD works in the non-perturbative regime.

Light quark mass ratios in $\eta/\eta' \to 3\pi$ decays

The decay of the η meson into 3π violates isospin symmetry, which is related to the difference of light quark masses, $m_u \neq m_d$. Therefore, the decay of $\eta \to 3\pi$ offers a unique way to determine the quark

[1]Institute of High Energy Physics, Chinese Academy of Sciences, Beijing 100049, China and [2]University of Chinese Academy of Sciences, Beijing 100049, China

E-mail: fangss@ihep.ac.cn

Received 18 November 2020; **Revised** 10 March 2021; **Accepted** 16 March 2021

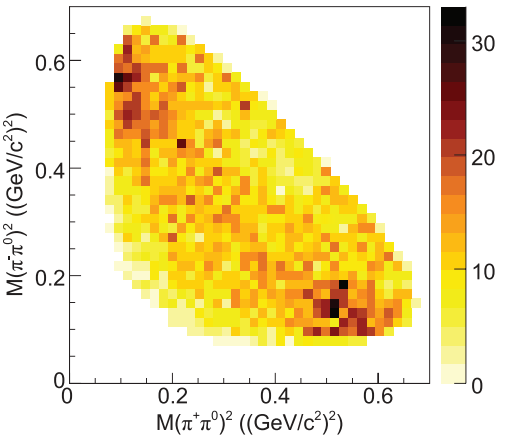

Figure 1. Dalitz plot of $M^2(\pi^+\pi^0)$ versus $M^2(\pi^-\pi^0)$ for the $\eta' \to \pi^+\pi^-\pi^0$ decay, where the two clear clusters correspond to the $\eta' \to \rho^{\mp}\pi^{\pm}$ decay [17].

mass ratio $Q^2 \equiv (m_s^2 - \hat{m}^2)/(m_d^2 - m_u^2)$ (where $\hat{m} = \frac{1}{2}(m_d + m_u)$). Extensive theoretical studies have been performed within the framework of combined ChPT and dispersion theory [4–9].

In addition to the recent results from the WASA-at-COSY [10] and KLOE-2 [11] experiments, BESIII reported a Dalitz plot analysis of $\eta \to 3\pi$ decays [12]. The measured matrix elements are in agreement with the most precise KLOE-2 determination and theoretical predictions. Taking experimental results as input, two dedicated analyses presented the results $Q = 22.0 \pm 0.7$ [13] and $Q = 21.6 \pm 1.1$ [14]. In the near future, the study of $\eta \to \pi^+\pi^-\pi^0$ and $\eta \to \pi^0\pi^0\pi^0$ decays at BESIII will provide an independent check of these results by directly fitting to differing theoretical models.

Historically, the $\eta' \to \pi^+\pi^-\pi^0$ decay was considered to proceed via π^0–η mixing [15], which offered the possibility of comparable strength $u - d$ quark mass difference from the branching fraction ratio of $r = \mathcal{B}(\eta' \to \pi\pi\pi)/\mathcal{B}(\eta' \to \pi\pi\eta)$. However, it was subsequently argued that the decay amplitudes are strongly affected by the intermediate resonances [16], e.g. the P-wave contribution from $\eta' \to \rho\pi$, and, thus, the $u - d$ quark mass difference could not be extracted in such a simple way.

In addition to the first observation of $\eta' \to \rho^{\pm}\pi^{\mp}$ (Fig. 1) by BESIII [17], the resonant π–πS wave, interpreted as the broad $f_0(500)$, is also expected to play an essential role in $\eta' \to \pi^+\pi^-\pi^0$ decays. The contribution of $f_0(500)$ provides a reasonable explanation for the negative slope parameter of the Dalitz plot of $\eta' \to \pi^0\pi^0\pi^0$ [12]. Because of limited statistics, it has been impossible to differentiate between S and D waves; larger event samples are crucial for carrying out amplitude analyses of these processes. Several theory groups have expressed interest in describing the decay using a dispersive approach. These improved theoretical studies along with more precise experimental measurements of $\eta/\eta' \to 3\pi$ decays from a variety of experiments are expected to improve the accuracy of the quark mass ratio.

Cusp effect in $\eta' \to \pi^0\pi^0\eta$ decays

In addition to the precision tests of effective theoretical models, common to all $\eta' \to \pi\pi\eta$ decays, the neutral decay $\eta' \to \pi^0\pi^0\eta$ also allows us to examine the cusp effect, i.e. an abrupt change in the $\pi^0\pi^0$ invariant mass distribution as it crosses the $2m_{\pi^+}$ threshold. An accurate measurement of the cusp effect may enable a determination of the S-wave pion–pion scattering lengths to high precision.

For $\eta' \to \pi^+\pi^-\eta$, BESIII results [18] are not particularly consistent with theoretical predictions based on the chiral unitary approach [19]. The discrepancies show up as about 4 SD on some of the parameters that are used to describe the Dalitz plot distribution. In the case of $\eta' \to \pi^0\pi^0\eta$, the results are in general consistent with theoretical predictions within the uncertainties and the latest results reported by the A2 experiment [20]. Because of the limited statistics, the present results are not precise enough to firmly establish isospin violation and additional effects, e.g. radiative corrections [21], and the π^+/π^0 mass difference should be considered in future experimental and theoretical studies.

A BESIII search for the cusp in $\eta' \to \eta\pi^0\pi^0$ performed by inspecting the $\pi^0\pi^0$ mass spectrum close to the $\pi^+\pi^-$ mass threshold [18] revealed no statistically significant effect. From an experimental perspective, the available high statistics of 10 billion J/ψ events at the BESIII experiment is expected to increase the η' decay event sample by nearly an order of magnitude. These additional data coupled with the incorporation of recent dispersive theoretical analyses [22] make investigation of the cusp effect in this channel very promising.

Box anomaly in the $\eta/\eta' \to \gamma\pi^+\pi^-$ decay

In the vector meson dominance (VMD) model, the main contribution to the decay $\eta' \to \gamma\pi^+\pi^-$ comes from $\eta' \to \gamma\rho$. However, a significant deviation in the dipion distribution between the theoretical predictions and data is observed, and this may be attributable to the Wess-Zumino-Witten box anomaly [23,24]. Previous measurements [25–30] sometimes give opposite conclusions on the presence of the box anomaly term.

Recently, a precision BESIII study of $\eta' \to \gamma\pi^+\pi^-$ [31] found, for the first time, that a fit that only included the components of ρ and ω and their

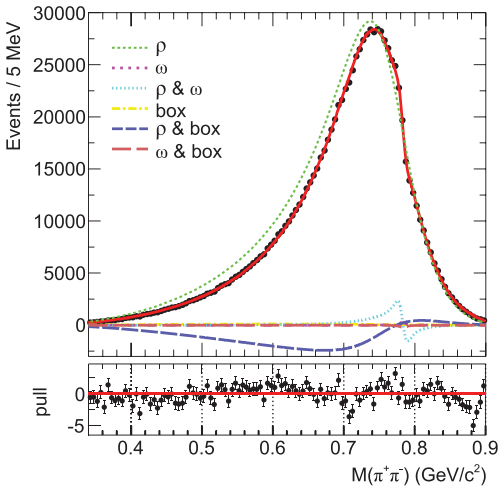

Figure 2. The results of model-dependent fits to $M(\pi^+\pi^-)$ with a ρ^0-ω box anomaly [31].

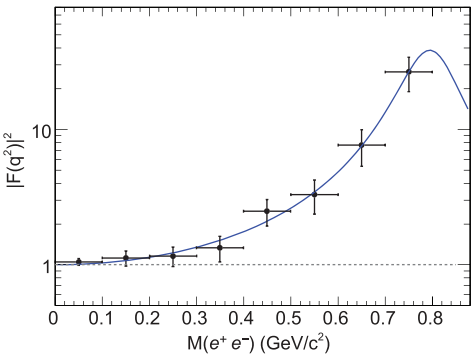

Figure 3. Fit to the single-pole form factor $|F(q^2)|^2$, where q^2 is the square of the e^+e^- invariant mass [43].

interference failed to describe the data; a significant additional contribution, either the box anomaly or a $\rho(1450)$ component, is found to be necessary, as indicated in Fig. 2, to provide a good description of the data. In this case, the influence of the box anomaly phenomenon, i.e. the presence of a well-defined contact term, still requires a definite and unambiguous demonstration.

The large and clean η/η' sample produced in J/ψ decays at the BESIII experiment is expected to promote the study of $\eta/\eta' \to \gamma\pi^+\pi^-$ to an unprecedented precision era. Along with a recently proposed model-independent approach [32], a combined analysis of $\eta/\eta' \to \gamma\pi^+\pi^-$ may present a consistent picture for the dynamics of these two decays.

Test of higher-order ChPT with $\eta/\eta' \to \gamma\gamma\pi^0$ and $\eta' \to \gamma\gamma\eta$ decays

The $\eta/\eta' \to \gamma\gamma\pi^0$ decays are of particular interest for tests of ChPT at the two-loop level. Since light vector mesons play a critical role in these models, the dynamical role of the vector mesons has to be systematically included in the context of either the VMD or Nambu-Jona-Lasinio model to reach a deeper understanding of these decays.

The $\eta \to \gamma\gamma\pi^0$ decay has been measured in many experiments [33]. Of interest is that the branching fraction of $\eta \to \gamma\gamma\pi^0$, $(8.4 \pm 2.7 \pm 1.4) \times 10^{-5}$ [34], as reported by KLOE is approximately a factor of 3 lower than that from the A2 experiment [35]. Experimentally, both the $\eta' \to \gamma\gamma\pi^0$ [36] and $\eta' \to \gamma\gamma\eta$ [37] decays were studied at BESIII. The measured branching fractions are in agreement with a recent theoretical calculation based on the linear sigma model with VMD couplings [38]. It was also found that the di-photon invariant mass dependence of the partial decay widths differs in shape from the predictions of different theoretical models [38]. Thus, a precision measurement of the di-photon mass spectrum would be a more sensitive tool for testing the reliability of theoretical calculations than just measurements of the branching fraction. In this case, an updated measurement for these double radiative decays using the full J/ψ sample at the BESIII experiment will provide an opportunity to have a combined analysis that will distinguish between different theoretical models.

Transition form factors of light mesons

The $\eta/\eta' \to \gamma l^+l^-(l = e, \mu)$ Dalitz decays, where the lepton pair is formed by internal conversion of an intermediate virtual photon and the decay rates are modified by the electromagnetic structure arising at the vertex of the transition, are of special interest. Deviations of measured quantity from their QED predictions are usually described in terms of a timelike transition form factor, which, in addition of being an important probe into the meson's structure [39], has an important role in the evaluation of the hadronic light-by-light contribution to the muon anomalous magnetic moment (see [40] for details).

In contrast to the SND and WASA experimental studies of $\eta \to \gamma l^+l^-$ [41,42], BESIII has a unique advantage in the study of Dalitz decays of both η and η' due to their high production rate in J/ψ radiative and hadronic decays. BESIII reported the first measurement of the e^+e^- invariant-mass distribution for $\eta' \to \gamma e^+e^-$ [43]. It was found that the single-pole parameterization provides a good description of data, as illustrated in Fig. 3. The corresponding slope parameter, $b_{\eta'} = 1.56 \pm 0.19$ GeV^{-2}, is in agreement with the predictions from different theoretical models [44–47] and a 1979 previous measurement of $\eta' \to \gamma\mu^+\mu^-$ [48].

The $\eta/\eta' \to l^+l^-l^+l^-$ decays address decays via two off-shell photons and indicate whether double vector meson dominance is realized in nature. To date, only the decay $\eta \to e^+e^-e^+e^-$ was observed by the KLOE experiment [49]. The corresponding form factor has neither been measured in the timelike nor the spacelike region. In accordance with the theoretical investigation in [50] of the predicted decay rates of $\eta' \to e^+e^-e^+e^-$ of the order of 10^{-4}, hundreds of events are expected to be observed by the BESIII experiment and significant progress could be made to test the latest theoretical prediction of 2.1×10^{-6} [51] based on a data-driven approach.

In addition, using the data sample collected at a center-of-mass energy of 3.773 GeV by the BESIII experiment, studies [52] show that the measurements of the spacelike transition form factors in the decay $e^+e^- \to e^+e^-\pi^0(\eta, \eta')$ via $\gamma\gamma$ interactions in the range of the transfer momentum Q^2 within $[0.3, 10]$ GeV/c^2 are feasible. It is worth mentioning that more data samples at 3.773 GeV and higher are planned for the BESIII experiment. They will be useful for the spacelike transition form factor measurements that are complementary to the data from other experiments and uniquely cover the Q^2 range that is relevant to the hadronic light-by-light correction for the evaluation of the muon anomaly moment.

Cross channel effect in $\omega \to \pi^+\pi^-\pi^0$ decays

The decay $\omega \to \pi^+\pi^-\pi^0$ is usually employed to investigate the ω decay mechanism by comparing a high-statistics Dalitz plot density distribution with theoretical predictions. In the dispersive theoretical framework [53,54], the Dalitz plot distribution and integrated decay width are sensitive to the so-called crossed-channel effect [54]. However, prior to BESIII, no experimental $\omega \to \pi^+\pi^-\pi^0$ data of sufficient precision were available to compare with the predictions.

Because of the high production rate of ω in J/ψ hadronic decays, BESIII was able to perform a precision Dalitz plot analysis with a sample of 2.6×10^5 $\omega \to \pi^+\pi^-\pi^0$ events [55], which is about 6 times larger than the samples in the previous work [56] by WASA-at-COSY. It was found that the Dalitz plot distribution of data significantly differs from the pure P-wave phase space, and additional contributions from resonances and/or final-state interactions are necessary. However, with the present statistics, the experimental results are consistent with the theoretical predictions without the need for incorporating crossed-channel effects, which may indicate that the crossed-channel effect contributions are overestimated in the dispersive calculations. Thus, investigation of this decay dynamics with higher precision by analyzing the full J/ψ data sample is needed to clarify this issue.

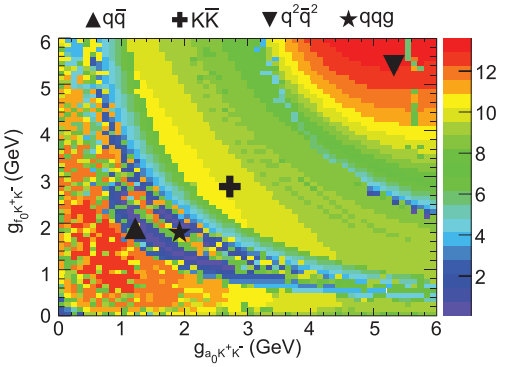

Figure 4. The statistical significance of the signal scanned in the two-dimensional space of $g_{a_0K^+K^-}$ and $g_{f_0K^+K^-}$ [64], where the markers indicate predictions from various illustrative theoretical models. The regions with higher statistical significance indicate larger probability for the emergence of the two coupling constants.

QUARK STRUCTURE OF LIGHT SCALAR MESONS

The nature of the light scalar mesons $f_0(500)$, $K_0^*(800)$, $a_0(980)$ and $f_0(980)$ has been a controversial issue for several decades. Taking into account the observations in heavy meson decays, the existence of these scalar mesons is not controversial, though $K_0^*(800)$ is still qualified as 'needs confirmation' in the Particle Data Group listings [33]. However, the properties of these scalar mesons cannot be understood as simple $q\bar{q}$ mesons, and non-$q\bar{q}$ interpretations of the light scalar nonet are supported by a variety of theoretical approaches [57–60].

Compared to scattering experiments, J/ψ decays provide a clean laboratory to explore these scalar states. At BESIII, a series of amplitude analyses were performed to study scalar mesons decay into pseudoscalar meson pairs $\pi\pi$, $K\bar{K}$ and πK in J/ψ decays [61–63] that established the existence of the $f_0(500)$ and $K^*(800)$.

At BESIII, the $a_0(980) - f_0(980)$ mixing effect, an essential approach for probing their nature, was observed for the first time in studies of $J/\psi \to \phi\eta\pi^0$ and $\chi_{c1} \to \pi^0\pi^+\pi^-$ decays [64]. The anomalous shape of $a_0(980)$ and the very narrow $f_0(980)$ peak produced by the mixing effect was clearly seen in the $\eta\pi^0$ and $\pi^+\pi^-$ mass spectra. The significance of the mixing effect was then investigated as a function of the two coupling constants $g_{a_0K^+K^-}$ and $g_{f_0K^+K^-}$, and compared with different models for the mesons' substructure, as shown in Fig. 4. The results favor the

tetraquark model, although other possibilities still cannot be completely ruled out.

In addition to their production via charmonium decays, other processes can also be used to explore the properties of scalar mesons at BESIII, including light meson and charm meson decays. Examples are the prominent $f_0(500)$ contribution in $\eta' \to 3\pi$ decays [17], and the evident effects of $a_0(980) - f_0(980)$ mixing in an amplitude analysis of $D_s^+ \to \pi^+\pi^0\eta$ [65]. Scalar mesons copiously produced in these decays are further evidence that the BESIII experiment is a unique facility for understanding the controversial nature of these particles.

PRECISION TESTS OF FUNDAMENTAL SYMMETRIES

The η and η' mesons are eigenstates of P, C and CP whose strong and electromagnetic decays are either anomalous or forbidden to lowest order by P, C, CP and angular momentum conservation. Therefore, their decays provide a unique laboratory for testing the fundamental symmetries in flavor-conserving processes, which was extensively reviewed in [66].

A straightforward way to test these symmetries is to search for P- and CP-violating η/η' decays into two pions. In the standard model (SM), the branching fractions for these modes are very tiny [67], but they may be enhanced by CP violation in the extended Higgs sector of the electroweak theory [68]. The high production rate for η' mesons in J/ψ decays enabled BESIII to report the best experimental limit to date, 4.5×10^{-4}, for $\mathcal{B}(\eta' \to \pi^0\pi^0)$ [69] at the 90% confidence level. More recently, BESIII made a search for the rare decay of $\eta' \to 4\pi^0$ and reported the branching upper limit, $\mathcal{B}(\eta' \to 4\pi^0) < 3.8 \times 10^{-5}$ at the 90% confidence level, for the first time [70].

Another interesting signal for possible CP-violating mechanisms would be an asymmetry in the angle between the $\pi^+\pi^-$ and e^+e^- planes in the η/η' rest frame, where the asymmetry would be caused by the interference between the usual CP allowed magnetic transition (driven by the chiral anomaly) and a CP-violating flavor-conserving electric dipole operator [71]. The experimental bound on this asymmetry for $\eta \to \pi^+\pi^-e^+e^-$, $A_\phi = (-0.6 \pm 3.1) \times 10^{-2}$ [72], from the KLOE experiment is compatible with zero. At BESIII, taking into account the measured branching fraction for $\eta' \to \pi^+\pi^-e^+e^-$, $(2.11 \pm 0.12 \pm 0.15) \times 10^{-3}$ [73], about 2×10^4 events could be used to explore the CP violation using the full data sample of 10 billion J/ψ events. More recently, the $\eta' \to \pi^+\pi^-\mu^+\mu^-$ decay was observed for the first time in the BESIII experiment [74].

Experimentally, $\eta/\eta' \to l^+l^-\pi^0$ decays could be used to test charge-conjugation invariance. In the SM, this process can proceed via a two-virtual-photon exchange whereas one-photon-exchange violates C parity. Within the framework of the VMD model, the most recent predictions [75] for the branching fraction are of the order of 10^{-9} for $\eta \to l^+l^-\pi^0$ and 10^{-10} for $\eta' \to l^+l^-\pi^0(\eta)$. Thus, a significant enhancement of the branching fractions exceeding the two-photon model may be indicative of C violation. With the available 10 billion J/ψ events, further improvement for these rare decays will be achieved.

LIGHT QUARK VECTOR MESONS IN e^+e^- ANNIHILATION

Information on light vector meson decays has been obtained from e^+e^- annihilations in, e.g. the KLOE, SND, CMD-2, BaBar and Belle experiments (see [76] for a review), where the vector mesons are observed as the peaks in the total cross section for the specific final states when the e^+e^- center of mass energy is varied by tuning the beam energy or by the initial state radiation (ISR) process. With energy scan data in the 2.0–3.08 GeV range, BESIII can perform direct searches for light vector mesons, especially the poorly studied vector strangeonium states.

The $\phi(2170)$, previously referred to as the Y(2175), has been established in the BaBar [77] and BES [78] experiments, but its measured mass and width remain controversial. There have been a number of different interpretations for $\phi(2170)$, such as a conventional $s\bar{s}$ state, a QCD hybrid, a tetraquark state, a $\Lambda\bar{\Lambda}$ bound state or a $\phi K\bar{K}$ resonance state. The situation will not be clarified without further experimental data. At BESIII, the line shapes of the cross sections for a number of measured channels, including $e^+e^- \to K^+K^-$ [79], $e^+e^- \to K^+K^-\pi^0\pi^0$ [80] and $e^+e^- \to \phi\eta'$ [81], were measured and a clear structure around 2.2 GeV was evident in each of them. The measured widths and masses are consistent with those from $J/\psi \to \phi\pi^+\pi^-\eta$ [82], as summarized in Table. 1. Of interest is the process of $e^+e^- \to K^+K^-K^+K^-$ [83], and its dominant submode $e^+e^- \to \phi K^+K^-$. The line shape for the latter is shown in Fig. 5. In both cases, a very narrow enhancement at $\sqrt{s} = 2.232$ GeV is observed, which is very close to the $e^+e^- \to \Lambda\overline{\Lambda}$ production threshold.

Another interesting possible strangeonium candidate is the $X(1750)$ observed in the photoproduction process [84], which was originally interpreted as the photoproduction mode of the $\phi(1680)$. However, the recent simultaneous observation of the $\phi(1680)$ and $X(1750)$ in $\psi(2S) \to K^+K^-\eta$

Table 1. Summary of the mass and width of $\phi(2170)$ obtained from the BESIII experiment.

Process	Mass (MeV/c^2)	Width (MeV)
$e^+e^- \to K^+K^-$ [79]	$2239.2 \pm 7.1 \pm 11.3$	$139.8 \pm 12.3 \pm 20.6$
$e^+e^- \to K^+K^-\pi^0\pi^0$ [80]	$2126.5 \pm 16.8 \pm 12.4$	$106.9 \pm 32.1 \pm 28.1$
$e^+e^- \to \phi\eta'$ [81]	$2177.5 \pm 4.8 \pm 19.5$	$149.0 \pm 15.6 \pm 8.9$
$J/\psi \to \phi\pi^+\pi^-\eta$ [82]	$2200 \pm 6 \pm 5$	$104 \pm 15 \pm 15$

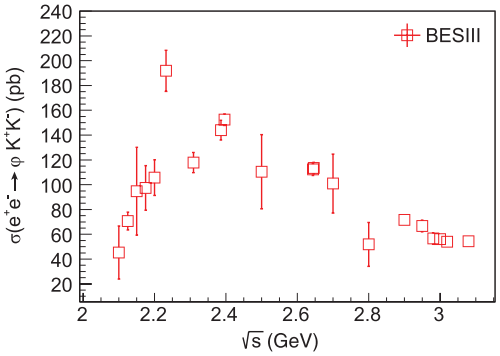

Figure 5. The measured Born cross section of $e^+e^- \to \phi K^+K^-$ [83].

decays [85] indicates that the $X(1750)$ is distinct from the $\phi(1680)$ and possibly a strangeonium state.

The above examples demonstrate that BESIII is a powerful instrument for investigating the light vector mesons. At present, more studies, such as $e^+e^- \to \phi\pi^+\pi^-$, $e^+e^- \to \phi\eta$ and $J/\psi \to K^+K^-\eta$, are ongoing to provide a deeper understanding of the nature of the $\phi(2170)$ and $X(1750)$, and to search for new strangeonium states.

SUMMARY AND PROSPECTS

The light meson decays, as described above, provide a unique opportunity to investigate many aspects of particle physics at low energy, with the advantages of high production rates and excellent performance of the detector. In addition to improved accuracy on many of the measured properties of well-known light meson decays, a series of first observations, such as new decay modes of η', $a_0(980) - f_0(980)$ mixing as well as possibly new strangeonium states, were reported. These significant advances demonstrate that BESIII is playing a leading role in the study of light meson decays.

Despite this impressive progress, many light meson decays are still unobserved and need to be explored. At BESIII, 10^{10} J/ψ events data are now available. This is 8 times larger than the subdata sample used in the present publications and offers great additional opportunities for research in light meson decays, especially for pseudoscalar and vector mesons, with unprecedented precision. Moreover, BESIII expects to take an additional 20 fb^{-1} of data at 3.773 GeV, which will support investigations of the light meson physics with different ISR and two-photon production techniques, such as the production of new vector mesons and measurements of the two-photon width of the light scalar mesons. In addition, different experimental techniques will give access to previously unexplored regions of the electromagnetic transition form factors, allowing a quantitative connection between the timelike and the spacelike regions.

In general, together with the other high-precision experiments, such as KLOE-2, A2, GlueX and BelleII, these very abundant and clean event samples that are accumulated at BESIII will bring the study of light meson decays into a precision era, and will definitely play an important role in the development of chiral effective field theory and lattice QCD, and make significant contributions to the understanding of hadron physics in the non-perturbative regime.

ACKNOWLEDGEMENTS

The author thanks Prof. S.L. Olsen for useful comments and suggestions.

FUNDING

This work was supported in part by the National Natural Science Foundation of China (11675184 and 11735014).

Conflict of interest statement. None declared.

REFERENCES

1. Ablikim M, An ZH and Bai JZ *et al.* Design and construction of the BESIII detector. *Nucl Instrum Meth A* 2010; **614**: 345–99.
2. Ablikim M, Achasov MN and Ai XC *et al.* Determination of the number of J/ψ events with J/ψ inclusive decays. *Chinese Phys C* 2017; **41**: 013001.
3. Ablikim M, Achasov MN and Ahmed S *et al.* Determination of the number of $\psi(3686)$ events at BESIII. *Chinese Phys C* 2018; **42**: 023001.
4. Gasser J and Leutwyler H. $\eta \to 3\pi$ to one loop. *Nucl Phys B* 1985; **250**: 539–60.

5. Bijnens J and Ghorbani K. $\eta \to 3\pi$ at two loops in chiral perturbation theory. *J High Energy Phys* 2007; **0711**: 030.
6. Schneider SP, Kubis B and Ditsche C. Rescattering effects in $\eta \to 3\pi$ decays. *J High Energy Phys* 2011; **1102**: 028.
7. Guo P, Danilkin IV and Schott D *et al.* Three-body final state interaction in $\eta \to 3\pi$. *Phys Rev D* 2015; **92**: 054016.
8. Colangelo G, Lanz S and Leutwyler H *et al.* Dispersive analysis of $\eta \to 3\pi$. *Eur Phys J C* 2018; **78**: 947.
9. Kampf K, Knecht M and Novotny J *et al.* Analytical dispersive construction of $\eta \to 3\pi$ amplitude: first order in isospin breaking. *Phys Rev D* 2011; **84**: 114015.
10. Adlarson P, Augustyniak W and Bardan W *et al.* Measurement of the $\eta \to \pi^+\pi^-\pi^0$ Dalitz plot distribution. *Phys Rev C* 2014; **90**: 045207.
11. Anastasi A, Babusci D and Bencivenni G *et al.* Precision measurement of the $\eta \to \pi^+\pi^-\pi^0$ Dalitz plot distribution with the KLOE detector. *J High Energy Phys* 2016; **1605**: 19.
12. Ablikim M, Achasov MN and Ai XC *et al.* Measurement of the matrix elements for the decays $\eta \to \pi^+\pi^-\pi^0$ and $\eta/\eta' \to \pi^0\pi^0\pi^0$. *Phys Rev D* 2015; **92**: 012014.
13. Colangelo G, Lanz S and Leutwyler H *et al.* $\eta \to 3\pi$: study of the Dalitz plot and extraction of the quark mass ratio Q. *Phys Rev Lett* 2017; **118**: 022001.
14. Guo P, Danilkin IV and Fernandez-Ramirez C *et al.* Three-body final state interaction in $\eta \to 3\pi$ updated. *Phys Lett B* 2016; **771**: 497–502.
15. Gross DJ, Treiman SB and Wilczek F. Light quark masses and isospin violation. *Phys Rev D* 1979; **19**: 2188–214.
16. Borasoy B, Meissner UG and Nissler R. On the extraction of the quark mass ratio $(m_d - m_u)/m_s$ from $\Gamma(\eta' \to \pi^0\pi^+\pi^-)/\Gamma(\eta' \to \eta\pi^+\pi^-)$. *Phys Lett B* 2006; **643**: 41–5.
17. Ablikim M, Achasov MN and Ahmed S *et al.* Amplitude analysis of the decays $\eta' \to \pi^+\pi^-\pi^0$ and $\eta' \to \pi^0\pi^0\pi^0$. *Phys Rev Lett* 2017; **118**: 012001.
18. Ablikim M, Achasov MN and Ahmed S *et al.* Measurement of the matrix elements for the decays $\eta' \to \eta\pi^+\pi^-$ and $\eta' \to \eta\pi^0\pi^0$. *Phys Rev D* 2018; **97**: 012003.
19. Borasoy B and Nissler R. Hadronic η and η' decays. *Eur Phys J A* 2005; **26**: 383–98.
20. Adlarson P, Afzal F and Ahmed Z *et al.* Measurement of the decay $\eta' \to \pi^0\pi^0\eta$ at MAMI. *Phys Rev D* 2018; **98**: 012001.
21. Kubis B and Schneider SP. The cusp effect in $\eta' \to \eta\pi\pi$ decays. *Eur Phys J C* 2009; **62**: 511–23.
22. Isken T, Kubis B and Schneider SP *et al.* Dispersion relations for $\eta' \to \eta\pi\pi$. *Eur Phys J C* 2017; **77**: 489.
23. Wess J and Zumino B. Consequences of anomalous ward identities. *Phys Lett B* 1971; **37**: 95–7.
24. Witten E. Global aspects of current algebra. *Nucl Phys B* 1983; **223**: 422–32.
25. Althoff M, Braunschweig W and Kirschfink FJ *et al.* Measurement of the radiative width of the η'(958) in two photon interactions. *Phys Lett B* 1984; **147**: 487–92.
26. Aihara H, Alston-Garnjost M and Avery RE *et al.* A study of η' formation in photon-photon collisions. *Phys Rev D* 1987; **35**: 2650–4.
27. Albrecht H, Andam AA and Binder U *et al.* Measurement of $\eta' \to \gamma\pi^+\pi^-$ in $\gamma\gamma$ collisions. *Phys Lett B* 1987; **199**: 457–61.
28. Bityukov SI, Borisov GV and Dorofeev VA *et al.* Study of the radiative decay $\eta' \to \pi^+\pi^-\gamma$. *Z Phys C* 1991; **50**: 451–4.
29. Benayoun M, Feindt M and Girone M *et al.* Experimental evidences for the box anomaly in η/η' decays and the electric charge of quarks. *Z Phys C* 1993; **58**: 31–54.
30. Abele A, Adomeit J and Amsler C *et al.* Measurement of the decay distribution of $\eta' \to \pi^+\pi^-\gamma$ and evidence for the box anomaly. *Phys Lett B* 1997; **402**: 195–206.
31. Ablikim M, Achasov MN and Ahmed S *et al.* Precision study of $\eta' \to \gamma\pi^+\pi^-$ decay dynamics. *Phys Rev Lett* 2018; **120**: 242003.
32. Stollenwerk F, Hanhart C and Kupsc A *et al.* Model-independent approach to $\eta \to \pi^+\pi^-\gamma$ and $\eta' \to \pi^+\pi^-\gamma$. *Phys Lett B* 2012; **707**: 184–90.
33. Zyla RA, Barnett RM and Beringer J *et al.* Review of particle physics. *Prog Theor Exp Phys* 2020; **2020**: 083C01.
34. Di Micco B, Ambrosino F and Antonelli A *et al.* The $\eta \to \pi^0\gamma\gamma$, η/η' mixing angle and the η mass measurement at KLOE. *Acta Phys Slovaca* 2006; **56**: 403–9.
35. Nefkens BMK, Prakhov S and Aguar-Bartolome P *et al.* New measurement of the rare decay $\eta \to \pi^0\gamma\gamma$ with the Crystal Ball/TAPS detectors at the Mainz Microtron. *Phys Rev C* 2014; **90**: 025206.
36. Ablikim M, Achasov MN and Ahmed S *et al.* Observation of the doubly radiative decay $\eta' \to \gamma\gamma\pi^0$. *Phys Rev D* 2017; **96**: 012005.
37. Ablikim M, Achasov MN and Adlarson P *et al.* Search for $\eta' \to \gamma\gamma\eta$. *Phys Rev D* 2019; **100**: 052015.
38. Escribano R, González-Solís S and Jora R *et al.* A theoretical analysis of the doubly radiative decays $\eta^{(\prime)} \to \gamma\gamma\pi^0$ and $\eta' \to \gamma\gamma\eta$. *Phys Rev D* 2020; **102**: 034026.
39. Landsberg LG. Electromagnetic decays of light mesons. *Phys Rep* 1985; **128**: 301–76.
40. Aoyama T, Asmussen N and Benayoun M *et al.* The anomalous magnetic moment of the muon in the standard model. *Phys Rept* 2020; **887**: 1–166.
41. Achasov MN, Aulchenko VM and Beloborodov KI *et al.* Study of conversion decays $\phi \to \eta e^+e^-$ and $\eta \to \gamma e^+e^-$ in the experiment with SND detector at the VEPP-2M collider. *Phys Lett B* 2001; **504**: 275–81.
42. Berlowski M, Bargholtz C and Bashkanov M *et al.* Measurement of eta meson decays into lepton-antilepton pairs. *Phys Rev D* 2008; **77**: 032004.
43. Ablikim M, Achasov MN and Ai XC *et al.* Observation of the Dalitz decay $\eta' \to \gamma e^+e^-$. *Phys Rev D* 2015; **92**: 012001.
44. Bramon A and Masso E. Q^2 duality for electromagnetic form-factors of mesons. *Phys Lett B* 1981; **104**: 311–4.
45. Ametller L, Bergstrom L and Bramon A *et al.* The quark triangle: application to pion and η decays. *Nucl Phys B* 1983; **228**: 301–15.
46. Ametller L, Bijnens J and Bramon A *et al.* Transition form-factors in π^0, η and η' couplings to gamma gamma. *Phys Rev D* 1992; **45**: 986.
47. Hanhart C, Kupsc A and Meißner UG *et al.* Dispersive analysis for $\eta \to \gamma\gamma^*$. *Eur Phys J C* 2013; **73**: 2668. Erratum: *Eur Phys J C* 2015; **75**: 242.
48. Dzhelyadin RI, Golovkin SV and Gritzuk MV *et al.* Observation of $\eta' \to \mu^+\mu^-\gamma$ decay. *Phys Lett B* 1979; **88**: 379–80.
49. Ambrosino F, Antonelli A and Antonelli M *et al.* Observation of the rare $\eta \to e^+e^-e^+e^-$ decay with the KLOE experiment. *Phys Lett B* 2011; **702**: 324.
50. Petri T. Anomalous decays of pseudoscalar mesons. arXiv:1010.2378.
51. Escribano R and Gonzàlez-Solís S. A data-driven approach to π^0, η and η' single and double Dalitz decays. *Chinese Phys C* 2018; **42**: 023109.
52. Czerwinsk E, Eidelman S and Hanhart C *et al.* MesonNet workshop on meson transition form factors. arXiv:1207.6556.
53. Niecknig F, Kubis B and Schneider SP. Dispersive analysis of $\omega \to 3\pi$ and $\phi \to 3\pi$. *Eur Phys J C* 2012; **72**: 2014.
54. Danilkin IV, Fernandez-Ramirez C and Guo P *et al.* Dispersive analysis of $\omega/\phi \to 3\pi, \pi\gamma^*$. *Phys Rev D* 2015; **91**: 094029.

55. Ablikim M, Achasov MN and Ahmed S *et al.* Dalitz plot analysis of the decay $\omega \to \pi^+\pi^-\pi^0$. *Phys Rev D* 2018; **98**: 112007.
56. Adlarson P, Augustyniakb W and Bardanc W *et al.* Measurement of the $\omega \to \pi^+\pi^-\pi^0$ Dalitz plot distribution. *Phys Lett B* 2017; **770**; 418–25.
57. Chen HX, Hosaka A and Zhu SL. Light scalar tetraquark mesons in the QCD sum rule. *Phys Rev D* 2007; **76**: 094025.
58. Ruiz de Elvira J, Pelaez JR and Pennington MR *et al.* Chiral perturbation theory, the $1/N_c$ expansion and Regge behaviour determine the structure of the lightest scalar meson. *Phys Rev D* 2011; **84**: 096006.
59. 't Hooft G, Isidori G and Maiani L *et al.* A theory of scalar mesons. *Phys Lett B* 2008; **662**: 424–30.
60. Parganlija D, Giacosa F and Rischke DH. Vacuum properties of mesons in a linear sigma model with vector mesons and global chiral invariance. *Phys Rev D* 2010; **82**: 054024.
61. Ablikim M, Bai JZ and Ban Y *et al.* The σ ploe in $J/\psi \to \omega\pi^+\pi^-$. *Phys Lett B* 2004; **598**: 149–58.
62. Ablikim M, Bai JZ and Ban Y *et al.* Evidence for κ meson production in $J/\psi \to K^*(892)^0 K^+\pi^-$ process. *Phys Lett B* 2006; **633**: 681–90.
63. Ablikim M, Bai JZ and Ban Y *et al.* Resonances in $J/\psi \to \phi\pi^+\pi^-$ and ϕK^+K^-. *Phys Lett B* 2005; **607**: 243–53.
64. Ablikim M, Achasov MN and Adlarson P *et al.* Observation of $a_0(980) - f_0(980)$ mixing. *Phys Rev Lett* 2018; **121**: 022001.
65. Ablikim M, Achasov MN and Adlarson P *et al.* Amplitude analysis of $D_s^+ \to \pi^+\pi^0\eta$ and first observation of the pure *W*-annihilation decays $D_s^+ \to \alpha_0(980)^+\pi^0$ and $D_s^+ \to \alpha_0(980)^0\pi^+$. *Phys Rev Lett* 2019; **123**: 112001.
66. Gan L, Kubis B and Passemar E *et al.* Precision tests of fundamental physics with η and η' mesons. arXiv:2007.00664.
67. Jarlskog C and Shabalin E. On searches for CP, T, CPT and C violation in flavour-changing and flavour-conserving interactions. *Phys Scripta T* 2002; **99**: 23–33.
68. Jarlskog C and Shabalin E. ϵ' and the decay $\eta \to \pi\pi$ in a theory with both explicit and spontaneous CP violation. *Phys Rev D* 1995; **52**: 6327–35.
69. Ablikim M, Achasov MN and Alberto D *et al.* Search for CP and *P* violating pseudoscalar decays into $\pi\pi$. *Phys Rev D* 2011; **84**: 032006.
70. Ablikim M, Achasov MN and Adlarson P *et al.* Search for the rare decay $\eta' \to \pi^0\pi^0\pi^0\pi^0$ at BESIII. *Phys Rev D* 2019; **101**: 032001.
71. Geng CQ, Ng JN and Wu TH. CP violation in the decay $\eta \to \pi^+\pi^-\gamma$. *Mod Phys Lett A* 2002; **17**: 1489–98.
72. Ambrosino F, Antonelli A and Antonelli M *et al.* Measurement of the branching ratio and search for a CP violating asymmetry in the $\eta \to \pi^+\pi^-e^+e^-(\gamma)$ decay at KLOE. *Phys Lett B* 2009; **675**: 283–8.
73. Ablikim M, Achasov MN and Adlarson P *et al.* Measurement of $\eta' \to \pi^+\pi^-e^+e^-$ and $\eta' \to \pi^+\pi^-\mu^+\mu^-$. *Phys Rev D* 2013; **87**: 092011.
74. Ablikim M, Achasov MN and Adlarson P *et al.* Observation of $\eta' \to \pi^+\pi^-\mu^+\mu^-$. *Phys Rev D* 2021; **103**: 072006.
75. Escribano R and Royo E. A theoretical analysis of the semileptonic decays $\eta^{(\prime)} \to \pi^0 l^+ l^-$ and $\eta' \to \eta l^+ l^-$. *Eur Phys J C* 2020; **80**: 1190.
76. Druzhinin VP, Eidelman SI and Serednyakov SI *et al.* Hadron production via e^+e^- collisions with initial state radiation. *Rev Mod Phys* 2011; **83**: 1545–88.
77. Aubert B, Bona M and Boutigny D *et al.* The $e^+e^- \to K^+K^-\pi^+\pi^-$, $K^+K^-\pi^0\pi^0$ and $K^+K^-K^+K^-$ cross-sections measured with initial-state radiation. *Phys Rev D* 2007; **76**: 012008.
78. Ablikim M, Bai JZ and Bai Y *et al.* Observation of $Y(2175)$ in $J/\psi \to \eta\phi f_0(980)$. *Phys Rev Lett* 2008; **100**: 102003.
79. Ablikim M, Achasov MN and Adlarson P *et al.* Measurement of $e^+e^- \to K^+K^-$ cross section at $\sqrt{s} = 2.0$–3.08 GeV. *Phys Rev D* 2019; **99**: 032001.
80. Ablikim M, Achasov MN and Adlarson P *et al.* Observation of a resonant structure in $e^+e^- \to K^+K^-\pi^0\pi^0$. *Phys Rev Lett* 2020; **124**: 112001.
81. Ablikim M, Achasov MN and Adlarson P *et al.* Observation of a structure in $e^+e^- \to \phi\eta'$ at $\sqrt{s}$ from 2.05 to 3.08 GeV. *Phys Rev D* 2020; **102**: 012008.
82. Ablikim M, Achasov MN and Adlarson P *et al.* Study of $J/\psi \to \eta\phi\pi^+\pi^-$ at BESIII. *Phys Rev D* 2015; **91**: 052017.
83. Ablikim M, Achasov MN and Adlarson P *et al.* Cross section measurements of $e^+e^- \to K^+K^-K^+K^-$ and ϕK^+K^- at center-of-mass energies from 2.10 to 3.08 GeV. *Phys Rev D* 2019; **100**: 032009.
84. Link JM, Reyes M and Yager PM *et al.* Observation of a 1750 MeV/c^2 enhancement in the diffractive photoproduction of K^+K^-. *Phys Lett B* 2002; **545**: 50–6.
85. Ablikim M, Achasov MN and Adlarson P *et al.* Partial wave analysis of $\psi(3686) \to K^+K^-\eta$. *Phys Rev D* 2010; **101**: 032008.

REVIEW

National Science Review
8: nwab182, 2021
https://doi.org/10.1093/nsr/nwab182
Advance access publication 5 October 2021

PHYSICS

Special Topic: Physics of the BESIII Experiment

Charmonium and charmoniumlike states at the BESIII experiment

Chang-Zheng Yuan [1,2]

ABSTRACT

Charmonium is a bound state of a charmed quark and a charmed antiquark, and a charmoniumlike state is a resonant structure that contains a charmed quark and antiquark pair but has properties that are incompatible with a conventional charmonium state. While operating at center-of-mass energies from 2 to 5 GeV, the BESIII experiment can access a wide mass range of charmonium and charmoniumlike states, and has contributed significantly in this field. We review BESIII results involving conventional charmonium states, including the first observation of the M1 transition $\psi(2S) \to \gamma\eta_c(2S)$ and the discovery of the $\psi_2(3823)$ state; and report on studies of charmoniumlike states, including the discoveries of the $Z_c(3900)$ and $Z_c(4020)$ tetraquark candidates, the resolution of the fine structure of the $Y(4260)$ state, the discovery of the new production process $e^+e^- \to \gamma X(3872)$ and the uncovering of strong evidence for the commonality among the $X(3872)$, $Y(4260)$ and $Z_c(3900)$ states. The prospects for further research at BESIII and proposed future facilities are also presented.

Keywords: charmonium states, charmoniumlike states, exotic hadrons, e^+e^- annihilation

INTRODUCTION

In the conventional quark model, mesons are comprised of a quark and antiquark pair, while baryons are comprised of three quarks. A bound state of a charmed quark (c) and a charmed antiquark ($\bar{c}$) is named charmonium. The first charmonium state, the J/ψ, was discovered at BNL [1] and at SLAC [2] in 1974, and since then, all the charmonium states below the open-charm threshold and a few vector charmonium states above the open-charm threshold have been established [3]; the measured spectrum of states agrees well with theoretical calculations based on QCD [4–6] and QCD-inspired potential models [7–9].

In addition to the charmonium states, the current QCD-based theoretical framework describes almost all of the other hadrons that have been observed to date quite well, including three-quark baryons and other quark-antiquark mesons [3]. Exotic hadronic states with configurations not limited to two or three quarks have been the subject of numerous theoretical proposals and experimental searches [10,11]. These proposed exotic hadrons include hadron-hadron molecules, diquark-diantiquark tetraquark states, hadro-quarkonia, quark-antiquark-gluon hybrids, multi-gluon glueballs and pentaquark baryons.

Many charmonium and charmoniumlike states were discovered at the BaBar [12] and Belle [13] B factories during the first decade of this century [14]. While some of these are good candidates for conventional charmonium states, there are other states that have properties that do not match those of any of the unassigned $c\bar{c}$ states, which may indicate that exotic states have already been observed [5,15–17]. These candidate exotic meson states are collectively called the XYZ particles, to indicate that their underlying nature is still unclear. Although this is not fully accepted within the high energy physics community, practitioners in the field use $Z_Q(\text{xxxx})$ to denote a quarkoniumlike state with mass roughly xxxx MeV/c^2 that contains a heavy quark pair $Q\bar{Q}$ and with non-zero isospin, $Y(\text{xxxx})$ for a vector quarkoniumlike state (called $\psi(\text{xxxx})$

[1]Institute of High Energy Physics, Chinese Academy of Sciences, Beijing 100049, China and [2]University of Chinese Academy of Sciences, Beijing 100049, China

E-mail: yuancz@ihep.ac.cn

Received 7 April 2021; **Revised** 23 September 2021; **Accepted** 24 September 2021

by PDG [3]) and X(xxxx) for states with other quantum numbers.

Although the BaBar [12] and Belle [13] experiments finished data taking in 2008 and 2010, respectively, the data are still used for various physics analyses. In 2008, two new experiments—BESIII [18], a τ-charm factory experiment at the BEPCII e^+e^- collider, and LHCb [19], a B-factory experiment at the LHC pp collider—started data taking, and have been contributing to the study of charmonium and charmoniumlike states ever since.

The BESIII experiment at the BEPCII double ring e^+e^- collider observed its first collisions in the τ-charm energy region in July 2008. The BESIII detector [18] is a magnetic spectrometer with an effective geometrical acceptance of 93% of 4π and state-of-the-art subdetectors for high precision charged and neutral particle measurements. After a few years of running at center-of-mass (c.m.) energies for its well-defined physics programs [20], i.e. at the J/ψ and $\psi(2S)$ peaks in 2009 and the $\psi(3770)$ peak in 2010 and 2011, the BESIII experiment began to collect data for the study of the XYZ particles, a program that was only mentioned tentatively in the BESIII Yellow Book [20]. The first data sample was collected at the $\psi(4040)$ resonance in May 2011 with an integrated luminosity of about 0.5 fb^{-1}. This sample was used to search for the production of the $X(3872)$ and the excited P-wave charmonium spin-triplet states via $\psi(4040)$ radiative transitions. The size of the sample was limited by the brief, one-month running time following the $\psi(3770)$ data taking in the 2010–11 run.

In summer 2012, the LINAC of the BEPCII was upgraded so that the highest beam energy was increased from 2.1 to 2.3 GeV, which made it possible to collect data at higher c.m. energies (up to 4.6 GeV). A data sample of 525 pb^{-1} was collected at a c.m. energy of 4.26 GeV from 14 December 2012 to 14 January 2013, with which the $Z_c(3900)$ charged charmoniumlike state was discovered [21]. This observation changed the data collection plan for the 2012–13 run and had considerable impact on the subsequent running schedule of the experiment; more data points between 4.13 and 4.60 GeV dedicated to the XYZ related analyses were recorded [22]. The highest beam energy was further increased from 2.3 to 2.5 GeV in summer 2019, making it possible to collect data at even higher c.m. energies (up to 5.0 GeV).

The data samples used for the XYZ study cover the energy range between 4.0 and 5.0 GeV, with a typical integrated luminosity of 500 pb^{-1} at each energy point. These data were also used for charmonium studies together with a 448 million $\psi(2S)$ event sample. Data samples with an integrated luminosity of 826 pb^{-1} at 104 energy points between 3.8 and 4.6 GeV [23] were also used for the XYZ study.

In this article, we review studies of charmonium and charmoniumlike states from the BESIII [18] experiment. We first introduce the study of conventional charmonium states and then the XYZ states. Finally, we discuss prospects for future studies with the BESIII experiment, and also point out possible studies at next generation facilities.

CONVENTIONAL CHARMONIUM STATES

The search for new charmonium states has always been a high priority topic. With the data taken at c.m. energies above 4 GeV, it is possible to search for states predicted by theories that are still unobserved [4–9]. These states include the excited P-wave spin-triplet states $\chi_{cJ}(2P)$ ($J = 0, 1, 2$), the excited P-wave spin-singlet state $h_c(2P)$, the D-wave spin-triplet states $\psi_J(1D)$ ($J = 2, 3$; the $J = 1$ state, the $\psi(3770)$, was observed many years ago [3]) and the D-wave spin-singlet state $\eta_{c2}(1D)$.

The predicted mass of the D-wave charmonium states (excluding the $\psi(3770)$, which is, in fact, a mixture of the $1\,^3D_1$ and $2\,^3S_1$ vector states) is in the 3.81–3.85 GeV/c^2 range predicted by several phenomenological calculations [7–9]. Since the mass of $\psi_2(1D)$ is above the $D\bar{D}$ threshold but below the $D\bar{D}^*$ threshold, and $\psi_2(1D) \to D\bar{D}$ violates parity, the $\psi_2(1D)$ is expected to be narrow and its dominant decay mode is $\psi_2(1D) \to \gamma\chi_{c1}$ [24]. The $\psi_2(1D)$ state, also called the $\psi_2(3823)$, was discovered at BESIII [25] in this final state, and the $\psi_3(1D)$ state was observed by LHCb in its decay into the $D\bar{D}$ final state [26].

The spin-triplet charmonium states are produced copiously in e^+e^- annihilation and in B decays and, thus, they are understood much better than the spin-singlet charmonium states, including the lowest lying S-wave state, the η_c, its radial excited partner, the $\eta_c(2S)$, and the P-wave spin-singlet state, the h_c. Since these three states are all produced in $\psi(2S)$ decays, the world's largest $\psi(2S)$ data sample at BESIII made it possible to study their properties with improved precision. In addition, the unexpected large production cross section for $e^+e^- \to \pi^+\pi^- h_c$ in the BESIII energy region [27] opened a new mechanism for studying the h_c and η_c (from $h_c \to \gamma\eta_c$), and BESIII contributed the world's best measurements of the properties of these states [28]. We report here the observation of the M1 transition $\psi(2S) \to \gamma\eta_c(2S)$ at BESIII [29], a transition that has been sought for since the first-generation BES experiment in the 1980s.

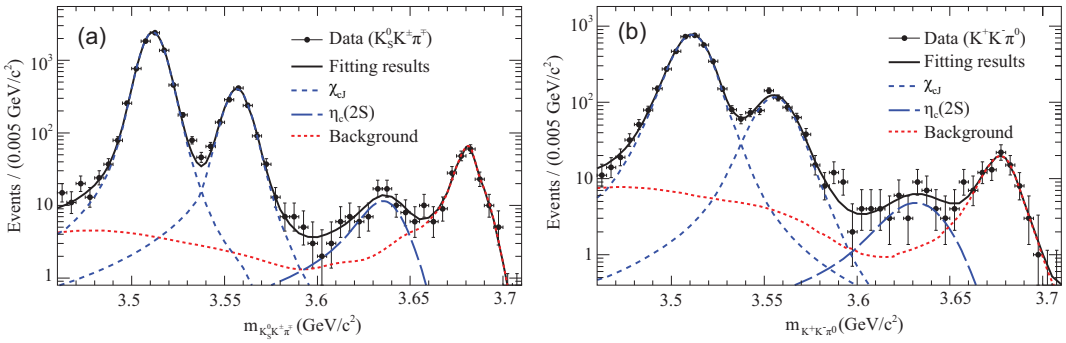

Figure 1. The fit to the invariant-mass spectra for (a) $K^0_S K^\pm\pi^\mp$ and (b) $K^+K^-\pi^0$ [29]. Dots with error bars are data, and the curves are total fits and individual components. The lowest peaks correspond to the $\eta_c(2S)$ signals.

Discovery of the M1 transition $\psi(2S) \to \gamma\eta_c(2S)$

The production of $\eta_c(2S)$ through a radiative transition from $\psi(2S)$ involves a charmed-quark spin-flip and, thus, proceeds via a magnetic dipole (M1) transition. The branching fraction has been calculated by many authors, with predictions in the range $\mathcal{B}(\psi(2S) \to \gamma\eta_c(2S)) = (0.1\text{–}6.2) \times 10^{-4}$ [30–32]. Experimentally, this transition has been searched for by Crystal Ball [33], BES [34,35] and CLEO [36]. No convincing signal was observed in any of these experiments.

With a sample of 106 million $\psi(2S)$ events collected at BESIII, the process $\psi(2S) \to \gamma\eta_c(2S)$ was observed for the first time with $\eta_c(2S) \to K^0_S K^\pm\pi^\mp$ and $K^+K^-\pi^0$ decay modes. The final $K\bar{K}\pi$ mass spectra and the fit results are shown in Fig. 1. For the number of $\eta_c(2S)$ signal events, the fit yields 81 $\pm$ 14 for the $K^0_S K^\pm\pi^\mp$ mode and 46 $\pm$ 11 for the $K^+K^-\pi^0$ mode; the overall statistical significance of the signal is larger than 10σ [29].

The mass of $\eta_c(2S)$ is measured to be $(3637.6 \pm 2.9 \pm 1.6)$ MeV/c^2, the width $(16.9 \pm 6.4 \pm 4.8)$ MeV, in good agreement with the PDG world average values [3], and the product branching fractions $\mathcal{B}(\psi(2S) \to \gamma\eta_c(2S)) \times \mathcal{B}(\eta_c(2S) \to K\bar{K}\pi) = (1.30 \pm 0.20 \pm 0.30) \times 10^{-5}$. Combining the production rate with a BaBar measurement of $\mathcal{B}(\eta_c(2S) \to K\bar{K}\pi)$, the M1 transition rate is determined to be $\mathcal{B}(\psi(2S) \to \gamma\eta_c(2S)) = (6.8 \pm 1.1_{\rm stat} \pm 4.5_{\rm sys}) \times 10^{-4}$. This agrees with theoretical calculations [30–32] and naive estimates based on the $J/\psi \to \gamma\eta_c$ transition [36].

This study benefited from the BESIII detector's high resolution electromagnetic calorimeter, which makes the detection of the radiative photon with 50 MeV energy possible [18]. Given the tiny transition rate and the low photon energy, it is understandable why this transition was not observed in previous studies [33,34,36]. This is the third M1 transition observed in a charmonium system (the other two are $J/\psi \to \gamma\eta_c$ and $\psi(2S) \to \gamma\eta_c$ observed in 1980 [37]); improved measurements of these transitions and discovery of more M1 transitions would improve the understanding of the high-order effects involved in these transitions [9,38,39].

Observation of the $\psi_2(1D)$ state

The processes of $e^+e^- \to \pi^+\pi^-\gamma\chi_{c1,2}$ are studied at the BESIII experiment using 4.1 fb^{-1} of data collected at c.m. energies from 4.23 to 4.60 GeV [25]. The $\chi_{c1,2}$ are reconstructed via their decays into $\gamma J/\psi$, with J/ψ to $\ell^+\ell^-$ ($\ell = e, \mu$). A clear signal is observed as a 19 $\pm$ 5 event peak in the $\gamma\chi_{c1}$ invariant mass distribution that is evident in Fig. 2(a). The statistical significance of the signal is 6.2σ, its mass is determined to be $(3821.7 \pm 1.3 \pm 0.7)$ MeV/c^2 and its properties are in good agreement with the $\psi_2(1D)$ charmonium state. The state is thus called the $\psi_2(3823)$ following the 3.8σ 'evidence' in B decays reported by Belle [40] in 2013. For the $\gamma\chi_{c2}$ mode, no significant $\psi_2(3823)$ signal is observed (Fig. 2(b)), and an upper limit on its production rate is determined. BESIII obtains the ratio $\mathcal{B}[\psi_2(3823) \to \gamma\chi_{c2}]/\mathcal{B}[\psi_2(3823) \to \gamma\chi_{c1}] < 0.42$ at the 90% confidence level (C.L.), which also agrees with expectations for the $\psi_2(1D)$ state [24].

With the observation of three D-wave spin-triplet states ($\psi(3770)$, $\psi_2(3823)$ and $\psi_3(3842)$), their center of gravity, 3822 MeV/c^2, is a good estimation of the mass of the D-wave spin-singlet state, $\eta_{c2}(1D)$. Since it cannot decay into open-charm final states, $\eta_{c2}(1D)$ is expected to be very narrow, and the identification of it should be clear, if it is produced with large enough rate, in $e^+e^- \to \gamma\eta_{c2}(1D)$, $e^+e^- \to \omega\eta_{c2}(1D)$ or $e^+e^- \to \pi^+\pi^- h_c(2P) \to \pi^+\pi^-\gamma\eta_{c2}(1D)$.

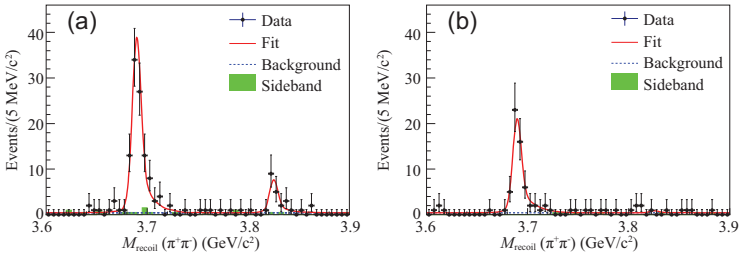

Figure 2. Simultaneous fit to the $M_{\rm recoil}(\pi^+\pi^-)$ distribution of (a) $\gamma\chi_{c1}$ events and (b) $\gamma\chi_{c2}$ events [25]. The small peak in (a) is the $\psi_2(3823)$ signal. Dots with error bars are data, red solid curves are total fits, dashed blue curves are background fits and the green shaded histograms are J/ψ mass sideband events.

EXOTIC CHARMONIUMLIKE STATES

A revival of the study of charmonium spectroscopy occurred in the early twenty-first century when the BaBar and Belle B factories started accumulating large data samples at the $\Upsilon(4S)$ peak. The high luminosity at these B factories enabled studies of charmonium states that are produced in a variety of ways, including B decays, initial-state-radiation (ISR) processes, double-charmonium production, two-photon processes, etc. While the discovery of the conventional charmonium states such as $\eta_c(2S)$ and $\chi_{c2}(2P)$ were more-or-less routine, the observations of the $X(3872)$ by Belle in 2003 [41] and the $Y(4260)$ by BaBar in 2005 [42], the first of the XYZ mesons, came as big surprises; although these new states decay to final states that contain both a c and a $\bar{c}$ quark, they have properties that do not match those of any $c\bar{c}$ meson [5,15–17].

All studies of XYZ states at the B factories have low statistics and limited precision. In contrast, BESIII can tune the c.m. energy to match the peaks of the Y states, where event rates are high enough to facilitate precise measurements of their resonance parameters and search for new states among their decay products.

New insights into the *Y* states

The Y states, such as $Y(4260)$ [42], $Y(4360)$ [43,44] and $Y(4660)$ [44], are produced directly or via the ISR process in e^+e^- annihilation and, thus, are vectors with quantum numbers $J^{PC}=1^{--}$. These states have strong couplings to hidden-charm final states in contrast to the established vector charmonium states in the same mass region, such as $\psi(4040)$, $\psi(4160)$ and $\psi(4415)$, which dominantly couple to open-charm meson pairs [45,46].

In potential models, five vector charmonium states are expected to be in the mass region between 4.0 and 4.7 GeV/c^2, namely $\psi(3S)$, $\psi(2D)$, $\psi(4S)$, $\psi(3D)$ and $\psi(5S)$, with the first three identified with the well-established $\psi(4040)$, $\psi(4160)$ and $\psi(4415)$ charmonium mesons; the masses of the as yet undiscovered $\psi(3D)$ and $\psi(5S)$ are expected to be higher than 4.4 GeV/c^2. However, six vector states in this mass region have been identified, as listed above. These make the $Y(4260)$, $Y(4360)$ and perhaps the $Y(4660)$ states good candidates for new types of exotic particles, stimulating many theoretical interpretations, including tetraquark states, molecular states, hybrid states or hadro-charmonia [5,15–17].

The $Y(4260)$ was first observed at the B factories as a distinct peak in the $\pi^+\pi^- J/\psi$ invariant mass distribution for ISR-produced $e^+e^- \to \gamma_{\rm ISR}\pi^+\pi^- J/\psi$ events [42,47]. Improved measurements from both BaBar [48] and Belle [49] with their full data samples confirmed the existence of both the $Y(4260)$ resonance and a non-$Y(4260)$-resonance component in $e^+e^- \to \pi^+\pi^- J/\psi$ around 4.0 GeV, but the line shape was parameterized with different models. The parameters of the $Y(4260)$ determined by fit to the combined data from the two B-factory experiments and the CLEO measurements [50] are $M_{Y(4260)} = (4251 \pm 9)$ MeV/c^2 and $\Gamma_{Y(4260)} = (120 \pm 12)$ MeV [51]. High precision BESIII measurements of the direct cross section for the $Y(4260)$ production in different final states supply new insight into its nature. These measurements include: $e^+e^- \to \pi^+\pi^- J/\psi$ [52], $e^+e^- \to \pi^+\pi^- h_c$ [27], $e^+e^- \to \omega\chi_{cJ}$ [53,54], $e^+e^- \to D^0D^{*-}\pi^+ + {\rm c.c.}$ [55], etc. [56].

Figure 3 shows the measured cross sections for each of these final states. The $Y(4260)$ structure is evident, but its line shape is in fact not well described by a single Breit-Wigner (BW) resonance function. Instead, its line shape is peaked at around 4.22 GeV, which is substantially lower than the average value from previous measurements [51], and a distinct shoulder is observed on its high-mass side that is especially pronounced in the $\pi^+\pi^- J/\psi$ mode. In order to describe this line shape, two resonant structures in the $Y(4260)$ peak region are needed. The lower one has a mass of $(4222.0 \pm 3.1 \pm 1.4)$ MeV/c^2 and a width of $(44.1 \pm 4.3 \pm 2.0)$ MeV, while the higher one has a mass of $(4320.0 \pm 10.4 \pm 7.0)$ MeV/c^2 and a width of $(101.4^{+25.3}_{-19.7} \pm 10.2)$ MeV. The mass of the first resonance is $\sim$30 MeV/c^2 lower than the world average value at that time [51] for $Y(4260)$ and its width is about a factor of 3 narrower. The second resonance is observed in the $e^+e^- \to \pi^+\pi^- J/\psi$ process for the first time. It is still not clear whether it is a new state or just a new decay mode of the $Y(4360)$ observed in $e^+e^- \to \pi^+\pi^-\psi(2S)$ [43,44]. The resonance parameters for the lower mass structure,

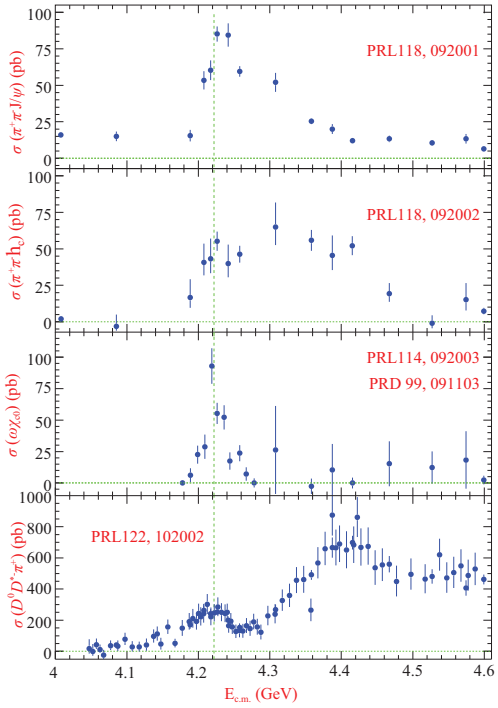

Figure 3. From top to bottom are the measured cross sections of $e^+e^- \to \pi^+\pi^- J/\psi$ [52], $e^+e^- \to \pi^+\pi^- h_c$ [27], $e^+e^- \to \omega\chi_{c0}$ [53,54] and $e^+e^- \to D^0D^{*-}\pi^+ + \text{c.c.}$ [55] as a function of the center-of-mass energy ($E_{c.m.}$). Dots with error bars are the data and the dotted vertical line is the peak of the $Y(4220)$.

the $Y(4220)$, are also measured in other decay channels and listed in Table 1.

Since the resonant structure around 4.2 GeV/c^2 is present in all of the above channels with similar resonance parameters, Gao *et al.* [57] applied a combined fit to the measured cross sections to determine the resonance parameters of the low-mass $Y(4220)$ peak with a resultant mass of $(4219.6 \pm 3.3 \pm 5.1)$ MeV/c^2 and width of $(56.0 \pm 3.6 \pm 6.9)$ MeV. These values are very different from those obtained in previous experiments [51]. The fit also gives the product of the leptonic decay width and the decay branching fraction to the considered final state. After accounting for the unmeasured isospin partners of the measured channels, a lower limit on the leptonic partial width of the $Y(4220)$ is determined to be $\Gamma_{e^+e^-} > (29.1 \pm 7.4)$ eV, where the error is the combined fit error and those from different fit scenarios. Cao *et al.* [58] analyzed BESIII, Belle and BaBar data on charmonium as well as open-charm final states, and a leptonic width of $O(0.1–1)$ keV was obtained. This partial width is much larger than LQCD predictions for a hybrid vector charmonium state [59].

In spite of the limited experimental information that has been available between the time of its discovery in 2005 and the recent BESIII measurements, the $Y(4260)$ has attracted considerable attention. The BESIII measurements of its production, decay and line shape in a variety of final states enable more sophisticated theoretical investigations, and some analyses have been performed, such as those in [58] and those quoted in [5,15–17]. The presence of the nearby $D_s^{*+}D_s^{*-}$, $D\bar{D}_1(2420)$ and $\omega\chi_{cJ}$ production thresholds, and its mass overlap with the $\psi(4160)$ and $\psi(4415)$ conventional charmonium states complicate its interpretation. Joint experimental and theoretical efforts will likely be required to gain a full understanding of the nature of this state; these include precision measurements of the cross sections of all the final states and applying a more sophisticated theoretical description of the coupled-channel effect and line shapes, and so on.

Discovery of the iso-triplet charmoniumlike $Z_c(3900)$ and $Z_c(4020)$ states

Searching for charged charmoniumlike states is one of the most promising ways of establishing the existence of the exotic hadrons, since such a state must contain at least four quarks and, thus, could not be a conventional meson. These searches have concentrated on decay final states that contain one charged pion and a charmonium state, such as J/ψ, $\psi(2S)$ and h_c, since they are narrow and their experimental identification is relatively unambiguous.

The first reported charged charmoniumlike state, $Z_c(4430)^-$, was found in the $\pi^-\psi(2S)$ invariant mass distribution in $B \to K\pi^-\psi(2S)$ decays by the Belle experiment in 2008 [60,61]. It was

Table 1. Resonance parameters of the $Y(4220)$ state from different modes measured at BESIII. The cross sections measured at a c.m. energy of 4.226 GeV are also listed.

Mode	Mass (MeV/c^2)	Width (MeV)	σ at $\sqrt{s} = 4.226$ GeV (pb)
$e^+e^- \to \pi^+\pi^- J/\psi$	$4222.0 \pm 3.1 \pm 1.4$	$44.1 \pm 4.3 \pm 2.0$	$85.1 \pm 1.5 \pm 4.9$
$e^+e^- \to \pi^+\pi^- h_c$	$4218.4^{+5.5}_{-4.5} \pm 0.9$	$66.0^{+12.3}_{-8.3} \pm 0.4$	$55.2 \pm 2.6 \pm 8.9$
$e^+e^- \to \omega\chi_{c0}$	$4218.5 \pm 1.6 \pm 4.0$	$28.2 \pm 3.9 \pm 1.6$	$55.4 \pm 6.0 \pm 5.9$
$e^+e^- \to \pi^+D^0D^{*-} + \text{c.c.}$	$4228.6 \pm 4.1 \pm 6.3$	$77.0 \pm 6.8 \pm 6.3$	$252 \pm 5 \pm 15$

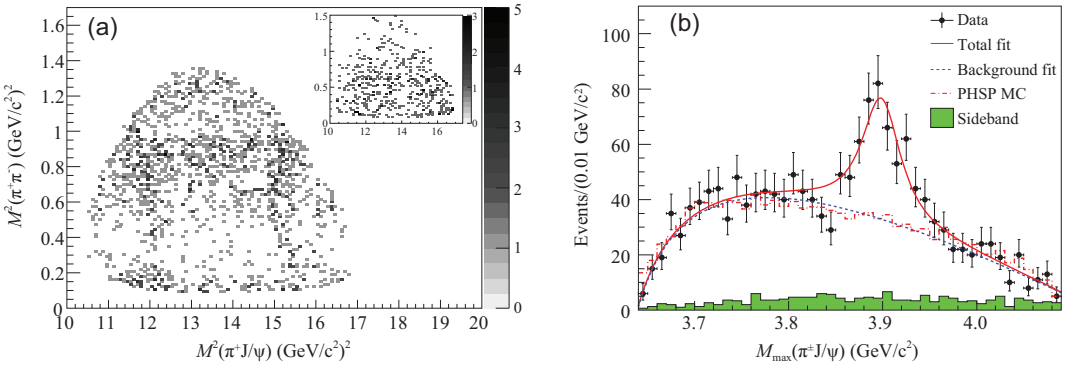

Figure 4. Dalitz plot for selected $e^+e^- \to \pi^+\pi^- J/\psi$ events in (a) the J/ψ signal region (the inset shows background events from the J/ψ mass sidebands) and (b) the $Z_c(3900)$ signal in $M_{\rm max}(\pi J/\psi)$ [21]. Points with error bars are data, the curves are best fits, the dashed histograms are the phase space distributions and the shaded histograms are the non-$\pi^+\pi^- J/\psi$ background estimated from the normalized J/ψ sidebands.

confirmed by the LHCb experiment seven years later [62]. The $Z_c(3900)^-$ state was observed in the $\pi^- J/\psi$ invariant mass distribution in the study of $e^+e^- \to \pi^+\pi^- J/\psi$ at BESIII [21] and Belle [49] experiments, and the $Z_c(4020)^-$ state was observed in the $\pi^- h_c$ system in $e^+e^- \to \pi^+\pi^- h_c$ [63] only at BESIII.

Observation of the $Z_c(3900)$ state

The BESIII experiment studied the $e^+e^- \to \pi^+\pi^- J/\psi$ process using a 525 pb^{-1} data sample at a c.m. energy of 4.26 GeV [21]. About 1500 signal events were observed and the cross section was measured to be $(62.9 \pm 1.9 \pm 3.7)$ pb, which agrees with the previous existing results from the Belle [47] and BaBar [48] experiments. The intermediate states in this three-body system were studied by examining the Dalitz plot of the selected candidate events, as shown in Fig. 4.

In addition to the known $f_0(500)$ and $f_0(980)$ structures in the $\pi^+\pi^-$ system, a structure at around 3.9 GeV/c^2 was observed in the $\pi^\pm J/\psi$ invariant mass distribution with a statistical significance larger than 8σ, which is referred to as the $Z_c(3900)$. A fit to the $\pi^\pm J/\psi$ invariant mass spectrum (see Fig. 4) determined its mass to be $(3899.0 \pm 3.6 \pm 4.9)$ MeV/c^2 and its width to be $(46 \pm 10 \pm 20)$ MeV.

A measurement performed at the Belle experiment that was released subsequent to the BESIII paper reported the observation of the $Z_c(3900)$ state (referred to as $Z(3900)^+$ in the Belle paper) produced via the ISR process with a mass of $(3894.5 \pm 6.6 \pm 4.5)$ MeV/c^2 and a width of $(63 \pm 24 \pm 26)$ MeV with a statistical significance larger than 5.2σ [49]. These observations were later confirmed by an analysis of CLEO-c data at a c.m. energy of 4.17 GeV [64], with a mass and width that agree with the BESIII and Belle measurements.

BESIII studied the spin-parity of the $Z_c(3900)$ with a partial wave analysis (PWA) of about 6000 $e^+e^- \to \pi^+\pi^- J/\psi$ events at $\sqrt{s} = 4.23$ and 4.26 GeV [65]. The fit indicated that the spin-parity $J^P = 1^+$ assignment for the $Z_c(3900)$ is favored over other quantum numbers (0^-, 1^-, 2^- and 2^+) by more than 7σ.

The $Z_c(3900)$ mass determined from its $\pi J/\psi$ invariant mass distribution is slightly above the $D\bar{D}^*$ mass threshold. The open-charm decay $Z_c(3900)^\pm \to (D\bar{D}^*)^\pm$ was observed with much larger rate than that to $\pi J/\psi$ [66,67], and the pole mass and width were determined with high precision to be $(3882.2 \pm 1.1 \pm 1.5)$ MeV/c^2 and $(26.5 \pm 1.7 \pm 2.1)$ MeV, respectively.

In both the QCD tetraquark and the molecular pictures, the $Z_c(3900)^\pm$ states are the $I_3 = \pm 1$ members of an isospin triplet. BESIII confirmed this by observing their neutral, isospin $I_3 = 0$ partners: the $Z_c(3900)^0$, in both the $\pi^0 J/\psi$ [68] and $(D\bar{D}^*)^0$ [69] decay modes. These observations establish $Z_c(3900)$ as an isovector state with even G parity. From a PWA to the $e^+e^- \to \pi^0\pi^0 J/\psi$ data in the vicinity of the $Y(4260)$ resonance, it is found that the cross-section line shape of $e^+e^- \to \pi^0 Z_c(3900)^0 \to \pi^0\pi^0 J/\psi$ is in agreement with that of $Y(4220)$ (see Fig. 5) [70].

BESIII also searched for the $Z_c(3900)$ isospin violating decay mode $\eta J/\psi$ [71] as well as to the light hadron final states $\omega\pi$ [72], $K\bar{K}\pi$ and $K\bar{K}\eta$ [73]. These modes were not observed and the upper limits of the decay rates are one order of magnitude or even smaller than that for $Z_c(3900) \to \pi J/\psi$, as naively expected.

Observation of the $Z_c(4020)$ state

The process $e^+e^- \to \pi^+\pi^- h_c$ was observed at c.m. energies of 3.90–4.42 GeV [63] with cross section that is similar to that for $e^+e^- \to \pi^+\pi^- J/\psi$ [52].

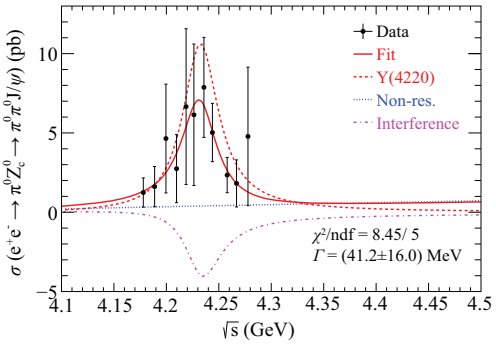

Figure 5. The cross sections of $e^+e^- \to \pi^0 Z_c(3900)^0 \to \pi^0\pi^0 J/\psi$ [70]. Points with error bars are data, the red solid curve is the total fit result, the red dashed (blue dotted) curve is the resonant (non-resonant) component and the magenta dash–dot line represents the interference of the two components.

Intermediate states of this three-body system were studied by examining the Dalitz plot of the selected $\pi^+\pi^- h_c$ candidate events, similar to what was done for the $e^+e^- \to \pi^+\pi^- J/\psi$ process [21]. Although there are no clear structures in the $\pi^+\pi^-$ system, there is distinct evidence for an exotic charmonium-like structure in the $\pi^\pm h_c$ system, as clearly evident in the Dalitz plot shown in Fig. 6. This figure also shows projections of the $M(\pi^\pm h_c)$ (two entries per event) distribution for the signal events as well as the background events estimated from normalized h_c mass sidebands. There is a significant peak at around 4.02 GeV/c^2 (the $Z_c(4020)$), and there are also some events at around 3.9 GeV/c^2 that could be due to the $Z_c(3900)$. The mass and width of the $Z_c(4020)$ were measured to be $(4022.9 \pm 0.8 \pm 2.7)$ MeV/c^2 and $(7.9 \pm 2.7 \pm 2.6)$ MeV, respectively. The statistical significance of the $Z_c(4020)$ signal is greater than 8.9σ.

In an analysis of the $e^+e^- \to \pi^0\pi^0 h_c$ process, the $Z_c(4020)^0$, the neutral isospin partner of the $Z_c(4020)^\pm$ was observed in the $\pi^0 h_c$ system. This indicates that the $Z_c(4020)$ is an isovector state [74]. The open-charm decay of the $Z_c(4020)$ was observed in $e^+e^- \to (D^*\bar{D}^*)\pi$, with a rate that is much larger than that for its decay into πh_c [75,76]. Partial wave analysis of $e^+e^- \to \pi^+\pi^-\psi(2S)$ is needed to confirm or deny the decay $Z_c(4020) \to \pi\psi(2S)$ [77].

Nature of the Z_c states

Although many measurements have been performed on the $Z_c(3900)$ and $Z_c(4020)$ states, the experimental information is still not very precise. From the experience of the $Z_c(4430)$ state, we know that the resonance parameters determined from a simple one-dimensional fit to the invariant mass distribution [60] may differ from those based on a full amplitude analysis with the interference effects between different amplitudes considered properly [61]. The same thing may happen with the $Z_c(3900)$ and $Z_c(4020)$ states. Amplitude analyses that are applied to the relevant final states that extract the resonant parameters as well as the couplings to different modes are essential to obtain more refined information for understanding the nature of these states. In addition, a PWA can also provide measurements of Argand plots of the Z_c amplitudes, which can be used to discriminate between different models for the Z_c states.

The production of Z_c states at a variety of c.m. energies can reveal whether these states are from resonance decays or continuum production. So far, only the $Z_c(3900)$ state has been observed both in e^+e^- annihilation [21] and in B-hadron decays [78,79]. Searches for these states in different production modes is of great importance.

These states seem to indicate that a new class of hadrons has been observed. Since there are at least four quarks within each of these Z_c states, they have

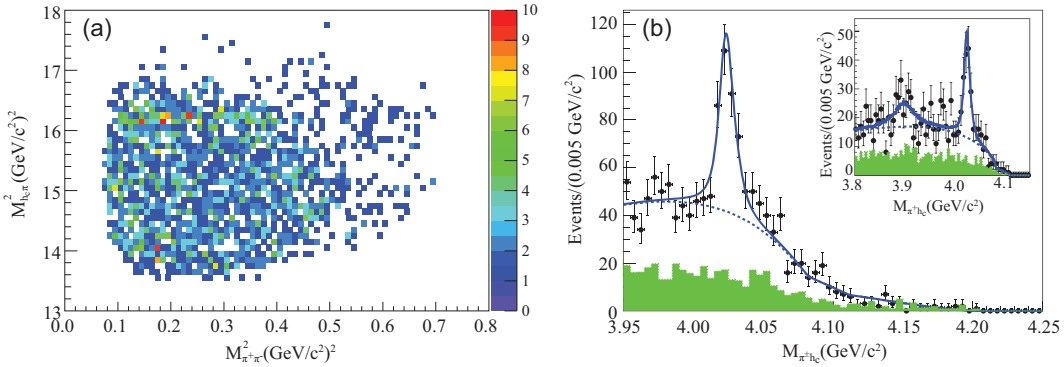

Figure 6. Dalitz plot ($M^2_{\pi^+h_c}$ versus $M^2_{\pi^+\pi^-}$) for (a) selected $e^+e^- \to \pi^+\pi^- h_c$ events and (b) the $Z_c(4020)$ signal observed in the πh_c invariant mass spectrum [63]. Points with error bars are data, the solid curves are best fits and the shaded histograms are the non-$\pi^+\pi^- h_c$ background estimated from the normalized h_c sidebands.

been alternatively interpreted as compact tetraquark states, molecular states of two charmed mesons ($D\bar{D}^* + D^*\bar{D}$, $D^*\bar{D}^*$, etc.), hadro-quarkonium states or other multiquark configurations; in some phenomenological studies they have been attributed to purely kinematical effects [5,15–17]. Since many of these models require assumptions that are hard to prove, it is essential that non-perturbative studies such as lattice QCD (LQCD) provide a way to understand their underlying nature; if the Z_c structures are not purely kinematical effects, they should appear on the lattice since they are strong interaction phenomena.

The currently available LQCD calculations that are relevant to the $Z_c(3900)$ state have a number of uncertainties, as has been recently reviewed in [80]. These include the lattice spacing, the volume, the physical π mass and the channels that are considered in the calculation.

An early lattice study performed by Prelovsek *et al.* [81] investigated the energy levels of two-meson systems, including $\pi J/\psi$, $\pi\psi(2S)$, $\rho\eta_c$, $D\bar{D}^*$, $D^*\bar{D}^*$, etc., as well as tetraquark operators. However, no convincing signals for extra new energy levels apart from the almost free scattering states of the two mesons were identified. Taking $D\bar{D}^*$ as the main relevant channel, the CLQCD collaboration performed a calculation that was based on the single-channel Lüscher finite-size formalism and found a slightly repulsive interaction between the two charmed mesons [82,83]. The results therefore do not support the possibility of a shallow bound state for the two mesons for the pion mass values of 300, 420 and 485 MeV/c^2. A preliminary study using staggered quarks found no $J^{PC} = 1^{+-}$ state distinct from the noninteracting scattering states either, but the authors also pointed out that future calculations with a larger interpolating operator basis may be able to resolve this state [84].

The HALQCD collaboration studied the problem using an approach where an effective potential is extracted from the lattice data and then used to solve the Schrödinger-like equations [85,86]. A fully coupled-channel potential for $\pi J/\psi$, $\rho\eta_c$ and $D\bar{D}^*$ interactions is obtained, and a strong off-diagonal transition between $\pi J/\psi$ and $D\bar{D}^*$ indicates that the $Z_c(3900)$ state can be explained as a threshold cusp within their current configuration ($m_\pi = 400-700$ MeV/c^2). In order to establish a definite conclusion on the structure of the $Z_c(3900)$ state in the real world, full QCD simulations near the physical point are being carried out [85,86].

Recently, in order to clarify the mismatch between these two approaches, CLQCD performed a two-channel lattice study using the two-channel Ross-Shaw effective range expansion [87]. They considered the $\pi J/\psi$ and $D\bar{D}^*$ channels that are most strongly coupled to $Z_c(3900)$ and found that the parameters of the Ross-Shaw matrix do not seem to support the HALQCD scenario. The parameters turn out to be large and the Ross-Shaw M matrix is far from singular, which is required for a resonance close to the threshold. However, since only two channels are studied, it is still not a direct comparison with the HALQCD approach, in which three channels were studied. In [80], the same three channels that the HALQCD collaboration analyzed were considered, namely $\pi J/\psi$, $\rho\eta_c$ and $D\bar{D}^*$. However, the final results will not come very soon.

Whatever the nature of the Z_c states turns out to be, they will teach us a lot about the hadronic structures. Unless all these structures are purely kinematical effects (in which case it would have to be an as yet unknown kinematic effect), they will suggest a new category of hadrons beyond the conventional meson and baryon picture. The observation of similar states in the bottom sector [88] and recent discoveries of structures with two pairs of charm-anticharm quarks [89] and with a minimal four-quark configuration $cs\bar{u}\bar{d}$ [90] confirm this expectation. Additional searches for other conceivable states should be performed and the theoretical consequences of these new types of hadrons should be investigated.

Comprehensive study of $X(3872)$ in the e^+e^- collision

The $X(3872)$ was first observed in $B^\pm \to K^\pm\pi^+\pi^- J/\psi$ decays in 2003 by Belle [41]. It was confirmed subsequently by several other experiments [91–94]. Prior to 2014, the $X(3872)$ was only observed in B meson decays and hadron collisions. Since the quantum numbers of $X(3872)$ are $J^{PC} = 1^{++}$, it can be produced via radiative decays of excited vector charmonium or charmoniumlike states such as the ψ and the Y.

The $X(3872)$ was observed at BESIII in the process $e^+e^- \to \gamma X(3872) \to \gamma\pi^+\pi^- J/\psi$, $J/\psi \to \ell^+\ell^-$ [95] (see Fig. 7(a)) and this first measurement was subsequently improved with more data [96]. The c.m. energy dependence of the product of the cross section $\sigma[e^+e^- \to \gamma X(3872)]$ and the branching fraction $\mathcal{B}[X(3872) \to \pi^+\pi^- J/\psi]$ is shown in Fig. 7(b), where the red curve shows the results of a fit to a BW resonance line shape with a mass of $(4200.6^{+7.9}_{-13.3} \pm 3.0)$ MeV/c^2 and a width of $(115^{+38}_{-26} \pm 12)$ MeV. These resonance parameters are consistent with those of the $\psi(4160)$

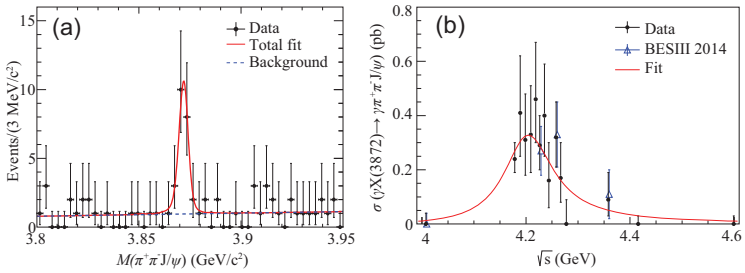

Figure 7. (a) Fit to the $M(\pi^+\pi^- J/\psi)$ distribution [95] and (b) fit to $\sigma^B[e^+e^- \to \gamma X(3872)] \times \mathcal{B}[X(3872) \to \pi^+\pi^- J/\psi]$ [96]. Dots/triangles with error bars are data and the curves are best fits.

charmonium state [3] or the $Y(4220)$ (see the section entitled 'New insights into the Y states') within errors.

Using all the data samples available at c.m. energies between 4.0 and 4.6 GeV, BESIII is able to observe for the first time significant signals of $X(3872) \to \omega J/\psi$ [96] and $X(3872) \to \pi^0\chi_{c1}$ [97], and search for other possible decays.

BESIII confirmed earlier observations of a large $X(3872) \to D^{*0}\bar{D}^0 + \text{c.c.}$ branching fraction and found evidence for $X(3872) \to \gamma J/\psi$ with a significance of 3.5σ [98]. No evidence was found for the decays $X(3872) \to \gamma\psi(2S)$. The upper limit on the ratio $\mathcal{B}(X(3872) \to \gamma\psi(2S))/\mathcal{B}(X(3872) \to \gamma J/\psi) < 0.59$ was obtained at the 90% C.L. [98], which is inconsistent with LHCb [99] and BaBar measurements [100] but consistent with a Belle upper limit [101]. No significant $X(3872) \to \pi^0\chi_{c0,2}$ signals were observed.

The hadronic transitions of the $X(3872)$ to low-mass charmonum states via a single pion or a rho meson violate isospin, and the large decay rates of $X(3872) \to \pi^0\chi_{c1}$ and $X(3872)$ to $\rho J/\psi \to \pi^+\pi^- J/\psi$ relative to the isospin-conserved mode $X(3872) \to \omega J/\psi$ indicate that $X(3872)$ is very unlikely to be a pure charmonium state, such as the $\chi_{c1}(2P)$. The order of magnitude larger decay rate to $D^{*0}\bar{D}^0 + \text{c.c.}$ than to the charmonium final state favors the $D^*\bar{D} + \text{c.c.}$ molecule interpretation of the $X(3872)$, as does the relatively smaller production rate of $X(3872) \to \gamma\psi(2S)$ compared with $X(3872) \to \gamma J/\psi$, or at least that there is a large fraction of molecular component in its wave function in addition to a charmonium component.

BESIII measured the ratios of branching fractions for $X(3872) \to \gamma J/\psi$, $\gamma\psi(2S)$, $\omega J/\psi$, $\pi^0\chi_{c1}$, $D^{*0}\bar{D}^0 + \text{c.c.}$, $\pi^0 D\bar{D}$ and $\gamma D\bar{D}$ to that for $X(3872) \to \pi^+\pi^- J/\psi$. By combining these with the measurements of the $X(3872)$ properties from the B factories, Li and Yuan [102] obtained the absolute branching fractions of the $X(3872)$ decays into six modes by globally fitting the measurements provided by the Belle, BaBar, BESIII and LHCb experiments (see Table 2). The branching fraction for $X(3872) \to \pi^+\pi^- J/\psi$ is determined to be $(4.1^{+1.9}_{-1.1})\%$, which is in good agreement with earlier estimates in [103] and [104]. By combining the branching fractions of all of the observed modes, the fraction of the unknown decays of the $X(3872)$ is found to be $(31.9^{+18.1}_{-31.5})\%$, which is an important challenge for future experimental studies of $X(3872)$ decays.

Table 2. The fitting results of the absolute branching fractions of the $X(3872)$ decays [102]. The branching fraction of the $X(3872)$ decays into unknown modes is calculated from the fit results.

Parameter index	Decay mode	Branching fraction (%)
1	$X(3872) \to \pi^+\pi^- J/\psi$	$4.1^{+1.9}_{-1.1}$
2	$X(3872) \to D^{*0}\bar{D}^0 + \text{c.c.}$	$52.4^{+25.3}_{-14.3}$
3	$X(3872) \to \gamma J/\psi$	$1.1^{+0.6}_{-0.3}$
4	$X(3872) \to \gamma\psi(2S)$	$2.4^{+1.3}_{-0.8}$
5	$X(3872) \to \pi^0\chi_{c1}$	$3.6^{+2.2}_{-1.6}$
6	$X(3872) \to \omega J/\psi$	$4.4^{+2.3}_{-1.3}$
	$X(3872) \to$ unknown	$31.9^{+18.1}_{-31.5}$

With a very large sample of $X(3872) \to \pi^+\pi^- J/\psi$ events, the LHCb experiment reported an improved measurement of its mass and a first measurement of its width [105]. Limited by its capability of D^{*0} reconstruction and mass resolution, it is still not possible for LHCb to measure the line shape of the resonance.

Commonality among the $X(3872)$, $Y(4260)$ and $Z_c(3900)$ states

With data taken with a c.m. energy at and near the $Y(4260)$ resonance peak, BESIII discovered a clear signal for $X(3872)$ production in association with a γ ray [95], as shown in Fig. 7, and a clear signal for $Z_c(3900)$ production in association with a π meson [70], as shown in Fig. 5. The c.m. energy dependence of the $e^+e^- \to \gamma X(3872)$ cross section is suggestive of a $Y(4260) \to \gamma X(3872)$ decay process, and that of the $e^+e^- \to \pi^0 Z_c(3900)^0$ cross section is suggestive of a $Y(4260) \to \pi Z_c(3900)$ decay process; these indicate that there might be some common features to the internal structures of the $Z_c(3900)$, $Y(4260)$ and $X(3872)$ states.

Many of the models developed to interpret the nature of one of these three states do not consider the possibility of a connection between them. With data supplied by the BESIII experiments, some of

Table 3. The numbers of observed events of discovery modes of the XYZ states at BESIII and other experiments. Here the states are detected with $X(3872) \to \pi^+\pi^- J/\psi$, $Y(4260) \to \pi^+\pi^- J/\psi$, $Z_c(3900)^\pm \to \pi^\pm J/\psi$, $Z_c(4020)^\pm \to \pi^\pm h_c$ and $Y(4660) \to \pi^+\pi^-\psi(2S)$. The numbers for the Belle II experiments are a simple scale according to those of the Belle experiment. Here '–' indicates not available. BESIII can detect other decay modes of these states while other experiments can barely do so.

Experiment	Data-taking time	$X(3872)$	$Y(4260)$	$Z_c(3900)$	$Z_c(4020)$	$Y(4660)$
BESIII	3 months	20	6000	1300	180	250
BaBar	1999–2008	90	270	80	–	45
Belle	1999–2010	170	550	160	–	90
LHCb	2011–12 (B decays)	4000	–	–	–	–
	2011–18 (pp collision)	16 000	–	–	–	–
Belle II	2019–30	8000	28 000	8000	–	5000

these models may be ruled out and others may need to be revisited in light of these new observations.

SUMMARY AND PERSPECTIVES

With the capability of adjusting the e^+e^- c.m. energy to the peaks of resonances, combined with the clean experimental environments due to near-threshold operation, BESIII is uniquely able to perform a broad range of critical measurements of charmonium physics, and the production and decays of many of the nonstandard XYZ states, as discussed above in the context of the studies of the $X(3872)$, $Y(4220)$, $Z_c(3900)$ and $Z_c(4020)$. Table 3 shows the operating times associated with the discoveries of the XYZ states at BESIII and other experiments, including the previous generation B factories, BaBar and Belle, and the new generation super-B factories, LHCb and Belle II. BESIII's special advantages for studying the XYZ states are evident.

We emphasize here that BESIII measured all the known decay modes of the $X(3872)$ and discovered its new decay modes even though the numbers of produced $X(3872)$ events are much smaller than those of other experiments. This is because the very clean experimental environment of e^+e^- collisions in the τ-charm threshold energy region uniquely facilitates the isolation of signals for $X(3872)$ decays into final states with one or more photons with high efficiency. This is especially true for final states that contain an h_c charmonium state like the BESIII discovery of the $Z_c(4020)$ state and measurements of $Y(4220)$ and $Y(4390) \to \pi^+\pi^- h_c$ decays. Neither the BaBar and Belle B factories nor the LHCb experiment has ever seen an h_c signal.

BESIII has produced a considerable amount of information about the XYZ and the conventional charmonium states. In addition, there are data that are still being analyzed and more data that will be accumulated at other c.m. energies [56,106]. Analyses with these additional data samples will provide an improved understanding of the XYZ states, especially the $X(3872)$, $Y(4260)$, $Z_c(3900)$, and $Z_c(4020)$ states. The maximum c.m. energy accessible at BEPCII was upgraded from 4.6 to 5.0 GeV in 2019, and a 5.6 fb^{-1} of data was accumulated in the 2019-20 and 2020–21 running periods, with more data planned for the future. This enables a full coverage of the $Y(4660)$ [44] resonance and a search for possible higher mass vector mesons and states with other quantum numbers, as well as improved measurements of their properties.

At the same time, other experiments will also supply information on these states. At the LHCb, in addition to the 3 fb^{-1} of data at 7 and 8 TeV that have been used for most of their published analyses, there is a 6 fb^{-1} of data sample at 13 TeV that is being used for improved analyses of many of the topics discussed above such as the $X(3872)$ decay properties and searches for the Y and $Z_c(3900)$ states in B decays.

Belle II [107] has collected about 200 fb^{-1} of data by mid-2021, and will accumulate 50 ab^{-1} data at the $\Upsilon(4S)$ peak by the end of 2030. These data samples can be used to study the XYZ and charmonium states in many different ways [14], among which ISR can produce events in the same energy range covered by BESIII. A 50 ab^{-1} Belle II data sample will correspond to 2.0–2.8 fb^{-1} of data for every 10 MeV from 4–5 GeV. Similar statistics will be available for modes like $e^+e^- \to \pi^+\pi^- J/\psi$ at Belle II and BESIII (after considering the fact that Belle II has lower efficiency). Belle II has the advantage that data at different energies will be accumulated at the same time, making the analysis much simpler than at BESIII.

There are two super τ-charm factories proposed, the STC in China [108] and the SCT in Russia [109]. Both machines would run at c.m. energies of up to 7 GeV with a peak luminosity of

10^{35} cm^{-2} s^{-1}, which is a factor of 100 improvement over the BEPCII. This would enable systematic studies of the XYZ and charmonium states with unprecedented precision.

ACKNOWLEDGEMENTS

I thank my BESIII collaborators for producing these fantastic results presented in this review; I thank Steve Olsen for comments and suggestions on the manuscript.

FUNDING

This work was supported in part by the National Key Research and Development Program of China (2020YFA0406301), the National Natural Science Foundation of China (11961141012, 11835012 and 11521505), and the CAS Center for Excellence in Particle Physics (CCEPP).

Note added. After submission of this manuscript, BESIII announced observation of a near-threshold structure in the K^+ recoil-mass spectra in $e^+e^- \to K^+(D_s^- D^{*0} + D_s^{*-} D^0)$ [110] and LHCb reported a resonance decaying into $K^{\pm}J/\psi$ that could be the strange partner of the $Z_c(3900)$ with the d quark replaced with an s quark [111].

Conflict of interest statement. None declared.

REFERENCES

1. Aubert JJ, Becker U and Biggs PJ *et al.* Experimental observation of a heavy particle *J. Phys Rev Lett* 1974; **33**: 1404–6.
2. Augustin JE, Boyarski AM and Breidenbach M *et al.* Discovery of a narrow resonance in e^+e^- annihilation. *Phys Rev Lett* 1974; **33**: 1406–8.
3. Zyla PA, Barnett RM and Beringer J *et al.* Review of particle physics. *Prog Theor Exp Phys* 2020; **2020**: 083C01.
4. Brambilla N, Pineda A and Soto J. Effective field theories for heavy quarkonium. *Rev Mod Phys* 2005; **77**: 1423–96.
5. Brambilla N, Eidelman S and Heltsley BK *et al.* Heavy quarkonium: progress, puzzles, and opportunities. *Eur Phys J C* 2011; **71**: 1534.
6. Brambilla N, Eidelman S and Foka P *et al.* QCD and strongly coupled gauge theories: challenges and perspectives. *Eur Phys J C* 2014; **74**: 2981.
7. Eichten E, Gottfried K and Kinoshita T *et al.* Charmonium: the model. *Phys Rev D* 1978; **17**: 3090–117.
8. Godfrey S and Isgur N. Mesons in a relativized quark model with chromodynamics. *Phys Rev D* 1985; **32**: 189–231.
9. Barnes T, Godfrey S and Swanson ES. Higher charmonia. *Phys Rev D* 2005; **72**: 054026.
10. Jaffe RL. Exotica. *Phys Rept* 2005; **409**: 1–45.
11. Klempt E and Zaitsev A. Glueballs, hybrids, multiquarks: experimental facts versus QCD inspired concepts. *Phys Rept* 2007; **454**: 1–202.
12. Aubert B, Bazana A and Boucham A *et al.* The BaBar detector. *Nucl Instrum Methods Phys Res A* 2002; 479: 1–116.
13. Abashian A, Gotowa K and Morgan N *et al.* The Belle detector. *Nucl Instrum Methods Phys Res A* 2002; **479**: 117–232.
14. Bevan AJ, Golob B and Mannel T *et al.* The physics of the *B* factories. *Eur Phys J C* 2014; **74**: 3026.
15. Brambilla N, Eidelman S and Hanhart C *et al.* The *XYZ* states: experimental and theoretical status and perspectives. *Phys Rept* 2020; **873**: 1–154.
16. Guo FK, Hanhart C and Meißner UG *et al.* Hadronic molecules. *Rev Mod Phys* 2018; **90**: 015004.
17. Chen HX, Chen W and Liu X *et al.* The hidden-charm pentaquark and tetraquark states. *Phys Rept* 2016; **639**: 1–121.
18. Ablikim M, An ZH and Bai JZ *et al.* Design and construction of the BESIII detector. *Nucl Instrum Methods Phys Res A* 2010; **614**: 345–99.
19. Alves AA, Jr, Andrade Filho LM and Barbosa AF *et al.* The LHCb detector at the LHC. *J Instrum* 2008; **3**: S08005.
20. Asner DM, Barnes T and Bian JM *et al.* Physics at BES-III. *Int J Mod Phys A* 2009; **24**: S1.
21. Ablikim M, Achasov MN and Ai XC *et al.* Observation of a charged charmoniumlike structure in $e^+e^- \to \pi^+\pi^- J/\psi$ at $\sqrt{s} = 4.26$ GeV. *Phys Rev Lett* 2013; **110**: 252001.
22. Ablikim M, Achasov MN and Ai XC *et al.* Precision measurement of the integrated luminosity of the data taken by BESIII at center of mass energies between 3.810 and 4.600 GeV. *Chin Phys C* 2015; **39**: 093001.
23. Ablikim M, Achasov MN and Ahmed S *et al.* Luminosity measurements for the R scan experiment at BESIII. *Chin Phys C* 2017; **41**: 063001.
24. Qiao CF, Yuan F and Chao KT. A crucial test for color octet production mechanism in Z^0 decays. *Phys Rev D* 1997; **55**: 4001–4.
25. Ablikim M, Achasov MN and Ai XC *et al.* Observation of the $\psi(1\,^3D_2)$ state in $e^+e^- \to \pi^+\pi^-\gamma\chi_{c1}$ at BESIII. *Phys Rev Lett* 2015; **115**: 011803.
26. Aaij R, Abellán Beteta C and Adeva B *et al.* Near-threshold $D\bar{D}$ spectroscopy and observation of a new charmonium state. *J High Energy Phys* 2019; **07**: 035.
27. Ablikim M, Achasov MN and Ahmed S *et al.* Evidence of two resonant structures in $e^+e^- \to \pi^+\pi^- h_c$. *Phys Rev Lett* 2017; **118**: 092002.
28. Ablikim M, Achasov MN and Ahmed S *et al.* Measurements of the branching fractions of $\eta_c \to K^+K^-\pi^0$, $K_S^0 K^{\pm}\pi^{\mp}$, $2(\pi^+\pi^-\pi^0)$, and $p\bar{p}$. *Phys Rev D* 2019; **100**: 012003.
29. Ablikim M, Achasov MN and Ambrose DJ *et al.* First observation of the M1 transition $\psi(3686) \to \gamma\eta_c(2S)$. *Phys Rev Lett* 2012; **109**: 042003.
30. Gao K. Study of radiative decays of $\psi(2S)$ mesons. arXiv: 0909.2812.
31. Li G and Zhao Q. Hadronic loop contributions to J/ψ and ψ' radiative decays into $\gamma\eta_c$ or $\gamma\eta_c'$. *Phys Lett B* 2008; **670**: 55–60.
32. Peng T and Ma B. Heavy quarkonium 2*S* states in light-front quark model. *Eur Phys J A* 2012; **48**: 66.
33. Edwards C, Partridge R and Peck C *et al.* Observation of an $\eta_c{}'$ candidate state with mass 3592 ± 5 MeV. *Phys Rev Lett* 1982; **48**: 70–3.

34. Yuan CZ. Search for $\eta_c(2S)$ and study of χ_{cJ} decays using $\psi(2S)$ data. Ph.D. Thesis. Institute of High Energy Physics, Chinese Academy of Sciences, 1997.
35. Yuan CZ. The initial $\psi(2S)$ physics program at the BES experiment. *Mod Phys Lett A* 2020; **35**: 2030009.
36. Cronin-Hennessy D, Gao KY and Gong DT *et al.* Search for $\psi(2S) \to \gamma\eta_c(2S)$ via fully reconstructed $\eta_c(2S)$ decays. *Phys Rev D* 2010; **81**: 052002.
37. Partridge R, Peck C and Porter F *et al.* Observation of an η_c candidate state with mass 2978 ± 9 MeV. *Phys Rev Lett* 1980; **45**: 1150–3.
38. Brambilla N, Jia Y and Vairo A. Model-independent study of magnetic dipole transitions in quarkonium. *Phys Rev D* 2006; **73**: 054005.
39. Pineda A and Segovia J. Improved determination of heavy quarkonium magnetic dipole transitions in potential nonrelativistic QCD. *Phys Rev D* 2013; **87**: 074024.
40. Bhardwaj V, Miyabayashi K and Adachi I *et al.* Evidence of a new narrow resonance decaying to $\chi_{c1}\gamma$ in $B \to \chi_{c1}\gamma K$. *Phys Rev Lett* 2013; **111**: 032001.
41. Choi SK, Olsen SL and Abe K *et al.* Observation of a narrow charmonium-like state in exclusive $B^{\pm} \to K^{\pm}\pi^+\pi^- J/\psi$ decays. *Phys Rev Lett* 2003; **91**: 262001.
42. Aubert B, Barate R and Boutigny D *et al.* Observation of a broad structure in the $\pi^+\pi^- J/\psi$ mass spectrum around 4.26 GeV/c^2. *Phys Rev Lett* 2005; **95**: 142001.
43. Aubert B, Barate R and Bona M *et al.* Evidence of a broad structure at an invariant mass of 4.32 GeV/c^2 in the reaction $e^+e^- \to \pi^+\pi^-\psi(2S)$ measured at *BABAR*. *Phys Rev Lett* 2007; **98**: 212001.
44. Wang XL, Yuan CZ and Shen CP *et al.* Observation of two resonant structures in $e^+e^- \to \pi^+\pi^-\psi(2S)$ via ISR at Belle. *Phys Rev Lett* 2007; **99**: 142002.
45. Ablikim M, Bai JZ and Ban Y *et al.* Determination of the $\psi(3770)$, $\psi(4040)$, $\psi(4160)$ and $\psi(4415)$ resonance parameters. *Phys Lett B* 2008; **660**: 315–9.
46. Uglov TV, Kalashnikova YS and Nefediev AV *et al.* Exclusive open-charm near-threshold cross sections in a coupled-channel approach. *JETP Lett* 2017; **105**: 1–7.
47. Yuan CZ, Shen CP and Wang P *et al.* Measurement of $e^+e^- \to \pi^+\pi^- J/\psi$ cross-section via initial state radiation at Belle. *Phys Rev Lett* 2007; **99**: 182004.
48. Lees JP, Poireau V and Tisserand V *et al.* Study of the reaction $e^+e^- \to \pi^+\pi^- J/\psi$ via initial-state radiation at *BABAR*. *Phys Rev D* 2012; **86**: 051102(R).
49. Liu ZQ, Shen CP and Yuan CZ *et al.* Study of $e^+e^- \to \pi^+\pi^- J/\psi$ and observation of a charged charmoniumlike state at Belle. *Phys Rev Lett* 2013; **110**: 252002.
50. He Q, Insler J and Muramatsu H *et al.* Confirmation of the $Y(4260)$ resonance production in ISR. *Phys Rev D* 2006; **74**: 091104.
51. Patrignani C, Agashe K and Aielli G *et al.* Review of particle physics. *Chin Phys C* 2016; **40**: 100001.
52. Ablikim M, Achasov MN and Ahmed S *et al.* Precise measurement of the $e^+e^- \to \pi^+\pi^- J/\psi$ cross section at center-of-mass energies from 3.77 to 4.60 GeV. *Phys Rev Lett* 2017; **118**: 092001.
53. Ablikim M, Achasov MN and Ai XC *et al.* Study of $e^+e^- \to \omega\chi_{cJ}$ at center-of-mass energies from 4.21 to 4.42 GeV. *Phys Rev Lett* 2015; **114**: 092003.
54. Ablikim M, Achasov MN and Adlarson P *et al.* Cross section measurements of $e^+e^- \to \omega\chi_{c0}$ from $\sqrt{s} = 4.178$ to 4.278 GeV. *Phys Rev D* 2019; **99**: 091103.
55. Ablikim M, Achasov MN and Ahmed S *et al.* Evidence of a resonant structure in the $e^+e^- \to \pi^+ D^0 D^{*-}$ cross section between 4.05 and 4.60 GeV. *Phys Rev Lett* 2019; **122**: 102002.
56. Ablikim M, Achasov MN and Adlarson P *et al.* Future physics programme of BESIII. *Chin Phys C* 2020; **44**: 040001.
57. Gao XY, Shen CP and Yuan CZ. Resonant parameters of the $Y(4220)$. *Phys Rev D* 2017; **95**: 092007.
58. Cao QF, Qi HR and Tang GY *et al.* On leptonic width of $X(4260)$. *Eur Phys J C* 2021; **81**: 83.
59. Chen Y, Chiu WF and Gong M *et al.* Exotic vector charmonium and its leptonic decay width. *Chin Phys C* 2016; **40**: 081002.
60. Choi SK, Olsen SL and Adachi I *et al.* Observation of a resonance-like structure in the $\pi^\pm\psi'$ mass distribution in exclusive $B \to K\pi^\pm\psi'$ decays. *Phys Rev Lett* 2008; **100**: 142001.
61. Chilikin K, Mizuk R and Adachi I *et al.* Experimental constraints on the spin and parity of the $Z(4430)^+$. *Phys Rev D* 2013; **88**: 074026.
62. Aaij R, Adeva B and Adinolfi M *et al.* Observation of the resonant character of the $Z(4430)^-$ state. *Phys Rev Lett* 2014; **112**: 222002.
63. Ablikim M, Achasov MN and Albayrak O *et al.* Observation of a charged charmoniumlike structure $Z_c(4020)$ and search for the $Z_c(3900)$ in $e^+e^- \to \pi^+\pi^- h_c$. *Phys Rev Lett* 2013; **111**: 242001.
64. Xiao T, Dobbs S and Tomaradze A *et al.* Observation of the charged hadron $Z_c^{\pm}$ (3900) and evidence for the neutral $Z_c^0(3900)$ in $e^+e^- \to \pi\pi J/\psi$ at $\sqrt{s} = 4170$ MeV. *Phys Lett B* 2013; **727**: 366.
65. Ablikim M, Achasov MN and Ai XC *et al.* Determination of the spin and parity of the $Z_c(3900)$. *Phys Rev Lett* 2017; **119**: 072001.
66. Ablikim M, Achasov MN and Albayrak O *et al.* Observation of a charged $(D\bar{D}^*)^{\pm}$ mass peak in $e^+e^- \to \pi^+ D\bar{D}^*$ at $\sqrt{s} = 4.26$ GeV. *Phys Rev Lett* 2014; **112**: 022001.
67. Ablikim M, Achasov MN and Ai XC *et al.* Confirmation of a charged charmoniumlike state $Z_c(3885)^{\mp}$ in $e^+e^- \to \pi^{\pm}(D\bar{D}^*)^{\mp}$ with double D tag. *Phys Rev D* 2015; **92**: 092006.
68. Ablikim M, Achasov MN and Ai XC *et al.* Observation of $Z_c(3900)^0$ in $e^+e^- \to \pi^0\pi^0 J/\psi$. *Phys Rev Lett* 2015; **115**: 112003.
69. Ablikim M, Achasov MN and Ai XC *et al.* Observation of a neutral structure near the $D\bar{D}^*$ mass threshold in $e^+e^- \to (D\bar{D}^*)^0\pi^0$ at $\sqrt{s} = 4.226$ and 4.257 GeV. *Phys Rev Lett* 2015; **115**: 222002.
70. Ablikim M, Achasov MN and Adlarson P *et al.* Study of the process $e^+e^- \to \pi^0\pi^0 J/\psi$ and neutral charmonium-like state $Z_c(3900)^0$. *Phys Rev D* 2020; **102**: 012009.
71. Ablikim M, Achasov MN and Ai XC *et al.* Search for the isospin violating decay $Y(4260) \to J/\psi\eta\pi^0$. *Phys Rev D* 2015; **92**: 012008.
72. Ablikim M, Achasov MN and Ai XC *et al.* Search for $Z_c(3900)^{\pm} \to \omega\pi^{\pm}$. *Phys Rev D* 2015; **92**: 032009.
73. Ablikim M, Achasov MN and Ahmed S *et al.* Measurements of $e^+e^- \to K_S^0 K^{\pm}\pi^{\mp}\pi^0$ and $K_S^0 K^{\pm}\pi^{\mp}\eta$ at center-of-mass energies from 3.90 to 4.60 GeV. *Phys Rev D* 2019; **99**: 012003.
74. Ablikim M, Achasov MN and Ai XC *et al.* Observation of $e^+e^- \to \pi^0\pi^0 h_c$ and a neutral charmoniumlike structure $Z_c(4020)^0$. *Phys Rev Lett* 2014; **113**: 212002.
75. Ablikim M, Achasov MN and Albayrak O *et al.* Observation of a charged charmoniumlike structure in $e^+e^- \to (D^*\bar{D}^*)^{\pm}\pi^{\mp}$ at $\sqrt{s} = 4.26$ GeV. *Phys Rev Lett* 2014; **112**: 132001.
76. Ablikim M, Achasov MN and Ai XC *et al.* Observation of a neutral charmoniumlike state $Z_c(4025)^0$ in $e^+e^- \to (D^*\bar{D}^*)^0\pi^0$. *Phys Rev Lett* 2015; **115**: 182002.
77. Ablikim M, Achasov MN and Ahmed S *et al.* Measurement of $e^+e^- \to \pi^+\pi^-\psi(3686)$ from 4.008 to 4.600 GeV and observation of a charged structure in the $\pi^\pm\psi(3686)$ mass spectrum. *Phys Rev D* 2017; **96**: 032004. Erratum: 2019; **99**: 019903.
78. Abazov VM, Abbott B and Acharya BS *et al.* Evidence for $Z_c^{\pm}$ (3900) in semi-inclusive decays of b-flavored hadrons. *Phys Rev D* 2018; **98**: 052010.

79. Abazov VM, Abbott B and Acharya BS *et al.* Properties of $Z_c^{\pm}$ (3900) produced in $P\bar{P}$ collision. *Phys Rev D* 2019; **100**: 012005.
80. Liu C, Liu L and Zhang K. Towards the understanding of Z_c(3900) from lattice QCD. *Phys Rev D* 2020; **101**: 054502.
81. Prelovsek S, Lang C and Leskovec L *et al.* Study of the Z_c^+ channel using lattice QCD. *Phys Rev D* 2015; **91**: 014504.
82. Chen Y, Gong M and Lei YH *et al.* Low-energy scattering of the $(D\bar{D}^*)^{\pm}$ system and the resonance-like structure Z_c(3900). *Phys Rev D* 2014; **89**: 094506.
83. Chen Y, Gong M and Lei Y-H *et al.* Low-energy scattering of $(D^*\bar{D}^*)^{\pm}$ system and the resonance-like structure Z_c(4025). *Phys Rev D* 2015; **92**: 054507.
84. Lee SH, DeTar C and Mohler D *et al.* Searching for the X(3872) and Z_c^+(3900) on HISQ lattices. arXiv:1411.1389.
85. Ikeda Y, Aoki S and Doi T *et al.* Fate of the tetraquark candidate Z_c(3900) from lattice QCD. *Phys Rev Lett* 2016; **117**: 242001.
86. Ikeda Y. The tetraquark candidate Z_c(3900) from dynamical lattice QCD simulations. *J Phys G* 2018; **45**: 024002.
87. Chen T, Chen Y and Gong M *et al.* A coupled-channel lattice study on the resonance-like structure Z_c(3900). *Chin Phys C* 2019; **43**: 103103.
88. Bondar A, Garmash A and Mizuk R *et al.* Observation of two charged bottomoniumlike resonances in $\Upsilon(5S)$ decays. *Phys Rev Lett* 2012; **108**: 122001.
89. Aaij R, Abellán Beteta C and Ackernley T *et al.* Observation of structure in the J/ψ-pair mass spectrum. *Sci Bull* 2020; **65**: 1983–93.
90. Aaij R, Abellán Beteta C and Ackernley T *et al.* Amplitude analysis of the $B^+ \to D^+D^-K^+$ decay. *Phys Rev D* 2020; **102**: 112003.
91. Acosta D, Affolder T and Ahn MH *et al.* Observation of the narrow state $X(3872) \to J/\psi\pi^+\pi^-$ in $\bar{p}p$ collisions at $\sqrt{s} = 1.96$ TeV. *Phys Rev Lett* 2004; **93**: 072001.
92. Abazov VM, Abbott B and Abolins M *et al.* Observation and properties of the X(3872) decaying to $J/\psi\pi^+\pi^-$ in $p\bar{p}$ collisions at $\sqrt{s} = 1.96$ TeV. *Phys Rev Lett* 2004; **93**: 162002.
93. Aubert B, Barate R and Boutigny D *et al.* Study of the $B \to J/\psi K^-\pi^+\pi^-$ decay and measurement of the $B \to X(3872)K^-$ branching fraction. *Phys Rev D* 2005; **71**: 071103.
94. Aaij R, Abellan Beteta C and Adeva B *et al.* Determination of the X(3872) meson quantum numbers. *Phys Rev Lett* 2013; **110**: 222001.
95. Ablikim M, Achasov MN and Ai XC *et al.* Observation of $e^+e^- \to \gamma X(3872)$ at BESIII. *Phys Rev Lett* 2014; **112**: 092001.
96. Ablikim M, Achasov MN and Adlarson P *et al.* Study of $e^+e^- \to \gamma\omega J/\psi$ and observation of $X(3872) \to \omega J/\psi$. *Phys Rev Lett* 2019; **122**: 232002.
97. Ablikim M, Achasov MN and Ahmed S *et al.* Observation of the decay $X(3872) \to \pi^0\chi_{c1}(1P)$. *Phys Rev Lett* 2019; **122**: 202001.
98. Ablikim M, Achasov MN and Adlarson P *et al.* Study of open-charm decay and radiative transitions of the X(3872). *Phys Rev Lett* 2019; **124**: 242001.
99. Aaij R, Adeva B and Adinolfi M *et al.* Evidence for the decay $X(3872) \to \psi(2S)\gamma$. *Nucl Phys B* 2014; **886**: 665.
100. Aubert B, Bona M and Karyotakis Y *et al.* Evidence for $X(3872) \to \psi_{2S}\gamma$ in $B^{\pm} \to X_{3872}K^{\pm}$ decays, and a study of $B \to c\bar{c}\gamma K$. *Phys Rev Lett* 2009; **102**: 132001.
101. Bhardwaj V, Trabelsi K and Singh JB *et al.* Observation of $X(3872) \to J/\psi\gamma$ and search for $X(3872) \to \psi'\gamma$ in B decays. *Phys Rev Lett* 2011; **107**: 091803.
102. Li C and Yuan CZ. Determination of the absolute branching fractions of X(3872) decays. *Phys Rev D* 2019; **100**: 094003.
103. Yuan C-Z. Exotic hadrons. arXiv:0910.3138.
104. Esposito A, Guerrieri AL and Piccinini F *et al.* Four-quark hadrons: an updated review. *Int J Mod Phys A* 2015; **30**: 1530002.
105. Aaij R, Abellán Beteta C and Ackernley T *et al.* Study of the lineshape of the χ_{c1}(3872) state. *Phys Rev D* 2020; **102**: 092005.
106. Yuan C-Z. Study of the XYZ states at the BESIII. *Front Phys* 2015; **10**: 101401.
107. Abe T, Adachi I and Adamczyk K *et al.* Belle II technical design report. arXiv:1011.0352.
108. Zhao ZG. Introduction to future high intensity collider @ 2–7 GeV in China. *International Workshop on Physics at Future High Intensity Collider @ 2–7 GeV in China*, University of Chinese Academy of Sciences (UCAS), Hefei, China, 13–16 January 2015.
109. Levichev E. Charm facilities. *The 9th International Workshop on Charm Physics*, Novosibirsk, Russia, 21–25 May 2018.
110. Ablikim M, Achasov MN and Adlarson P *et al.* Observation of a near-threshold structure in the K^+ recoil-mass spectra in $e^+e^- \to K^+(D_s^-D^{*0} + D_s^{*-}D^0)$. *Phys Rev Lett* 2021; **126**: 102001.
111. Aaij R, Abellán Beteta C and Ackernley T *et al.* Observation of new resonances decaying to $J/\psi K^+$ and $J/\psi\phi$. *Phys Rev Lett* 2021; **127**: 082001.

REVIEW

National Science Review
8: nwab181, 2021
https://doi.org/10.1093/nsr/nwab181
Advance access publication 5 October 2021

PHYSICS

Special Topic: Physics of the BESIII Experiment

Study of the standard model with weak decays of charmed hadrons at BESIII

Hai-Bo Li[1,2,*] and Xiao-Rui Lyu[2,*]

ABSTRACT

A comprehensive review of weak decays of charmed hadrons ($D^{0/+}$, D_s^+ and Λ_c^+) based on analyses of the threshold data from e^+e^- annihilation in the BESIII experiment is presented. Current experimental challenges and successes in understanding decays of the charmed hadrons are discussed. Precise calibrations of quantum chromodynamics and tests of the standard model are provided by measurements of purely leptonic and semi-leptonic decays of charmed hadrons, and lepton universality is probed in purely leptonic decays of charmed mesons to three generations of leptons. Quantum correlations in threshold data samples provide access to strong phases in the neutral D meson decays and probe the decay dynamics of the charmed Λ_c baryon. Charm physics studies with near-threshold production of charmed particle pairs are unique to BESIII, and provide many important opportunities and challenges.

Keywords: charmed mesons, charmed baryon, leptonic decay, semi-leptonic decay, lepton flavor universality

INTRODUCTION

The discovery of the J/ψ in 1974 marked a new era in particle physics. The arrival of the first heavy quark indicated that the standard model (SM) provided a correct low-energy description of particle physics. Four decades later, the charmed quark still plays unique roles in studies of strong and weak interactions [1]. Recent observation of *CP* violation in charmed meson decays has attracted significant and renewed interest to charm physics [2,3]. It paves the road to precise tests of the SM in interesting weak interaction transitions and maybe even to searches for new physics beyond the SM.

A distinctive feature of all the charmed hadrons is that their masses place them at the edge of the region where non-perturbative hadronic physics is operative, forcing us to develop new means to cope with such scales. This point has been made in prescient reviews [4,5] that posed many of the questions that are still awaiting answers. While this fact does not markedly affect the theoretical description of leptonic and semi-leptonic decays of charmed hadrons, it poses challenges to analyses of their hadronic transitions. We expect that detailed experimental studies would provide some hints on the dynamics of charm hadronic decays, so that eventually those problems will be overcome. In this review we focus on the weak decays of ground-state charmed hadrons, i.e. three charmed mesons $D^+(c\bar{d})$, $D^0(c\bar{u})$ and $D_s^+(c\bar{s})$ as well as one charmed baryon $\Lambda_c^+(cud)$, with internal quark constituents as depicted in Fig. 1, that can be extensively studied using data collected at the BESIII experiment. There are mainly three classes of charmed hadron decays: purely leptonic, semi-leptonic and hadronic decays. Measurements of the charmed hadron decays can be used to calibrate lattice quantum chromodynamics (LQCD) calculations. In addition, BESIII data provide stringent constraints on the Cabibbo-Kobayashi-Maskawa (CKM) six-quark flavor-mixing matrix [7] via: (1) precision measurements of the CKM matrix elements $|V_{cs}|$ and $|V_{cd}|$ that parameterize the strengths of $c \to s$ and $c \to d$ weak transitions, respectively; (2) determinations of the strong-interaction phases in D-meson decays that are essential inputs to measurements of the *CP*-violating phase

[1]Institute of High Energy Physics, Chinese Academy of Sciences, Beijing 100049, China and [2]University of Chinese Academy of Sciences, Beijing 100049, China

*Corresponding authors. E-mails: lihb@ihep.ac.cn; xiaorui@ucas.ac.cn

Received 9 April 2021; **Revised** 24 September 2021; **Accepted** 24 September 2021

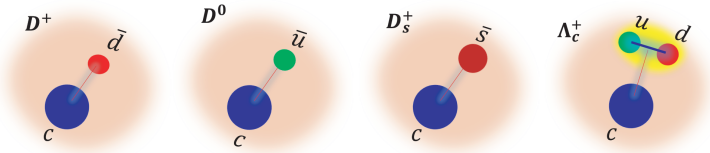

Figure 1. Quark constituents for the ground-state charmed hadrons of $D^+(c\bar{d})$, $D^0(c\bar{u})$, $D_s^+(c\bar{s})$ and $\Lambda_c^+(cud)$. Taken from [6].

γ of the CKM matrix element V_{ub} in B-meson decays [8].

ADVANTAGES NEAR THRESHOLD PRODUCTION FROM e^+e^- ANNIHILATION

Experiments at e^+e^- machines operating at the $\psi(3770)$ and $\psi(4140)$ resonances and $\Lambda_c^+\bar{\Lambda}_c^-$ threshold, such as CLEO-c and BESIII [9], have several important advantages. First, the cross section for charm production is relatively high, for example, $\sigma(e^+e^- \to D^0\bar{D}^0) = (3.615 \pm 0.010 \pm 0.038)$ nb and $\sigma(e^+e^- \to D^+D^-) = (2.830 \pm 0.011 \pm 0.026)$ nb at the $\psi(3770)$ peak [10]. Second, the $D\bar{D}$ and $\Lambda_c^+\bar{\Lambda}_c^-$ pairs are produced in the exclusive two-body channel with no additional particles. Thus, one can employ a double-tag technique pioneered by the Mark III experiment [11]: a full reconstruction of an anti-D meson on one side of tagged events together with the known momentum and energy of colliding beams provides a 'beam' of D particles of known four-momentum on the other side. The tag yield, which provides the normalization for the branching fraction measurement, is extracted from the distribution of beam-constrained mass $M_{\rm BC} = \sqrt{E_{\rm beam}^2 - |\vec{p}_{\rm tag}|^2}$, where $\vec{p}_{\rm tag}$ is the three-momentum of the tag $\bar{D}$ candidate and $E_{\rm beam}$ is the beam energy, both evaluated in the e^+e^- center-of-mass system. When a tagged D^+ decays to a muon and a muonic neutrino, $\mu^+\nu_\mu$, the mass of the (missing) nearly zero-mass neutrino can be inferred from energy-momentum conservation. This tagging technique, which obviates the need for knowledge of the luminosity or the production cross section, is a powerful tool for charmed particle decay measurements that is most accurately performed by the near-threshold experiments.

Furthermore, the charmed hadron pairs at BESIII are produced via e^+e^- annihilation through a virtual photon (with spin, parity and C parity of $J^{PC} = 1^{--}$), e.g. in the process $e^+e^- \to \gamma^* \to \psi(3770) \to D^0\bar{D}^0$ ($e^+e^- \to \gamma^* \to \Lambda_c^+\bar{\Lambda}_c^-$). Hence, the wave function of the produced charm hadron pairs is analogous to that of photons in an aligned, spin-1 state with odd charge parity $C = -1$, and the $D^0\bar{D}^0$ ($\Lambda_c^+\bar{\Lambda}_c^-$) pair are in a quantum-entangled state. This allows for unique probes of the structure of decay amplitudes and relative phases between D^0 and $\bar{D}^0$ decays, as well as novel measurements of neutral D mixing and CP violation in D^0 and Λ_c^+ decays [12–15].

PRECISION TESTS OF THE STANDARD MODEL

In the SM, quark-flavor mixing is characterized by the unitary 3×3 CKM matrix [7]:

$$V_{\rm CKM} = \begin{pmatrix} V_{ud} & V_{us} & V_{ub} \\ V_{cd} & V_{cs} & V_{cb} \\ V_{td} & V_{ts} & V_{tb} \end{pmatrix}. \qquad (1)$$

The CKM matrix induces flavor-changing transitions within and among generations in the charged currents in tree-level $W^\pm$-exchange interactions. Experiments have revealed a strong hierarchy among the CKM matrix elements: transitions within the same generation are described by $V_{\rm CKM}$ elements of $\mathcal{O}(1)$, whereas there is a suppression of $\mathcal{O}(10^{-1})$ for transitions between the first and the second generations, $\mathcal{O}(10^{-2})$ between the second and the third, and $\mathcal{O}(10^{-3})$ between the first and the third. Following the observation of this hierarchy, Wolfenstein [16] proposed an expansion of the CKM matrix in terms of four parameters (which was further modified by Buras [17]), λ, A, $\bar{\rho}$ and $\bar{\eta}$, under the relations

$$\begin{aligned} \lambda^2 &= \frac{|V_{us}|^2}{|V_{ud}|^2 + |V_{us}|^2}, \\ A^2\lambda^4 &= \frac{|V_{cb}|^2}{|V_{ud}|^2 + |V_{us}|^2}, \\ \bar{\rho} + i\,\bar{\eta} &= -\frac{V_{ud}V_{ub}^*}{V_{cd}V_{cb}^*}, \end{aligned} \qquad (2)$$

which are used to fully characterize the matrix. Any deviation of $V_{\rm CKM}$ from unitarity would indicate new physics beyond the SM. Therefore, improving our knowledge of the CKM matrix elements to test unitarity is one of the principal goals of flavor physics. BESIII data provide direct precise measurements of the CKM matrix elements $|V_{cs}|$ and $|V_{cd}|$ using the purely leptonic and semi-leptonic charmed-hadron decay rates, as discussed in detail below.

Purely leptonic and semi-leptonic decays of hadrons have a special characteristic advantage in studies of the weak interaction [18,19]. A key feature is their relative simplicity, a consequence of the

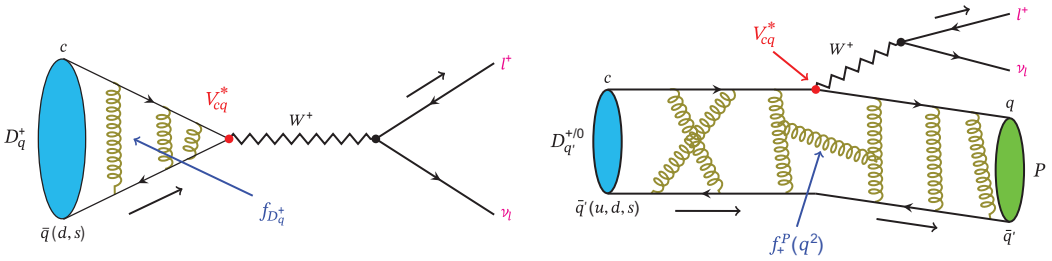

Figure 2. Diagrams for purely leptonic (left) and semi-leptonic (right) decays of $D_{(s)}$ mesons. (Courtesy of Hao-Kai Sun, Institute of High Energy Physics, Chinese Academy of Sciences.)

fact that in these processes the effects of the strong interactions can be isolated. For each decay type, the decay amplitude can be written as the product of a well-understood leptonic current for the process $W^+ \to \ell^+\nu_\ell$ (ℓ denotes charged leptons) and a more complicated hadronic current for the quark transition. Figure 2 shows the Feynman diagrams for the purely leptonic (left diagram) and semi-leptonic (right diagram) decays. In purely leptonic decays, the hadronic current describes an annihilation of the quark and the anti-quark in the initial-state charmed mesons, while in semi-leptonic decays it describes the evolution from the initial-charmed hadron to the final-state hadrons. Because strong interactions affect only one of the two currents, purely leptonic and semi-leptonic decays are relatively simple from a theoretical perspective; they provide bilateral means both to measure fundamental SM parameters and to perform detailed studies of the decay dynamics [20].

A bridge between quarks and leptons: decay constants and lepton flavor universality

Purely leptonic decays of the D^+ and D_s^+ mesons are among the simplest and best-understood probes of $c \to d$ and $c \to s$ quark transitions. In each case, the effects of the strong interaction can be parameterized in terms of just one factor, called the decay constant $f_{D_q^+}$. In the SM, the corresponding decay rate, ignoring radiative corrections, is given in a simple form:

$$\Gamma(D_q^+ \to \ell^+\nu_\ell) = \frac{G_F^2 f_{D_q^+}^2}{8\pi} |V_{cq}|^2 m_\ell^2 m_{D_q^+} \times \left(1 - \frac{m_\ell^2}{m_{D_q^+}^2}\right)^2. \quad (3)$$

Here $q = d$ or s quark and $\ell = e$, μ or τ (electron, muon or tau lepton), and ν_ℓ stands for the neutrino with the corresponding lepton flavor. The D_q^+ mass ($m_{D_q^+}$), the mass of the charged lepton (m_ℓ) and the Fermi coupling constant (G_F) are all known to high precision [21]. Thus, the determination of $\Gamma(D_q^+ \to \ell^+\nu_\ell)$ directly measures the product $f_{D_q^+}|V_{cq}|$ of the D_q^+ decay constant and the magnitude of the $c \to q$ CKM matrix element. One can then either extract $|V_{cq}|$ by using the predicted value of $f_{D_q^+}$, e.g. from LQCD [22], or obtain $f_{D_q^+}$ by using the experimentally measured $|V_{cq}|$ to test the LQCD prediction.

Since the purely leptonic decays of pseudoscalar mesons are helicity suppressed, their decay rates are proportional to the square of the charged lepton mass. According to Equation (3), the SM-expected relative decay widths for the $\tau\nu_\tau$, $\mu\nu_\mu$ and $e\nu_e$ modes are $2.67 : 1 : 2.35 \times 10^{-5}$ for D^+ and $9.75 : 1 : 2.35 \times 10^{-5}$ for D_s^+ with negligible uncertainties. Therefore, the SM $D_q^+ \to e^+\nu_e$ branching fractions are expected to be $\mathcal{B}_{e^+\nu_e} < 10^{-8}$ and not yet experimentally observable.

Using a data sample with an integrated luminosity of 2.93 fb^{-1} collected with BESIII at the $\psi(3770)$ peak, a total of about 1.7 million single-tag D^- mesons are selected using nine hadronic decay modes (summing up to 30% of all D^- decays) on the tagging side. Throughout this article, charge-conjugate modes are implicitly assumed, unless otherwise stated. Signal candidates of $D^+ \to \mu^+\nu_\mu$ are required to have a signature in which the tagging D^- mesons are accompanied by exactly one track that is identified as a muon with charge opposite to that of the tagging D^-. Since the massless neutrino is undetected, the yields of the signal $D^+ \to \mu^+\nu_\mu$ decays are measured based on the missing-mass-squared variable $M_{\rm miss}^2 = (E_{\rm beam} - E_\mu)^2 - (-\vec{p}_{\rm tag} - \vec{p}_\mu)^2$, where E_μ and $\vec{p}_\mu$ are the energy and three-momentum of the muon, respectively, and $\vec{p}_{\rm tag}$ is the three-momentum of the tagged D^- candidate. Here $M_{\rm miss}$ corresponds to the invariant mass of the neutrino, and hence the signal for $D^+ \to \mu^+\nu_\mu$ events is the peak around $M_{\rm miss}^2 = 0$, as shown in Fig. 3(a), where a tiny background is smoothly distributed under the signal

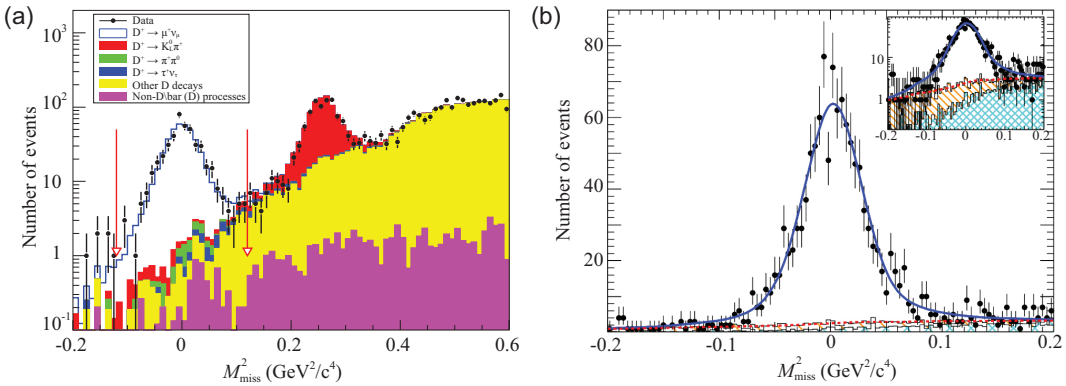

Figure 3. The missing-mass $M^2_{\rm miss}$ distribution of the selected (a) $D^+ \to \mu^+\nu_\mu$ and (b) $D_s^+ \to \mu^+\nu_\mu$ candidates from [23] and [25], respectively. The error bars show the statistical uncertainty in experimental data. Arrows in plot (a) are the boundaries of the signal region, and the inset in plot (b) shows the same distribution on the logarithmic scale. Plots are from [23] and [25].

Table 1. Measurements of D^+ and D_s^+ purely leptonic decays with threshold data at BESIII, and comparisons between experimental results and theoretical expectation or SM-global fit results. (Here, '–' indicates not available.)

Observable	Measurement	Prediction/fit
$\mathcal{B}(D^+ \to \mu^+\nu_\mu)$	$(3.71 \pm 0.19_{\rm stat} \pm 0.06_{\rm syst}) \times 10^{-4}$ [23]	–
$f_{D^+}\lvert V_{cd}\rvert$	$(45.75 \pm 1.20_{\rm stat} \pm 0.39_{\rm syst})$ MeV	–
f_{D^+}	$(203.8 \pm 5.2_{\rm stat} \pm 1.8_{\rm syst})$ MeV	(212.7 ± 0.6) MeV [22]
$\lvert V_{cd}\rvert$	$0.2150 \pm 0.0055_{\rm stat} \pm 0.0020_{\rm syst}$	0.22438 ± 0.00044 [21]
$\mathcal{B}(D^+ \to \tau^+\nu_\tau)$	$(1.20 \pm 0.24_{\rm stat} \pm 0.12_{\rm syst}) \times 10^{-4}$ [24]	–
$\Gamma(D^+ \to \tau^+\nu_\tau)/\Gamma(D^+ \to \mu^+\nu_\mu)$	$3.21 \pm 0.64_{\rm stat} \pm 0.43_{\rm syst}$ [24]	2.67
$\mathcal{B}(D_s^+ \to \mu^+\nu_\mu)$	$(5.49 \pm 0.16_{\rm stat} \pm 0.15_{\rm syst}) \times 10^{-3}$ [25]	–
$f_{D_s^+}\lvert V_{cs}\rvert$	$(246.2 \pm 3.6_{\rm stat} \pm 3.5_{\rm syst})$ MeV	–
$f_{D_s^+}$	$(252.9 \pm 3.7_{\rm stat} \pm 3.6_{\rm syst})$ MeV	(249.9 ± 0.5) MeV [22,26]
$\lvert V_{cs}\rvert$	$0.985 \pm 0.014_{\rm stat} \pm 0.014_{\rm syst}$	0.97359 ± 0.00011 [21]
$\Gamma(D_s^+ \to \tau^+\nu_\tau)/\Gamma(D_s^+ \to \mu^+\nu_\mu)$	9.98 ± 0.52 [25]	9.74
$f_{D_s^+}/f_{D^+}$	$1.24 \pm 0.04_{\rm stat} \pm 0.02_{\rm syst}$ [25]	1.1783 ± 0.0016 [28]

peak. From this, BESIII obtained the world's most accurate branching fraction measurement for $D^+ \to \mu^+\nu_\mu$ decay [23], as shown in Table 1. By inputting either the LQCD-calculated value for the decay constant [22] or the CKM matrix element values from a global SM fit [21], the $|V_{cd}|$ or f_{D^+} can be extracted; the corresponding results are listed in Table 1. Using the same data sample, BESIII recently reported the first measurement of the absolute decay branching fraction for $D^+ \to \tau^+\nu_\tau$ with a significance of 5.1σ [24]. The presence of additional final-state neutrinos from the τ^+ decays results in more background and a relatively larger systematic uncertainty than in the $D^+ \to \mu^+\nu_\mu$ decay measurement.

To study the $D_s^+ \to \mu^+\nu_\mu$ signal channel, BESIII uses $e^+e^- \to D_s^+D_s^{*-}$ collisions at the center-of-mass energy of 4178 MeV and performs a similar analysis as was used for the $D^+ \to \mu^+\nu_\mu$ decay measurement [25]; the $D_s^+ \to \mu^+\nu_\mu$ signal peak is shown in Fig. 3(b). The absolute branching fraction and the product $f_{D_s^+}|V_{cs}|$ are obtained as listed in Table 1. Taking the CKM matrix element $|V_{cs}|$ from the latest global SM fit [21], the D_s^+ decay constant is determined. Alternatively, taking the averaged decay constant from recent LQCD calculations [22,26], the CKM matrix element is extracted as listed in Table 1. These are the most precise measurements to date, and provide an important calibration of the theoretical calculations of $f_{D_s^+}$ and a stringent test of the unitarity of the CKM matrix with an improved accuracy.

Using the world average values from the Particle Data Group (PDG) [21], we determine the ratio

$$R^{D^+}_{\tau/\mu} = \Gamma(D^+ \to \tau^+\nu_\tau)/\Gamma(D^+ \to \mu^+\nu_\mu) = 3.21 \pm 0.64_{\rm stat} \pm 0.43_{\rm syst}, \quad (4)$$

which, although still statistically limited, is consistent with the SM prediction of 2.67. With BESIII's expected future 20 fb^{-1} data set at the $\psi(3770)$ peak, as discussed in [9] and approved by the collaboration, the precision on $R^{D_s^+}_{\tau/\mu}$ will be statistically improved to about 8%, which will provide an important test of the lepton flavor universality (LFU). For the D_s^+, we obtain

$$R^{D_s^+}_{\tau/\mu} = \Gamma(D_s^+ \to \tau^+\nu_\tau)/\,\Gamma(D_s^+ \to \mu^+\nu_\mu) = 9.98 \pm 0.52, \quad (5)$$

which agrees with the SM-predicted value of 9.74. Meanwhile, $D_s^+ \to \tau^+\nu_\tau$ decays are currently being studied at BESIII with an expected result that will have a precision comparable to that achieved for the $D_s^+ \to \mu^+\nu_\mu$ decay mode. This result should improve the accuracy of the $f_{D_s^+}|V_{cs}|$ measurement and can also be used to test LFU in the ratio $R^{D_s^+}_{\tau/\mu}$ with a precision of 4.7% based on the current data set [9]. With the expected 6 fb^{-1} data set at 4178 MeV, as discussed in [9], the precision on $R^{D_s^+}_{\tau/\mu}$ will be systematically limited at about 3% or less, which will provide for the most stringent test of the μ–τ LFU in heavy quark decays [27].

Finally, combining the measured $f_{D_s^+}|V_{cs}|$ value with its $f_{D^+}|V_{cd}|$ counterpart, along with the $|V_{cd}/V_{cs}|$ value from the global SM fit [21], BESIII made a direct measurement of the $f_{D_s^+}/f_{D^+}$ decay constant ratio [25] that is 1.5σ higher than the Flavour Lattice Averaging Group (FLAG) world average value [28], as shown in Table 1. Since LQCD can make a very accurate prediction of $f_{D_s^+}/f_{D^+}$, which is a unique property of purely leptonic D^+/D_s^+ decays, BESIII can make unambiguous measurements of fundamental SM parameters and perform detailed studies of the charmed hadron decay dynamics. For these purposes, more data are needed at the $D\bar{D}$ and $D_s^+D_s^{*-}$ thresholds to pursue high-precision calibrations of LQCD calculations [9].

Precision measurements of the transition form factors

In the SM, semi-leptonic decays of charmed hadrons involve the interaction of a leptonic current with a hadronic current. The latter is non-perturbative and cannot be calculated from first principles; thus, it is usually parameterized in terms of form factors. Still, the weak and strong effects in semi-leptonic decays can be well separated, since there are no strong final-state interactions between the leptonic and hadronic systems. Among the semi-leptonic decays, the simplest case is $D^{0/+} \to P\ell^+\nu_\ell$ (where P denotes a pseudoscalar meson), for which the differential partial decay width is given, in the limit of negligible charged lepton mass, by

$$\frac{\mathrm{d}\Gamma(D^{0/+} \to P\,\ell^+\nu_\ell)}{\mathrm{d}q^2} = \frac{G_F^2|V_{cq}|^2}{24\pi^3}\,p_P^3\,|f_+^P(q^2)|^2. \quad (6)$$

Here p_P is the magnitude of the three-momentum of the P meson in the $D^{0/+}$ rest frame and $f_+^P(q^2)$ is the form factor of the hadronic weak current depending on $q^2 = |M(\ell^+\nu_\ell)|^2$, the square of the four-momentum transfer between the initial state $D^{0/+}$ and final state P. Thus, semi-leptonic decays can be used to extract the product of a form factor normalization chosen to be at $q^2 = 0$ and a CKM matrix element: $|V_{cq}|\,f_+^P(0)$. These decays allow for a robust determination of the $|V_{cs}|$ and $|V_{cd}|$ CKM matrix elements in conjunction with form factors determined from LQCD calculations. Alternatively, by inputting CKM matrix elements one can determine the form factors to provide high-precision tests of LQCD calculations.

The CLEO experiment had made precision measurements of semi-leptonic charm-decay rates using a data set accumulated at the $\psi(3770)$ peak [29]. With a three-times-larger data set, BESIII reported improved measurements of the absolute decay rates and the form factors, thereby assuming an important role in the precision tests of LQCD calculations [9].

Notably, measurements of the exclusive $D^0 \to K^-\ell^+\nu_\ell$ and $\pi^-\ell^+\nu_\ell$ decays, as well as $D^+ \to \bar{K}^0\ell^+\nu_\ell$ and $\pi^0\ell^+\nu_\ell$ decay modes, with $\ell = e$ or μ, have been reported [30,31]. Results for the absolute branching fractions are summarized in Table 2. From studies of the differential decay rates (see Equation (6)), the products of the hadronic form factor at $q^2 = 0$ and the magnitude of the CKM matrix element, $|V_{cs}|\,f_+^K(0)$ and $|V_{cd}|\,f_+^\pi(0)$, are shown in Table 2. Combining these products with the values of $|V_{cs}|$ and $|V_{cd}|$ from the SM-constrained fit [21], we extract the transition form factors

$$f_+^K(0) = 0.7368 \pm 0.0026_{\mathrm{stat}} \pm 0.0036_{\mathrm{syst}}$$

and

$$f_+^\pi(0) = 0.6372 \pm 0.0080_{\mathrm{stat}} \pm 0.0044_{\mathrm{syst}},$$

and their ratio

$$\frac{f_+^\pi(0)}{f_+^K(0)} = 0.865 \pm 0.013,$$

which is in good agreement with the present average (0.834 ± 0.023) of LQCD calculations [27,28] and a light cone sum rule value 0.84 ± 0.04 [32]. The experimental precision is better than that of the

Table 2. Measurements of D^0/D^+, D_s^+ and Λ_c semi-leptonic decays with near-threshold data at BESIII, and comparisons between experimental results and theoretical expectation or SM-global fit results. (Here '–' indicates not available.)

Observable	Measurement	Prediction/fit
$\mathcal{B}(D^0 \to K^- e^+ \nu_e)$	$(3.505 \pm 0.014_{\rm stat} \pm 0.033_{\rm syst})\%$ [30]	–
$\lvert V_{cs}\rvert f_+^K(0)$	$0.7172 \pm 0.0025_{\rm stat} \pm 0.0035_{\rm syst}$ [30]	–
$f_+^K(0)$	$0.7368 \pm 0.0026_{\rm stat} \pm 0.0036_{\rm syst}$ [30]	$0.747 \pm 0.011 \pm 0.015$ [28]
$\mathcal{B}(D^0 \to \pi^- e^+ \nu_e)$	$(0.295 \pm 0.004_{\rm stat} \pm 0.003_{\rm syst})\%$ [30]	–
$\lvert V_{cd}\rvert f_+^\pi(0)$	$0.1435 \pm 0.0018_{\rm stat} \pm 0.0009_{\rm syst}$ [30]	–
$f_+^\pi(0)$	$0.6372 \pm 0.0080_{\rm stat} \pm 0.0044_{\rm syst}$ [30]	$0.66 \pm 0.02 \pm 0.02$ [28]
$\mathcal{B}(D^+ \to \bar{K}^0 e^+ \nu_e)$	$(8.60 \pm 0.06_{\rm stat} \pm 0.15_{\rm syst})\%$ [31]	–
$f_+^K(0)$	$0.725 \pm 0.004_{\rm stat} \pm 0.012_{\rm syst}$ [31]	$0.747 \pm 0.011 \pm 0.015$ [28]
$\mathcal{B}(D^+ \to \pi^0 e^+ \nu_e)$	$(0.363 \pm 0.008_{\rm stat} \pm 0.005_{\rm syst})\%$ [31]	–
$f_+^\pi(0)$	$0.622 \pm 0.012_{\rm stat} \pm 0.003_{\rm syst}$ [31]	$0.66 \pm 0.02 \pm 0.02$ [28]
$f_+^\pi(0)/f_+^K(0)$	0.865 ± 0.013 [31]	0.84 ± 0.04 [32]
$\mathcal{B}(\Lambda_c^+ \to \Lambda e^+ \nu_e)$	$(3.63 \pm 0.38_{\rm stat} \pm 0.20_{\rm syst})\%$ [33]	–
$\mathcal{B}(\Lambda_c^+ \to \Lambda \mu^+ \nu_\mu)$	$(3.49 \pm 0.46_{\rm stat} \pm 0.27_{\rm syst})\%$ [34]	–
$\mathcal{B}(\Lambda_c^+ \to \Lambda \mu^+ \nu_\mu)/\mathcal{B}(\Lambda_c^+ \to \Lambda e^+ \nu_e)$	$0.96 \pm 0.16_{\rm stat} \pm 0.04_{\rm syst}$ [34]	≈ 1.0

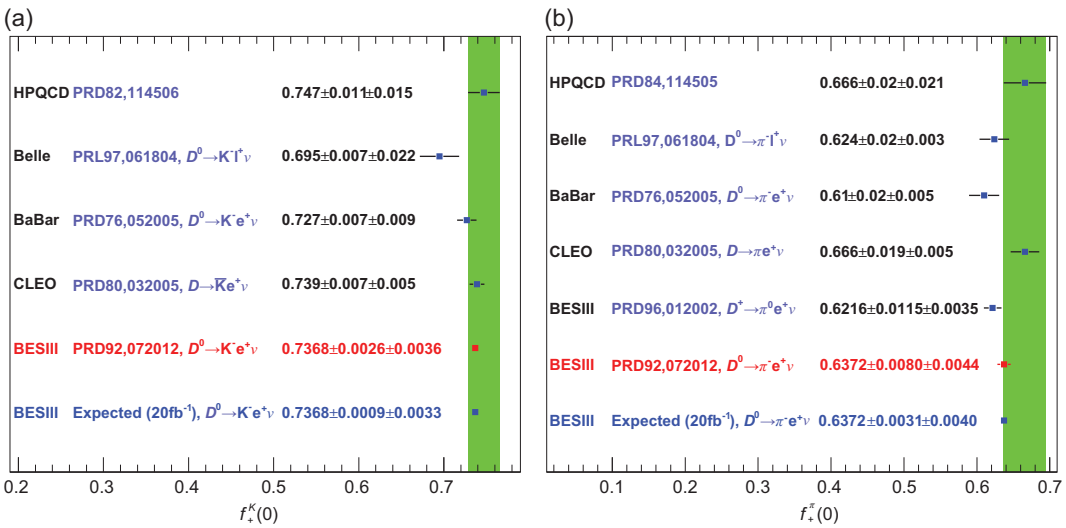

Figure 4. Comparison of the results for (a) $f_+^K(0)$ and (b) $f_+^\pi(0)$ measured by the Belle, BaBar, CLEO-c and BESIII experiments. The green bands present the LQCD uncertainties. The value marked in red denotes the best measurement from BESIII, and the value marked in dark blue denotes the expected precision from BESIII with ten times the current data set [9]. (Courtesy of Hai-Long Ma, Institute of High Energy Physics, Chinese Academy of Sciences.)

theoretical calculation. The measurement of $f_+^\pi(0)$ is dominated by statistical uncertainties. More data will reduce these uncertainties as discussed in the BESIII future physics programme [9]. Figure 4 shows the form factors $f_+^K(0)$ and $f_+^\pi(0)$ measured by various experiments together with results from LQCD calculations [27,28].

Based on a 567 pb^{-1} data set collected at 4.6 GeV, an energy point slightly above the $\Lambda_c^+\bar{\Lambda}_c^-$ production threshold, BESIII made the first absolute branching fraction measurement of $\Lambda_c^+ \to \Lambda e^+ \nu_e$ [33]. Similar to the tagging technique employed in the $D\bar{D}$ threshold production, the $\bar{\Lambda}_c^-$ is tagged via its hadronic decay modes. As an example, Fig. 5 shows the beam-constrained mass $M_{\rm BC}$ distribution for the $\bar{\Lambda}_c^- \to \bar{p}K^+\pi^-$ tagging mode, where the background level is very low. This is typical for most tagging modes and demonstrates that the threshold data sets provide unique opportunities for nearly background-free charmed baryon decay measurements. Since the massless neutrino is undetected, the kinematic variable $U_{\rm miss} = E_{\rm miss} - c|\vec{p}_{\rm miss}|$ is used to infer its presence, where $E_{\rm miss}$ and $\vec{p}_{\rm miss}$ are the missing energy and missing

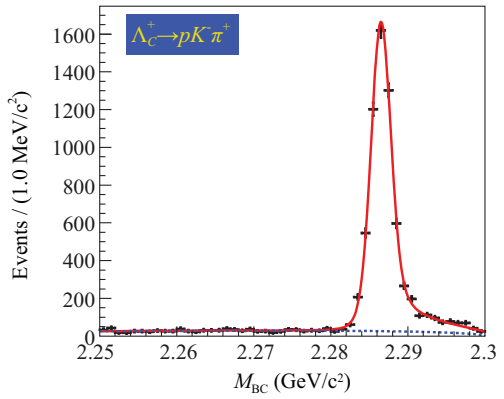

Figure 5. Fit to the $M_{\rm BC}$ distribution for $\bar{\Lambda}_c^- \to \bar{p}K^+\pi^-$ decay in the tag side. The points with error bars are data, the solid curves show the total fits and the dashed curves are the background shapes. (Courtesy of Pei-Rong Li, Lanzhou University.)

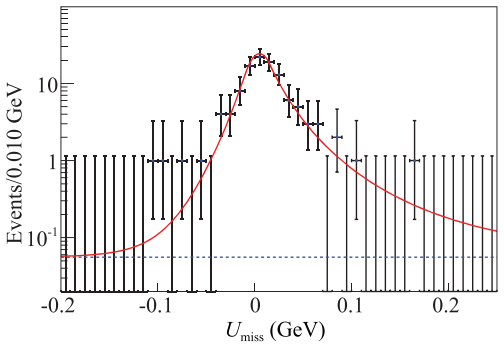

Figure 6. Fit to the $U_{\rm miss}$ distribution within the Λ signal region [33]. The points with error bars are data, the solid curves show the total fits and the dashed curves are the background shapes. Plot is from [33].

momentum carried by the neutrino, respectively. The calculation methods of $E_{\rm miss}$ and $\vec{p}_{\rm miss}$ can be found in [33]. The $U_{\rm miss}$ distribution is presented in Fig. 6, and a tiny background under the signal peak is inferred. From this, the absolute branching fractions for $\Lambda_c^+ \to \Lambda e^+\nu_e$ and $\Lambda_c^+ \to \Lambda\mu^+\nu_\mu$ decays are determined. For the $\Lambda_c^+ \to \Lambda e^+\nu_e$ case, the BESIII result listed in Table 2 corresponds to a two-fold improvement in the precision of the world average value. Since the branching fraction for $\Lambda_c^+ \to \Lambda e^+\nu_e$ is the benchmark and serves as a normalization mode for all other Λ_c^+ semi-leptonic channels, the BESIII result allows for stringent tests of different theoretical models. For the muonic decay $\Lambda_c^+ \to \Lambda\mu^+\nu_\mu$, the BESIII result is the first direct measurement [34], and with it the branching fraction ratio is determined to be

$$\mathcal{B}(\Lambda_c^+ \to \Lambda\mu^+\nu_\mu)/\mathcal{B}(\Lambda_c^+ \to \Lambda e^+\nu_e) = 0.96 \pm 0.16_{\rm stat} \pm 0.04_{\rm syst},$$

which is consistent with $e-\mu$ LFU. The form factors for charmed baryon transition to light hyperons/baryons will be studied with high precision when more threshold data samples are collected by BESIII [9]. The detailed q^2-dependent transition form factors can be studied at BESIII, and will provide unique calibrations of LQCD calculations. Alternatively, with LQCD predictions as input, BESIII measurements can be used to test LFU at any given q^2 value.

Impact on CKM matrix elements: $|V_{cs}|$ and $|V_{cd}|$

If precision LQCD calculations of the decay constants and form factors are taken as inputs, measurements of branching fractions for the purely leptonic and semi-leptonic decays can be used to confront weak-interaction physics. In the past decade, great progress has been made in the LQCD calculations of decay constants. The uncertainties of the results have been reduced from the level of 1%–2% to 0.2% [28]. With these, the BESIII leptonic-decay measurements have uncertainties of 2.5% and 1.5% for $|V_{cd}|$ and $|V_{cs}|$, respectively, and dominate the PDG world average values. For leptonic decays, the statistical error on $|V_{cd}|$ is larger than the systematic error, while the statistical and systematic uncertainties of $|V_{cs}|$ are comparable, as shown in Fig. 7. The BESIII result for $|V_{cd}|$ listed in Fig. 7(a) is within 1.7σ of the value obtained from a global SM fit to the other CKM matrix element measurements that assumes unitarity.

With additional data from the next 10-year physics programme for BESIII [9], the relative errors on the $|V_{cs}|$ and $|V_{cd}|$ determinations with purely leptonic decays will both reach the 1% level; if the $|V_{cd}|$ result is the same as its current central value, the significance of the discrepancy would increase to about the 4σ level, as shown in Fig. 7(a).

In addition, with the FLAG [28] world average value for $(f_{D_s^+}/f_{D^+})^{\rm FLAG} = 1.1783 \pm 0.0016$, BESIII obtained $|V_{cd}/V_{cs}|^2 = 0.048 \pm 0.003_{\rm stat} \pm 0.001_{\rm syst}$, which is consistent with that expected with the values of $|V_{cs}|$ and $|V_{cd}|$ given by the CKMfitter group to within 2σ [36]. The error on the ratio $|V_{cd}/V_{cs}|^2$ is currently dominated by the limited experimental statistics, and with the planned BESIII final data sample, we expect that the statistical uncertainty will be comparable to the systematic uncertainty that arises mainly from the LQCD decay constant calculations.

The matrix elements $|V_{cs}|$ and $|V_{cd}|$ can also be determined from the measured partial widths for the semi-leptonic decays $D^{0(+)} \to \bar{K}\ell\nu_\ell$ and $D^{0(+)} \to \pi\ell\nu_\ell$ with the computed values of the form

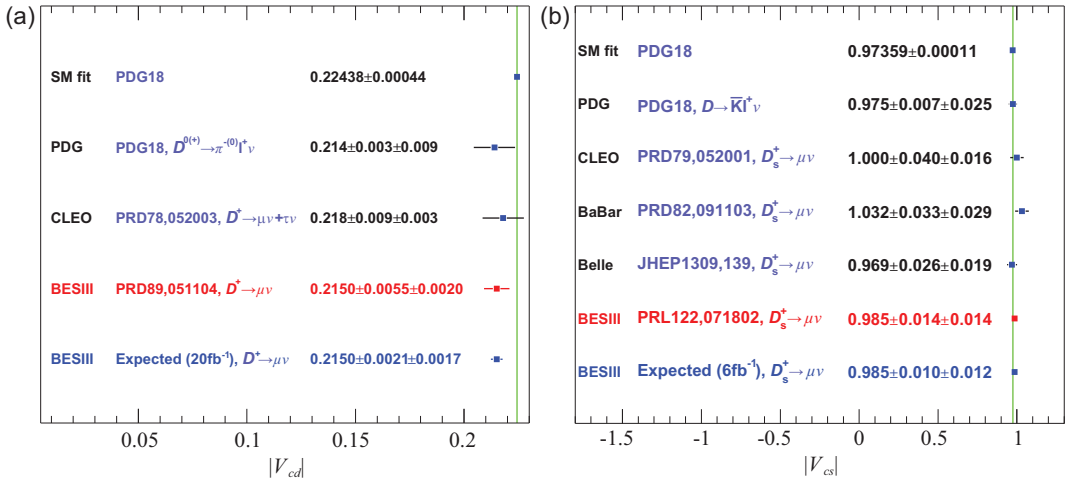

Figure 7. Precision of the measurements of (a) $|V_{cd}|$ and (b) $|V_{cs}|$. The green bands indicate the uncertainties of the average values from the global fit in the SM [35]. The circles, dots and rectangles with error bars are results derived from semi-leptonic D decays, purely leptonic D decays and other methods, respectively. The results marked in red denote the best measurements, and the values marked in light blue denote the expected precisions with the BESIII data sets that will be accumulated in the future [9]. (Courtesy of Hai-Long Ma, Institute of High Energy Physics, Chinese Academy of Sciences.)

factors from LQCD taken as inputs [28]. The results using this method are also shown in Fig. 7. At present, the uncertainties from LQCD calculations are 2.4% for $f_+^K(0)$ and 4.4% for $f_+^\pi(0)$, which are significantly larger than the uncertainties from the associated experimental measurements, and, therefore, limit the determinations of $|V_{cs}|$ and $|V_{cd}|$ with this approach.

With the future BESIII data and improvements in the LQCD calculations on the decay constants and form factors that are expected circa 2025, we can anticipate significantly improved constraints on the $(|V_{cs}|, |V_{cd}|)$ plane as shown in Fig. 8 [9], where direct contributions from the BESIII experiment are indicated. This will allow for precise tests of the consistency of CKM determinations from different quark sectors [9,36].

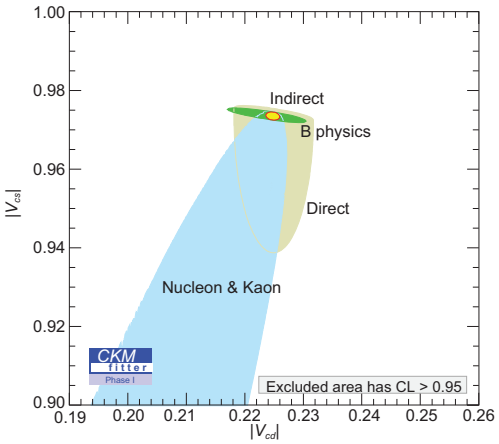

Figure 8. Constraints on the $(|V_{cs}|, |V_{cd}|)$ plane expected with the future BESIII data-taking plan as described in the BESIII white paper [9]. The indirect (green) constraints (from B decays) are related to $|V_{cs}|$ and $|V_{cd}|$ by unitarity [36]. The direct (gray) constraints combine purely leptonic and semi-leptonic $D_{(s)}$ decays from the BESIII experiment. The red circled region of the global combination corresponds to the 68% confidence level. Plot is from [9].

Impact on the charm lifetime and SU(3)$_F$ symmetry from inclusive semi-leptonic decays

Isospin symmetry requires that the charged and neutral D mesons have the same inclusive semi-leptonic partial widths for Cabibbo-favored decays [37], and this is confirmed by experiments within measurement uncertainties [21]. This prediction is expected to be reliable, since the lepton cannot interact strongly with the final-state hadrons, and the charged and neutral D mesons differ only in the isospin of the light quark. Therefore, a precise measurement of the $\Gamma(D^0\to Xe^+\nu_e)/\Gamma(D^+\to Xe^+\nu_e)$ ratio (X refers to any accessible hadronic system) provides a test of isospin symmetry. With current values from the PDG [21], one has $\Gamma(D^0\to Xe^+\nu_e) = (1.583\pm0.027)\times10^{11}\ \mathrm{s}^{-1}$ and $\Gamma(D^+\to Xe^+\nu_e) = (1.545\pm0.031)\times10^{11}\ \mathrm{s}^{-1}$, and the observed ratio is

$$R_{Xe\nu}^{D^0/D^+} = \frac{\Gamma(D^0\to Xe^+\nu_e)}{\Gamma(D^+\to Xe^+\nu_e)} = 1.025\pm0.027. \quad (7)$$

It indicates the need for reduction of experimental uncertainties on the branching fraction measurements before the predicted deviations of this ratio

from unity can be identified. On the other hand, assuming the equality of semi-leptonic D^0 and D^+ partial widths, one obtains

$$\frac{\tau_{D^+}}{\tau_{D^0}} = \frac{\Gamma(D^0 \to \text{all})}{\Gamma(D^+ \to \text{all})} = \frac{\Gamma(D^0 \to \text{all})}{\Gamma(D^0 \to Xe^+\nu_e)} \times \frac{\Gamma(D^+ \to Xe^+\nu_e)}{\Gamma(D^+ \to \text{all})} = \frac{\mathcal{B}_{\text{SL}}^{D^+}}{\mathcal{B}_{\text{SL}}^{D^0}},$$

where $\mathcal{B}_{\text{SL}}^{D^+}(\mathcal{B}_{\text{SL}}^{D^0})$ is the inclusive semi-leptonic branching fraction for D^+ (D^0). Therefore, comparison of $\mathcal{B}_{\text{SL}}^{D^+}/\mathcal{B}_{\text{SL}}^{D^0}$ with τ_{D^+}/τ_{D^0} from direct lifetime measurements from other experiments provides a test of isospin symmetry in charm decays and QCD calculations. This analysis is currently ongoing at BESIII with triple the amount of CLEO-c data, and the sensitivity will be significantly improved.

Furthermore, inclusive semi-leptonic width measurements of strange and non-strange D mesons have revealed a clean determination of SU(3) breaking effects. According to the operator product expansion methods [38], the partial widths for the inclusive semi-leptonic decays of the D^+, D^0 and D_s^+ mesons should be equal up to SU(3)_F symmetry breaking and non-factorizable contributions (although their phase-space differences may not be trivial [38]). With the current values from the PDG [21], one has $\Gamma(D_s^+ \to Xe^+\nu_e) = (1.300 \pm 0.082) \times 10^{11}\ \text{s}^{-1}$, and the observed ratio is

$$R_{Xe\nu}^{D_s/D} = \frac{\Gamma(D_s^+ \to Xe^+\nu_e)}{\Gamma(D \to Xe^+\nu_e)} = 0.830 \pm 0.053. \quad (8)$$

Thus, the semi-leptonic D_s^+ decay rate is $(17.0 \pm 5.3)\%$ lower than the charge-averaged non-strange D semi-leptonic rate. This difference not only sheds light on strong-interaction dynamics, but can serve as a useful calibration for measurements using D_s^+ decays [38]. Inclusive $D_s^+ \to Xe^+\nu_e$ decay is currently being studied at BESIII with an expected precision that will be comparable to that achieved for the corresponding $D \to Xe^+\nu_e$ mode.

Similar to the cases for the charmed mesons ($D^0/D^+/D_s^+$), the lifetime of the Λ_c^+ charmed baryon is dominated by the weak decay of the charm quark, but is somewhat affected by the influence of the two accompanying light quarks (u and d) in the hadron state in contrast to the single light quark component in the meson case. Therefore, it will be interesting to make a comparison between the partial widths of the inclusive semi-leptonic decays $\Lambda_c^+ \to Xe^+\nu_e$ and $D \to Xe^+\nu_e$, so that one can further understand the internal interactions and structures in the charmed baryon and mesons. Information about exclusive semi-leptonic decays of the Λ_c^+ is sparse [21], and only the $\Lambda_c^+ \to \Lambda\ell^+\nu_\ell$ ($\ell = e$ and μ) decay mode has been measured. The measurement of the branching fraction of $\Lambda_c^+ \to \Lambda\ell^+\nu_\ell$ was first performed by the ARGUS collaboration [39] and subsequently by the CLEO collaboration [40]. Recently, the BESIII collaboration measured the absolute branching fraction of $\Lambda_c^+ \to \Lambda\ell^+\nu_\ell$, as discussed in the section entitled 'Precision measurements of the transition form factors' [33,34]. A comparison of the exclusive semi-leptonic decay and the inclusive semi-leptonic decay will guide searches for new semi-leptonic decay modes. Based on the threshold data at BESIII, the absolute branching fraction of the inclusive semi-leptonic decays of the Λ_c^+ baryon is determined to be $\mathcal{B}(\Lambda_c^+ \to Xe^+\nu_e) = (3.95 \pm 0.34_{\text{stat}} \pm 0.09_{\text{syst}})\%$ [41], from which we obtain [41]

$$\mathcal{B}(\Lambda_c^+ \to \Lambda e^+\nu_e)/\mathcal{B}(\Lambda_c^+ \to Xe^+\nu_e) = (91.9 \pm 12.5_{\text{stat}} \pm 5.4_{\text{syst}})\%$$

and determine the ratio

$$\Gamma(\Lambda_c^+ \to Xe^+\nu_e)/\Gamma(D \to Xe^+\nu_e) = 1.26 \pm 0.12,$$

which can be used to restrict different QCD models and understand the internal interactions and structures in the charmed baryon and mesons [38,42,43].

UNIQUE PROBES WITH QUANTUM ENTANGLED $D^0\bar{D}^0$ AND $\Lambda_c^+\bar{\Lambda}_c^-$ STATES

BESIII operating at the $\psi(3770)$ resonance is a 'charm factory' that produces $D^0\bar{D}^0$ pairs in a state of definite charge-conjugation eigenvalue $C = -$. The antisymmetry of the wave function of the $D^0\bar{D}^0$ state induces quantum entanglement between the decay amplitudes of two D mesons. In particular, if one D meson is reconstructed in a CP eigenstate, the other D meson is required to have the opposite CP quantum number, provided CP is conserved in D decays. Thus, the transition $\psi(3770) \to D^0\bar{D}^0$ occupies a special place in the charm experimentalist's and theorist's arsenal [44]. BESIII data at $\psi(3770)$ offer crucial experimental advantages for the determination of absolute branching fractions and interference between the two decay amplitudes from the entangled D^0 and $\bar{D}^0$ mesons [45–48], that can be used to access their relative strong phases [12]. This suite of measurements is important to the international program in precision flavor physics and widely considered to be one of the main motivations for a charm factory [9]. Particularly pertinent to this

review, BESIII offers unique opportunities to search for *CP* violation by exploiting quantum coherence in an almost background-free environment.

Analogously, the reaction $e^+e^- \to \Lambda_c^+\bar{\Lambda}_c^-$ produces charmed and anti-charmed baryon pairs. The $\Lambda_c^+\bar{\Lambda}_c^-$ pair must be in a *C*-odd quantum entangled state, which provides a unique opportunity to study the spin observables in the charmed baryon decays at BESIII.

In this section, we discuss some selected measurements, including: (1) the unique quantum-coherent measurement of strong phases in neutral D^0 hadronic decays and (2) the absolute branching fraction measurements of the Λ_c^+ hadronic decays firstly implemented in the cleanest way near threshold. Both of these topics are highlight results in charm physics at BESIII.

Relative strong phase and constraints on the *CP*-violation phase γ

The complex phases that result from the strong interactions between the hadrons in the final states cannot be reliably calculated in theory and must be determined experimentally [12]. The values of the strong phase differences between the Cabibbo-favored (CF) and doubly Cabbibo-suppressed (DCS) amplitudes in charmed meson decays are crucial inputs for the extraction of the *CP*-violation phase angle γ, i.e. the phase of the CKM matrix element V_{ub} [16,49], determined from measurements of *b*-hadron decays. A precise measurement of γ provides a benchmark for tests of the SM that can be used as a probe to search for evidence of physics beyond the SM [36,50,51]. Three methods have so far been proposed to determine γ: GLW [52,53], ADS [54,55] and Dalitz (GGSZ) [56] analyses. One of the most sensitive decay modes for measuring γ is $B^- \to DK^-$ with $D \to K_S\pi^+\pi^-$ [56], where D represents a superposition of D^0 and $\bar{D}^0$ mesons. The model-independent approach [57,58] requires a binned Dalitz plot analysis of the amplitude-weighted average cosine and sine of the relative strong phase between D^0 and $\bar{D}^0 \to K_S\pi^+\pi^-$ decay amplitudes to determine γ. These relative strong phases can be uniquely determined from quantum-correlated $\psi(3770) \to D^0\bar{D}^0$ decays.

In 2009 and 2010, the CLEO experiment presented first measurements of the strong-phase parameters by using 0.82 fb^{-1} of data [59,60]. The limited precision of these strong phase parameters translates into a systematic uncertainty for the measurement of γ of approximately 4° [61]. In the coming decade, the statistical uncertainty of γ is expected to be 1.5° or less, in which case the overall precision will be limited by the strong-phase inputs.

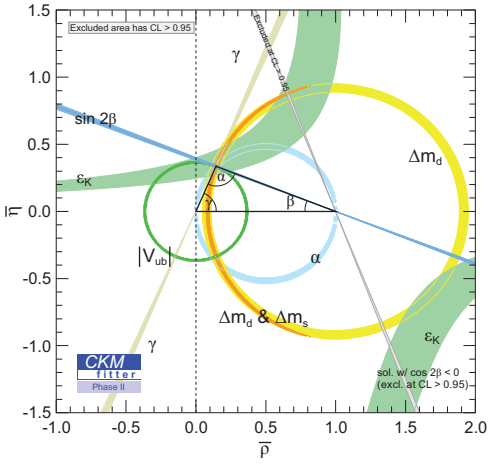

Figure 9. Evolving constraints and the global fit in the $(\bar{\rho}, \bar{\eta})$ plane (for $\bar{\rho}$ and $\bar{\eta}$, see Equation (2)) with the anticipated improvements by considering the LHCb upgrade [1] and final data set from the Belle II experiment [65]. The *CP*-violation phase γ is expected to have an accuracy around 0.4°, with the input from 20 fb^{-1} of data accumulated at the $D\bar{D}$ threshold [9] at BESIII. The shaded areas have the 95% confidence level. The plot is from the CKM fitter group [36] for the BESIII future physics programme [9]. Plot is from [9].

Hence, measurements of the relative strong-phase parameters with improved precision are a high priority activity that is critical for a range of *CP*-phase measurements. At present, BESIII is the only running experiment that can take data at the $D^0\bar{D}^0$-pair-production threshold. Based on 2.93 fb^{-1} of data, BESIII recently explored several methods to improve the analysis by incorporating more hadronic D^0 decays to increase statistics, including the development of partial reconstruction techniques to improve signal efficiency, and taking the effects of bin migration into account to reduce possible deviations of the results [62–64]. These improvements are critical to provide better precision and accuracy compared to previous measurements [61]. Using the new BESIII results, the effect of the strong-phase uncertainty on the value of γ will be reduced to around 1.0°, which is approximately a factor of 3 smaller than what was possible with the CLEO measurements [59,60]. This will ensure that the anticipated statistical improvements in the measurements of *CP*-phase γ at the LHCb and Belle II experiments over the next decade will have a deep impact on precision tests of the SM.

Given the future sensitivities resulting from the LHCb upgrade [1] and the final data set from Belle II [65], the overall constraints and the global CKM fit on the $(\bar{\rho}, \bar{\eta})$ plane (for $\bar{\rho}$ and $\bar{\eta}$, see Equation (2)) are shown in Fig. 9. The *CP*-phase γ is expected to have an accuracy of around 0.4° [66], thanks to the BESIII charm input that will be

available with the full data sample of 20 fb^{-1} at the $D\bar{D}$ mass threshold that is part of the experiment's future running plan [9]. Based on the future largest $D\bar{D}$ sample, quantum-coherence measurements of strong phases of more charm decay modes, as stated in [9], facilitate stringent cross checks of independent approaches of determining the γ angle and provide constraints in worldwide averaging the D^0–$\bar{D}^0$ mixing parameters and the involved indirect *CP* violation. The future high-statistics *B* decay data at future LHCb upgrade provide sensitivity in accessing the strong phase parameters in principle. However, the final BESIII measurement is a necessary input for reaching the target γ sensitivity.

Absolute branching fraction measurements of the Λ_c decays

Measurements of weak decays of charmed baryons provide useful information for understanding the interplay of weak and strong interactions, and are complementary to the information obtained from charmed mesons. The lightest charmed baryon Λ_c^+, with quark configuration *udc*, serves as the cornerstone of charmed baryon spectroscopy. However, the progress of the theoretical understanding of Λ_c^+ decays has been slow [51,67–73], mostly due to limited understanding of the non-perturbative effects in QCD theory in the charmed baryon sector.

Before 2014, most Λ_c^+ decay branching fractions were obtained by measuring their ratios to the reference mode $\Lambda_c^+ \to pK^-\pi^+$, thus introducing strong correlations and compounding uncertainties. The old, experimentally averaged branching fraction, $\mathcal{B}(\Lambda_c^+ \to pK^-\pi^+) = (5.0 \pm 1.3)\%$, had a large uncertainty due to the introduction of model assumptions on Λ_c^+ inclusive decays in these measurements [74]. Furthermore, only about 40% of the total decay rate had been measured and many modes were not identified, such as those with final-state neutrons. Therefore, comprehensive experimental measurements of various Λ_c^+ hadronic decays play an important role in improving different theoretical calculations [75] and developing the QCD methodology in handling non-perturbative effects.

Based on a 567 pb^{-1} data sample accumulated at 4.6 GeV, BESIII has systematically investigated the production and decays of the Λ_c^+ [9] for the first time using near-threshold data, which guarantee clean background and controllable systematics. BESIII provided absolute measurement of $\mathcal{B}(\Lambda_c^+ \to pK^-\pi^+)$ by counting the relative yields of the detected $\Lambda_c^+\bar{\Lambda}_c^-$ pairs over the single Λ_c^+, with the result $(5.84 \pm 0.27_{\text{stat}} \pm 0.23_{\text{syst}})\%$ [76]. This has competitive precision to the result $(6.84 \pm 0.24^{+0.21}_{-0.27})\%$ reported by Belle [77] at nearly the same time, and the combined precision of the two measurements is 5.2%, a five-fold reduction of the previous uncertainty [78]. Since this mode is the golden channel for detecting Λ_c^+ baryons in hadron collider experiments, the BESIII result impacts many aspects of heavy flavor physics. For instance, since the Λ_b^0 decays primarily to Λ_c^+ [42,79], it constrains the measurement of $|V_{ub}|$ via $\Lambda_b^0 \to \Lambda_c^+\mu^-\nu$. Improved measurements of Λ_c^+ hadronic decays can be used to constrain charm and bottom quark fragmentation functions by counting inclusive heavy flavor baryons [80].

In addition, BESIII reported numerous absolute branching fraction measurements of two-body CF and singly Cabibbo-suppressed (SCS) decays with improved precision, as listed in Table 3. The calculated branching fractions for these modes still have large uncertainties, and precise experimental measurements are essential to calibrate different models and explore the dynamics in charmed baryon decays. For instance, the improved precision provides crucial input to the theoretical predictions [88] for the observation channels of the doubly charmed baryon Ξ_{cc}^{++} at LHCb [89]. In particular, the improved precision of the SCS modes is useful for testing $\text{SU}(3)_\text{F}$ symmetry in the charm sector and provides insight of the size of *CP* violation in the charmed baryon sector [90].

Moreover, BESIII observed, for the first time, decay modes with a neutron in the final state, including $\Lambda_c^+ \to nK_S^0\pi^+$ [84] and $\Sigma^-\pi^+\pi^+\pi^0$ with $\Sigma^- \to n\pi^-$ [85]. These analyses were carried out by using the missing-mass technique to infer the presence of a final-state neutron that is only possible because of the kinematic constrains of pair production in near-threshold data at BESIII. The results provide useful input to tests of isospin symmetry in the charm sector.

The hadronic weak decays of charmed baryons are expected to violate parity conservation. For instance, in a two-body decay $\Lambda_c^+ \to BP$ (B denotes a $J^P = \frac{1}{2}^+$ baryon and P denotes a $J^P = 0^-$ pseudoscalar meson) the parity asymmetry is defined as $\alpha_{BP}^+ \equiv 2\text{Re}(s^*p)/(|s|^2 + |p|^2)$, where s and p stand for the parity-violating *s*-wave and parity-conserving *p*-wave amplitudes in the decay, respectively. For the process $\Lambda_c^+ \to \Lambda\pi^+$, which proceeds via a W interaction, $c \to W^+ + s$, the effects of parity violation are mainly determined by studying the polarization of the produced Λ via its decays to $p\pi^-$ from the initially (polarized) charmed baryons [75,91]. If *CP* is violated, the decay asymmetry parameters α_{BP}^+ for Λ_c^+ and $\bar{\alpha}_{\bar{B}\bar{P}}^-$ for $\bar{\Lambda}_c^-$ have different magnitudes but are opposite in sign. Hence, separate determinations of α_{BP}^+ and $\bar{\alpha}_{\bar{B}\bar{P}}^-$ would facilitate searching for the effects of *CP*

Table 3. Measurements of the Λ_c^+ hadronic decays (two-body CF, neutron-involved and SCS decays) at BESIII, and their comparisons to the previous world averages. For BESIII results, the first uncertainties are statistical and the second are systematic.

Decay channel	BESIII (%)	Previous world averages (%) [78]
Two-body CF		
pK_S^0	$1.52 \pm 0.08 \pm 0.03$ [76]	1.15 ± 0.30
$\Lambda\pi^+$	$1.24 \pm 0.07 \pm 0.03$ [76]	1.07 ± 0.28
$\Sigma^0\pi^+$	$1.27 \pm 0.08 \pm 0.03$ [76]	1.05 ± 0.28
$\Sigma^+\pi^0$	$1.18 \pm 0.10 \pm 0.03$ [76]	1.00 ± 0.34
$\Sigma^+\omega$	$1.56 \pm 0.20 \pm 0.07$ [76]	2.7 ± 1.0
Ξ^0K^+	$0.590 \pm 0.086 \pm 0.039$ [81]	0.50 ± 0.12
$\Xi(1530)^0K^+$	$0.502 \pm 0.099 \pm 0.031$ [81]	0.4 ± 0.1
$\Sigma^+\eta$	$0.41 \pm 0.19 \pm 0.05$ [82]	0.70 ± 0.23
$\Sigma^+\eta'$	$1.34 \pm 0.53 \pm 0.19$ [82]	First evidence
$\Sigma(1385)^+\eta$	$0.91 \pm 0.18 \pm 0.09$ [83]	1.22 ± 0.37
Neutron-involved		
$nK_S^0\pi^+$	$1.82 \pm 0.23 \pm 0.11$ [84]	First observation
$\Sigma^-\pi^+\pi^+$	$1.81 \pm 0.17 \pm 0.09$ [85]	2.1 ± 0.4
$\Sigma^-\pi^+\pi^+\pi^0$	$2.11 \pm 0.33 \pm 0.14$ [85]	First observation
SCS		
$p\phi$	$0.106 \pm 0.019 \pm 0.014$ [86]	0.082 ± 0.027
$p\eta$	$0.124 \pm 0.028 \pm 0.010$ [87]	First evidence
$p\pi^0$	< 0.027at90%C.L. [87]	First measurement
$p\pi^+\pi^-$	$0.391 \pm 0.028 \pm 0.039$ [86]	0.35 ± 0.2
pK^+K^- (non-ϕ)	$0.0547 \pm 0.0130 \pm 0.0074$ [86]	0.035 ± 0.017

violation. So far, only a few decay asymmetry parameters, e.g. $\alpha_{\Lambda\pi}$ for $\Lambda_c^+ \to \Lambda\pi^+$, and $\alpha_{\Sigma^+\pi^0}$ for $\Lambda_c^+ \to \Sigma^+\pi^0$, have been studied, and even those with limited precision [21]. Therefore, improved or new decay asymmetry measurements are desirable, as they could shed light on the decay mechanism and allow searches for *CP* asymmetries in the charmed baryon sector. In addition the decay asymmetry values allow for discrimination between different theoretical models, as listed in [75,92].

In the near-threshold production of $\Lambda_c^+\bar{\Lambda}_c^-$ pairs, non-zero transverse polarization of the Λ_c^+ will aid the determinations of the decay asymmetries. The decay asymmetry parameters are determined by analyzing the multi-dimensional angular distributions, where the full cascade decay chains are considered. The detailed method can be found in [93], in which a joint extraction of the four decay parameters of $\alpha_{\Lambda\pi}, \alpha_{\Sigma^+\pi^0}, \alpha_{\Sigma^0\pi^+}$ and $\alpha_{p\bar{K}^0}$ at the same time was carried out based on the Λ_c^+ sample at 4.6 GeV. An indiction of a non-zero transverse polarization is seen with a significance of 2.1σ, as shown in Fig. 10, which makes the measurement of the asymmetry parameter $\alpha_{p\bar{K}^0}$ accessible experimentally for the first time. The asymmetry parameters [93] for the $p\bar{K}^0$, $\Lambda\pi^+$, $\Sigma^+\pi^0$ and $\Sigma^0\pi^+$ modes are measured to be $0.18 \pm 0.43_{\rm stat} \pm 0.14_{\rm syst}$, $-0.80 \pm 0.11_{\rm stat} \pm 0.02_{\rm syst}$, $-0.57 \pm 0.10_{\rm stat} \pm 0.07_{\rm syst}$ and $-0.73 \pm 0.17_{\rm stat} \pm 0.07_{\rm syst}$, respectively. In comparison with previous results, the measurements for the $\Lambda\pi^+$ and $\Sigma^+\pi^0$ modes are consistent but have an improved precision, while the parameters for the $p\bar{K}^0$ and $\Sigma^0\pi^+$ modes are measured for the first time. At present, no theoretical model provides predictions that are fully consistent with all these measurements and BESIII measurements have become benchmarks to calibrate the QCD-derived theoretical models. During BESIII's 2020 data taking, about 10 times larger Λ_c^+ samples were accumulated at the center-of-mass energies between 4.6 and 4.7 GeV, and the significance of Λ_c^+ polarization could improve to more than 5σ. In this case the precision of the decay asymmetries will be improved at least by a factor of 3. With this information, tests of *CP* violations can be pursued for the two-body decays by comparing decay asymmetry parameters measured separately for Λ_c^+ and $\bar{\Lambda}_c^-$.

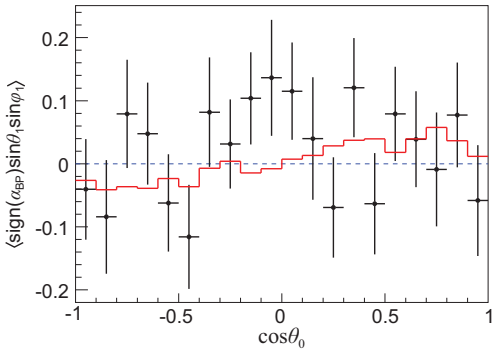

Figure 10. The effect of the Λ_c^+ transverse polarization versus $\cos\theta_0$ in $e^+e^- \to \Lambda_c\bar{\Lambda}_c$ at a center-of-mass energy of 4.6 GeV. Here θ_0 is the Λ_c^+ production angle relative to the e^--beam direction. The solid curve is a fit to the data; the dotted line is the expectation for zero polarization. Detailed description can be found in [93]. Plot is from [9].

SUMMARY AND PROSPECTS

Charm particle weak decays remain an exciting field for both theoretical and experimental investigations. In this article, we summarize results on charm decays that have been obtained in the BESIII experiment with data sets collected at the production thresholds of $D\bar{D}$, $D_s^{*+}D_s^-$ and $\Lambda_c^+\bar{\Lambda}_c^-$. These data samples allow the application of double-tag methods to fully reconstruct events even when invisible particles, such as neutrons or neutrinos, are present in the final states. This provides a unique environment to obtain the absolute branching fractions of charmed hadron decays to purely leptonic, semi-leptonic and hadronic final states with very low background levels. These BESIII measurements provide rigorous

Table 4. Prospects of some key measurements with the future data-taking plan in the BESIII white paper [9].

Observable	Measurement	BESIII [9]
$\mathcal{B}(D^+ \to \ell^+\nu_\ell)$	$f_{D^+}\lvert V_{cd}\rvert$	1.1%
$\mathcal{B}(D_s^+ \to \ell^+\nu_\ell)$	$f_{D_s^+}\lvert V_{cs}\rvert$	1.0%
$d\Gamma(D^{0/+} \to \bar{K}\ell^+\nu_\ell)/dq^2$	$f_+^K(0)\lvert V_{cs}\rvert$	0.5%
$d\Gamma(D^{0/+} \to \pi\ell^+\nu_\ell)/dq^2$	$f_+^\pi(0)\lvert V_{cd}\rvert$	0.6%
$d\Gamma(D_s^+ \to \eta\ell^+\nu_\ell)/dq^2$	$f_+^\eta(0)\lvert V_{cs}\rvert$	0.8%
Strong phases in D^0	Constraint on γ	$<0.4^\circ$
$\Lambda_c^+ \to pK^-\pi^+$	$\mathcal{B}(\Lambda_c^+ \to pK^-\pi^+)$	2%
$\Lambda_c^+ \to \Lambda\ell^+\nu_\ell$	$\mathcal{B}(\Lambda_c^+ \to \Lambda\ell^+\nu_\ell)$	3.3%

tests of QCD-based models and measurements of the CKM matrix elements $|V_{cs}|$ and $|V_{cd}|$, supply inputs to CKM weak phase measurements and test leptonic-flavor universality.

Charmed hadron studies will continue during the future upgrade of the BESIII experiment. By the end of the BESIII program, which will include some important machine upgrades, 10 times the current amount of data will be collected [9], and this will usher in a precision charm flavor era. High statistics data near the production thresholds with quantum-coherent initial states at BESIII will provide key measurements of the phase differences between the decay amplitudes while no reliable QCD-based computation is available. This suite of measurements is important to the worldwide flavor physics program. New inputs from future BESIII analyses based on larger data samples will deepen our understanding of the detailed dynamics of charm decays and hopefully facilitate reliable theoretical predictions for the *CP* asymmetry in the charm sector [3], therefore allowing us to search for new physics beyond the SM.

In addition, other experiments, such as LHCb and Belle II, are running and will produce huge statistics of charm hadrons, providing stringent constraints on *CP*-violation observables [3]. The sensitivity of the observed *CP* asymmetry in charmed meson decays by LHCb is about 3×10^{-4} [2], which is consistent with the SM expectation $\mathcal{O}(10^{-4} - 10^{-3})$ [94]. BESIII, with 20 fb^{-1} of data at the $\psi(3770)$ peak, can only reach a sensitivity level of a few percent on the *CP*-violation measurements, and the corresponding sensitivity at a super-τ-charm factory [95,96] is only $\mathcal{O}(10^{-3})$, which is still one order of magnitude lower than that for the current LHCb data set [97]. However, a super-τ-charm factory has the potential to provide constraints on the decay dynamics of charmed hadrons [98]. All these experiments plus their future upgrades will continue the studies of charmed hadron physics that will deepen our understanding of strong interactions in the charm sector, and constrain the SM parameters. Finally, Table 4 presents the precision prospects for some key charmed hadron measurements that are based on the BESIII future data-taking plan.

ACKNOWLEDGEMENTS

The authors especially thank Prof. S.L. Olsen for useful comments and suggestion.

FUNDING

This work was supported in part by the National Key Research and Development Program of China (2020YFA0406400), the National Natural Science Foundation of China (11822506, 11875054, and 11935018), the Chinese Academy of Sciences (CAS) (QYZDJ-SSW-SLH003), the CAS Large-Scale Scientific Facility Program, and the Fundamental Research Funds for the Central Universities.

Conflict of interest statement. None declared.

REFERENCES

1. Cerri A, Gligorov VV and Malvezzi S *et al.* Report from working group 4: opportunities in flavour physics at the HL-LHC and HE-LHC. *CERN Yellow Rep Monogr* 2019; **7**: 867–1158.
2. Aaij R, Abellan Beteta C and Adeva B *et al.* Observation of CP violation in charm decays. *Phys Rev Lett* 2019; **122**: 211803.
3. Saur M and Yu F-S. Charm CPV: observation and prospects. *Sci Bull* 2020; **65**: 1428–31.
4. Bianco S, Fabbri FL and Benson D *et al.* A Cicerone for the physics of charm. *Riv Nuovo Cim* 2003; **26N7**: 1–200.
5. Artuso M, Meadows B and Petrov AA. Charm meson decays. *Annu Rev Nucl Part Sci* 2008; **58**: 249–91.
6. Huang GS, Li HB and Lyu X-R. Highlights of the experiments performed on the Beijing spectrometer. *Physics* 2020; **49**: 499–512.
7. Kobayashi M and Maskawa T. CP violation in the renormalizable theory of weak interaction. *Prog Theor Phys* 1973; **49**: 652–7.
8. Ceccucci A, Gershon T and Kenzie M *et al.* Origins of the method to determine the CKM angle γ using $B^\pm \to DK^\pm$, $D \to K_S{}^0\pi^\pm\pi^-$ decays. arXiv:2006.12404.
9. Ablikim M, Achasov MN and Adlarson P *et al.* Future physics programme of BESIII. *Chin Phys C* 2020; **44**: 040001.
10. Ablikim M, Achasov MN and Ahmed S *et al.* Measurement of $e^+e^- \to D\bar{D}$ cross sections at the ψ(3770) resonance. *Chin Phys C* 2018; **42**: 083001.
11. Baltrusaitis RM, Becker J and Blaylock G *et al.* Direct measurements of charmed-*D*-meson hadronic branching fractions. *Phys Rev Lett* 1986; **56**: 2140–3.
12. Xing Z-Z. $D^0-\bar{D}^0$ mixing and CP violation in neutral *D*-meson decays. *Phys Rev D* 1997; **55**: 196–218.
13. Kang XW, Li HB and Lu GR *et al.* Study of CP violation in $\Lambda_c{}^+$ decay. *Int J Mod Phys A* 2011; **26**: 2523–35.
14. Kang XW and Li HB. Study of CP violation in $D \to VV$ decay at BESIII. *Phys Lett B* 2010; **684**: 137–40.

15. Charles J, Descotes-Genon S and Kang XW *et al.* Extracting CP violation and strong phase in D decays by using quantum correlations in $\psi(3770) \to D^0\bar{D}^0 \to (V_1V_2)(V_3V_4)$ and $\psi(3770) \to D^0\,\bar{D}^0 \to (V_1V_2)(K\pi)$. *Phys Rev D* 2010; **81**: 054032.
16. Wolfenstein L. Parametrization of the Kobayashi-Maskawa matrix. *Phys Rev Lett* 1983; **51**: 1945–7.
17. Buras AJ, Lautenbacher ME and Ostermaier G. Waiting for the top quark mass, $K^+ \to \pi^+ \nu\bar{\nu}$, B_s^0-$\bar{B}_s^0$ mixing, and CP asymmetries in B decays. *Phys Rev D* 1994; **50**: 3433–46.
18. Khlopov MY. Effects of symmetry violation in semileptonic meson decays. *Yad Fiz* 1978; **28**: 1134–6 (in Russian). English translation: *Sov J Nucl Phys* 1978; **28**: 583–5.
19. Gershtein SS and Khlopov MY. SU(4) symmetry breaking and lepton decays of heavy pseudoscalar mesons. *JETP Lett* 1976; **23**: 338.
20. Richman JD and Burchat PR. Leptonic and semi-leptonic decays of charm and bottom hadrons. *Rev Mod Phys* 1995; **67**: 893–976.
21. Zyla PA, Barnett RM and Beringer J *et al.* Review of particle physics. *Prog Theor Exp Phys* 2020; **2020**: 083C01.
22. Bazavov A, Bernard C and Brambilla N *et al.* Up-, down-, strange-, charm-, and bottom-quark masses from four-flavor lattice QCD. *Phys Rev D* 2018; **98**: 054517.
23. Ablikim M, Achasov MN and Ai XC *et al.* Precision measurements of $B(D^+ \to \mu^+\nu_\mu)$, the pseudoscalar decay constant $f_D{}^+$, and the quark mixing matrix element $|V_{cd}|$. *Phys Rev D* 2014; **89**: 051104.
24. Ablikim M, Achasov MN and Adlarson P *et al.* Observation of the leptonic decay $D^+ \to \tau^+\nu_\tau$. *Phys Rev Lett* 2019; **123**: 211802.
25. Ablikim M, Achasov MN and Ahmed S *et al.* Determination of the pseudoscalar decay constant $f_{D_s^+}$ via $D_s^+ \to \mu^+\nu_\mu$. *Phys Rev Lett* 2019; **122**: 071802.
26. Carrasco N, Dimopoulos P and Frezzotti R *et al.* Leptonic decay constants f_K, f_D, and f_{Ds} with $N_f = 2 + 1 + 1$ twisted-mass lattice QCD. *Phys Rev D* 2015; **91**: 054507.
27. Amhis YS, Banerjee SW and Ben-Haim E *et al.* Averages of b-hadron, c-hadron, and τ-lepton properties as of 2018. arXiv:1909.12524.
28. Aoki S, Aoki Y and Bečirević D *et al.* FLAG review 2019. *Eur Phys J C* 2020; **80**: 113.
29. Besson D, Pedlar TK and Xavier J *et al.* Improved measurements of D meson semi-leptonic decays to π and K mesons. *Phys Rev D* 2009; **80**: 032005.
30. Ablikim M, Achasov MN and Ai XC *et al.* Study of dynamics of $D^0 \to K^-e^+\nu_e$ and $D^0 \to \pi^-e^+\nu_e$ decays. *Phys Rev D* 2015; **92**: 072012.
31. Ablikim M, Achasov MN and Ahmed S *et al.* Analysis of $D^+ \to \bar{K}^0e^+\nu_e$ and $D^+ \to \pi^0e^+\nu_e$ semi-leptonic decays. *Phys Rev D* 2017; **96**: 012002.
32. Ball P. Testing QCD sum rules on the light-cone in $D \to (\pi, K)\ell\nu$ decays. *Phys Lett B* 2006; **641**: 50–6.
33. Ablikim M, Achasov MN and Ai XC *et al.* Measurement of the absolute branching fraction for $\Lambda_c^+ \to \Lambda\, e^+\nu_e$. *Phys Rev Lett* 2015; **115**: 221805.
34. Ablikim M, Achasov MN and Ahmed S *et al.* Measurement of the absolute branching fraction for $\Lambda_c^+ \to \Lambda\, \mu^+\nu_\mu$. *Phys Lett B* 2017; **767**: 42–7.
35. Tanabashi M, Hagiwara K and Hikasa K *et al.* Review of particle physics. *Phys Rev D* 2018; **98**: 030001.
36. Charles J, Hocker A and Lacker H *et al.* CP violation and the CKM matrix: assessing the impact of the asymmetric B factories. *Eur Phys J C* 2005; **41**: 1–131 and updates at http://ckmfitter.in2p3.fr.
37. Pais A and Treiman SB. Charmed meson lifetime ratios and production in $e^+ - e^-$ collisions. *Phys Rev D* 1977; **15**: 2529–32.
38. Gronau M and Rosner JL. Ratios of heavy hadron semi-leptonic decay rates. *Phys Rev D* 2011; **83**: 034025.
39. Albrecht H, Ehrlichmann H and Hamacher T *et al.* Observations of $\Lambda_c{}^+$ semi-leptonic decay. *Phys Lett B* 1991; **269**: 234–42.
40. Bergfeld T, Eisenstein BI and Gollin G *et al.* Study of the decay $\Lambda_c^+ \to \Lambda l^+\nu_l$. *Phys Lett B* 1994; **323**: 219–26.
41. Ablikim M, Achasov MN and Ahmed S *et al.* Measurement of the absolute branching fraction of the inclusive semi-leptonic Λ_c^+ decay. *Phys Rev Lett* 2018; **121**: 251801.
42. Rosner JL. Prospects for improved Λ_c branching fractions. *Phys Rev D* 2012; **86**: 014017.
43. Manohar AV and Wise MB. Inclusive semi-leptonic B and polarized Λ_b decays from QCD. *Phys Rev D* 1994; **49**: 1310–29.
44. Wilkinson G. Charming synergies: the role of charm-threshold studies in the search for physics beyond the Standard Model. *Sci Bull* 2021; **66**: 2251–3.
45. Ablikim M, Achasov MN and Ai XC *et al.* Amplitude analysis of the $D^+ \to K^0{}_S\,\pi^+\,\pi^0$ Dalitz plot. *Phys Rev D* 2014; **89**: 052001.
46. Ablikim M, Achasov MN and Ahmed S *et al.* Observation of the W-annihilation decay $D_s^+ \to \omega\,\pi^+$ and evidence for $D_s^+ \to \omega\,K^+$. *Phys Rev D* 2019; **99**: 091101.
47. Ablikim M, Achasov MN and Ai XC *et al.* Measurement of the branching fractions of $D_s^+ \to \eta'\,X$ and $D_s^+ \to \eta'\rho^+$ in $e^+e^- \to D_s^+D_s^-$. *Phys Lett B* 2015; **750**: 466–74.
48. Ablikim M, Achasov MN and Ai XC *et al.* Observation of the singly Cabibbo-suppressed decay $D^+ \to \omega\pi^+$ and evidence for $D^0 \to \omega\pi^0$. *Phys Rev Lett* 2016; **116**: 082001.
49. Chau LL and Keung WY. Comments on the parametrization of the Kobayashi-Maskawa matrix. *Phys Rev Lett* 1984; **53**: 1802–5.
50. Brod J and Zupan J. The ultimate theoretical error on γ from $B \to DK$ decays. *J High Energy Phys* 2014; **1401**: 051.
51. Asner DM, Barnes T and Bian JM *et al.* Physics at BES-III. *Int J Mod Phys A* 2009; **24**: S1–794.
52. Gronau M and London D. How to determine all the angles of the unitarity triangle from $B_d^0 \to D\,K_s$ and $B_s^0 \to D\phi$. *Phys Lett B* 1991; **253**: 483–8.
53. Gronau M and Wyler D. On determining a weak phase from CP asymmetries in charged B decays. *Phys Lett B* 1991; **265**: 172–6.
54. Atwood D, Dunietz I and Soni A. Enhanced CP violation with $B \to \mathrm{KD}^0(\bar{D}^0$ modes and extraction of the Cabibbo-Kobayashi-Maskawa angle γ. *Phys Rev Lett* 1997; **78**: 3257–60.
55. Atwood D, Dunietz I and Soni A. Improved methods for observing CP violation in $B^\pm \to KD$ and measuring the CKM phase γ. *Phys Rev D* 2001; **63**: 036005.
56. Giri A, Grossman Y and Soffer A *et al.* Determining γ using $B^\pm \to DK^\pm$ with multibody D decays. *Phys Rev D* 2003; **68**: 054018.
57. Bondar A and Poluektov A. Feasibility study of model-independent approach to ϕ_3 measurement using Dalitz plot analysis. *Eur Phys J C* 2006; **47**: 347–53.
58. Bondar A and Poluektov A. The use of quantum-correlated D^0 decays for ϕ_3 measurement. *Eur Phys J C* 2008; **55**: 51–6.
59. Briere RA, Vogel H and Onyisi PUE *et al.* First model-independent determination of the relative strong phase between D^0 and $\bar{D}^0 \to K_S{}^0\,\pi^+\pi^-$ and its impact on the CKM angle γ/ϕ_3 measurement. *Phys Rev D* 2009; **80**: 032002.

60. Libby J, Kornicer M and Mitchell RE *et al.* Model-independent determination of the strong-phase difference between D^0 and $\bar{D}^0 \to K^0_{S,L}\, h^+\, h^-$ ($h = \pi, K$) and its impact on the measurement of the CKM angle γ/ϕ_3. *Phys Rev D* 2010; **82**: 112006.
61. Aaij R, Adeva B and Adinolf M *et al.* Measurement of the CKM angle γ using $B^{\pm} \to DK^{\pm}$ with $D \to K_S{}^0\pi^+\pi^-$, $K_S{}^0K^+K^-$ decays. *J High Energy Phys* 2018; **1808**: 176. Erratum: 2018; 1810: 107 (2018).
62. Ablikim M, Achasov MN and Adlarson P *et al.* Model-independent determination of the relative strong-phase difference between D^0 and $\bar{D}^0 \to K^0_{S,L}\pi^+\pi^-$ and its impact on the measurement of the CKM angle γ/ϕ_3. *Phys Rev D* 2020; **101**: 112002.
63. Ablikim M, Achasov MN and Adlarson P *et al.* Determination of strong-phase parameters in $D \to K^0_{S,L}\pi^+\pi^-$. *Phys Rev Lett* 2020; **124**: 241802.
64. Ablikim M, Achasov MN and Ahmed S *et al.* Improved model-independent determination of the strong-phase difference between D^0 and $\bar{D}^0 \to K^0_{S,L}\, K^+K^-$ decays. *Phys Rev D* 2020; **102**: 052008.
65. Kou E, Urquijo P and Altmannshofer W *et al.* The Belle II physics book. *Prog Theor Exp Phys* 2019; **2019**: 123C01. Erratum: 2020; **2020**; 029201.
66. Aaij R, Bediaga I and Cruz Torres M *et al.* Physics case for an LHCb upgrade II—opportunities in flavour physics, and beyond, in the HL-LHC era. arXiv:1808.08865.
67. Körner JG and Krämer M. Exclusive nonleptonic charm baryon decays. *Z Phys C* 1992; **55**: 659–70.
68. Uppal T, Verma RC and Khanna MP. Constituent quark model analysis of weak mesonic decays of charm baryons. *Phys Rev D* 1994; **49**: 3417–25.
69. Zenczykowski P. Quark and pole models of nonleptonic decays of charmed baryons. *Phys Rev D* 1994; **50**: 402–11.
70. Chau LL, Cheng HY and Tseng B. Analysis of two-body decays of charmed baryons using the quark diagram scheme. *Phys Rev D* 1996; **54**: 2132–60.
71. Sharma KK and Verma RC. $SU(3)_{flavor}$ analysis of two-body weak decays of charmed baryons. *Phys Rev D* 1997; **55**: 7067–74.
72. Kohara Y. Two-body nonleptonic decays of charmed baryons. *Nuovo Cim A* 1998; **111**: 67–73.
73. Ivanov MA, Körner JG and Lyubovitskij VE *et al.* Exclusive nonleptonic decays of bottom and charm baryons in a relativistic three quark model: evaluation of nonfactorizing diagrams. *Phys Rev D* 1998; **57**: 5632–52.
74. Jaffe DE, Masek G and Paar HP *et al.* Measurement of $B(\Lambda_c^+ \to p\, K^-\, \pi^+)$. *Phys Rev D* 2000; **62**: 072005.
75. Cheng HY. Charmed baryons circa 2015. *Front Phys (Beijing)* 2015; **10**: 101406.
76. Ablikm M, Achasov MN and Ai XC *et al.* Measurements of absolute hadronic branching fractions of Λ_c^+ baryon. *Phys Rev Lett* 2016; **116**: 052001.
77. Zupanc A, Bartel C and Gabyshev N *et al.* Measurement of the branching fraction $B(\Lambda_c^+ \to p\, K^-\, \pi^+)$. *Phys Rev Lett* 2014; **113**: 042002.
78. Olive KA, Agashe K and Amsler C *et al.* Review of particle physics. *Chin Phys C* 2014; **38**: 090001.
79. Dytman SA, Mueller JA and Nam S *et al.* Measurement of exclusive B decays to final states containing a charmed baryon. *Phys Rev D* 2002; **66**: 091101.
80. Aaij R, Abellan Beteta C and Adeva B *et al.* Measurement of *b*-hadron production fractions in 7 TeV pp collisions. *Phys Rev D* 2012; **85**: 032008.
81. Ablikim M, Achasov MN and Ahmed S *et al.* Measurements of absolute branching fractions for $\Lambda_c^+ \to \Xi^0 K^+$ and $\Xi(1530)^0 K^+$. *Phys Lett B* 2018; **783**: 200–6.
82. Ablikim M, Achasov MN and Ahmed S *et al.* Evidence for the decays of $\Lambda_c^+ \to \Sigma^+\eta$ and $\Sigma^+\eta'$. *Chin Phys C* 2019; **43**: 083002.
83. Ablikim M, Achasov MN and Ahmed S *et al.* Measurement of the absolute branching fractions of $\Lambda_c{}^+ \to \Lambda\eta\pi^+$ and $\Sigma(1385)^+\eta$. *Phys Rev D* 2019; **99**: 032010.
84. Ablikim M, Achasov MN and Ahmed S *et al.* Observation of $\Lambda^+{}_c \to nK^0{}_S\pi_+$. *Phys Rev Lett* 2017; **118**: 112001.
85. Ablikim M, Achasov MN and Ahmed S *et al.* Observation of the decay $\Lambda_c{}^+ \to \Sigma^-\, \pi^+\pi^+\pi^0$. *Phys Lett B* 2017; **772**: 388–93.
86. Ablikm M, Achasov MN and Ahmed S *et al.* Measurement of singly Cabibbo suppressed decays $\Lambda_c^+ \to p\pi^+\pi^-$ and $\Lambda_c^+ \to pK^+K^-$. *Phys Rev Lett* 2016; **117**: 232002.
87. Ablikim M, Achasov MN and Ahmed S *et al.* Evidence for the singly-Cabibbo-suppressed decay $\Lambda_c^+ \to p\eta$ and search for $\Lambda_c^+ \to p\pi^0$. *Phys Rev D* 2017; **95**: 111102.
88. Yu FS, Jiang HY and Li RH *et al.* Discovery potentials of doubly charmed baryons. *Chin Phys C* 2018; **42**: 051001.
89. Aaij R, Adeva B and Adinolf M *et al.* Observation of the doubly charmed baryon Ξ_{cc}^{++}. *Phys Rev Lett* 2017; **119**: 112001.
90. Geng CQ, Hsiao YK and Liu CW *et al.* Charmed baryon weak decays with SU(3) flavor symmetry. *J High Energy Phys* 2017; **1711**: 147.
91. Wang D, Ping RG and Li L *et al.* Charmed baryon decay asymmetry in e^+e^- annihilation. *Chin Phys C* 2017; **41**: 023106.
92. Cheng HY. Charmed baryon physics circa 2021. arXiv:2109.01216.
93. Ablikim M, Achasov MN and Adlarson P *et al.* Measurements of weak decay asymmetries of $\Lambda_c^+ \to pK_S^0$, $\Lambda\pi^+$, $\Sigma^+\pi^0$, and $\Sigma^0\pi^+$. *Phys Rev D* 2019; **100**: 072004.
94. Cheng HY and Chiang CW. SU(3) symmetry breaking and CP violation in D -> PP decays. *Phys Rev D* 2012; **86**: 014014.
95. Bondar AE, Anashin VV and Aulchenko VM *et al.* Project of a super Charm-Tau factory at the Budker Institute of Nuclear Physics in Novosibirsk. *Yad Fiz* 2013; **76**: 1132–45.
96. Luo Q, Gao W and Lan J *et al.* Progress of conceptual study for the accelerators of a 2-7 GeV super Tau Charm facility at China. In: *10th International Particle Accelerator Conference*, Melbourne, Australia, 2019.
97. Xing ZZ. A U-spin prediction for the CP-forbidden transition $e^+\, e^- \to D^0\bar{D}^0 \to (K^+\, K^-)_D\, (\pi^+\, \pi^-)_D$. *Mod Phys Lett A* 2019; **34**: 1950238.
98. Bondar A, Poluektov A and Vorobiev V. Charm mixing in the model-independent analysis of correlated $D^0\ \bar{D}^0$ decays. *Phys Rev D* 2010; **82**: 034033.

REVIEW

National Science Review
8: nwab187, 2021
https://doi.org/10.1093/nsr/nwab187
Advance access publication 14 October 2021

PHYSICS

Special Topic: Physics of the BESIII Experiment

Probing the internal structure of baryons

Guangshun Huang [1,2,*], Rinaldo Baldini Ferroli[3,4,*] and BESIII Collaboration

ABSTRACT

Electromagnetic form factors are fundamental observables that describe the electric and magnetic structure of hadrons and provide keys to understand the strong interaction. At the Beijing Spectrometer (BESIII), form factors have been measured for different baryons in the time-like region for the first time or with the best precision. The results are presented with examples focused on but not limited to the proton/neutron, the Λ, with a strange quark, and the Λ_c, with a charm quark.

Keywords: baryon structure, form factor, threshold effect, abnormal production

[1]Department of Modern Physics, University of Science and Technology of China, Hefei 230026, China; [2]State Key Laboratory of Particle Detection and Electronics, Hefei 230026, China; [3]INFN Laboratori Nazionali di Frascati, I-00044 Frascati, Italy and [4]Institute of High Energy Physics, Chinese Academy of Sciences, Beijing 100049, China

*__Corresponding authors__. E-mails: hgs@ustc.edu.cn; baldini@lnf.infn.it

Received 24 January 2021; **Revised** 8 October 2021; **Accepted** 8 October 2021

INTRODUCTION

Baryons and mesons are both hadrons, i.e. bound systems of quarks in a naive quark model [1] or, more accurately, also gluons in modern theory. Baryons are half-integer spin fermions, comprised, in a first approximation, of three quarks held together by the strong interactions. Protons (p) and neutrons (n), collectively known as nucleons (N), are the lightest baryons, and are the major components of the observable matter of the Universe. A nucleon has three valence light quarks (u or d); if one or more of its u or d quarks are replaced by heavier quarks (s, c, b or t), it becomes a hyperon. The most known baryons are the spin 1/2 SU(3) octet, including the isospin doublet p/n, singly stranged isospin singlet Λ, singly stranged isospin triplet $\Sigma^-/\Sigma^0/\Sigma^+$ and the doubly stranged isospin doublet Ξ^-/Ξ^0 [2]. The lightest charmed baryon is the Λ_c^+ [2]. Hadrons are not point-like particles, and their internal electric and magnetic structure is characterized by their electromagnetic form factors (FFs).

The particles are so tiny (of the order of 10^{-15} m, or a femtometre) that they cannot be observed directly by the human eye (ability of 10^{-4} m, or 0.1 mm), an optical microscope (resolution of 10^{-7} m, or 0.1 μm) or even an electric microscope (resolution of 10^{-10} m, or 0.1 nm, the size of an atom). Instead, their properties are studied through collisions. When two particles traverse each other, they interact by exchanging force carriers called bosons that transfer some energy and momentum (i.e. four momentum) from one to the other. For electron-nucleon scattering, the electron is a probe that spies the secrets hidden inside the nucleon, and in this case the four-momentum transfer squared has a negative value ($q^2 < 0$), and is categorized as a space-like process. When a particle and an anti-particle meet, for example in the case of an electron and a positron, they can annihilate—i.e. disappear into a virtual photon—and then produce an fermion-antifermion pair that eventually materializes as a system of hadrons, of which a baryon-antibaryon pair is one possibility. In this case the four-momentum transfer squared has a positive value ($q^2 > 0$), and is classified as a time-like process. The Feynman diagrams for these two processes are shown in Fig. 1(a) and (b), respectively. For the latter, the form factors of the participating baryon can be deduced from the behavior of the outgoing baryon-antibaryon pair, which is the subject of the study covered in this paper.

Hadronic production data from electron-positron annihilations at low energies (around the giga-electron-volt order) are important to the understanding of the structure of hadrons and the strong interactions of their constituent quarks. Moreover, since hyperons are not stable, they can be studied only in the time-like domain. The Beijing Spectrometer (BESIII) [3] at the Beijng Electron Positron Collider (BEPCII) [4] operates in the

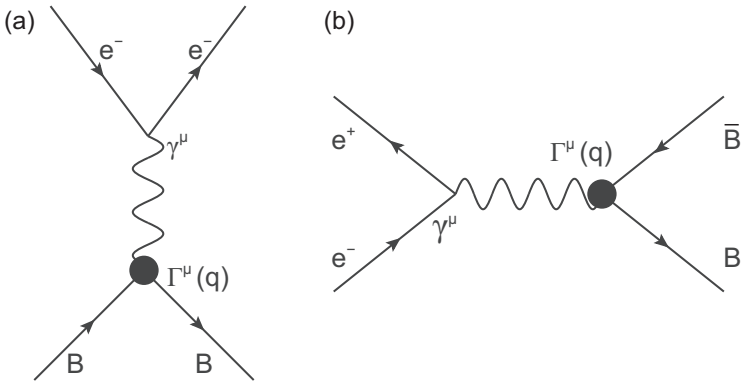

Figure 1. Lowest-order Feynman diagrams for elastic electron-hadron scattering $e^- B \to e^- B$ (a), and for the annihilation process $e^+ e^- \to B\bar{B}$ (b).

center-of-mass energy range from 2.0 and 4.6 GeV, which is a transition region between perturbative and non-perturbative quantum chromodynamics (QCD). Using the initial state radiation (ISR) technique, BESIII can also access energies below 2.0 GeV. The e^+e^- collision data that are used for QCD studies at BESIII include an integrated luminosity of 12 pb^{-1} at four energies (2.23, 2.4, 2.8 and 3.4 GeV) in the continuum taken in 2012, about 800 pb^{-1} at 104 energies between 3.85 and 4.6 GeV taken in the 2013–14 run, and about 650 pb^{-1} at 22 energies from 2.0 to 3.08 GeV taken in 2015. These are the so-called scan data, with moderate luminosity at each energy point; nonetheless, for these energies, they are the largest data samples in the world. There are also much larger samples for charm physics or XYZ particle search, some as large as a few fb^{-1} at a single energy, which are suitable for ISR-type analyses. With these huge data samples, BESIII is uniquely well suited to make baryon form factor measurements with unprecedentedly high precision.

BARYON MYSTERIES

The standard wisdom is that baryons are bound states of three quarks, but this description is incomplete. For example, though nucleons are the basic building blocks of observable matter in the Universe, not all of their basic properties such as their size, spin, magnetic moment and mass are fully understood, even after 100 years of study [5,6].

The charge radius of a proton measured by muonic Lamb shift once differed from that determined by electron-proton scattering or electronic Lamb shift by as much as five standard deviations [7], but recent measurements from electron scattering [8] and hydrogen spectroscopy [9] eliminated the discrepancies, and this so-called proton-radius puzzle has been essentially solved [10,11].

The proton spin has also been in a crisis in the era of the constituent quark model. The European Muon Collaboration (EMC) experiment found that the baryon spin is not only due to the spins of the valence quark [12]. It has been commonly assumed that the proton's spin of 1/2 was formed by two quarks with parallel spins and a third quark with opposite spin. In the EMC experiment, a quark of a polarized proton target was struck by a polarized muon beam, and the quark's instantaneous spin was measured. It was expected that the spin of two of the three quarks would cancel out and the spin of the third quark would be polarized in the direction of the proton's spin. Thus, the sum of the quarks' spin was expected to be equal to the proton's spin. Surprisingly, it was found that the number of quarks with spin in the proton's spin direction was almost the same as the number of quarks whose spin was in the opposite direction. Similar results have been obtained in many experiments afterwards, demonstrating clearly that both generalized parton distributions and transverse momentum distributions are important in the nucleon spin structure [13]. Our modern understanding is that the nucleon spin comes not only from quarks but also from gluons, and various contributions can be calculated using, e.g. Ji's sum rule [14]. The abnormal magnetic moment of a proton (much larger than that for a Dirac point-like particle) is generally considered an indication of a more complicated internal structure than simply three spin-1/2 quarks in a relative S wave.

Moreover, the mass of a proton cannot be explained by the Higgs mechanism, since the sum of the quarks masses inside a proton is too small, which means that there are considerable contributions to its mass from the strong interactions among quarks and gluons. Nowadays, these contributions can be calculated precisely in the lattice QCD, so the proton mass is largely understood [15,16].

BARYON FORM FACTOR MEASUREMENTS AT BESIII

The differential cross section of electron-positron annihilation to a baryon-antibaryon pair can be written as a function of the center-of-mass (c.m.) energy squared s as [17]

$$\frac{d\sigma_{B\bar{B}}(s)}{d\Omega} = \frac{\alpha^2\beta C}{4s}\left[|G_M(s)|^2(1+\cos^2\theta) + \frac{4m_B^2}{s}|G_E(s)|^2\sin^2\theta\right], \quad (1)$$

where θ is the polar angle of the baryon in the e^+e^- c.m. frame and $\beta = \sqrt{1-4m_B^2/s}$ is the

speed of the baryon. The Gamov-Sommerfeld factor C [18–20] describes the Coulomb enhancement effect: for a charged baryon pair, $C = y/(1 - e^{-y})$ with $y = \pi\alpha\sqrt{1-\beta^2}/\beta$ accounts for the electromagnetic interaction between the outgoing baryons; while for a neutral baryon pair, $C = 1$. The form factors, G_E and G_M, essentially describe the electric and magnetic distributions inside the baryon and basically provide a measure of its boundary or size. These are functions of the four-momentum transfer $s = q^2$, so should more accurately be written as $G_E(q^2)$ and $G_M(q^2)$. In the time-like domain, the form factors are complex with nonzero imaginary parts, and the translation into the internal structure is not straightforward, contrary to the case in the space-like region. It is noteworthy that final-state interactions become prevailing close to threshold and should thus be properly dealt with. By definition, the electric and magnetic form factors should be equal at the baryon-antibaryon pair's mass threshold where only s-wave production contributes [21], i.e. $G_E(4m_B^2) = G_M(4m_B^2)$, but generally they are not. In analyses of data with limited statistics it is often assumed that they are equal and the two form factors are replaced by an effective form factor, $G_{\rm eff} = G_E = G_M$.

In principle, the Coulomb interaction between the outgoing charged baryon pair B^+B^- should play an important role, in particular, by producing an abrupt jump in the cross section at threshold, since the phase space factor β is canceled by a $1/\beta$ factor in the Coulomb correction (however, there is no full consensus on that), which is a non-perturbative correction to the Born approximation to account for the Coulomb interaction between the outgoing charged baryons. In fact, the cross section for $e^+e^- \to p\bar{p}$ at threshold has been measured to be very close to the point-like value, which is consistent with the prediction, but then it is followed by a flat behavior, which is unexpected. While, for a neutral-baryon pair $B^0\bar{B}^0$, the cross section at threshold should be zero according to equation (1). The minimum c.m. energy for BESIII data is 2.0 GeV, which is about 122 MeV above the nucleon-antinucleon threshold, so no solid conclusion can be drawn for the proton-pair and neutron-pair cases, but BESIII can test these effects for charged baryons by seeing if there is a step with a value close to the point-like one for $\Lambda_c^+\bar{\Lambda}_c^-$ production, and for neutral baryons by seeing if the cross section is vanishing at the $\Lambda\bar{\Lambda}$ at threshold. Present BESIII results seem to indicate that at both the $\Lambda_c^+\bar{\Lambda}_c^-$ and $\Lambda\bar{\Lambda}$ thresholds there is a step that is close to the point-like value for charged particles, although maybe not exactly the same.

Proton

Space-like proton form factors have been measured with very high precision in many experiments [22,23]. In the time-like region, there have been a few measurements of $G_{\rm eff}$ by DM2 [24,25], E760 [26], PS170 [27], FENICE [28], E835 [29,30], BaBar [31,32] and CMD-3 [33,34], but these have relatively poor precision and mutual agreement. For the $|G_E/G_M|$ ratio, the measurements were rare and there is a long-time tension between PS170 and BaBar. The BESII experiment also measured the proton effective form factor, but with poor statistical precision [35]. BESIII continued this effort using the 2012 and 2015 scan data, and produced the most accurate $|G_E/G_M|$ ratio measurements at 16 c.m. energies between 2.0 and 3.08 GeV [36,37] that favor BaBar over PS170 and helped clarify the puzzle. BESIII also performed the measurements using the ISR technique [38,39], with results that are consistent with those of BaBar. The BESIII measurements are shown in panel (a) of Fig. 2 for a $p\bar{p}$ production cross section in the range 2.0–3.08 GeV, in panel (b) for the effective proton time-like form factor, in panel (c) for the form factor ratio $R = |G_E/G_M|$ and in panel (d) for the effective form factor residual, together with results from other experiments. The best precision in the time-like region was reported by BESIII, and the electric form factor was extracted for the first time. The unprecedented 3.5% uncertainty that was achieved at 2.125 GeV by BESIII is close to that of the best measurements in the space-like region, which have been at per cent levels for a long time. The CMD-3 experiment measured the production cross section of the proton pair and observed an abrupt rise at the nucleon-antinucleon threshold [34], as expected for point-like charged particles according to equation (1). BESIII did not extend down to the threshold energy, but the results around 2 GeV agree with CMD-3. This information improves our understanding of the proton inner structure from a different dimension and helps us to test theoretical models that depend on non-perturbative QCD, e.g. charge distribution within the proton can be deduced [40,41]. The near threshold behavior of the electromagnetic form factor of a hadron is mostly determined by the interaction of the hadron and antihadron in the final state, and therefore measurements of the form factor properties can also serve as a fruitful source of information about hadron-antihadron interaction [42].

Interestingly there are oscillations in the effective proton form factor, first seen by BaBar and later confirmed by BESIII [38]. These oscillations were subsequently studied with more precise data by

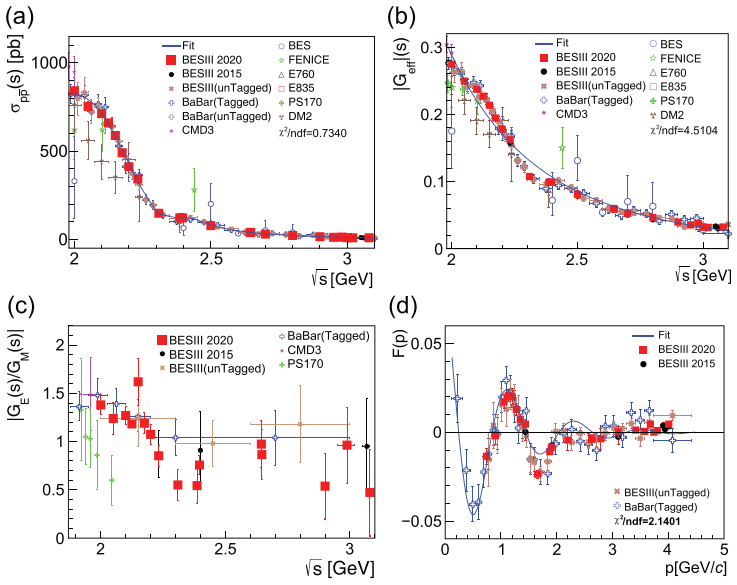

Figure 2. (a) The cross sections for $e^+e^- \to p\bar{p}$. (b) The effective proton time-like form factor. The blue curve is the result of an attempt to fit the measurements with a smooth dipole-like function. (c) The ratio $R = |G_E/G_M|$. (d) Effective form factor residual $F(p)$ after subtracting the one calculated by QCD theory (the blue curve shown in (b)), as a function of the relative motion p of the final proton and antiproton. Plots are from [37].

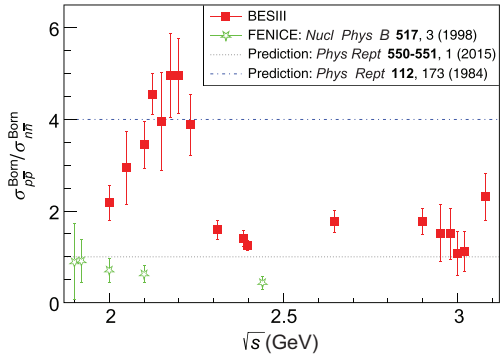

Figure 3. Ratio of the Born cross section of $e^+e^- \to p\bar{p}$ to that of $e^+e^- \to n\bar{n}$.

BESIII [37]. Bianconi and Tomasi-Gustafsson [43] speculated that possible origins of this curious behavior are rescattering processes at relative distances of 0.7–1.5 fm between the centers of the forming hadrons, leading to a large fraction of inelastic processes in p-$\bar{p}$ interactions, and a large imaginary component to the rescattering processes.

Neutron

Prior to the BESIII experiment, there was a long-standing puzzle related to the differences between the neutron and proton production rates. QCD-motivated models predict that the cross section for the proton should be 4 times larger than for the neutron [44], or they should be same [45]. In contrast, the FENICE experiment found that the neutron cross section was twice as large as the proton's, albeit with statistics that were very limited, only 74 $n\bar{n}$ events in total for five energy bins [28]. More recent measurements in the vicinity of the nucleon-antinucleon threshold are from the SND experiment [46,47]. The cross sections of $e^+e^- \to n\bar{n}$ and the neutron form factors between 2 and 3.08 GeV have been measured by BESIII with a good deal more data, over 2000 $n\bar{n}$ events at 18 energies [48]. Because the final-state neutron and anti-neutron are both neutral, with no tracks recorded in the drift chamber, the event selection is a challenge. The information in the calorimeter and the time-of-flight counters has to be used to identify the signal; as such, the selection efficiency is much lower and the number of observed neutron events is significantly less than that for protons. Neutron measurements from SND [46,47] and BESIII [48] overlap and roughly agree at 2 GeV, where a cross-section behavior that is close to the $e^+e^- \to p\bar{p}$ case is observed, in particular, a flat behavior above threshold up to 2 GeV, as seen by CMD-3 [34]; however, this challenges the expected behavior from equation (1). For energies above 2 GeV, the BESIII measurements of the ratio of the proton-to-neutron cross sections is more compatible with the QCD-motivated model predictions: as shown in Fig. 3, the cross section for $e^+e^- \to p\bar{p}$ is larger than for $e^+e^- \to n\bar{n}$ in general.

From BESIII measurements of the angular distributions for $e^+e^- \to N\bar{N}$ events, the S-wave and D-wave contributions are disentangled for the first time, which is currently under further investigation in the collaboration. Moreover, from comparisons of the $e^+e^- \to n\bar{n}$ and $e^+e^- \to p\bar{p}$ cross sections, the isoscalar and isovector components of $e^+e^- \to N\bar{N}$ can, in principle, be separated [49]. One of the components dominates and is nearly constant up to 2 GeV, similar to $e^+e^- \to p\bar{p}$, but at present it is difficult to identify whether this component is the isoscalar (very likely the largest) or the isovector one. With more data in the future, this identification could be achieved by BESIII.

The Λ hyperon

The Λ, which is the lightest hyperon that contains an s quark, is more difficult to study than the nucleon because of its smaller production cross section. It was measured previously in the DM2 [25] and BaBar [50] experiments, but the results were not conclusive. BESIII has studied the channel $e^+e^- \to \Lambda\bar{\Lambda}$ [51] with an analysis that used a 40.5 pb^{-1} data sample that was collected

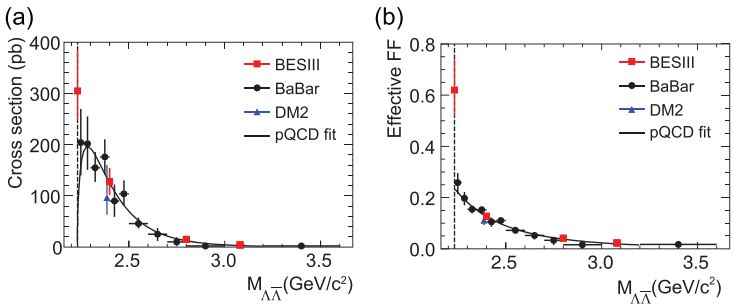

Figure 4. (a) Measurements of the $e^+e^- \to \Lambda\bar{\Lambda}$ cross section. (b) The Λ effective form factor. Plots are from [51].

at four different energy scan points during 2011 and 2012. The lowest energy point is 2.2324 GeV, only 1 MeV above the $\Lambda\bar{\Lambda}$ threshold. These data made it possible to measure the Born cross section very near threshold. To use the data as efficiently as possible, both events where Λ and $\bar{\Lambda}$ decayed to the charged mode $(\mathrm{Br}(\Lambda \to p\pi^-) = 64\%)$ and events where the $\bar{\Lambda}$ decayed to the neutral mode $(\mathrm{Br}(\bar{\Lambda} \to \bar{n}\pi^0) = 36\%)$ were selected. In the first case, the identification relied on finding two mono-energetic charged pions with evidence for a $\bar{p}$ annihilation in the material of the beam pipe or the inner wall of the tracking chamber. In the second case, the $\bar{n}$ annihilation was identified with a multi-variate analysis of variables provided by the electromagnetic calorimeter. Additionally, a mono-energetic π^0 was reconstructed to fully identify this decay channel. For the higher energy points, only the charged decay modes of Λ and $\bar{\Lambda}$ were reconstructed by identifying all the charged tracks and using the event kinematics. The resulting measurements [51] of the Born cross section are shown in Fig. 4(a) together with previous measurements [25,50]. The Born cross section near threshold is found to be $312 \pm 51(\mathrm{stat.})^{+72}_{-45}(\mathrm{sys.})$ pb. This result confirms BaBar's measurement [50], but with much higher momentum transfer squared accuracy. Since the Coulomb factor is equal to 1 for neutral baryon pairs, the cross section is expected to go to zero at threshold. Therefore, the observed threshold enhancement implies the existence of a complicated underlying physics scenario. The unexpected features of baryon pair production near threshold have driven a lot of theoretical studies, including scenarios that invoke bound states or unobserved meson resonances [42,52,53]. It was also interpreted as an attractive Coulomb interaction on the constituent quark level [54,55]. Another possible explanation is that the final-state interactions play an important role near the threshold [56–58]. The BESIII measurement improves previous results at low invariant masses at least by 10% and even more above 2.4 GeV/c. The Λ effective form factor extracted from the cross-section measurement is shown in Fig. 4(b).

According to the optical theorem, there is a nonzero relative phase between G_E and G_M. At $M_{\Lambda\bar{\Lambda}} = 2.396$ GeV, where we have the largest $\Lambda\bar{\Lambda}$ sample of 555 events from 66.9 pb^{-1} data, a multi-dimensional analysis was used to make a full determination of the Λ electromagnetic form factors for the first time for any baryon; the relative phase difference is $\Delta\Phi = 37^\circ \pm 12^\circ \pm 6^\circ$ [59] with the input parameter $\alpha_\Lambda = 0.750 \pm 0.010$ measured from J/ψ decays [60]. The improved determination of α_Λ also has profound implications for the baryon spectrum, since fits to such observables by theoretical models are a crucial element in determining the light baryon resonance spectrum, which provides a point of comparison for theoretical approaches [61]. The $|G_E/G_M|$ ratio was determined to be $R = 0.96 \pm 0.14(\mathrm{stat.}) \pm 0.02(\mathrm{sys.})$ and the effective form factor at $M_{\Lambda\bar{\Lambda}} = 2.396$ GeV was determined to be $|G_{\mathrm{eff}}| = 0.123 \pm 0.003(\mathrm{stat.}) \pm 0.003(\mathrm{sys.})$. The Λ angular distribution and the polarization as a function of the scattering angle are shown in Fig. 5(a) and (b), respectively. This first complete measurement of the hyperon electromagnetic form factor is a milestone in the study of the hyperon structure, while the long-term goal is to describe charge and magnetization densities of the hyperons.

The Λ_c charmed baryon

Experimental studies on charmed baryons have been rather sparse. The only previous study of the process $e^+e^- \to \Lambda_c^+\bar{\Lambda}_c^-$ is from the Belle experiment, which measured the cross section using the ISR technique [62], and reported a lineshape that implied the existence of a likely resonance, called the Y(4660). Based on 631.3 pb^{-1} data collected in 2014 at the four energy points $\sqrt{s} = 4.5745$, 4.5809, 4.5900 and 4.5995 GeV, BESIII measured the $\Lambda_c^+\bar{\Lambda}_c^-$ cross section with unprecedented precision [63]. The lowest energy point is only 1.6 MeV above the $\Lambda_c^+\bar{\Lambda}_c^-$ threshold. At each of the energy points, ten Cabibbo-favored hadronic decay modes, $\Lambda_c^+ \to pK^-\pi^+$, pK_S^0, $\Lambda\pi^+$, $pK^-\pi^+\pi^0$, $pK^0\pi^0$, $\Lambda\pi^+\pi^0$, $pK_S\pi^+\pi^-$, $\Lambda\pi^+\pi^+\pi^-$, $\Sigma^0\pi^+$ and $\Sigma^+\pi^+\pi^-$, as well as the corresponding charge-conjugate modes were studied. The total Born cross section is obtained from the weighted average of the 20 individual measurements, and the results are shown in Fig. 6(a). Similar to the case for $e^+e^- \to p\bar{p}$, an abrupt rise in the cross section just above threshold that is much steeper than phase-space expectations is discerned, which was not seen by

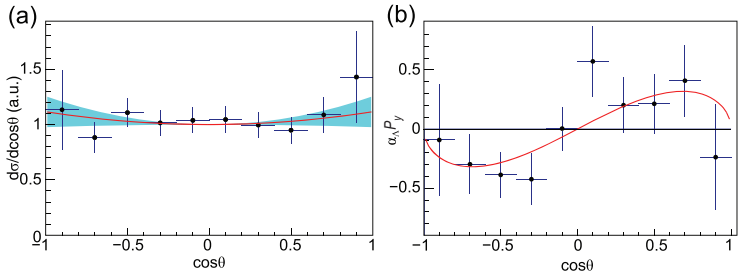

Figure 5. (a) The acceptance corrected Λ scattering angle distribution for $e^+e^- \to \Lambda\bar{\Lambda}$ at $M_{\Lambda\bar{\Lambda}} = 2.396$ GeV. (b) The product of the Λ decay parameter α_Λ and Λ polarization P_y as a function of the scattering angle. Plots are from [59].

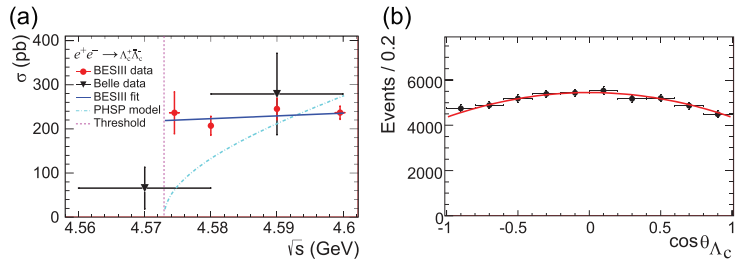

Figure 6. (a) The Born cross section of $e^+e^- \to \Lambda_c^+\bar{\Lambda}_c^-$ obtained by BESIII and Belle. (b) The angular distribution and corresponding fit results in data at $\sqrt{s} = 4.5995$ GeV. Plots are from [63].

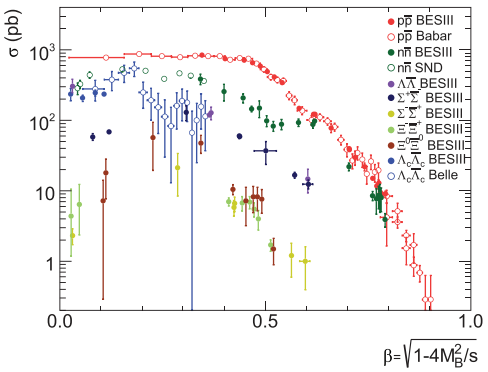

Figure 7. A compilation of cross sections, revealing similar patterns for all $B\bar{B}$ pairs measured so far: $p\bar{p}$ by BaBar [31,32] and BESIII [37], $n\bar{n}$ by SND [46,47] and BESIII [48], $\Lambda\bar{\Lambda}$ by BESIII [51], $\Sigma^+\bar{\Sigma}^-/\Sigma^-\bar{\Sigma}^+$ by BESIII [65], $\Xi^-\bar{\Xi}^+/\Xi^0\bar{\Xi}^0$ by BESIII [66,67], $\Lambda_c^+\bar{\Lambda}_c^-$ by Belle [62] and BESIII [63].

Belle due to limitations in the ISR method. BESIII's measured cross-section lineshape is different from Belle's, disfavoring a resonance like $\Upsilon(4660)$ in the $\Lambda_c^+\bar{\Lambda}_c^-$ channel. The BESIII results have driven discussions in the theoretical literature [64].

High statistic data samples at $\sqrt{s} = 4.5745$ and 4.5995 GeV enabled studies of the polar angular distribution of Λ_c in the e^+e^- center-of-mass system. The shape function $f(\theta) \propto (1 + \alpha_{\Lambda_c}\cos^2\theta)$ is fitted to the combined data containing the yields of Λ_c^+ and $\bar{\Lambda}_c^-$ for all ten decay modes, as shown in Fig. 6(b). The ratio between the electric and magnetic form factors $|G_E/G_M|$ can be extracted using $|G_E/G_M|^2(1-\beta^2) = (1-\alpha_{\Lambda_c})/(1+\alpha_{\Lambda_c})$. From these distributions, the ratios $|G_E/G_M|$ of Λ_c^+ have been extracted for the first time: they are $1.14 \pm 0.14\,(\text{stat.}) \pm 0.07\,(\text{sys.})$ and $1.23 \pm 0.05\,(\text{stat.}) \pm 0.03\,(\text{sys.})$ at $\sqrt{s} = 4.5745$ and 4.5995 GeV, respectively.

BARYON CHALLENGES AT BESIII

The energy thresholds for pair production of all of the ground-state spin-1/2 SU(3) octet and spin-3/2 decuplet are accessible to BESIII. Baryon form factor measurements are among the most important reasons why BESIII has collected an unprecedented amount of off-resonance data. From the analysis of existing data, it is expected that the ratio of the absolute values of the Λ electromagnetic form factors, $|G_E/G_M|$, can be measured at five energy points. The most interesting findings are the abrupt cross-section jumps at threshold followed by a nearly flat behavior that has been observed for $\Lambda\bar{\Lambda}$, $\Lambda_c^+\bar{\Lambda}_c^-$, $p\bar{p}$, $n\bar{n}$, etc. If the BEPCII energy could be lowered to the vicinity of nucleon-antinucleon threshold, BESIII will be able to confirm the $p\bar{p}$ and $n\bar{n}$ cases with much better precision. Figure 7 shows the cross-section lineshapes for a variety of baryon-antibaryon pairs, including those that were recently measured for singly stranged $\Sigma^+\bar{\Sigma}^-/\Sigma^-\bar{\Sigma}^+$ [65], doubly stranged $\Xi^-\bar{\Xi}^+$ [66] and $\Xi^0\bar{\Xi}^0$ [67]. They all seem to share the common feature of a plateau starting from the baryon pair production threshold, though for some channels, more statistics are ideally needed. The behaviors of $\Sigma^0\bar{\Sigma}^0$ (the last member to be covered for the spin-1/2 SU(3) octet baryons) and other baryon pairs will be reported in the near future.

SUMMARY AND PROSPECTS

The measurements of baryon form factors have been an important ongoing activity at BESIII. Form factors of the proton with the best precision were obtained in the time-like region, and the electric form factor of the proton was measured for the first time. Measurements of the neurtron time-like form factor with unprecedented precision have also been reported. The Λ and Λ_c were studied and in both cases abnormal cross-section enhancements were observed near the production thresholds. The form factors of the Λ_c were extracted for the first time.

In addition, Σ^+/Σ^- [65], Ξ^- [66] and Ξ^0 [67] form factor measurements were recently reported, and results for Σ^0 will soon be released. BESIII also has a plan to explore the nucleon production thresh-

old by taking data in the range 1.8–2.0 GeV for $\sim$100 pb^{-1} at 23 energy points [68], in order to study the anomalous threshold cross-section behavior in more detail. With numerous first measurements and interesting discoveries, these studies shed new light on the understanding of interactions and the fundamental structure of particles.

It will take a long time to ultimately unravel the fundamental structure of baryons. Further improvements in the form factor measurement of baryons will continue to be the focus of future powerful electron-ion colliders in America (EiC) [69] and China (EicC) [70], super electron-positron colliders in China [71] and Russia [72] for the space-like and time-like regions, respectively.

ACKNOWLEDGMENTS

The authors thank Prof. S. L. Olsen for helpful suggestions and proofreading.

FUNDING

This work was supported in part by the National Natural Science Foundation of China (NSFC) (12035013, 12061131003, 11911530140 and 11335008), the Joint Large-Scale Scientific Facility Funds of the NSFC and the Chinese Academy of Sciences (U1832103), the National Key Research and Development Program of China (2020YFA0406403), and the National Key Basic Research Program of China (2015CB856705).

Conflict of interest statement. None declared.

REFERENCES

1. Gell-Mann M. Schematic model of baryons and mesons. *Phys Lett* 1964; **8**: 214–5.
2. Zyla PA, Barnett RM and Beringer J *et al.* Review of particle physics. *Prog Theor Exp Phys* 2020; **2020**: 083C01.
3. Ablikim M, An ZH and Bai JZ *et al.* Design and construction of the BESIII detector. *Nucl Instrum Methods Phys Res A* 2010; **614**: 345–99.
4. Yu CH, Duan Z and Gu SD *et al.* BEPCII performance and beam dynamics studies on luminosity. *Seventh International Particle Accelerator Conference (IPAC 2016)*, Busan, Korea, 8–13 May, 2016.
5. Rutherford E. Collision of α particles with light atoms. IV. An anomalous effect in nitrogen. *Philos Mag* 1919; **6**: 31–7.
6. Chadwick J. Possible existence of a neutron. *Nature* 1932; **129**: 312.
7. Pohl R, Antognini A and Nez F *et al.* The size of the proton. *Nature* 2010; **466**: 213–6.
8. Xiong W, Gasparian A and Gao H *et al.* A small proton charge radius from an electron–proton scattering experiment. *Nature* 2019; **575**: 147–50.
9. Bezginov N, Valdez T and Horbatsch M *et al.* A measurement of the atomic hydrogen Lamb shift and the proton charge radius. *Science* 2019; **365**: 1007–12.
10. Hammer HW and Meißner UG. The proton radius: from a puzzle to precision. *Sci Bull* 2020; **65**: 257–8.
11. Karr JP, Marchand D and Voutier E. The proton size. *Nat Rev Phys* 2020; **2**: 601–14.
12. Ashman J, Badelek B and Baum G *et al.* A measurement of the spin asymmetry and determination of the structure function g(1) in deep inelastic muon-proton scattering. *Phys Lett B* 1988; **206**: 364–70.
13. Deur A, Brodsky SJ and de Téramond GF. The spin structure of the nucleon. *Rep Prog Phys* 2019; **82**: 076201.
14. Ji X. Gauge-invariant decomposition of nucleon spin. *Phys Rev Lett* 1997; **78**: 610–3.
15. Huang JH, Sun TT and Chen H. Evaluation of pion-nucleon sigma term in Dyson-Schwinger equation approach of QCD. *Phys Rev D* 2020; **101**: 054007.
16. Borsanyi S, Durr S and Fodor Z *et al.* Ab initio calculation of the neutron-proton mass difference. *Science* 2015; **347**: 1452–5.
17. Zichichi A, Berman SM and Cabibbo N *et al.* Proton anti-proton annihilation into electrons, muons and vector bosons. *Nuovo Cim* 1962; **24**: 170–80.
18. Sommerfeld A. Über die beugung und bremsung der elektronen. *Ann Phys* 1931; **403**: 257–330.
19. Brodsky SJ and Lebed RF. Production of the smallest QED atom: true muonium ($\mu^+\mu^-$). *Phys Rev Lett* 2009; **102**: 213401.
20. Sakharov AD. Interaction of an electron and positron in pair production. *Sov Phys Usp* 1991; **34**: 375–7.
21. Griffiths D. *Introduction to Elementary Particles*, 2nd edn. Weinheim: Wiley-VCH, 2008.
22. Gayou O, Aniol KA and Averett T *et al.* Measurement of G_{E_p}/G_{M_p} in $\vec{e}\ p \rightarrow e\ \vec{p}$ to $Q^2 = 5.6\text{GeV}^2$. *Phys Rev Lett* 2002; **88**: 092301.
23. Zhan X, Allada K and Armstrong DS *et al.* High-precision measurement of the proton elastic form factor ratio $\mu_p G_E/G_M$ at low Q^2. *Phys Lett B* 2011; **705**: 59–64.
24. Bisello D, Limentani S and Nigro M *et al.* A measurement of $e^+e^- \rightarrow \bar{p}\,p$ for 1975 MeV $\leq \sqrt{s} \leq$ 2250 MeV. *Nucl Phys B* 1983; **224**: 379–95.
25. Bisello D, Busetto G and Castro A *et al.* Baryon pairs production in e^+e^- annihilation at $\sqrt{(s)} = 2.4$ GeV. *Z Phys C* 1990; **48**: 23–8.
26. Armstrong TA, Bettoni D and Bharadwaj V *et al.* Proton electromagnetic form factors in the timelike region from 8.9 to 13.0 GeV^2. *Phys Rev Lett* 1993; **70**: 1212–5.
27. Bardin G, Burgun G and Calabrese R *et al.* Determination of the electric and magnetic form factors of the proton in the time-like region. *Nucl Phys B* 1994; **411**: 3–32.
28. Antonelli A, Baldini R and Benasi P *et al.* The first measurement of the neutron electromagnetic form-factors in the timelike region. *Nucl Phys B* 1998; **517**: 3–35.
29. Ambrogiani M, Bagnasco S and Baldini W *et al.* Measurements of the magnetic form-factor of the proton in the timelike region at large momentum transfer. *Phys Rev D* 1999; **60**: 032002.
30. Ambrogiani M, Bagnasco S and Baldini W *et al.* Measurements of the magnetic form-factor of the proton for timelike momentum transfers. *Phys Lett B* 2003; **559**: 20–5.

31. Lees JP, Poireau V and Tisserand V *et al.* Study of $e^+e^- \to p\bar{p}$ via initial-state radiation at BABAR. *Phys Rev D* 2013; **87**: 092005.
32. Lees JP, Poireau V and Tisserand V *et al.* Measurement of the $e^+e^- \to p\bar{p}$ cross section in the energy range from 3.0 to 6.5 GeV. *Phys Rev D* 2013; **88**: 072009.
33. Akhmetshin RR, Amirkhanov AN and Anisenkov AV *et al.* Study of the process $e^+e^- \to p\bar{p}$ in the c.m. energy range from threshold to 2 GeV with the CMD-3 detector. *Phys Lett B* 2016; **759**: 634–40.
34. Akhmetshin RR, Amirkhanov AN and Anisenkov AV *et al.* Observation of a fine structure in $e^+e^- \to$ hadrons production at the nucleon-antinucleon threshold. *Phys Lett B* 2019; **794**: 64–8.
35. Ablikim M, Bai JZ and Ban Y *et al.* Measurement of the cross section for $e^+e^- \to p\bar{p}$ at center-of-mass energies from 2.0 to 3.07 GeV. *Phys Lett B* 2005; **630**: 14–20.
36. Ablikim M, Achasov MN and Ai XC *et al.* Measurement of the proton form factor by studying $e^+e^- \to p\bar{p}$. *Phys Rev D* 2015; **91**: 112004.
37. Ablikim M, Achasov MN and Adlarson P *et al.* Measurement of proton electromagnetic form factors in $e^+e^- \to p\bar{p}$ in the energy region 2.00-3.08 GeV. *Phys Rev Lett* 2020; **124**: 042001.
38. Ablikim M, Achasov MN and Adlarson P *et al.* Study of the process $e^+e^- \to p\bar{p}$ via initial state radiation at BESIII. *Phys Rev D* 2019; **99**: 092002.
39. Ablikim M, Achasov MN and Adlarson P *et al.* Measurement of proton electromagnetic form factors in the time-like region using initial state radiation at BESIII. *Phys Lett B* 2021; **817**: 136328.
40. Adamuscin C, Dubnicka S and Dubnickova AZ *et al.* A unitary and analytic model of nucleon EM structure, the puzzle of JLab proton polarization data and new insight into the proton charge distribution. *Prog Part Nucl Phys* 2005; **55**: 228–41.
41. Dubnickova AZ and Dubnicka S. Proton em form factors data are in disagreement with new $\sigma_{tot}(e^+e^- \to p\bar{p})$ measurements. arXiv:2010.15872.
42. Dalkarov OD, Khakhulin PA and Voronin AY. On the electromagnetic form factors of hadrons in the time-like region near threshold. *Nucl Phys A* 2010; **833**: 104–18.
43. Bianconi A and Tomasi-Gustafsson E. Periodic interference structures in the timelike proton form factor. *Phys Rev Lett* 2015; **114**: 232301.
44. Chernyak VL and Zhitnitsky AR. Asymptotic behavior of exclusive processes in QCD. *Phys Rep* 1984; **112**: 173–318.
45. Pacetti S, Baldini Ferroli R and Tomasi-Gustafsson E. Proton electromagnetic form factors: basic notions, present achievements and future perspectives. *Phys Rep* 2015; **550–551**: 1–103.
46. Achasov MN, Barnyakov AY and Beloborodov KI *et al.* Study of the process $e^+e^- \to n\bar{n}$ at the VEPP-2000 e^+e^- collider with the SND detector. *Phys Rev D* 2014; **90**: 112007.
47. Druzhinin VP and Serednyakov SI. Measurement of the $e^+e^- \to n\bar{n}$ cross section with the SND detector at the VEPP-2000 collider. *EPJ Web Conf* 2019; **212**: 07007.
48. The BESIII Collaboration. Oscillating features in the electromagnetic structure of the neutron. *Nat Phys* 2021; **17**: 1200–4.
49. Dmitriev VF, Milstein AI and Salnikov SG. Isoscalar amplitude dominance in e^+e^- annihilation to $N\overline{N}$ pair close to the threshold. *Phys At Nucl* 2014; **77**: 1173–7.
50. Aubert B, Bona M and Boutigny D *et al.* Study of $e^+e^- \to \Lambda\bar{\Lambda}$, $\Lambda\bar{\Sigma}^0$, $\Sigma^0\bar{\Sigma}^0$ using initial state radiation with BABAR. *Phys Rev D* 2007; **76**: 092006.
51. Ablikim M, Achasov MN and Ahmed S *et al.* Observation of a cross-section enhancement near mass threshold in $e^+e^- \to \Lambda\bar{\Lambda}$. *Phys Rev D* 2018; **97**: 032013.
52. El-Bennich B, Lacombe M and Loiseau B *et al.* Paris $N\overline{N}$ potential constrained by recent antiprotonic-atom data and $\overline{n}p$ total cross sections. *Phys Rev C* 2009; **79**: 054001.
53. Xiao LY, Weng XZ and Zhong XH *et al.* A possible explanation of the threshold enhancement in the process $e^+e^- \to \Lambda\bar{\Lambda}$. *Chinese Phys C* 2019; **43**: 113105.
54. Baldini R, Pacetti S and Zallo A *et al.* Unexpected features of $e^+e^- \to p\overline{p}$ and $e^+e^- \to \Lambda\overline{\Lambda}$ cross-sections near threshold. *Eur Phys J A* 2009; **39**: 315–21.
55. Baldini Ferroli R, Pacetti S and Zallo A. No Sommerfeld resummation factor in $e^+e^- -> p\bar{p}$? *Eur Phys J A* 2012; **48**: 33.
56. Zou BS and Chiang HC. One-pion-exchange final-state interaction and the $p\overline{p}$ near threshold enhancement in $J/\psi \to \gamma p\overline{p}$ decays. *Phys Rev D* 2004; **69**: 034004.
57. Haidenbauer J, Hammer HW and Meißner UG *et al.* On the strong energy dependence of the $e^+e^- \leftrightarrow p\bar{p}$ amplitude near threshold. *Phys Lett B* 2006; **643**: 29–32.
58. Haidenbauera J and Meißner UG. The electromagnetic form factors of the Λ in the timelike region. *Phys Lett B* 2016; **761**: 456–61.
59. Ablikim M, Achasov MN and Adlarson P *et al.* Complete measurement of the Λ electromagnetic form factors. *Phys Rev Lett* 2019; **123**: 122003.
60. Ablikim M, Achasov MN and Ahmed S *et al.* Polarization and entanglement in baryon-antibaryon pair production in electron-positron annihilation. *Nat Phys* 2019; **15**: 631–4.
61. Ireland DG, Döring M and Glazier DI *et al.* Kaon photoproduction and the Λ decay parameter α_-. *Phys Rev Lett* 2019; **123**: 182301.
62. Pakhlova G, Adachi I and Aihara H *et al.* Observation of a near-threshold enhancement in the $e^+e^- \to \Lambda_c^+\Lambda_c^-$ cross section using initial-state radiation. *Phys Rev Lett* 2008; **101**: 172001.
63. Ablikim M, Achasov MN and Ahmed S *et al.* Precision measurement of the $e^+e^- \to \Lambda_c^+\bar{\Lambda}_c^-$ cross section near threshold. *Phys Rev Lett* 2018; **120**: 132001.
64. Dai LY, Haidenbauer J and Meißner UG. Re-examining the *X*(4630) resonance in the reaction $e^+e^- \to \Lambda_c^+\bar{\Lambda}_c^-$. *Phys Rev D* 2017; **96**: 116001.
65. Ablikim M, Achasov MN and Adlarson P *et al.* Measurements of Σ^+ and Σ^- time-like electromagnetic form factors for center-of-mass energies from 2.3864 to 3.0200 GeV. *Phys Lett B* 2021; **814**: 136110.
66. Ablikim M, Achasov MN and Adlarson P *et al.* Measurement of cross section for $e^+e^- \to \Xi^-\bar{\Xi}^+$ near threshold at BESIII. *Phys Rev D* 2021; **103**: 012005.
67. Ablikim M, Achasov MN and Adlarson P *et al.* Measurement of cross section for $e^+e^- \to \Xi^0\bar{\Xi}^0$ near threshold. *Phys Lett B* 2021; **820**: 136557.
68. Ablikim M, Achasov MN and Adlarson P *et al.* Future physics programme of BESIII. *Chinese Phys C* 2020; **44**: 040001.
69. Accardi A, Albacete JL and Anselmino M *et al.* Electron ion collider: the next QCD frontier—understanding the glue that binds us all. *Eur Phys J A* 2016; **52**: 268.
70. Anderle DP, Bertone V and Cao X *et al.* Electron-ion collider in China. *Front Phys* 2021; **16**: 64701.
71. Luo Q and Xu D. Progress on preliminary conceptual study of HIEPA, a Super Tau-Charm factory in China. *Ninth International Particle Accelerator Conference (IPAC 2018)*, Vancouver, Canada, 29 April–4 May, 2018.
72. Barnyakov AY. The project of the Super Charm-Tau factory in Novosibirsk. *J Phys Conf Ser* 2020; **1561**: 012004.

REVIEW

National Science Review
8: nwab189, 2021
https://doi.org/10.1093/nsr/nwab189
Advance access publication 20 October 2021

PHYSICS

Special Topic: Physics of the BESIII Experiment

New physics searches at the BESIII experiment

Shenjian Chen [1,2,*] and Stephen Lars Olsen[3,4,*]

ABSTRACT

The standard model (SM) of particle physics, comprised of the unified electroweak and quantum chromodynamic theories, accurately explains almost all experimental results related to the micro-world, and has made a number of predictions for previously unseen particles, most notably the Higgs scalar boson, that were subsequently discovered. As a result, the SM is currently universally accepted as the theory of the fundamental particles and their interactions. However, in spite of its numerous successes, the SM has a number of apparent shortcomings, including: many free parameters that must be supplied by experimental measurements; no mechanism to produce the dominance of matter over antimatter in the universe; and no explanations for gravity, the dark matter in the universe, neutrino masses, the number of particle generations, etc. Because of these shortcomings, there is considerable incentive to search for evidence for new, non-SM physics phenomena that might provide important clues about what a new, beyond the SM theory (BSM) might look like. Although the center-of-mass energies that BESIII can access are far below the energy frontier, searches for new, BSM physics are an important component of its research program. This report reviews some of the highlights from BESIII's searches for signs of new, BSM physics by: measuring rates for processes that the SM predicts to be forbidden or very rare; searching for non-SM particles such as dark photons; performing precision tests of SM predictions; and looking for violations of the discrete symmetries *C* and *CP* in processes for which the SM expectations are immeasurably small.

Keywords: new physics, dark photons, lepton flavor violation, *C* and *CP* violation

[1]School of Physics, Nanjing University, Nanjing 210093, China; [2]Nanjing Proton Source Research and Design Center, Nanjing 210093, China; [3]University of Chinese Academy of Sciences, Beijing 100049, China and [4]Institute for Basic Science, Daejeon 34126, South Korea

*__Corresponding authors__. E-mails: sjchen@nju.edu.cn; solsensnu@gmail.com

Received 15 April 2021; **Revised** 12 October 2021; **Accepted** 12 October 2021

INTRODUCTION

The standard model consistently predicts the results of experimental measurements and has emerged as the only viable candidate theory for describing elementary particle interactions [1–4]. In spite of its great success, there are a number of reasons to believe that the standard model (SM) is not the ultimate theory, including the following.

- The SM has 19 free parameters that must be supplied by experimental measurements. These include the quark, lepton and Higgs masses, the mixing angles of the Cabibbo–Kobayashi–Maskawa (CKM) quark-flavor mixing matrix, and the couplings of the electric, weak and quantum chromodynamic (QCD) color forces.
- As first pointed out by Sakharov [5], the matter-antimatter asymmetry of the universe implies the existence of sizable *CP*-violating interactions in nature. However, the established SM mechanism for *CP* violation fails to explain the matter-dominated universe by about 10 orders of magnitude; there must be additional *CP*-violating mechanisms in nature beyond those contained in the SM.
- The model has no explanation for dark matter, which is, apparently, the dominant component of the mass of the universe.
- The particles in the SM are arranged in three generations of colored quarks and three generations of leptons; particle interactions are mediated by three forces: the color, electromagnetic and weak forces. The theory provides no explanation for why the number of generations is three and it does not account in any way for gravity, the fourth force that is known to exist.

As a result, there have been a huge number of experimental efforts aimed at finding 'new physics,' which refers to new physical phenomena beyond

the standard model (BSM) of particle physics. This may be, for example, a new fundamental particle, such as a fourth generation quark or lepton, or a new fundamental force carrier, such as a dark photon, high-mass gauge boson, a new Higgs-like meson, etc. Searches for new physics can be performed in two ways. One method is to look for direct production of new particles in collisions at high-energy accelerators, for example at the Large Hadron Collider, and reconstruct it from its SM decay products. Another way is to measure precisely a decay process that can be accurately described by the SM, and look for deviations from the SM prediction of the decay rate. According to quantum field theory (QFT), new heavy particles can contribute to the decay process through virtual loop diagrams. These make precision measurements sensitive to new physics, and this technique is widely used in high intensity collider experiments such as BESIII [6–8].

Here we review highlights of some of these activities at BESIII.

RARE PROCESSES

Search for flavor changing neutral currents

Flavor changing neutral current (FCNC) processes transform an up-type (u, c, t) or down-type (d, s, b) quark into another quark of the same type but with a different flavor. In the SM, these processes are mediated by the Z boson and are known as neutral currents. However, they are strongly suppressed by the Glashow-Iliopoulos-Maiani (GIM) cancelation [9] and only occur as second-order loop processes. In many extensions of the SM, virtual TeV-scale particles can contribute competing processes that lead to measurable deviations from SM-inferred transition rates or other properties. Hence, studies of rare FCNC processes are suitable probes for new physics.

Recently, hints of discrepancies have been observed in the semi-leptonic FCNC processes of the b quark, $b \to s\ell^+\ell^-$ ($\ell = e, \mu$), by the LHCb experiment [10]. (1) The differential branching fractions measured as a function of the squared four-momentum transferred to the two leptons, Q^2, for several B-meson decay modes are below the theoretical predictions [11–15]. The largest local discrepancy is a 3.3σ difference in the rate for $B_s^0 \to \phi\mu^+\mu^-$ decay from its SM-predicted value. (2) The ratios of branching fractions for decays involving muons and electrons, defined as

$$R_K = \frac{\mathcal{B}(B^+ \to K^+\mu^+\mu^-)}{\mathcal{B}(B^+ \to K^+e^+e^-)}$$

$$\text{and} \quad R_{K^*} = \frac{\mathcal{B}(B^+ \to K^{*+}\mu^+\mu^-)}{\mathcal{B}(B^+ \to K^{*+}e^+e^-)},$$

which are unity in the SM (i.e. lepton-flavor universality), were measured to be [16,17]

$$R_K = 0.745^{+0.090}_{-0.074} \pm 0.036 \text{ at central}$$
$$Q^2 \in [1.0, 6.0]\,\text{GeV}/c^2, \quad 2.6\sigma,$$
$$R_{K^*} = 0.66^{+0.11}_{-0.07} \pm 0.03 \text{ at low}$$
$$Q^2 \in [0.045, 1.1]\text{GeV}/c^2, \quad 2.1\sigma - 2.3\sigma,$$
$$R_{K^*} = 0.69^{+0.11}_{-0.07} \pm 0.05 \text{ at central}$$
$$Q^2 \in [1.1, 6.0]\,\text{GeV}/c^2, \quad 2.4\sigma - 2.5\sigma,$$

where the levels of deviations from the SM predictions are indicated. (3) Measurements of the quantity P_5', which is the chiral asymmetry produced by the interference between the transversely and longitudinally polarized amplitudes in the decay $B \to K^{*+}\ell^+\ell^-$, are 2.8σ and 3.0σ lower than the SM prediction in two Q^2 intervals below the J/ψ resonance mass [18]. Since these discrepancies could be evidence for new particles that would extend the SM, it is important to check if there are similar deviations in the charm sector.

While SM rates for FCNC transitions in the down-type b- or s-quark sectors are relatively frequent because of the large mass of the top quark contribution to the loop, those in the up-type c-quark sector are especially rare due to the small masses of the intermediate down-like quarks in the loop that result in a strong GIM cancelation. For $c \to u$ transition rates for charmed and charmonia particles that proceed via the SM loop contribution, dubbed short distance effects, the expected branching fractions are typically between $<10^{-8}$ [19–24] and 10^{-10}–10^{-14} [25–27], respectively. For FCNC decays of charmed mesons, the measured rates are enhanced by a few orders of magnitude by SM contributions from long distance effects that proceed via di-lepton decays of ordinary ρ, ω and ϕ vector mesons [23,24]. However, some extensions to the SM further enhance these FCNC processes, sometimes by orders of magnitude [22,28–32].

The BESIII experiment has searched for c-quark FCNC processes in both charmed meson and charmonium decays. No significant signals for new physics are found in any of the investigated decay modes, and the inferred 90% confidence level (CL) upper limits on the branching fractions are summarized in Table 1.

- For the $D^0 \to \gamma\gamma$ mode, the upper limit is consistent with that previously set by the BaBar experiment [33]. The BESIII result is the first experimental study of this decay that uses D^0 mesons produced at the open-charm threshold.

Table 1. Results for the upper limit at the 90% CL on the branching fractions for various FCNC process searches performed at BESIII. Also listed are the best previous results and the SM predictions, where the branching fraction calculations for charmed meson and charmonium decays are based on long distance and short distance contributions, respectively.

Mode	Data	$\mathcal{B}^{UL}$ at 90% CL	Ref.	Previous best $\mathcal{B}^{UL}$	Ref.	SM prediction	Ref.
$D^0 \to \gamma\gamma$	2.92 fb^{-1} $\psi(3770)$	3.8×10^{-6}	[36]	2.2×10^{-6}	[33]	3.5×10^{-8}	[20]
$D^+ \to \pi^+\pi^0 e^+e^-$	2.93 fb^{-1} $\psi(3770)$	1.4×10^{-5}	[37]				
$D^+ \to K^+\pi^0 e^+e^-$	2.93 fb^{-1} $\psi(3770)$	1.5×10^{-5}	[37]				
$D^+ \to K^0_S\pi^+ e^+e^-$	2.93 fb^{-1} $\psi(3770)$	2.6×10^{-5}	[37]				
$D^+ \to K^0_S\, K^+e^+e^-$	2.93 fb^{-1} $\psi(3770)$	1.1×10^{-5}	[37]				
$D^0 \to K^-K^+e^+e^-$	2.93 fb^{-1} $\psi(3770)$	1.1×10^{-5}	[37]	3.15×10^{-4}	[34]	6.5×10^{-7}	[24]
$D^0 \to \pi^+\pi^-e^+e^-$	2.93 fb^{-1} $\psi(3770)$	0.7×10^{-5}	[37]	3.73×10^{-4}	[34]	2.0×10^{-6}	[24]
$D^0 \to K^-\pi^+e^+e^-$	2.93 fb^{-1} $\psi(3770)$	4.1×10^{-5}	[37]	3.85×10^{-4}	[34]	1.6×10^{-5}	[24]
$D^0 \to \pi^0e^+e^-$	2.93 fb^{-1} $\psi(3770)$	0.4×10^{-5}	[37]	0.45×10^{-4}	[34]	0.8×10^{-6}	[21]
$D^0 \to \eta e^+e^-$	2.93 fb^{-1} $\psi(3770)$	0.3×10^{-5}	[37]	1.1×10^{-4}	[34]		
$D^0 \to \omega e^+e^-$	2.93 fb^{-1} $\psi(3770)$	0.6×10^{-5}	[37]	1.8×10^{-4}	[34]		
$D^0 \to K^0_S e^+e^-$	2.93 fb^{-1} $\psi(3770)$	1.2×10^{-5}	[37]	1.1×10^{-4}	[34]		
$J/\psi \to D^0e^+e^-$	1.31 B J/ψ	8.5×10^{-8}	[38]	1.1×10^{-5}	[35]	4.8×10^{-14}	[27]
$\psi(2S) \to D^0e^+e^-$	448 M $\psi(2S)$	1.4×10^{-7}	[38]				
$\psi(2S) \to \Lambda_c^+ \bar{p}e^+e^-$	448 M $\psi(2S)$	1.7×10^{-6}	[39]				

- For the rare decays $D \to h(h^{(\prime)})e^+e^-$, where h indicates a meson that is comprised of u, d, and s quarks, searches for four-body decays of D^+ mesons are performed for the first time, and the upper limits for D^0 meson decays are, in general, one order of magnitude better than previous measurements [34].
- Searches for the FCNC decays $\psi(2S) \to D^0e^+e^-$ and $\psi(2S) \to \Lambda_c^+ \bar{p}e^+e^-$ are performed for the first time. The upper limit on $J/\psi \to D^0e^+e^-$ is 2 orders of magnitude more stringent than the best previous result, which was set by the BESII collaboration [35].

Prospects for BESIII rare decay searches

The BESIII FCNC search results mentioned above are based on data collected in 2009–2012, which included 1.31B J/ψ and 448M $\psi(2S)$ event samples and a 2.93 fb^{-1} data sample that was accumulated at $E_{\rm CM} = 3.773$ MeV, the peak energy of the $\psi(3770) \to D\bar{D}$ resonance. BESIII has recently increased the J/ψ data sample to 10B events and will eventually increase the $\psi(2S)$ sample to 3B events, and the $\psi(3770) \to D\bar{D}$ data to 20 fb^{-1} (see Table 7.1 of [40]). Since the results listed in Table 1 are mainly limited by statistics, when the full data are available and analyzed, the sensitivity levels of FCNC searches should improve, in most cases, by factors of $\sim$7, and decay branching fractions will be probed at the 10^{-6}–10^{-8} levels. If no interesting signals are found, more stringent upper limits would be established that should further constrain the parameter spaces of a number of new physics models.

In contrast to FCNC processes, charged-current weak decays of charmonium states are allowed, but are expected to occur as very rare processes; the SM-predicted branching fractions are of the order 10^{-10}–10^{-8} [25], which means that they would be difficult to detect at BESIII, even with the full 10B event J/ψ data sample. However, some BSM calculations based on a two-Higgs-doublet model predict that the branching ratios of charmonium weak decays could be enhanced to be as large as 10^{-5} [41]. BESIII searched for several Cabibbo-favored weak decays, such as the hadronic processes $J/\psi \to D_s^-\rho^+$ and $J/\psi \to \bar{D}^0\bar{K}^{*0}$ [42], and the semileptonic process $J/\psi \to D_s^{(*)-}e^+\nu_e$ [43], and established 90% CL branching fraction upper limits in the $\sim 10^{-5}$–10^{-6} range. Searches for some Cabibbo-suppressed weak decays of the J/ψ are currently underway at BESIII, with expected branching fraction sensitivity levels of about 10^{-7}.

TESTING SM PREDICTIONS FOR LEPTON COUPLINGS AND CKM MATRIX ELEMENTS

In the SM, the strength of charged-current weak interactions is governed by a single universal parameter, the Fermi constant $G_{\rm F}$. The three charged leptons (e^-, μ^-, τ^-) all couple to the W boson with this strength, a feature called lepton-flavor universality (LFU). Although the quarks appeared, at first, to have different coupling strengths, this is because of a misalignment between the charge $=-1/3$ strong-interaction flavor eigenstates (d, s, b) and their weak-interaction counterparts (d', s', b'), as was first

Table 2. BESIII measurements of charmed particle semi-leptonic and purely leptonic branching-fraction measurements, and comparisons of the $\Gamma_{e(\tau)}/\Gamma_\mu$ to SM expectations for LFU.

Mode	$n_{\rm evts}$	$\mathcal{B}$ ($\times 10^{-3}$)	Ref.	$\Gamma_{e(\tau)}/\Gamma_\mu$	SM pred.	$\sqrt{\frac{\Gamma_{e(\tau)}/\Gamma_\mu}{\rm SM}} - 1$
$D^0 \to K^-\mu^+\nu_\mu$	47.1K	$34.13 \pm 0.19 \pm 0.35$	[54]	1.027 ± 0.014	1.026 ± 0.001	0.001 ± 0.008
$D^0 \to K^-e^+\nu_e$	70.7K	$35.05 \pm 0.14 \pm 0.33$	[55]			
$D^0 \to \pi^-\mu^+\nu_\mu$	2.3K	$2.72 \pm 0.08 \pm 0.06$	[56]	1.085 ± 0.037	1.015 ± 0.002	0.034 ± 0.019
$D^0 \to \pi^-e^+\nu_e$	6.3K	$2.95 \pm 0.04 \pm 0.03$	[55]			
$D^+ \to \bar{K}^0\mu^+\nu_\mu$	20.7K	$87.2 \pm 0.7 \pm 1.8$	[57]	1.012 ± 0.033	≈ 1.03	
$D^+ \to \bar{K}^0e^+\nu_e$	26.0K	$86.0 \pm 0.6 \pm 1.5$	[58]			
$D^+ \to \pi^0\mu^+\nu_\mu$	1.3K	$3.50 \pm 0.11 \pm 0.10$	[56]	1.037 ± 0.045	1.015 ± 0.002	0.011 ± 0.023
$D^+ \to \pi^0e^+\nu_e$	3.4K	$3.63 \pm 0.08 \pm 0.05$	[58]			
$D^+ \to \omega\mu^+\nu_\mu$	194	$1.77 \pm 0.18 \pm 0.11$	[59]	0.92 ± 0.14	$0.93 - 0.97$	
$D^+ \to \omega e^+\nu_e$	491	$1.63 \pm 0.11 \pm 0.08$	[60]			
$D^+ \to \eta\mu^+\nu_\mu$	234	$1.04 \pm 0.10 \pm 0.05$	[61]	1.03 ± 0.13	$1.0 - 1.03$	
$D^+ \to \eta e^+\nu_e$	373	$1.07 \pm 0.08 \pm 0.05$	[62]			
$\Lambda_c^+ \to \Lambda\mu^+\nu_\mu$	79	$34.9 \pm 4.6 \pm 2.7$	[63]	1.04 ± 0.31	≈ 1.0	
$\Lambda_c^+ \to \Lambda e^+\nu_e$	104	$36.3 \pm 3.8 \pm 2.0$	[64]			
$D^+ \to \tau^+\nu_\tau$	137	$1.20 \pm 0.24 \pm 0.12$	[65]	3.21 ± 0.77	2.67	0.096 ± 0.132
$D^+ \to \mu^+\nu_\mu$	409	$0.37 \pm 0.02 \pm 0.01$	[66]			
$D_s^+ \to \tau^+\nu_\tau$	4.9K	$52.7 \pm 1.0 \pm 1.2$	[67]	9.72 ± 0.37	9.75	-0.002 ± 0.019
$D_s^+ \to \mu^+\nu_\mu$	1.1K	$5.49 \pm 0.16 \pm 0.15$	[68]			

realized by Cabibbo in 1963 [44]. He hypothesized that the weak interaction flavor states were related to the strong-interaction states by an orthogonal rotation; the most general rotation matrix for three quark generations was first written down by Kobayashi and Maskawa in 1973 [45]. The universality of the quark-W couplings is reflected by the unitarity of the CKM matrix. The equality of the weak interaction-coupling strengths for the quarks and leptons is a feature that is specific to the SM and is violated by many beyond-the-SM theories, such as those that include fourth generation quarks, additional weak vector bosons or multiple Higgs particles.

Search for violations of charged lepton flavor universality

The equality of the electron and muon couplings, g_e and g_μ, has been established at the $\mathcal{O}(0.2\%)$ level, i.e. $(g_e/g_\mu - 1) = 0.002 \pm 0.002$, by a comparison between the $K^+ \to e^+\nu_e$ and $K^+ \to \mu^+\nu_\mu$ partial decay widths measured by the NA62 experiment [46] together with values from the Particle Data Group (PDG) for the K^+ lifetime and the electron and muon masses [47]. The best test of the equality of the τ-lepton coupling and muon couplings, $(g_\tau/g_\mu - 1) = 0.0008 \pm 0.0021$, has similar precision and is from a BESIII measurement of the tau mass [48] together with PDG values of the tau-lepton's lifetime and leptonic decay branching fractions.

The possibility of LFU violation has attracted considerable recent attention because of measurements from BaBar [49], Belle [50] and LHCb [51] of the relative decay rates for the semi-leptonic processes $\bar{B} \to D^{(*)}\tau^-\nu$ and $\bar{B} \to D^{(*)}\ell^-\nu$ ($\ell^- = \mu^-$ or e^-) that seem to violate SM expectations. Specifically, the Heavy Flavor Averaging Group's recent averages of experimental measurements are [52]

$$\begin{aligned}\mathcal{R}_D &= \frac{\mathcal{B}(\bar{B} \to D\tau^-\nu)}{\mathcal{B}(\bar{B} \to D\ell^-\nu)} \\ &= 0.340 \pm 0.027 \pm 0.013(\text{expt.}) \\ &\quad [\mathbf{SM}{:}0.299 \pm 0.003], \\ \mathcal{R}_{D^*} &= \frac{\mathcal{B}(\bar{B} \to D^*\tau^-\nu)}{\mathcal{B}(\bar{B} \to D^*\ell^-\nu)} \\ &= 0.295 \pm 0.011 \pm 0.008\ (\text{expt.}) \\ &\quad [\mathbf{SM}{:}0.258 \pm 0.005]. \end{aligned} \quad (1)$$

Here the discrepancies with LFU, if they are real and not just statistical fluctuations, are of order 10%, and motivate more careful checks of LFU in semi-leptonic and purely leptonic charmed particle decays with BESIII data.

BESIII tests of LFU

Charmed particle decay measurements at BESIII are summarized in detail elsewhere in this journal volume [53]. Table 2 summarizes measurements that are relevant for LFU tests, where all the measurements agree with SM expectations within $1 \sim 2\sigma$. The quantities in the last column,

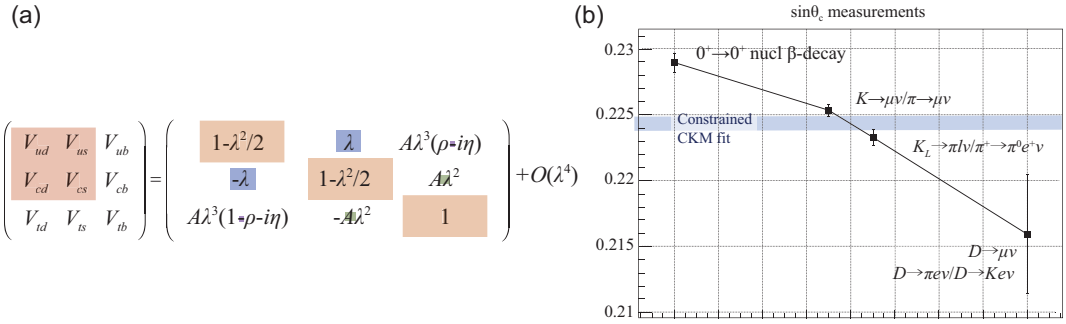

Figure 1. (a) The CKM matrix and its Wolfenstein parameterization. The shaded rectangles in the latter have areas $\propto |V_{ij}|$. (b) Values of $\sin\theta_C$ derived from different measurements. The value based on nuclear β decay is from [70], the one from $K_{\mu 2}$ ($K_{\ell 3}$) decays is from [72] ([75]), and the one from D decays is the average of BESIII $\mathcal{B}(D^+ \to \mu^+\nu)$ [66] and $\mathcal{B}(D^0 \to \pi^- e^+\nu)/\mathcal{B}(D^0 \to K^- e^+\nu)$ [55] measurements. The shaded blue band is the PDG 2018 $\sin\theta_C$ value based on a unitarity-constrained fit to all CKM elements [47].

$\sqrt{(\Gamma_{e(\tau)}/\Gamma_\mu)/\mathrm{SM}} - 1$, which would be $(g_{e(\tau)}/g_\mu - 1)$ if radiative corrections and detailed considerations of the relevant form factors were properly applied, are included as indicators of the sensitivity levels. According to these values, the most stringent BESIII sensitivity levels for LFU-violating effects are a factor of 5 better than those of the $\bar{B} \to D^{(*)}\tau^-\nu$ measurements (equation (1)) but an order of magnitude poorer than the limits on g_e/g_μ from the K^+ decay.

Future prospects for LFU tests at BESIII

The most stringent BESIII tests for LFU-violating effects in charmed-particle decays are derived from measurements of $D \to \bar{K}\ell^+\nu$ and $\pi\ell^+\nu$ semi-leptonic decays, where the current $(g_e/g_\mu - 1)$ sensitivities are at the 1% $\sim$ 2% level. These results are based on the analysis of the 2.97 fb^{-1} data sample accumulated at $\psi(3770) \to D\bar{D}$ resonance. When the analysis of the full 20 fb^{-1} data set is complete, the sensitivity levels of the LFU tests, which are now mostly statistically limited, will improve by factors of $\sim$2.5, and be in the sub-1% range. In this case, if the current 1.8σ discrepancy that BESIII sees in $D^0 \to K^-\ell^-\nu$ is real and the central value reported in Table 2 persists, its significance will increase to more than 4σ. The other BESIII measurement with interesting potential is the ratio of the $D_s^+ \to \tau^+\nu$ and $D_s^+ \to \mu^+\nu$ purely leptonic decay rates that is based on analyses of a 3.19 fb^{-1} data sample collected at $E_{\mathrm{CM}} = 4178$ MeV, where $\sigma(e^+e^- \to D_s^{*+}\bar{D}_s^-)$ has a local maximum of $\sim$1 nb. In this case, the BESIII long-range plan includes an additional 3 fb^{-1} data sample at 4178 MeV, which would provide a $\sqrt{2}$ improvement in $(g_\tau/g_\mu - 1)$ sensitivity.

Unitarity of the CKM matrix and the Cabibbo angle anomaly

The CKM matrix (see Fig. 1(a)) is the DNA of flavor physics; its elements characterize all of the SM weak charged current interactions of quarks. It defines a rotation in three dimensions of flavor space and, in the SM where there are three quark generations, it must be exactly unitary; any deviation from this would be a clear signal for new physics.

The unitarity condition for the top row of the CKM matrix is: $|V_{ud}|^2 + |V_{us}|^2 + |V_{ub}|^2 = 1$. Experimentally, a high-precision value of $|V_{ud}|$ comes from an analysis of eight superallowed $0^+ \to 0^+$ nuclear β decays [69] corrected for electroweak effects. The latest result is $|V_{ud}| = 0.97370(4)$ [70]. A precise value of the ratio $|V_{us}|/|V_{ud}| = 0.2313(5)$ is determined from a KLOE measurement of $\mathcal{B}(K^+ \to \mu^+\nu)$ [71], the PDG 2018 world average for $\mathcal{B}(\pi^+ \to \mu^+\nu)$ [47] and a Flavour Lattice Averaging Group average of LQCD evaluations of the pseudoscalar form-factor ratio f_{K^+}/f_{π^+} [72]. The value of $|V_{ub}|^2$, determined from B-meson decays, is $\sim \mathcal{O}(10^{-5})$ and is a negligible contributor to the unitarity condition [47]. The combination of these results [70],

$$|V_{ud}|^2 + |V_{us}|^2 + |V_{ub}|^2 = 0.9983(5), \qquad (2)$$

indicates a nominal $\sim 3.5\sigma$ deviation from unitarity that, if taken at face value, is strong evidence for a SM violation.

Since deviations from CKM unitarity would be a clear sign of new physics, the equation (2) result inspired further investigation. These included: independent determinations of $|V_{ud}|$ based on the neutron lifetime [73,74] that returned consistent results, albeit with a slightly larger error; an

independent evaluation of $|V_{us}|/|V_{ud}|$ using $\mathcal{B}(K_L \to \pi \ell \nu)$ and $\mathcal{B}(\pi^+ \to \pi^0 e^+ \nu)$ [75] that found an even larger deviation from unitarity, but with a correspondingly larger error; and re-examinations of the nuclear physics corrections used in the nuclear β-decay analyses for $|V_{ud}|$ [76,77] that did not change the central value, but indicated that the previous error that was assigned to these effects may have been somewhat underestimated. The current state of affairs is that the best current analyses of the existing data find an $\mathcal{O}(0.1\%)$ deviation from unitarity for the top row of the CKM matrix with a significance level that is somewhere in the $2\sigma \sim 5\sigma$ range.

The strong generational hierarchy of the CKM quark-flavor mixing matrix is illustrated in Fig. 1(a), where the Wolfenstein parameterization [78] is shown with shaded rectangles with areas that are proportional to $|V_{i,j}|$. Transitions between different generations (i.e. further off-diagonal elements) are successively suppressed by additional factors of $\lambda = \sin\theta_C \simeq 0.225$, where θ_C is the Cabibbo angle. A striking feature of the Wolfenstein formulation, and a characteristic of the SM, is that, to $\mathcal{O}(\lambda^6) \sim 10^{-4}$, the four entries in the upper-left corner of the matrix, i.e. all transitions involving (u, d) and (c, s) quarks, are well characterized by the single parameter, $\sin\theta_C$. Grossman *et al.* [79] argued that comparing the $\sin\theta_C$ values derived from different $q_i \leftrightarrow q_j$ ($i = u, c$; $j = d, s$) subprocesses is a more sensitive test for new physics than tests of the CKM matrix unitarity, and provided, in support of this claim, an example of a toy model that has a heavy gauge boson with different *d*- and *s*-quark couplings that demonstrates this. In Fig. 1(b), values of $\sin\theta_C$ derived from the nuclear β decay ($u \leftrightarrow d$) and $K_{\ell 2}$ and $K_{\ell 3}$ decay ($u \leftrightarrow s$) transitions discussed in the previous paragraph are shown. The apparent discrepancy from a single, universal value is referred to as the *Cabibbo angle anomaly*.

Studies of $c \to d$ transitions provide independent $\sin\theta_C$ determinations. In the SM, $|V_{cd}| = |V_{us}| = \sin\theta_C$; a deviation between the $\sin\theta_C$ value inferred from $c \to d$ decays and that evaluated from $K_{\ell 2}$ and $K_{\ell 3}$ decays would be another clear indication of new physics. To date, this relation has not been strenuously tested. The PDG 2018 world-average value, $|V_{us}| = 0.2243 \pm 0.0005$, differs from that for $|V_{cd}| = 0.218 \pm 0.004$ by 1.5σ, with an uncertainty that is nearly an order of magnitude poorer [47]. The best determinations of $|V_{cd}|$ to date are from statistically limited BESIII measurements of $\mathcal{B}(D^+ \to \mu^+\nu)$ [66] and the ratio $\mathcal{B}(D^0 \to \pi^- e^+ \nu)/\mathcal{B}(D^0 \to K^- e^+ \nu)$ [55], both of which are based on analyses of BESIII's 2.97 fb^{-1} sample of $\psi(3770) \to D\bar{D}$ events that are discussed elsewhere in this journal volume [53]. The average value of the two $|V_{cd}|$ measurements is plotted in Fig. 1(b).

With the full 20 fb^{-1} $\psi(3770)$ data sample, the BESIII precision on $|V_{cd}|$ should be improved by at least a factor of 2.5; if the result is the same as the current central value, the significance of the discrepancy would increase to about the 4σ level.

SEARCHES FOR NON-SM SOURCES OF *CP* VIOLATION

Searches for new sources of *CP* violation have been elevated to a new level of interest by the recent LHCb discovery of a *CP*-violating asymmetry in the charmed quark sector; a 5σ difference between the branching fractions for $D^0 \to K^+K^-$ or $\pi^+\pi^-$ and $\bar{D}^0$ to the same final states, with a magnitude of order 10^{-3} [80]. The measured *CP*-violating asymmetry is at the high end of theoretical estimates for its SM value, which range from 10^{-3} [81–84] to 10^{-4} [85]. Although the LHCb result is intriguing in that it may be a sign of the long-sought-for non-SM mechanism for *CP* violation, uncertainties in the SM calculations for this asymmetry make it impossible to either establish or rule out this possibility [86].

Violations of *CP* have never been observed in weak decays of strange hyperons; the current limit on *CP*-violating asymmetry in Λ hyperon decay is of order 10^{-2} [87], which is 2 orders of magnitude above the highest conceivable SM effects [88]. A non-zero measurement of a *CP*-violating asymmetry at the level of $\sim 10^{-3}$ would be an unambiguous signature for new physics.

Search for *CP* violation in $\Lambda \to p\pi^-$ decay

Parity violation in the weak interactions was discovered in 1957 [89,90]. Immediately thereafter there was considerable interest is studying parity violations in strange hyperon decays that were predicted by Lee and Yang [91]. For the $Y \to B\pi$ weak decay process, where Y is one of the spin $=1/2$ strange hyperons and B is an octet baryon, parity violation allows for both *S*- and *P*-wave transitions, and the final states are characterized by the Lee-Yang parameters

$$\alpha = \frac{2\mathrm{Re}(S^*P)}{|S|^2 + |P|^2}, \qquad \beta = \frac{2\mathrm{Im}(S^*P)}{|S|^2 + |P|^2},$$
$$\gamma = \frac{|S|^2 - |P|^2}{|S|^2 + |P|^2}, \tag{3}$$

where $\alpha^2 + \beta^2 + \gamma^2 = 1$. If the initial state Y has a non-zero polarization $\vec{\mathcal{P}}_Y$, the B flight direction in

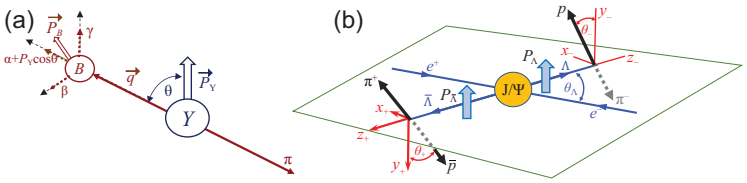

Figure 2. (a) Polarized $Y \to B\pi$ decay illustrating the α, β, γ dependence of the daughter B polarization, where $\vec{q}$ is a vector along the B momentum in the Y rest frame. (b) The $J/\psi \to \Lambda\bar{\Lambda}$ reaction. Parity conservation in J/ψ decay guarantees that the ($\cos\theta$-dependent) Λ and $\bar{\Lambda}$ polarizations are equal and perpendicular to the production plane.

the Y rest frame relative to the polarization direction, θ, is distributed as $dN/d\cos\theta \propto 1 + \alpha|\vec{\mathcal{P}}_Y|\cos\theta$ and, if α is also non-zero, has an explicit parity-violating up-down asymmetry. The polarization of the daughter baryon, $\vec{\mathcal{P}}_B$, depends on $\mathcal{P}_Y$, θ and the α, β, γ parameters, as illustrated in Fig. 2(a). If CP is conserved, the decay parameters for Y and $\bar{Y}$ are equal in magnitude but opposite in sign. (The parameters for $\bar{Y}$ are denoted by $\bar{\alpha}$ and $\bar{\beta}$.) Violations of CP symmetry would result in non-zero values for the parameters A_{CP} and B_{CP}, defined as

$$A_{CP} \equiv \frac{\alpha + \bar{\alpha}}{\alpha - \bar{\alpha}} \quad \text{and} \quad B_{CP} \equiv \frac{\beta + \bar{\beta}}{\beta - \bar{\beta}}. \tag{4}$$

Measuring α_Λ for $\Lambda \to p\pi^-$ decay is not straightforward. Measurements of the up-down parity-violating asymmetry in $\Lambda \to p\pi^-$ determine the product $\alpha_\Lambda \mathcal{P}_\Lambda$, where $\mathcal{P}_\Lambda$ is generally unknown. To extract α_Λ, the polarization of the final-state proton must be measured. This was done in a series of pre-1975 experiments by scattering the final-state proton on carbon, with a world-average result of $\alpha_\Lambda = 0.642 \pm 0.013$ [92]; this was the PDG value for 43 years, from 1976 until 2019.

BESIII measured α_Λ and $\bar{\alpha}_\Lambda$ with fully reconstructed $e^+e^- \to J/\psi \to (\Lambda \to p\pi^-)(\bar{\Lambda} \to \bar{p}\pi^+)$ events. For this reaction, the joint angular distribution can be expressed as [93]

$$\begin{aligned} d\Gamma &\propto (1 + \alpha_\psi \cos^2\theta_\Lambda) \\ &\times [1 + \mathcal{P}_\Lambda(\cos\theta_\Lambda)(\alpha_\Lambda \cos\theta_- + \bar{\alpha}_\Lambda \cos\theta_+)] \\ &+ \alpha_\Lambda\bar{\alpha}_\Lambda[\mathcal{F}_1(\xi) + (1-\alpha_\psi^2)^{1/2}\cos\Delta\Phi\mathcal{F}_2(\xi)], \end{aligned} \tag{5}$$

where θ_Λ is the Λ production angle relative to the e^+-beam direction (the $\cos\theta_\Lambda$ distribution is $1 + \alpha_\psi\cos^2\theta_\Lambda$); $\Delta\Phi$ is the complex phase difference between the $A_{+,+}$ and $A_{+,-}$ helicity amplitudes; and ξ denotes $(\theta_\Lambda, \theta_-, \phi_- \theta_+, \phi_+)$, where θ_-, ϕ_- (θ_+, ϕ_+) are the Λ ($\bar{\Lambda}$) decay angles (see Fig. 2(b)). The $\cos\theta_\Lambda$-dependent Λ (and $\bar{\Lambda}$) polarization is given by

$$\mathcal{P}_\Lambda(\cos\theta_\Lambda) = \frac{(1-\alpha_\psi^2)^{1/2}\cos\theta_\Lambda \sin\theta_\Lambda \sin\Delta\Phi}{1 + \alpha_\psi\cos^2\theta_\Lambda}. \tag{6}$$

The Λ polarization is zero if the $A_{+,+}$ and $A_{+,-}$ helicity amplitudes are relatively real (i.e. $\Delta\Phi = 0$), in which case it is apparent from equation (5) that only the product $\alpha_\Lambda\bar{\alpha}_\Lambda$ can be measured and individual determinations of α_Λ and $\bar{\alpha}_\Lambda$ cannot be extracted from the data. (Expressions for $\mathcal{F}_1(\xi)$ and $\mathcal{F}_2(\xi)$ are provided in [93].)

When BESIII was being planned, it was generally thought that $\mathcal{P}_\Lambda \approx 0$ and that $J/\psi \to \Lambda\bar{\Lambda}$ events would not be useful for CP tests. It was somewhat of a surprise when BESIII subsequently discovered that, in fact, the polarization of Λ and $\bar{\Lambda}$ hyperons produced in J/ψ decays is substantial [94], as shown in Fig. 3(a). With a sample of 420K fully reconstructed $J/\psi \to (\Lambda \to p\pi^-)(\bar{\Lambda} \to \bar{p}\pi^+)$ events in a 1.3B J/ψ event sample, BESIII measured $A_{CP}^\Lambda = -0.006 \pm 0.012 \pm 0.007$. This null result improved on the precision of the best previous measurement, $A_{CP}^\Lambda = +0.013 \pm 0.022$ [87], that was based on 96K $p\bar{p} \to \Lambda\bar{\Lambda}$ events, by a factor of 2. As a byproduct of this measurement, BESIII made the world's most precise measurement of $\alpha_\Lambda = 0.750 \pm 0.010$, a result that is more than 5 standard deviations higher than the previous PDG average value. It is likely that all previous measurements were biased by a common systematic problem, probably related to the spin analyzing properties of carbon; the PDG 2019 value for α_Λ is solely based on the BESIII value [47].

Prospects for BESIII *CP* violation studies

The BESIII values for A_{CP}^Λ and α_Λ mentioned in the previous paragraph were realized by an analysis of 1.3B J/ψ decays, which is a small subset of BESIII's total 10B J/ψ event sample. The analysis of the full data set is currently underway, which, when completed, will provide a factor-of-3 improvement in sensitivity.

BESIII is currently applying a similar analysis to $J/\psi \to (\Xi^- \to \Lambda\pi^-)(\bar{\Xi}^+ \to \bar{\Lambda}\pi^+)$ hyperon pairs, where preliminary results [95] demonstrate that there is substantial transverse Ξ polarization (see Fig. 3(b)). In $\Xi^-\bar{\Xi}^+$ events, the α_Ξ decay parameter influences both the up-down decay asymmetry in the primary $\Xi \to \Lambda\pi$ process, and the polarization of the daughter Λ hyperons (see Fig. 3(a)) that can be determined from the decay asymmetry in the secondary $\Lambda \to p\pi^-$ decay. For a given sample of J/ψ decays, the number of fully

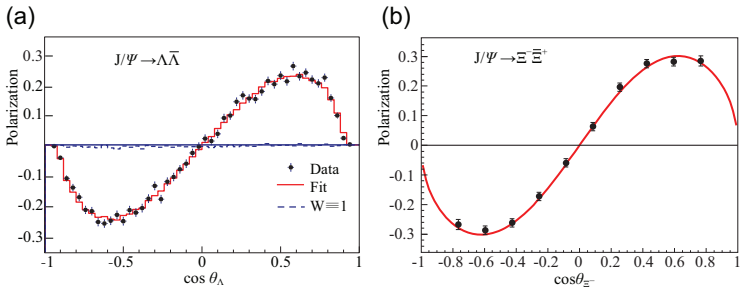

Figure 3. Polarization versus $\cos\theta_{\Lambda(\Xi^-)}$ for (a) $J/\psi \to \Lambda\bar{\Lambda}$ [94] and (b) $J/\psi \to \Xi^-\bar{\Xi}^+$ [95] events. The red curves are fits to the data; the blue (black) curves are expectations for zero polarization.

reconstructed $\Xi^-\bar{\Xi}^+$ events in which $\Lambda \to p\pi^-$ and $\bar{\Lambda} \to \bar{p}\pi^+$ are only about one-quarter of the number of reconstructed $J/\psi \to \Lambda\bar{\Lambda}$ events because of the smaller $J/\psi \to \Xi^-\bar{\Xi}^+$ branching fraction and a lower detection efficiency. Nevertheless, this lower event number is compensated by the added information from the daughter Λ decays. As a result, the sensitivity per event for the Ξ^- decay parameters is higher than that for Λ parameters with $J/\psi \to \Lambda\bar{\Lambda}$ events, and simulations show comparable precisions for α_{Ξ^-} and α_Λ [96]. In contrast to $\Lambda \to p\pi$, where measuring the daughter proton's polarization is impractical, in $\Xi \to \Lambda\pi$ decays the daughter Λ polarization is measured and $B^{\Xi^-}_{CP}$ can be determined; $B^{\Xi^-}_{CP}$ is potentially more sensitive to new physics than $A^{\Xi^-}_{CP}$ [97].

In addition to the Λ hyperons produced by $J/\psi \to \Lambda\bar{\Lambda}$, those produced as daughters in $J/\psi \to (\Xi^- \to \Lambda\pi^-)(\bar{\Xi}^+ \to \bar{\Lambda}\pi^+)$ events are also useful for A^{Λ}_{CP} measurements. The rms polarization of Λ hyperons produced via $J/\psi \to \Lambda\bar{\Lambda}$ (see Fig. 3(a)) is $\langle\mathcal{P}_{J/\psi,\Lambda}\rangle_{\rm rms} \approx 0.13$. In contrast, the rms polarization for Λ hyperons produced as a daughter particle in $\Xi^- \to \Lambda\pi^-$ decay is $\langle\mathcal{P}_{\Xi^-,\Lambda}\rangle_{\rm rms} \approx |\alpha_{\Xi^-}| = 0.39 \pm 0.01$ (see Fig. 2(a)). Thus, $\langle\mathcal{P}_{\Xi^-,\Lambda}\rangle_{\rm rms} \approx 3\langle\mathcal{P}_{J/\psi,\Lambda}\rangle_{\rm rms}$ and, since the A^{Λ}_{CP} sensitivity is proportional to $\sqrt{n_{\rm evts}}$ but linear in $\langle\mathcal{P}_\Lambda\rangle_{\rm rms}$, a Λ from $\Xi^- \to \Lambda\pi^-$ decay has 9 times the equivalent statistical power of a Λ from $J/\psi \to \Lambda\bar{\Lambda}$. Detailed estimates of BESIII's ultimate statistical error for A_{CP} with the existing 10B J/ψ event sample, including Λ hyperons from $\Xi \to \Lambda\pi$ decays, are reported in [96] and summarized here in Table 3. The projected ultimate A^{Λ}_{CP} sensitivity is $\mathcal{O}(2 \times 10^{-3})$, which is an order of magnitude improvement on the pre-BESIII result [87].

STANDARD MODEL FORBIDDEN PROCESSES

Cross sections for $e^+e^- \to$ *hadrons* in the BESIII accessible $E_{\rm CM}$ regions are $\mathcal{O}(10^{-}{\rm nb})$ and the experiment typically records $\mathcal{O}(10^5)$ events/day. However, at the J/ψ resonance peak, the cross section is $\approx$3.6 μb, and in a typical day of operation BESIII collects $\mathcal{O}(10^8)$ events. The cross section at the $\psi(2S)$ peak is $\approx$2 μb and the event rate is $\mathcal{O}(5 \times 10^7)$ events/day. Thus, at the J/ψ and $\psi(2S)$ peaks, BESIII has a high rate of events in a very clean experimental environment that is well suited for high sensitivity searches for a number of SM-model forbidden processes. About one-third of the $\psi(2S)$ events decay via $\psi(2S) \to \pi^+\pi^- J/\psi$, where the triggering on, and detection of only the $\pi^+\pi^-$ pair provides an unbiased 'beam' of tagged J/ψ mesons that can be used to search for decays to final states that would otherwise be undetectable. Table 4 summarizes published BESIII results for forbidden J/ψ decay processes.

Search for the Landau–Yang theorem forbidden $J/\psi \to \gamma\gamma$ decay

The Landau–Yang theorem states that a massive spin-1 meson cannot decay to two photons [103,104]. As a consequence, the $J/\psi \to \gamma\gamma$ decay mode is strictly forbidden. An unambiguous signal for $J/\psi \to \gamma\gamma$ would signal a breakdown of the spin-symmetry theorem of QFT, the underlying framework of the SM and its many proposed new physics extensions. (For a discussion of how QFT might be modified to accommodate a Landau–Yang theorem violation, see [105].)

Table 3. The expected numbers of fully reconstructed events and the extrapolated 1σ statistical errors on $\langle\alpha\rangle = (\alpha - \bar{\alpha})/2$ and A_{CP} from a complete analysis of $J/\psi \to \Lambda\bar{\Lambda}$, $\Xi^-\bar{\Xi}^+$ and $\Xi^0\bar{\Xi}^0$ events in BESIII's 10B J/ψ event data sample (from [96]). Here the full reconstruction of the $\Lambda \to p\pi^-$ and $\bar{\Lambda} \to \bar{p}\pi^+$ decay channels are required.

Reaction	$\mathcal{B}$ ($\times 10^{-4}$)	$n_{\rm evts}$	$\delta\langle\alpha_\Lambda\rangle$	δA^{Λ}_{CP}	$\delta\langle\alpha_{\Xi^-}\rangle$	$\delta A^{\Xi^-}_{CP}$	$\delta\langle\alpha_{\Xi^0}\rangle$	$\delta A^{\Xi^0}_{CP}$
$J/\psi \to \Lambda\bar{\Lambda}$	18.9	3200K	0.0010	0.0049				
$J/\psi \to \Xi^-\bar{\Xi}^+$	9.7	810K	0.0018	0.0034	0.0016	0.0039		
$J/\psi \to \Xi^0\bar{\Xi}^0$	11.6	670K	0.0019	0.0041			0.0017	0.0049
Combined			0.0013	0.0023				

Table 4. Results of the SM forbidden J/ψ decay searches performed at BESIII, showing the data sample size, the upper limit at 90% CL on the branching fractions and the best previous results.

Mode	Data	$\mathcal{B}^{UL}$ at 90% CL	Ref.	Previous best $\mathcal{B}^{UL}$	Ref.
$J/\psi \to \gamma\gamma$	106M $\psi(2S)$	2.7×10^{-7}	[98]	5×10^{-6}	[99]
$J/\psi \to \gamma\phi$	106M $\psi(2S)$	1.4×10^{-6}	[98]		
$J/\psi \to e\mu$	225M J/ψ	1.6×10^{-7}	[100]	1.1×10^{-6}	[101]
$J/\psi \to \Lambda_c^+ e^-$	1.31B J/ψ	6.9×10^{-8}	[102]		

The PDG 2018 upper limit, $\mathcal{B}(J/\psi \to \gamma\gamma) < 2.7 \times 10^{-7}$ [47], is entirely based on a BESIII measurement that uses tagged J/ψ mesons that recoil from the $\pi^+\pi^-$ system in $\psi(2S) \to \pi^+\pi^- J/\psi$ decays [98], and is a factor of 20 times more sensitive than previous measurements [99]. In a data sample containing 106M $\psi(2S)$ decays, events with two oppositely charged tracks and two γ-rays that satisfy a four-constraint energy-momentum kinematic fit to the $\pi^+\pi^-\gamma\gamma$ hypothesis were selected. Figure 4(a) shows the mass recoiling against the $\pi^+\pi^-$ tracks where there is a 29 ± 7 event peak at the J/ψ mass that is consistent with being entirely due to the expected background from roughly equal numbers of $J/\psi \to \gamma\pi^0$ and $\gamma\eta$ events in which the π^0 and η decay to a pair of γ-rays with a large energy asymmetry and the low energy γ is undetected either because its energy is below the detection threshold or outside of the fiducial acceptance region of the detector ($|\cos\theta_\gamma| > 0.92$).

Search for the charge-conjugation parity (C) violating $J/\psi \to \gamma\phi$ decay

A similar BESIII analysis searched for $J/\psi \to \gamma\phi$ [98]. Although this process does not violate the Landau–Yang theorem, it violates C conservation. The weak interactions are known to violate C conservation, but the expected branching fractions for weak-interaction-mediated J/ψ decays are below the level of 10^{-9} [106]. If $J/\psi \to \gamma\phi$ were seen with a branching fraction that is higher than this, it would imply a violation of C conservation in the electromagnetic interaction and be an indicator of new physics. This measurement is based on a search for J/ψ decays to $\gamma\phi$; $\phi \to K^+K^-$, with tagged J/ψ mesons from $\psi(2S) \to \pi^+\pi^- J/\psi$ decays. In this case kinematically constrained $\gamma\pi^+\pi^-K^+K^-$ events, where the K^+ and K^- are positively identified as such by the BESIII PID systems and the $\pi^+\pi^-$ recoil mass is within ± 15 MeV of $m_{J/\psi}$. Figure 4(b) shows the K^+K^- invariant mass where there is no sign of a $\phi \to K^+K^-$ peak at $M_{K^+K^-} \approx m_\phi = 1020$ MeV. A 90% CL upper limit on the size of the ϕ signal is <6.9 events, which translates into a branching fraction upper limit of $\mathcal{B}(J/\psi \to \gamma\phi) < 1.4 \times 10^{-6}$. This is the first experimental limit for this decay.

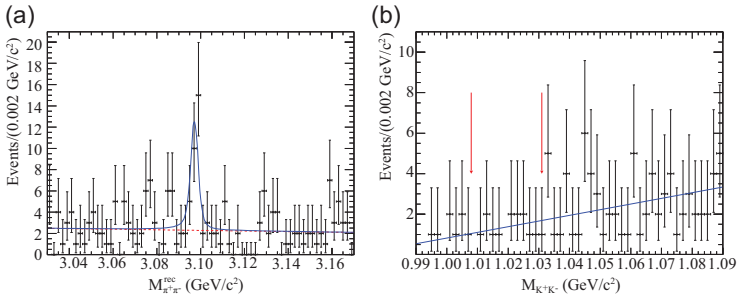

Figure 4. (a) The $\pi^+\pi^-$ recoil mass spectrum for selected $\psi(2S) \to \pi^+\pi^-\gamma\gamma$ events. The peak at the $\pi^+\pi^-$ recoil mass $\approx m_{J/\psi} = 3.097$ GeV is entirely attributable to backgrounds from $J/\psi \to \gamma\pi^0$ and $\gamma\eta$. (b) The K^+K^- invariant mass distribution for $\psi(2S) \to \gamma\pi^+\pi^-K^+K^-$ events with $M(\gamma K^+K^-) = m_{J/\psi} \pm 15$ MeV. A $J/\psi \to \gamma\phi$ decay would show up as a narrow peak with $M(K^+K^-) \approx m_\phi = 1.02$ GeV. Both plots are from [98].

Search for lepton flavor violation in $J/\psi \to e\mu$ decays

The discovery of neutrino oscillations [107] provided clear evidence for violations of lepton flavor conservation (LFV) in the neutrino sector. However, the SM translation of the neutrino results to the charged-lepton sector predicts LFV effects that are proportional to powers of the neutrino masses with branching fractions that are immeasurably small ($<10^{-51}$). Thus, any observation of LFV at levels much higher than this would be clear evidence for new physics, such as grand unified theories or the presence of extra dimensions. Although most attention is given to LFV searches in muon decay, tau decay and $\mu \to e$ conversion experiments, in some theories LFV quarkonium decays, including $V \to \ell_i^- \ell_j^+$ decays, where $i \neq j$, are promising reactions [108]. BESIII searched for the LFV decay $J/\psi \to e^-\mu^+$.

The best previous limit was a 2003 BESII result, $\mathcal{B}(J/\psi \to e^-\mu^-) < 1.1 \times 10^{-6}$ [101], that was based on an analysis of a sample of 58M J/ψ events. This was improved by a 2013 BESIII result that was based on a sample of 225M J/ψ events. In this analysis, the variables $|\sum \vec{p}|/\sqrt{s}$ and $E_{\rm vis}/\sqrt{s}$ are examined for events with two back-to-back and

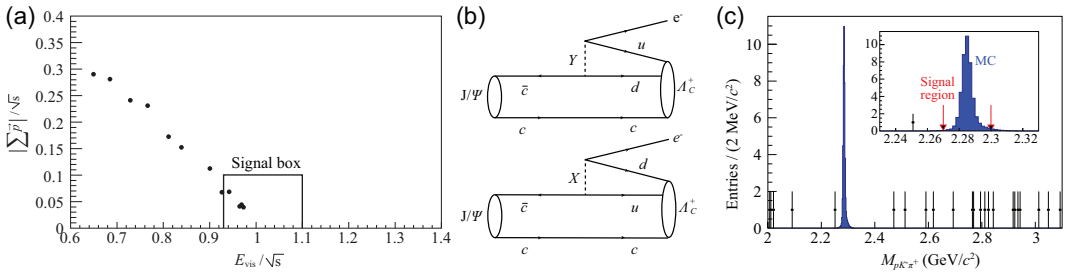

Figure 5. (a) Plot of $|\sum \vec{p}|/\sqrt{s}$ versus $E_{\rm vis}/\sqrt{s}$ for selected $J/\psi \to e^-\mu^+$ candidate events in BESIII [100]. (b) Diagrams for leptoquark-mediated $J/\psi \to e^-\Lambda_c^+$ decay as per the model of [109]. (c) The $pK^-\pi^+$ invariant mass distribution for selected, kinematically constrained $J/\psi \to e^- pK^-\pi^+$ events (from BESIII [102]). The expected shape of a $J/\psi \to \Lambda_c^+ e^-$; $\Lambda_c^+ \to pK^-\pi^+$ signal is shown as the blue histogram.

oppositely charged tracks, with one track positively identified as an electron and the other as a muon. Events with detected γ-rays or additional tracks are rejected, and selected events are required to satisfy a four-constraint energy-momentum kinematic fit. The main background is expected to be from $J/\psi \to \mu^+\mu^-$ events in which one of the muons passes the electron identification requirements. Figure 5(a) shows a scatterplot of $|\sum \vec{p}|/\sqrt{s}$ versus $E_{\rm vis}/\sqrt{s}$ for selected events, where the four events in the signal box are consistent with the 4.75 ± 1.09 background events that are expected. (This background level corresponds to a muon to electron misidentification probability of $\sim 10^{-7}$.) The 90% CL upper limit of $\mathcal{B}(J/\psi \to e^-\mu^+) < 1.6 \times 10^{-7}$ that is established [100] is a factor of 7 more stringent than the previous result.

Search for lepton/baryon number violations in $J/\psi \to \Lambda_c^+ e^-$

In addition to *CP* violation, another requirement that Sakharov listed for the production of the matter-antimatter symmetry of the universe is the existence of a mechanism for baryon/lepton number violation [5]. Processes that violate baryon (B) and lepton (L) number but conserve their difference (B-L) occur in grand unified theories [109]. Experiments that search for B-violating decays of the proton have reported lifetime upper limits with spectacular sensitivities: e.g. $\tau(p \to e^+\pi^0) > 1.6 \times 10^{34}$ years [110]. In contrast, limits for B-violating decays in the heavy quark sector are sparse and not remotely as sensitive. These include a 90% CL upper limit $\mathcal{B}(D^0 \to pe^-) < 1.0 \times 10^{-5}$ from CLEO [111] and BaBar branching fraction limits for $B^0 \to \Lambda_c^+\ell^-$ and $B^- \to \Lambda(\bar{\Lambda})\ell^-$ (here $\ell = e$, μ) that range from a few $\times 10^{-6}$ for the Λ_c^+ modes to a few $\times 10^{-8}$ for the $\Lambda(\bar{\Lambda})$ modes [112].

The only result on B-violating quarkonium decays is a BESIII upper limit on $J/\psi \to \Lambda_c^+ e^-$ that is based on an analysis of a sample of 1.3B J/ψ decays. Quark line diagrams for this process in the context of the Pati–Salam model [109] are shown in Fig. 5(b), where X and Y are virtual leptoquarks that mediate the decay. BESIII searched for exclusive $J/\psi \to \Lambda_c^+ e^-$ decay events where the Λ_c^+ decays to $pK^-\pi^+$ ($\mathcal{B} = 6.3\%$). The $pK^-\pi^+$ invariant mass distribution for candidate events, shown as data points in Fig. 5(c), has no events in the mass interval that is ± 4 times the resolution and centered on the Λ_c^+ mass. The absence of any event candidates translates into a 90% CL frequentist upper limit of $\mathcal{B}(J/\psi \to \Lambda_c^+ e^-) < 6.9 \times 10^{-8}$ [102].

SEARCHES FOR NEW, BEYOND THE STANDARD MODEL PARTICLES

In spite of the success of the SM, particle physics still faces a number of mysteries and challenges, including the origin of elementary particle masses and the nature of dark matter (DM). The Higgs mechanism [113] is a theoretically attractive way to explain the mass of elementary particles. However, the SM relation for the Higgs mass is a potentially divergent infinite sum of quadratically increasing terms that somehow add up to the finite value $m_{\rm Higgs} = 125$ GeV, a SM feature that many theoretical physicists consider to be *unnatural* [114]. The existence of DM is inferred from a number of astrophysical and cosmological observations [115]. One possibility is that DM may be comprised of electrically neutral, weakly interacting, stable particles with a mass at the electroweak scale. However, none of the SM particles are good DM candidates and, from the perspective of theory and phenomenology, this implies that the SM is deficient and the quest for a more fundamental theory beyond the SM is strongly motivated. In some extensions of the SM, the naturalness and DM problems can be solved at once.

The naturalness problem can be solved by supersymmetry (SUSY) [116], where every SM

particle has an as yet undiscovered partner with the same quantum numbers and gauge interactions but differs in spin by $\frac{1}{2}$. The most economical and intensively studied version of SUSY is the minimal supersymmetric model (MSSM) [116], with superpartners that include

spin zero	*sfermions*:	left handed $\tilde{f}_L$, right handed $\tilde{f}_R$,
spin-$\frac{1}{2}$	*gauginos*:	a bino $\tilde{B}$, three winos $\tilde{W}_i$, gluinos $\tilde{g}$,
spin-$\frac{1}{2}$	*higgsinos*:	two $\tilde{H}_i$.

The two higgsinos can mix with the bino and the three winos to produce two *chargino* $\chi^{\pm}_{1,2}$ and four *neutralino* $\chi^0_{1,2,3,4}$ physical states. A discrete symmetry called *R*-parity is introduced to make the lightest SUSY particle, usually the χ^0_1, stable, which makes it a nearly ideal DM candidate that is often denoted as simply χ. A further extension is the so-called next-to-minimal MSSM (NMSSM) [117–119], in which a complex isosinglet field is added. The NMSSM has a rich Higgs sector containing three *CP*-even, two *CP*-odd, and two charged Higgs bosons. The mass of the lightest *CP*-odd scalar Higgs boson, the A^0, may be less than twice the mass of charm quark, in which case it would be accessible at BESIII.

Although the lightest neutralino is an attractive DM candidate, the lack of any experimental evidence for it in either LHC experiments or direct detection experiments suggests that DM might be more complex than the neutralino of the SUSY models. Attempts to devise a unified explanation have led to a vast and diverse array of dark-sector models. These models necessarily have several sectors: a *visible sector* that includes all of the SM particles, a *dark sector* of particles that do not interact with the known strong, weak or electromagnetic forces and a *portal sector* that consists of particles that couple the visible and dark sectors. The latter may be vectors, axions, Higgs-like scalars or neutrino-like fermions [120,121], of which vectors are the most frequently studied. The simplest scenario for the vector portal invokes a new force that is mediated by a $U(1)$ gauge boson [122] that couples very weakly to charged particles via kinetic mixing with the SM photon γ, with a mixing strength ε that is in the range between 10^{-5} and 10^{-2} [123]. This new boson is variously called a dark photon, hidden photon or *U* boson, and is denoted as γ'. The γ' mass is expected to be low, of the order of MeV/c^2 to GeV/c^2 [123] and, thus, it could be produced at the BEPCII collider in a variety of processes, depending on its mass.

Search for A^0, γ' and invisible decays of light mesons

Both the light *CP*-odd NMSSM Higgs boson A^0 and dark photon γ' have been searched for by BESIII. Since it is Higgs-like, the A^0 couples to SM fermions with a strength proportional to the fermion mass. For an A^0 with a mass below the τ pair production threshold, the decay $A^0 \to \mu^+\mu^-$ is expected to be dominant. The A^0 can also serve as a portal to the dark sector with the invisible-final-state decay process $A^0 \to \chi\bar{\chi}$. Similarly, as a portal between the SM and dark sectors, the γ' can, in turn, either decay to $\chi\bar{\chi}$, or visibly to a pair of light leptons or quarks, provided it is kinematically allowed.

BESIII results on searches for the A^0, γ' and invisible decays of light meson states are summarized in Table 5. The A^0 was searched for in $J/\psi \to \gamma A^0$ ($A^0 \to \mu^+\mu^-$) and $\psi(2S) \to \pi^+\pi^- J/\psi$ ($J/\psi \to \gamma A^0$) ($A^0 \to \mu^+\mu^-$) decay candidate events in BESIII's J/ψ [124] and $\psi(2S)$ [125] data samples. The sensitivity obtained with the J/ψ data is 5 times better than that with the $\psi(2S)$ data. The combination of BaBar [126] and BESIII [124] measurements constrain the A^0 to be mostly singlet. BESIII published three results on dark photon (γ') searches in J/ψ and $\psi(3770)$ decays with resulting 90% CL exclusion regions for ε as a function of the dark photon mass that are shown in Fig. 6. BESIII dark photon searches in $J/\psi \to \eta\gamma'$ ($\gamma' \to e^+e^-$) decays [127] and $J/\psi \to \eta'\gamma'$ ($\gamma' \to e^+e^-$) decays [128] were among the first searches that were based on these channels [129]. BESIII results for dark photon searches in $e^+e^- \to \gamma_{\rm ISR}\gamma'$($\gamma' \to \ell^+\ell^-, \ell = e, \mu$) initial state radiation events were based on 2 years of data taking and are competitive with BaBar results [130] based on 9 years of running. Invisible decays of light mesons that are produced in J/ψ decays were also searched for at BESIII. These include the first measurements for the ω and ϕ vector mesons that are copiously produced via $J/\psi \to \omega\eta$ and $\phi\eta$ decays [131]. For $J/\psi \to \phi\eta$ ($\eta \to$ *invisible*) and $J/\psi \to \phi\eta'$ ($\eta' \to$ *invisible*) decays, the BESIII limits [132] are factors of 6 and 3 improvements over previous results from BESII [133]. These results provide complementary information to studies of the nature of DM and constrain parameters of the phenomenological models.

INTERACTIONS WITH OTHER EXPERIMENTS

The standard model of particle physics is a seamless structure in which measurements in one sector have profound impact on other, seemingly unrelated areas. Thus, for example, BESIII

Table 5. BESIII results on searches for the light *CP*-odd Higgs boson A^0, the dark photon γ', and invisible decays of quarkonium and light mesons. The first column lists the decay modes and the third column lists the measured 90% CL branching fractions upper limits. For the visible dark photon decays, the corresponding $\gamma - \gamma'$ mixing strength ε limits are shown in the fourth column.

Mode	Data	$\mathcal{B}^{UL}$ at 90% CL	ε ($\times 10^{-3}$)	Ref.
$J/\psi \to \gamma A^0(\to \mu^+\mu^-)$	225M J/ψ	$(2.8 - 495.3) \times 10^{-8}$		[124]
$\psi' \to \pi\pi J/\psi(\to \gamma A^0(\to \mu^+\mu^-))$	106M $\psi(2S)$	$(4 - 210) \times 10^{-7}$		[125]
$J/\psi \to \eta\gamma'(\to e^+e^-)$	1.31B J/ψ	$(1.9 - 91.1) \times 10^{-8}$	$10 - 1$	[127]
$J/\psi \to \eta'\gamma'(\to e^+e^-)$		$(1.8 - 20) \times 10^{-8}$	$3.4 - 26$	[128]
$e^+e^- \to \gamma_{\rm ISR}\gamma'(\to e^+e^-/\mu^+\mu^-)$	2.93 fb^{-1} $\psi(3770)$		$0.1 - 1$	[129]
$J/\psi \to \eta\omega(\omega \to invisible)$	1.31B J/ψ	7.3×10^{-5}		[131]
$J/\psi \to \eta\phi(\phi \to invisible)$		1.7×10^{-4}		
$J/\psi \to \phi\eta(\eta \to invisible)$	225M J/ψ	1.0×10^{-4}		[132]
$J/\psi \to \phi\eta'(\eta' \to invisible)$		5.3×10^{-4}		

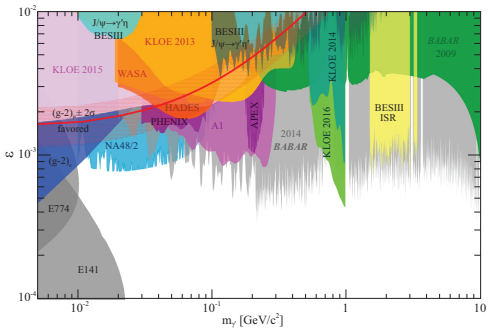

Figure 6. Exclusion limits at the 90% confidence level for the mixing strength parameter ε as a function of the dark photon mass $m_{\gamma'}$. Also shown are exclusion limits from other experiments. The ε values that would explain the discrepancy between the measured and SM-calculated value of the anomalous magnetic moment of the muon [134] are displayed as the bold solid red line along with its 2σ band. Plot is from [129], overlaid with the BESIII limits of $J/\psi \to \eta\gamma'$ and $J/\psi \to \eta'\gamma'$.

measurements of strong-interaction phases in hadronic decays of charmed mesons provide important input into determinations of the *CP*-violating angle γ in *B*-meson decays by BelleII and LHCb. Similarly, BESIII measurements of the annihilation cross section for $e^+e^- \to hadrons$ at energies below 2 GeV provide critical input to the interpretation of high-energy tests of the SM at the Higgs (126 GeV) and top-quark (173 GeV) mass scales as well as the measurements of $(g-2)_\mu$, the anomalous magnetic moment of the muon. The relation between BESIII measurements of strong phases in the charmed sector to *CP*-violating measurements in the beauty sector are discussed elsewhere in this journal volume [53]. Here we briefly review the impact of the BESIIII cross-section results on the interpretation of $(g-2)_\mu$ measurements.

BESIII impact on the determination of $(g-2)_\mu$

The measured value of $(g-2)_\mu$ from BNL experiment E821 [135] is ~3.7 standard deviations higher than the SM prediction [136], a discrepancy that has inspired elaborate follow-up experiments at Fermilab [137] and J-PARC [138]. As illustrated in Fig. 7(a), the SM predicted value for $(g-2)_\mu$ is very sensitive to the effects of hadronic vacuum polarization (HVP) of the virtual photon, which are about 100 times larger than the current experimental uncertainty. The contributions from higher-order radiative corrections to the μ-γ vertex, so-called hadron light-by-light (HLbL) scattering, is of the same order as the current experimental error, but it has a 20% theoretical uncertainty that will be comparable to the expected error from the new round of experiments.

Vacuum polarization also has critical influence on precision tests of the electroweak theory, which rely on a precise knowledge of $\alpha(s)$, the running QED coupling constant. Because of vacuum polarization, $\alpha^{-1}(m_Z^2) = 128.95 \pm 0.01$ [139], about 6% below its long distance value of $\alpha^{-1}(s=0) = 137.04$. About half of this change is due to HVP.

Precision measurement of vacuum polarization of virtual photons

Since HVP effects are non-perturbative, they cannot be directly computed from first-principle QCD. Recent computer-based lattice QCD (LQCD) calculations have made significant progress but the uncertainties are still large [152,153]. The most reliable determinations to date of HVP contributions to $(g-2)_\mu$ and $\alpha(m_Z^2)$ use dispersion relations with input from experimental measurements of cross sections for e^+e^- annihilation into hadrons [136]. The data used for the most recent determinations are mostly

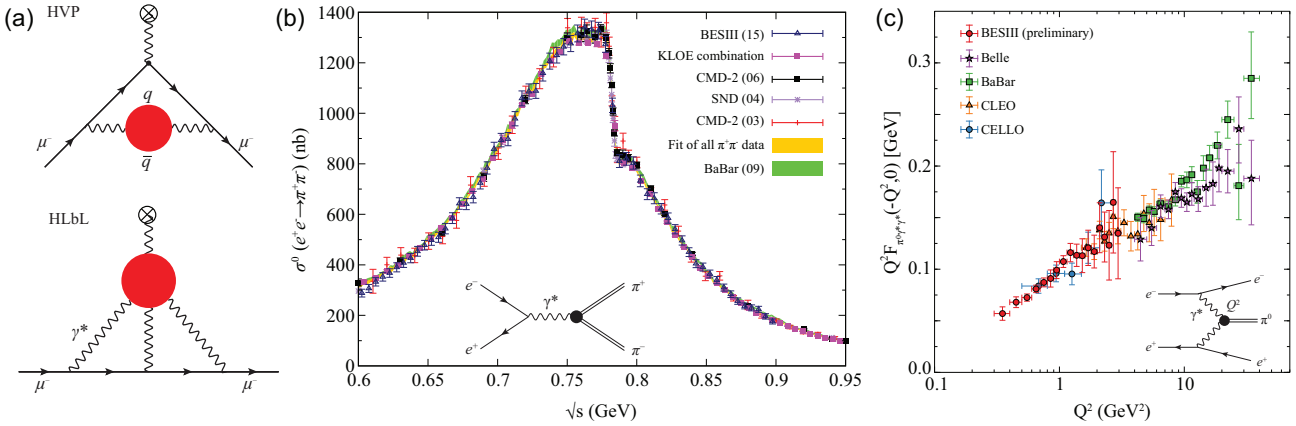

Figure 7. (a) Hadron vacuum polarization (HVP) and hadron light-by-light scattering (HLbL) contributions to the SM calculation of $(g-2)_\mu$. The red circles represent hadronic contributions. (b) Measurements of $\sigma(e^+e^- \to \pi^+\pi^-)$ from SND [140], CMD-2 [141,142], BaBar [143], KLOE [144] and BESIII [145]. The structure near $E_{\rm CM} = 0.78$ GeV is caused by interference between $\rho \to \pi^+\pi^-$ and $\omega \to \pi^+\pi^-$ (from [146]). (c) Preliminary BESIII results for the π^0 form factor [147] together with results from CELLO [148], CLEO [149], BaBar [150] and Belle[151] (from [136]).

from the SND [140], BaBar [143], BESIII [145], CMD-2 [141,142] and KLOE [144] experiments. BaBar and KLOE operations have been terminated, leaving SND, CMD-3 [154] and BESIII as the only running facilities with the capability to provide the improvements in precision that will be essential for the evaluation of $(g-2)_\mu$ with a precision that will match those of the new experimental measurements.

With data taken at $E_{\rm CM} = 3.773$ GeV (primarily for studies of D-meson decays), BESIII measured the cross sections for $e^+e^- \to \pi^+\pi^-$ at $E_{\rm CM}$ between 0.6 and 0.9 GeV [145], which covers the $\rho \to \pi^+\pi^-$ peak, the major contributor to the HVP dispersion relation integral. These measurements used initial state radiation (ISR) events in which one of the incoming beam particles radiates a γ-ray with energy $E_{\rm ISR} = xE_{\rm CM}/2$ before annihilating at a reduced CM energy of $E_{\rm CM} = \sqrt{1-x}E_{\rm CM}$. The relative uncertainty of the BESIII measurements is 0.9%, which is similar to the precisions of the BaBar [143] and KLOE [144] results. The BESIII measured values agree well with KLOE results for energies below 0.8 GeV, but are systematically higher at higher energies; in contrast, BESIII results agree with BaBar at higher energies, but are lower at lower energies. Detailed comparisons are shown in Fig. 7(b). Nevertheless, the contributions of $e^+e^- \to \pi^+\pi^-$ to the $(g-2)_\mu$ HVP calculation from these experiments have overall agreement within 2 standard deviations, and the observed ∼3.7 standard deviation difference between the calculated muon magnetic moment value and the E821 experimental measurement persists.

Experimental input for data-driven HLbL determinations

The HLbL scattering contribution to the SM $(g-2)_\mu$ value has a hadron loop (see Fig. 7(a)) that is non-perturbative and in a more complex environment than the HVP loop. As a result, its determination is not straightforward and has a rather volatile history (see [155]). In this case, the loop integral is dominated by single mesons (π^0, η, η') but, since they couple to virtual photons, their time-like form factors at low Q^2 values are involved. Until now, only high Q^2 measurements of these form factors have been reported and models were used to extrapolate these to the low Q^2 regions of interest. Recently, however, BESIII reported preliminary π^0 form-factor results for Q^2 values in the range 0.3–1.5 GeV^2 [147] (see Fig. 7(c)). These are the first experimental results that include momentum transfers below $Q^2 = 0.5$ GeV^2, the relevant region for HLbL calculations. These, and measurements of the η and η' form factors that are currently underway, will reduce the model dependence and, thus, the theoretical errors of the HLbL contribution to $(g-2)_\mu$.

Prospects for $(g-2)_\mu$-related measurements at BESIII

Currently, the precision of the $(g-2)_\mu$ measurement (54 ppm [135]) is comparable to that of the SM calculation (37 ppm [136]). However, since a 4-fold improvement in the experimental precision is imminent, improvements in the theoretical precision are needed. These will require improved experimental input for the data-driven evaluations of the HVP and HLbL terms and/or improved LQCD calculations. BESIII is improving the $\sigma(e^+e^- \to hadrons)$ measurements used for the HVP term and providing light meson form factors for the HLbL determination. Moreover, precision BESIII measurements of various decay constants and form factors

provide calibration points that are used to validate LQCD techniques.

SUMMARY AND PERSPECTIVES

In the search for new, beyond the standard model physics, there is no compelling theoretical guidance for where it might first show up. It may first appear at the energy frontier that is explored at the LHC, or at the intensity frontier that is pursued at lower energies. (Interestingly, the current most prominent candidate for BSM physics is the $\sim 3.7\sigma$ discrepancy in $(g-2)_\mu$, which is about as far removed from the energy frontier as one can get.) A key aspect of any experiment is *reach*, i.e. the range of unexplored SM-parameter space that is explored. In this quest, BESIII is accumulating huge numbers of J/ψ and $\psi(2S)$ events that support high sensitivity searches for low-mass non-SM particles, SM-forbidden decay processes and non-SM *CP* violations in hyperon decays. In addition, high statistics samples of D and D_s mesons produced just above threshold in very clean experimental environments provide the means to search for new physics in the (u, d)-(c, s) quark sector with the world's best precision. BESIII is continuing the BES program's long history of steadily improving the precision of $e^+e^- \to hadrons$ annihilation cross-section measurements and light meson form-factor determinations that are used to evaluate HVP and HLbL corrections that are needed for the interpretation of SM tests being done by other experiments.

Results highlighted here are primarily based on data samples that were accumulated at the peaks of the narrow J/ψ and $\psi(2S)$ charmonium states and the $\psi(3770) \to D\bar{D}$ resonance. These data samples correspond to 1.3B J/ψ events, 448M $\psi(2S)$ events and a 2.93 fb^{-1} integrated luminosity exposure at $\psi(3770)$. Thanks to the excellent operation of the BEPCII collider, BESIII recently collected a total of 10B J/ψ events that are now being analyzed. And, as this report is being written, a data-taking run is in progress that has the goal of collecting a total of 4M $\psi(2S)$ events. When this run is completed, the BEPCII energy will be set at the $\psi(3770)$ peak, where it will stay until the total exposure at this energy reaches 20 fb^{-1}. These nearly 10-fold increases in the amount of available data will extend the BESIII discovery reach for new, BSM physics by a factor of 3 for most channels, and by almost an order of magnitude for processes with zero backgrounds.

FUNDING

This work was supported in part by the National Natural Science Foundation of China (NSFC) (12035009), the Joint Large-Scale Scientific Facility Funds of the NSFC and CAS (U1532257), the National Key Basic Research Program of China (2015CB856700), the CAS President's International Fellowship Initiative, and the Korean Institute for Basic Science (IBS-R016-D1).

Conflict of interest statement. None declared.

REFERENCES

1. Weinberg S. Essay: half a century of the standard model. *Phys Rev Lett* 2018; **121**: 220001.
2. Weinberg S. A model of leptons. *Phys Rev Lett* 1967; **19**: 1264–6.
3. Glashow SL. Partial symmetries of weak interactions. *Nucl Phys* 1961; **22**: 579–88.
4. Salam A. Weak and electromagnetic interactions. *Conf Proc C* 1968; **680519**: 367–77.
5. Sakharov AD. Violation of CP invariance, C asymmetry, and baryon asymmetry of the universe. *Pisma Zh Eksp Teor Fiz* 1967; **5**: 32–5.
6. Prasad V. Dark matter/ new physics searches at BESIII. *PoS* 2020; **ALPS2019**: 030.
7. Wang B. Searches for new physics at the Belle II experiment. arXiv:1511.00373.
8. Godang R. Search for new physics at BABAR. *EPJ Web Conf* 2013; **49**: 15002.
9. Glashow SL, Iliopoulos J and Maiani L. Weak interactions with lepton-hadron symmetry. *Phys Rev D* 1970; **2**: 1285–92.
10. Capriotti L. Flavour anomalies in rare decays at LHCb. *PoS* 2019; **ICHEP2018**: 233.
11. Aaij R, Adeva B and Adinolfi M *et al.* Differential branching fractions and isospin asymmetries of $B \to K^{(*)}\mu^+\mu^-$ decays. *J High Energy Phys* 2014; **06**: 133.
12. Aaij R, Adeva B and Adinolfi M *et al.* Angular analysis and differential branching fraction of the decay $B_s^0 \to \phi\mu^+\mu^-$. *J High Energy Phys* 2015; **09**: 179.
13. Aaij R, Adeva B and Adinolfi M *et al.* Measurements of the S-wave fraction in $B^0 \to K^+\pi^-\mu^+\mu^-$ decays and the $B^0 \to K^*(892)^0\mu^+\mu^-$ differential branching fraction. *J High Energy Phys* 2016; **11**: 47. Erratum: 2017; **04**: 142.
14. Aaij R, Adeva B and Adinolfi M *et al.* Differential branching fraction and angular analysis of $\Lambda_b^0 \to \Lambda\mu^+\mu^-$ decays. *J High Energy Phys* 2015; **06**: 115. Erratum: 2018; **09**: 145.
15. Detmold W and Meinel S. $\Lambda_b \to \Lambda\ell^+\ell^-$ form factors, differential branching fraction, and angular observables from lattice QCD with relativistic *b* quarks. *Phys Rev D* 2016; **93**: 074501.
16. Aaij R, Adeva B and Adinolfi M *et al.* Test of lepton universality using $B^+ \to K^+\ell^+\ell^-$ decays. *Phys Rev Lett* 2014; **113**: 151601.
17. Aaij R, Adeva B and Adinolfi M *et al.* Test of lepton universality with $B^0 \to K^{*0}\ell^+\ell^-$ decays. *J High Energy Phys* 2017; **08**: 055.
18. Aaij R, Abellán Beteta C and Adeva B *et al.* Angular analysis of the $B^0 \to K^{*0}\mu^+\mu^-$ decay using 3 fb^{-1} of integrated luminosity. *J High Energy Phys* 2016; **02**: 104.

19. Greub C, Hurth T and Misiak M *et al*. The $c \to u\gamma$ contribution to weak radiative charm decay. *Phys Lett B* 1996; **382**: 415–20.
20. Fajfer S, Singer P and Zupan J. The rare decay $D^0 \to \gamma\gamma$. *Phys Rev D* 2001; **64**: 074008.
21. Burdman G, Golowich E and Hewett JL *et al*. Rare charm decays in the standard model and beyond. *Phys Rev D* 2002; **66**: 014009.
22. Fajfer S, Prelovsek S and Singer P. Rare charm meson decays $D \to Pl^+l^-$ and $c \to ul^+l^-$ in SM and MSSM. *Phys Rev D* 2001; **64**: 114009.
23. Paul A, Bigi II and Recksiegel S. On $D \to X_u l^+ l^-$ within the standard model and frameworks like the littlest Higgs model with T parity. *Phys Rev D* 2011; **83**: 114006.
24. Cappiello L, Cata O and D'Ambrosio G. Standard model prediction and new physics tests for $D^0 \to h^+h^-\ell^+\ell^-(h = \pi, K; \ell = e, \mu)$. *J High Energy Phys* 2013; **04**: 135.
25. Sanchis-Lozano MA. On the search for weak decays of heavy quarkonium in dedicated heavy quark factories. *Z Phys C* 1994; **62**: 271–80.
26. Wang YM, Zou H and Wei ZT *et al*. The transition form-factors for semileptonic weak decays of J/ψ in QCD sum rules. *Eur Phys J C* 2008; **54**: 107–21.
27. Wang YM, Zou H and Wei ZT *et al*. FCNC-induced semileptonic decays of J/ψ in the standard model. *J Phys G* 2009; **36**: 105002.
28. Prelovsek S and Wyler D. $c \to u\gamma$ in the minimal supersymmetric standard model. *Phys Lett B* 2001; **500**: 304–12.
29. Paul A., Bigi II and Recksiegel S. $D^0 \to \gamma\gamma$ and $D^0 \to \mu^+\mu^-$ rates on an unlikely impact of the littlest Higgs model with T-parity. *Phys Rev D* 2010; **82**: 094006. Erratum: 2011; **83**: 019901.
30. Hill CT. Topcolor assisted technicolor. *Phys Lett B* 1995; **345**: 483–9.
31. Aulakh CS and Mohapatra RN. Neutrino as the supersymmetric partner of the majoron. *Phys Lett B* 1982; **119**: 136–40.
32. Glashow SL and Weinberg S. Natural conservation laws for neutral currents. *Phys Rev D* 1977; **15**: 1958.
33. Lees JP, Poireau V and Prencipe E *et al*. Search for the decay $D^0 \to \gamma\gamma$ and measurement of the branching fraction for $D^0 \to \pi^0\pi^0$. *Phys Rev D* 2012; **85**: 091107.
34. Patrignani C, Agashe K and Aielli G *et al*. Review of particle physics. *Chin Phys C* 2016; **40**: 100001.
35. Ablikim M, Bai JZ and Ba Y *et al*. Search for the rare decays $J/\psi \to D_s^- e^+\nu_e$, $J/\psi \to D^- e^+\nu_e$ and $J/\psi \to \overline{D^0} e^+e^-$. *Phys Lett B* 2006; **639**: 418–23.
36. Ablikim M, Achasov MN and Ai XC *et al*. Search for $D^0 \to \gamma\gamma$ and improved measurement of the branching fraction for $D^0 \to \pi^0\pi^0$. *Phys Rev D* 2015; **91**: 112015.
37. Ablikim M, Achasov MN and Ahmed S *et al*. Search for the rare decays $D \to h(h^{(')})e^+e^-$. *Phys Rev D* 2018; **97**: 072015.
38. Ablikim M, Achasov MN and Ahmed S *et al*. Search for the rare decays $J/\psi \to D^0 e^+e^- + c.c.$ and $\psi(3686) \to D^0 e^+e^- + c.c.$ *Phys Rev D* 2017; **96**: 111101.
39. Ablikim M, Achasov MN and Ahmed S *et al*. Search for the rare decay of $\psi(3686) \to \Lambda_c^+ \overline{p} e^+e^- + c.c.$ at BESIII. *Phys Rev D* 2018; **97**: 091102.
40. Ablikim M, Achasov MN and Adlarson P *et al*. Future physics programme of BESIII. *Chin Phys C* 2020; **44**: 040001.
41. Datta A, O'Donnell PJ and Pakvasa S *et al*. Flavor changing processes in quarkonium decays. *Phys Rev D* 1999; **60**: 014011.
42. Ablikim M, Achasov MN and Ai XC *et al*. Search for the rare decays $J/\psi \to D_s^- \rho^+$ and $J/\psi \to \overline{D}^0 \overline{K}^{*0}$. *Phys Rev D* 2014; **89**: 071101.
43. Ablikim M, Achasov MN and Ai XC *et al*. Search for the weak decays $J/\psi \to D_s^{(*)} e\nu_e + c.c.$. *Phys Rev D* 2014; **90**: 112014.
44. Cabibbo N. Unitary symmetry and leptonic decays. *Phys Rev Lett* 1963; **10**: 531–3.
45. Kobayashi M and Maskawa T. CP violation in the renormalizable theory of weak interaction. *Prog Theor Phys* 1973; **49**: 652–7.
46. Lazzeroni C, Romano A and Ceccucci A *et al*. Precision measurement of the ratio of the charged kaon leptonic decay rates. *Phys Lett B* 2013; **719**: 326–36.
47. Tanabashi M, Hagiwara K and Hikasa K *et al*. Review of particle physics. *Phys Rev D* 2018; **98**: 030001.
48. Ablikim M, Achasov MN and Ai XC *et al*. Precision measurement of the mass of the τ lepton. *Phys Rev D* 2014; **90**: 012001.
49. Lees JP, Poireau V and Tisserand V *et al*. Evidence for an excess of $\bar{B} \to D^{(*)}\tau^-\bar{\nu}_\tau$ decays. *Phys Rev Lett* 2012; **109**: 101802.
50. Abdesselam A, Adachi I and Adamczyk K *et al*. Measurement of $\mathcal{R}(D)$ and $\mathcal{R}(D^*)$ with a semileptonic tagging method. arXiv:1904.08794.
51. Aaij R, Adeva B and Adinolfi M *et al*. Test of lepton flavor universality by the measurement of the $B^0 \to D^{*-}\tau^+\nu_\tau$ branching fraction using three-prong τ decays. *Phys Rev D* 2018; **97**: 072013.
52. Amhis YS, Banerjee SW and Ben-Haim E *et al*. Averages of *b*-hadron, *c*-hadron, and τ-lepton properties as of 2018. *Eur Phys J C* 2021; **81**: 226.
53. Li HB and Lyu XR. Study of the standard model with weak decays of charmed hadrons at BESIII. *Natl Sci Rev* 2021; **8**: nwab181.
54. Ablikim M, Achasov MN and Ahmed S *et al*. Study of the $D^0 \to K^-\mu^+\nu_\mu$ dynamics and test of lepton flavor universality with $D^0 \to K^-\ell^+\nu_\ell$ decays. *Phys Rev Lett* 2019; **122**: 011804.
55. Ablikim M, Achasov MN and Ai XC *et al*. Study of dynamics of $D^0 \to K^-e^+\nu_e$ and $D^0 \to \pi^-e^+\nu_e$ decays. *Phys Rev D* 2015; **92**: 072012.
56. Ablikim M, Achasov MN and Ahmed S *et al*. Measurement of the branching fraction for the semi-leptonic decay $D^{0(+)} \to \pi^{-(0)}\mu^+\nu_\mu$ and test of lepton universality. *Phys Rev Lett* 2018; **121**: 171803.
57. Ablikim M, Achasov MN and Ai XC *et al*. Improved measurement of the absolute branching fraction of $D^+ \to \bar{K}^0\mu^+\nu_\mu$. *Eur Phys J C* 2016; **76**: 369.
58. Ablikim M, Achasov MN and Ahmed S *et al*. Analysis of $D^+ \to \bar{K}^0 e^+\nu_e$ and $D^+ \to \pi^0 e^+\nu_e$ semileptonic decays. *Phys Rev D* 2017; **96**: 012002.
59. Ablikim M, Achasov MN and Adlarson P *et al*. Observation of the semimuonic decay $D^+ \to \omega\mu^+\nu_\mu$. *Phys Rev D* 2020; **101**: 072005.
60. Ablikim M, Achasov MN and Ai XC *et al*. Measurement of the form factors in the decay $D^+ \to \omega e^+\nu_e$ and search for the decay $D^+ \to \phi e^+\nu_e$. *Phys Rev D* 2015; **92**: 071101.
61. Ablikim M, Achasov MN and Adlarson P *et al*. First observation of $D^+ \to \eta\mu^+\nu_\mu$ and measurement of its decay dynamics. *Phys Rev Lett* 2020; **124**: 231801.
62. Ablikim M, Achasov MN and Ahmed S *et al*. Study of the decays $D^+ \to \eta^{(\prime)}e^+\nu_e$. *Phys Rev D* 2018; **97**: 092009.
63. Ablikim M, Achasov MN and Ahmed S *et al*. Measurement of the absolute branching fraction for $\Lambda_c^+ \to \Lambda\mu^+\nu_\mu$. *Phys Lett B* 2017; **767**: 42–7.
64. Ablikim M, Achasov MN and Ai XC *et al*. Measurement of the absolute branching fraction for $\Lambda_c^+ \to \Lambda e^+\nu_e$. *Phys Rev Lett* 2015; **115**: 221805.
65. Ablikim M, Achasov MN and Adlarson P *et al*. Observation of the leptonic decay $D^+ \to \tau^+\nu_\tau$. *Phys Rev Lett* 2019; **123**: 211802.
66. Ablikim M, Achasov MN and Ai XC *et al*. Precision measurements of $B(D^+ \to \mu^+\nu_\mu)$, the pseudoscalar decay constant f_{D^+}, and the quark mixing matrix element $|V_{cd}|$. *Phys Rev D* 2014; **89**: 051104.

67. Ablikim M, Achasov MN and Adlarson P *et al.* Measurement of the absolute branching fraction of $D_s^+ \to \tau^+\nu_\tau$ via $\tau^+ \to e^+\nu_e\bar{\nu}_\tau$. *Phys Rev Lett* 2021; **127**: 171801.
68. Ablikim M, Achasov MN and Ahmed S *et al.* Determination of the pseudoscalar decay constant $f_{D_s^+}$ via $D_s^+ \to \mu^+\nu_\mu$. *Phys Rev Lett* 2019; **122**: 071802.
69. Hardy J and Towner IS. $|V_{ud}|$ from nuclear β decays. *PoS* 2016; **CKM2016**: 028.
70. Seng CY, Gorchtein M and Patel HH *et al.* Reduced hadronic uncertainty in the determination of V_{ud}. *Phys Rev Lett* 2018; **121**: 241804.
71. Ambrosino F, Antonelli A and Antonelli M *et al.* Measurement of the absolute branching ratio for the $K^+ \to \mu^+\nu(\gamma)$ decay with the KLOE detector. *Phys Lett B* 2006; **632**: 76–80.
72. Aoki S, Aoki Y and Bečirević D *et al.* FLAG review 2019. *Eur Phys J C* 2020; **80**: 113.
73. Czarnecki A, Marciano WJ and Sirlin A. Radiative corrections to neutron and nuclear beta decays revisited. *Phys Rev D* 2019; **100**: 073008.
74. Seng CY, Feng X and Gorchtein M *et al.* Joint lattice QCD-dispersion theory analysis confirms the quark-mixing top-row unitarity deficit. *Phys Rev D* 2020; **101**: 111301.
75. Bazavov A, Bernard C and DeTar C *et al.* $|V_{us}|$ from $K_{\ell 3}$ decay and four-flavor lattice QCD. *Phys Rev D* 2019; **99**: 114509.
76. Seng CY, Gorchtein M and Ramsey-Musolf MJ. Dispersive evaluation of the inner radiative correction in neutron and nuclear β decay. *Phys Rev D* 2019; **100**: 013001.
77. Gorchtein M. γW-box inside-out: nuclear polarizabilities distort the beta decay spectrum. *Phys Rev Lett* 2019; **123**: 042503.
78. Wolfenstein L. Parametrization of the Kobayashi-Maskawa matrix. *Phys Rev Lett* 1983; **51**: 1945.
79. Grossman Y, Passemar E and Schacht S. On the statistical treatment of the Cabibbo angle anomaly. *J High Energy Phys* 2020; **07**: 68.
80. Aaij R, Abellán Beteta C and Adeva B *et al.* Observation of CP violation in charm decays. *Phys Rev Lett* 2019; **122**: 211803.
81. Golden M and Grinstein B. Enhanced CP violations in hadronic charm decays. *Phys Lett B* 1989; **222**: 501–6.
82. Buccella F, Lusignoli M and Miele G *et al.* Nonleptonic weak decays of charmed mesons. *Phys Rev D* 1995; **51**: 3478–86.
83. Bianco S, Fabbri FL and Benson D *et al.* A Cicerone for the physics of charm. *Riv Nuovo Cim* 2003; **26**: 1–200.
84. Grossman Y, Kagan AL and Nir Y. New physics and CP violation in singly Cabibbo suppressed D decays. *Phys Rev D* 2007; **75**: 036008.
85. Khodjamirian A and Petrov AA. Direct CP asymmetry in $D \to \pi^-\pi^+$ and $D \to K^-K^+$ in QCD-based approach. *Phys Lett B* 2017; **774**: 235–42.
86. Saur M and Yu FS. Charm *CPV*: observation and prospects. *Sci Bull* 2020; **65**: 1428–31.
87. Barnes PD, Diebold G and Franklin G *et al.* Observables in high statistics measurements of the reaction $\bar{p}p \to \bar{\Lambda}\Lambda$. *Phys Rev C* 1996; **54**: 1877–86.
88. Donoghue JF, He XG and Pakvasa S. Hyperon decays and CP nonconservation. *Phys Rev D* 1986; **34**: 833.
89. Lee TD and Yang CN. Question of parity conservation in weak interactions. *Phys Rev* 1956; **104**: 254–8.
90. Wu CS, Ambler E and Hayward RW *et al.* Experimental test of parity conservation in β decay. *Phys Rev* 1957; **105**: 1413–4.
91. Lee TD and Yang CN. General partial wave analysis of the decay of a hyperon of spin 1/2. *Phys Rev* 1957; **108**: 1645–7.
92. Bricman C, Dionisi C and Hemingway RJ *et al.* Review of particle properties. *Phys Lett B* 1978; **75**: 1–250.
93. Fäldt G and Kupsc A. Hadronic structure functions in the $e^+e^- \to \bar{\Lambda}\Lambda$ reaction. *Phys Lett B* 2017; **772**: 16–20.
94. Ablikim M, Achasov MN and Ahmed S *et al.* Polarization and entanglement in baryon-antibaryon pair production in electron-positron annihilation. *Nat Phys* 2019; **15**: 631–4.
95. Ablikim M, Achasov MN and Adlarson P *et al.* Weak phases and CP-symmetry tests in sequential decays of entangled double-strange baryons. arXiv:2105.11155.
96. Adlarson P and Kupsc A. CP symmetry tests in the cascade-anticascade decay of charmonium. *Phys Rev D* 2019; **100**: 114005.
97. Gonzalez E and Illana JI. CP violation in nonleptonic hyperon decays at the tau charm factory. In: *3rd Workshop on the Tau-Charm Factory*, 1994, 525–38.
98. Ablikim M, Achasov MN and Ai XC *et al.* Search for C-parity violation in $J/\psi \to \gamma\gamma$ and $\gamma\phi$. *Phys Rev D* 2014; **90**: 092002.
99. Adams GS, Anderson M and Cummings JP *et al.* Observation of $J/\psi \to 3\gamma$. *Phys Rev Lett* 2008; **101**: 101801.
100. Ablikim M, Achasov MN and Albayrak O *et al.* Search for the lepton flavor violation process $J/\psi \to e\mu$ at BESIII. *Phys Rev D* 2013; **87**: 112007.
101. Bai JZ, Ban Y and Bian JG *et al.* Search for lepton flavor violation process $J/\psi \to e\mu$. *Phys Lett B* 2003; **561**: 49–54.
102. Ablikim M, Achasov MN and Ahmed S *et al.* Search for baryon and lepton number violation in $J/\psi \to \Lambda_c^+ e^- + c.c.$ *Phys Rev D* 2019; **99**: 072006.
103. Landau LD. On the angular momentum of a system of two photons. *Dokl Akad Nauk SSSR* 1948; **60**: 207–9.
104. Yang CN. Selection rules for the dematerialization of a particle into two photons. *Phys Rev* 1950; **77**: 242–5.
105. Gninenko SN, Ignatiev AY and Matveev VA. Two photon decay of Z′ as a probe of bose symmetry violation at the CERN LHC. *Int J Mod Phys A* 2011; **26**: 4367–85.
106. Wang T, Jiang Y and Yuan H *et al.* Weak decays of J/ψ and $\Upsilon(1S)$. *J Phys G* 2017; **44**: 045004.
107. Fukuda Y, Hayakawa T and Ichihara E *et al.* Evidence for oscillation of atmospheric neutrinos. *Phys Rev Lett* 1998; **81**: 1562–7.
108. Bordes J, Chan HM and Tsou ST. Implications of a rotating mass matrix. *Phys Rev D* 2001; **63**: 016006.
109. Pati JC and Salam A. Lepton number as the fourth color. *Phys Rev D* 1974; **10**: 275–89. Erratum: 1975; **11**: 703.
110. Abe K, Haga Y and Hayato Y *et al.* Search for proton decay via $p \to e^+\pi^0$ and $p \to \mu^+\pi^0$ in 0.31 megaton-years exposure of the Super-Kamiokande water Cherenkov detector. *Phys Rev D* 2017; **95**: 012004.
111. Rubin P, Lowrey N and Mehrabyan S *et al.* Search for $D^0 \to \bar{p}e^+$ and $D^0 \to pe^-$. *Phys Rev D* 2009; **79**: 097101.
112. del Amo Sanchez P, Lees JP and Poireau V *et al.* Searches for the baryon- and lepton-number-violating decays $B^0 \to \Lambda_c^+\ell^-$, $B^- \to \Lambda\ell^-$, and $B^- \to \bar{\Lambda}\ell^-$. *Phys Rev D* 2011; **83**: 091101.
113. Higgs PW. Broken symmetries and the masses of gauge bosons. *Phys Rev Lett* 1964; **13**: 508–9.
114. Susskind L. Dynamics of spontaneous symmetry breaking in the Weinberg-Salam theory. *Phys Rev D* 1979; **20**: 2619–25.
115. Jibrail AW, Elahi PJ and Lewis GF. Cosmological signatures of dark sector physics: the evolution of haloes and spin alignment. *Mon Notices Royal Astron Soc* 2020; **492**: 2369–82.
116. Martin SP. A supersymmetry primer. *Adv Ser Dir High Energy Phys* 1998; **18**: 1–98.

117. Ellwanger U, Hugonie C and Teixeira AM. The next-to-minimal supersymmetric standard model. *Phys Rep* 2010; **496**: 1–77.
118. Maniatis M. The next-to-minimal supersymmetric extension of the standard model reviewed. *Int J Mod Phys A* 2010; **25**: 3505–602.
119. Djouadi A, Drees M and Ellwanger U *et al.* Benchmark scenarios for the NMSSM. *J High Energy Phys* 2008; **07**: 2.
120. Essig R, Jaros JA and Wester W *et al.* Dark sectors and new, light, weakly-coupled particles. arXiv:1311.0029.
121. Alexander J, Battaglieri M and Echenard B *et al.* Dark sectors 2016 workshop: community report. arXiv:1608.08632.
122. Holdom B. Two U(1)'s and ϵ charge shifts. *Phys Lett B* 1986; **166**: 196–8.
123. Arkani-Hamed N, Finkbeiner DP and Slatyer TR *et al.* A theory of dark matter. *Phys Rev D* 2009; **79**: 015014.
124. Ablikim M, Achasov MN and Ai XC *et al.* Search for a light CP-odd Higgs boson in radiative decays of J/ψ. *Phys Rev D* 2016; **93**: 052005.
125. Ablikim M, Achasov MN and Ambrose DJ *et al.* Search for a light exotic particle in J/ψ radiative decays. *Phys Rev D* 2012; **85**: 092012.
126. Lees JP, Poireau V and Tisserand V *et al.* Search for di-muon decays of a low-mass Higgs boson in radiative decays of the $\Upsilon(1S)$. *Phys Rev D* 2013; **87**: 031102. Erratum: 2013; **87**: 059903.
127. Ablikim M, Achasov MN and Adlarson P *et al.* Study of the Dalitz decay $J/\psi \to e^+e^-\eta$. *Phys Rev D* 2019; **99**: 012006.
128. Ablikim M, Achasov MN and Ahmed S *et al.* Measurement of $\mathcal{B}(J/\psi \to \eta' e^+e^-)$ and search for a dark photon. *Phys Rev D* 2019; **99**: 012013.
129. Ablikim M, Achasov MN and Ai XC *et al.* Dark photon search in the mass range between 1.5 and 3.4 GeV/c^2. *Phys Lett B* 2017; **774**: 252–7.
130. Lees JP, Poireau V and Tisserand V *et al.* Search for a dark photon in e^+e^- collisions at BaBar. *Phys Rev Lett* 2014; **113**: 201801.
131. Ablikim M, Achasov MN and Ahmed S *et al.* Search for invisible decays of ω and ϕ with J/ψ data at BESIII. *Phys Rev D* 2018; **98**: 032001.
132. Ablikim M, Achasov MN and Albayrak O *et al.* Search for η and η' invisible decays in $J/\psi \to \phi\eta$ and $\phi\eta'$. *Phys Rev D* 2013; **87**: 012009.
133. Ablikim M, Bai JZ and Ban Y *et al.* Search for invisible decays of η and η' in the processes $J/\psi \to \phi\eta$ and $\phi\eta'$. *Phys Rev Lett* 2006; **97**: 202002.
134. Pospelov M. Secluded U(1) below the weak scale. *Phys Rev D* 2009; **80**: 095002.
135. Bennett GW, Bousquet B and Brown HN *et al.* Final report of the muon E821 anomalous magnetic moment measurement at BNL. *Phys Rev D* 2006; **73**: 072003.
136. Aoyama T, Asmussen N and Benayoun M *et al.* The anomalous magnetic moment of the muon in the standard model. *Phys Rep* 2020; **887**: 1–166.
137. Grange J, Guarino V and Winter P *et al.* Muon (g-2) technical design report. arXiv:1501.06858.
138. Otani M. Status of the muon g-2/EDM experiment at J-PARC (E34). *JPS Conf Proc* 2015; **8**: 025008.
139. Davier M, Hoecker A and Malaescu B *et al.* Reevaluation of the hadronic vacuum polarisation contributions to the standard model predictions of the muon $g-2$ and $\alpha(m_Z^2)$ using newest hadronic cross-section data. *Eur Phys J C* 2017; **77**: 827.
140. Achasov MN, Beloborodov KI and Berdyugin AV *et al.* Update of the $e^+e^- \to \pi^+\pi^-$ cross-section measured by SND detector in the energy region $400 < \sqrt{s} < 1000$ MeV. *J Exp Theor Phys* 2006; **103**: 380–4.
141. Akhmetshin RR, Anashkin EV and Arbuzov AB *et al.* Reanalysis of hadronic cross-section measurements at CMD-2. *Phys Lett B* 2004; **578**: 285–9.
142. Akhmetshin RR, Aulchenko VM and Banzarov VSH *et al.* High-statistics measurement of the pion form factor in the ρ-meson energy range with the CMD-2 detector. *Phys Lett B* 2007; **648**: 28–38.
143. Lees JP, Poireau V and Tisserand V *et al.* Precise measurement of the $e^+e^- \to \pi^+\pi^-(\gamma)$ cross section with the initial-state radiation method at BABAR. *Phys Rev D* 2012; **86**: 032013.
144. Anastasi A, Babusci D and Berlowski M *et al.* Combination of KLOE $\sigma(e^+e^- \to \pi^+\pi^-\gamma(\gamma))$ measurements and determination of $a_\mu^{\pi^+\pi^-}$ in the energy range $0.10 < s < 0.95$ GeV^2. *J High Energy Phys* 2018; **03**: 173.
145. Ablikim M, Achasov MN and Ai XC *et al.* Measurement of the $e^+e^- \to \pi^+\pi^-$ cross section between 600 and 900 MeV using initial state radiation. *Phys Lett B* 2016; **753**: 629. Eerratum: 2021; **812**: 135982.
146. Keshavarzi A, Nomura D and Teubner T. Muon $g-2$ and $\alpha(M_Z^2)$: a new data-based analysis. *Phys Rev D* 2018; **97**: 114025.
147. Redmer CF. Measurement of meson transition form factors at BESIII. arXiv:1810.00654.
148. Behrend HJ, Criegee L and Field JH *et al.* A measurement of the π^0, η and η' electromagnetic form-factors. *Z Phys C* 1991; **49**: 401–10.
149. Gronberg J, Hill TS and Kutschke R *et al.* Measurements of the meson-photon transition form-factors of light pseudoscalar mesons at large momentum transfer. *Phys Rev D* 1998; **57**: 33–54.
150. Aubert B, Karyotakis Y and Lees JP *et al.* Measurement of the $\gamma\gamma^* \to \pi^0$ transition form factor. *Phys Rev D* 2009; **80**: 052002.
151. Uehara S, Watanabe Y and Nakazawa H *et al.* Measurement of $\gamma\gamma^* \to \pi^0$ transition form factor at Belle. *Phys Rev D* 2012; **86**: 092007.
152. Miura K. Review of lattice QCD studies of hadronic vacuum polarization contribution to muon $g-2$. *PoS* 2019; **LATTICE2018**: 010.
153. Davies CTH, DeTar C and El-Khadra AX *et al.* Hadronic-vacuum-polarization contribution to the muon's anomalous magnetic moment from four-flavor lattice QCD. *Phys Rev D* 2020; **101**: 034512.
154. Akhmetshin RR, Amirkhanov AN and Anisenkov AV *et al.* Study of the process $e^+e^- \to \pi^+\pi^-\pi^+\pi^-$ in the C.M. energy range 920–1060 MeV with the CMD-3 detector. *Phys Lett B* 2017; **768**: 345–50.
155. Melnikov K. Theory review of the muon $g-2$. *EPJ Web Conf* 2016; **118**: 01020.

INTERVIEW

National Science Review
8: nwab008, 2021
https://doi.org/10.1093/nsr/nwab008
Advance access publication 20 January 2021

Special Topic: Physics of the BESIII Experiment

The search for charmed states of matter

By Philip Ball

With the discovery of the Higgs boson in 2012, the Standard Model of particle physics was completed. This description encompasses all known subatomic particles and their interactions. Much of the public interest in high-energy physics now focuses on experimental searches for 'new physics' beyond the Standard Model. Yet it would be a mistake to imagine that the Standard Model is now fully understood. Many questions remain about the ways in which known fundamental particles interact and unite, especially at the very high energies needed to produce the most exotic varieties, such as heavy quarks (quarks are the constituents of hadrons, which include the ordinary nuclear particles protons and neutrons) and heavy leptons (leptons are members of the family that includes electrons).

The Beijing Electron-Positron Collider (BEPC), operated by the Chinese Academy of Sciences' Institute of High Energy Physics, is one of the installations that are probing these questions. It has been running since 1988, using a detector called the Beijing Spectrometer (BES). (The site also houses the Beijing Synchrotron Radiation Facility for conducting studies in condensed matter using intense X-rays.) Since 2008, these two instruments have been operating in upgraded form: the BESIII detector and BEPCII accelerator. The facility is now one of the key international centers for investigating the properties and behavior of new exotic hadrons, in particular those that include the charm quark. Italian physicist Luciano Maiani, Director of the European particle physics center CERN in Switzerland from 1999 to 2003, is one of the world leaders in this area of high-energy physics, and played a central role in the identification of the charm quark itself. NSR spoke to him about the aims of the latest work at the BEPCII, and the prospects for new discoveries.

***NSR*:** What are the main improvements that were made for BESIII and BEPCII, and what new regimes of energy, beam intensity and/or sensitivity do they access?

***Maiani*:** BEPCII is a particle accelerator of a special kind called a collision ring. The first of these devices was realized by Austrian physicist Bruno Touschek in Italy in the 1960s. In this machine, two beams of particles, one with electrons (e^-) and the other with positrons (e^+, the electron's antiparticle), are accelerated and kept in two circular orbits under extreme vacuum. Where the orbits intersect, electrons and positrons collide head on. In a few cases, an electron and a positron interact so closely that they annihilate one another, giving rise to a wealth of subatomic particles that can be studied by appropriate particle detectors. BESIII is one such detector, and measures the energy, direction of flight, electric charge and other physical properties of the particles created in the annihilation event, thus identifying their nature and the correlations among them. Collision rings are characterized by the beam energy, which determines the maximum mass of the particles produced, and the luminosity, related to the density of particles in the beam and which determines the collision rate.

BEPC can produce particles containing a pair of charm quarks, such as the J/Ψ meson discovered by Burton Richter and Samuel Ting (which won them the 1976 Nobel Prize). Particle detectors are characterized by the precision with which particle energies can be measured, the energy resolution, and by their capability for detecting neutral particles such as photons, which are an important tool for identifying new particles produced in e^+e^- annihilation. The labels II and III indicate progressive increases in luminosity (for BEPC) and in energy resolution and neutral particle detection (for BES), with respect to the original design.

Italian physicist Luciano Maiani, Director of the European particle physics center CERN in Switzerland from 1999 to 2003 *(courtesy of Luciano Maiani).*

> Among facilities of this kind, BEPCII currently has the highest luminosity in the world.
>
> —Luciano Maiani

***NSR*:** How, in short, does BESIII work?

***Maiani*:** The annihilation of an e^+e^- pair can produce a single unstable particle, called a 'resonance', which appears as a bump in the annihilation probability as a function of beam energy (that is the 'spectroscopy'), with a width inversely proportional to the particle's lifetime. (The amount of this indeterminacy in energy is inversely related to the lifetime of the particle via Heisenberg's Uncertainty Principle.) In this way, we can determine lifetimes of the order of 10^{-20}–10^{-23} seconds, which is something we could never assess from direct measurements of this timescale. That is how the J/Ψ particle and many other charm-anticharm states were first observed in the 1970s at the SLAC collider in Stanford, California.

As well as the resonance, the annihilation produces many other particles. However, particular clusters of the final particles may themselves arise from the decay of an unstable particle. To identify the parent particle, one plots the distribution of the total mass of the cluster. A bump in this distribution, and the corresponding width, gives the mass and lifetime of the parent resonance. In this way, BESIII has discovered the resonances denoted $Z_C(3900)$ and $Z_C(4020)$, where the numbers indicate the masses in MeV. These resonances are made of a pair of charm quarks accompanied by a pair of lighter quarks, as indicated by the fact that they are electrically charged (unlike the J/Ψ). These Z_C resonances are among the first examples of subnuclear particles that require, in their constitution, at least two quark–antiquark pairs. The $Z_C{}^+$, for example, is made from a $c\bar{c}$ and a $u\bar{d}$ pair [Here c, u and d denote the charm, up and down quarks, and the bars indicate their antiparticles.].

***NSR*:** Are there any other instruments in the world that could perform experiments like those at BESIII? How do its capabilities compare with those at CERN, for example?

***Maiani*:** The particles studied with BESIII are in the range of particles made by a $c\bar{c}$ pair (called charmonia) plus, eventually, other constituents. These particles are called hidden charm particles, because they have zero net charm quantum number: the charm and anticharm quarks 'cancel out'. Hidden charm particles are produced in high-energy hadron colliders like the Large Hadron Collider (LHC) at CERN—but there they feature in events with a large background of other particles, and so it is hard to see the resonances. Low background is a crucial feature of e^+e^- colliders like BEPCII.

Among facilities of this kind (called charm-tau factories), BEPCII currently has the highest luminosity in the world. A lower-luminosity machine, VEPP2000, is working at the Budker Institute in Novosibirsk, Russia, with plans for a considerable upgrade in the coming years. At higher energy, the $b\bar{b}$ factory at KEK in Tsukuba, Japan, with the Belle detector, can reach the hidden charm range by restricting the observation of events to those in which one of the initial particles (the electron or positron) loses energy by radiating a photon so as to bring the center-of-mass energy of the annihilation into the charm-tau range.

The Belle and LHCb collaborations have produced valuable results on exotic hadrons. But as far as resolution and luminosity are concerned, BEPCII and BESIII are firmly in the forefront of global research on hidden charm particles.

TESTING THE THEORY OF QUARK BINDING

***NSR*:** There is a well-established theory—quantum chromodynamics (QCD)—for describing the properties of 'light' hadrons in terms of the interactions of light quarks and gluons. And yet it seems that there are still questions to be asked about this sector of high-energy physics. What are the key issues here?

***Maiani*:** QCD has been tested in phenomena such as high-energy, large-angle scattering of electrons off protons (called deep inelastic scattering). In these conditions, the coupling that regulates the QCD interaction is small—this property is called asymptotic freedom, the discovery of which won David Gross, David Politzer and Franck Wilczek the 2004 Nobel Prize. In these conditions the interaction can be treated in close analogy to quantum electrodynamics (the quantum description of matter–light interactions), and the theory satisfactorily describes the experimental results. But the binding of quarks into baryons and mesons (hadrons) puts QCD in the very strong interaction regime, and the connection of the fundamental theory to the details of the binding is not (yet) well-established. This makes hadron spectroscopy of great interest, because those experiments can give us clues about how to build a theory of the bound states, in particular to determine the dominant forces binding multiquark mesons such as the resonance $Z_C{}^+$, in comparison to the simplest $c\bar{c}$ states (that is, charmonia). Multiquark spectroscopy is thus the new, largely unexplored, frontier of quantum chromodynamics.

***NSR*:** There seem to be some exotic particles and states predicted in the low-energy light-hadron regime, such as 'glueballs'. What are these, and why are they important?

***Maiani*:** In QCD, the strong interactions are transmitted by gluons: massless particles with spin 1, analogous in many respects to the photons that transmit the electromagnetic force, except that they are able to interact strongly with each other. As a consequence, one can conceive of bound states called 'glueballs' made of gluons only, which would be neutral under all possible elementary particle symmetries. Theoretically, it is difficult to distinguish gluons from quark–antiquark states in which the quarks are arranged so as to neutralize all possible quantum numbers related to symmetry: these are called 'singlet' configurations. At the moment, among the observed resonances,

there are few cases where more singlet particles have been seen than are

> Multiquark spectroscopy is the new, largely unexplored, frontier of quantum chromodynamics.
>
> —Luciano Maiani

predicted by the quark model—and so these can be considered to be candidates for these elusive glueballs.

***NSR*:** One of the primary goals of BESIII seems to be to probe the physics of heavy quarks such as the charm quark. You yourself played a key role in the discovery of this particle. Can you tell us how that came about?

***Maiani*:** If hadrons are made of three quark types only (up, down and strange), as originally proposed by Murray Gell-Mann and George Zweig in 1963, it implies that the weak force would be mediated by a particular boson that produces the so-called Cabibbo transition, by which a u quark and the weak-force particle W^- interconvert with a particular combination of d and s quarks introduced by Nicola Cabibbo. Attention was focused in 1968 on the so-called 'neutral current processes', which are forbidden in the first approximation but can be generated by including 'corrections' with amplitudes that can in principle grow without limit. In 1970, Sheldon Glashow, John Iliopoulos and I (collectively, GIM) proposed that these processes might involve a fourth quark, designated 'charm' (c). (Such a quark had already been suggested by others for completely different reasons.) This idea turned a puzzle in the three-quark theory into a way of estimating the mass of this putative fourth quark.

The predicted c quark mass was sufficiently large to explain the unsuccessful searches for mesons containing it that had been conducted in the 1960s. The GIM mechanism has been an important step towards a unified theory of the electromagnetic and weak interactions, allowing hadrons (governed by strong interactions) to be included in the picture. The existence of the charm quark was confirmed by the discovery of the J/Ψ particle in 1974.

THE WORLD OF CHARMONIA

***NSR*:** In charm physics, the notion of 'charmonium' states seems to play a central role. What is this?

***Maiani*:** Calculations of the neutral-current processes that motivated the GIM mechanism have been carried out in the electroweak theory and have confirmed the large mass of the charm quark: $M_C \approx 1.8$ GeV. With the advent of QCD, the large value of charm mass appeared in a different light. It is known that electron–positron pairs form bound states known as 'positronium'. In 1974, Thomas Appelquist and David Politzer considered the analogous state formed by a $c\bar{c}$ pair bound by QCD forces, which they called 'charmonium'. The idea was taken up by Sheldon Glashow, Alvaro de Rujula and Howard Georgi, to explain the surprisingly narrow width of the just-discovered J/Ψ, which implied that that particle might be the first manifestation of the charm quark (in hidden-charm disguise). In the following years, many authors presented accurate quantitative calculations of the numerous charmonia states discovered in electron–positron colliders after the J/Ψ . That success was repeated at higher mass, after the discovery of similar resonances of $b\bar{b}$ quark pairs.

***NSR*:** There seems to be a dizzying array of possible particles, resonances and transitions involving charm quarks. Can you help us navigate this 'zoo' by explaining what some of the key issues are?

***Maiani*:** Heavy quark pairs are difficult both to create and to destroy by QCD forces. The first examples of such exotic hadrons were resonances whose decay products contain a charmonium (and therefore a $c\bar{c}$ pair) but do not fit the spectrum of charmonia accurately computed by QCD. Such resonances have been dubbed 'unanticipated charmonia' and classified, provisionally, as X, Y and Z states. The first unanticipated charmonium, $X(3872)$, was found by the Belle collaboration in Japan in 2003; this state decayed into J/Ψ and pion particles. $X(3872)$ cannot be a charmonium state, however, because its mass does not fit with predictions and because its pion decays do not follow the rules obeyed by pure charmonia. A second unanticipated resonance, $Y(4260)$, was found by the Babar experiment at SLAC, with a mass that also does not fit the charmonium spectrum. The first example of electrically charged unanticipated charmonium, $Z(4430)$, was found by Belle in 2007, but its existence as a genuine resonance was put in doubt by Babar. However, in 2014 the LHCb instrument at CERN, with improved statistics, confirmed $Z(4430)$ as a genuine resonance.

In 2013, as indicated earlier, BESIII discovered two other charged resonances with charmonium decay: $Z_C(3900)$ (which decays into J/Ψ and a pion) and $Z_C(4020)$ (which decays into a pion and a charmonium state with the same spin as J/Ψ but opposite parity, denoted h_c). Over the past 10 years, BESIII has produced a wealth of results on the Y states, including analogies among the $X(3872)$, $Y(4260)$ and $Z_C(3900)$ states.

Even so, no consensus has been reached yet about how quarks are organized inside X, Y and Z resonances. One possibility is the 'compact tetraquark', where a diquark (cq) is bound to an anti-diquark ($\bar{c}\bar{q}'$) by QCD forces, similar to those that bind $c\bar{c}$ into a meson. With improved statistics and resolution, BESIII might be able to help distinguish among this and other models.

THE SEARCH FOR NEW PHYSICS

***NSR*:** What are the prospects for discovering new physics (that is, physics beyond the Standard Model) at BESIII? Can you speculate on what this might be? Is there any prospect, for example, of shedding new light on dark matter, or on the origin of

the asymmetry in the amounts of matter and antimatter in the universe?

***Maiani*:** One fascinating proposal is that dark matter consists of new particles not coupled to the forces of the Standard Model.

> BESIII could perhaps even discover a signature of dark photons.
>
> —Luciano Maiani

There could be a new photon, called a 'dark photon', for which all known particles have zero charge (meaning that they do not interact with it). But by a quantum-mechanical effect, this dark photon could spend a small fraction of its time as a normal photon, thus acquiring a small coupling to, for example, electrons and muons. That would mean a small fraction of the particles produced by an e^+e^- collider could be dark photons that would produce anomalous signals, for example in the spectrum of e^+e^- pairs in the final state. Previous low-energy colliders have set limits on the coupling and mass of dark photons. BESIII could extend considerably the regime that could be explored for such coupling, and perhaps even discover a signature of dark photons.

Matter/antimatter symmetry is violated both in fundamental interactions and in the universe at large scales—the Sun, for example, is made of matter, and there is no evidence of anti-stars or anti-galaxies made of antimatter. We do not know if these two asymmetries are related, or whether one can explain the latter by the former. BESIII may shed light on this fundamental question by measuring the matter/antimatter asymmetries in the weak decays of charmed mesons, by comparing the asymmetry in charm decays to the known asymmetries in strange and beauty mesons. This is largely unexplored at the moment.

COLLABORATIONS IN CHALLENGING TIMES

***NSR*:** This is evidently a highly international collaboration, albeit with a strong Chinese representation. As a previous Director General of CERN, you will doubtless know very well the challenges of maintaining such a vast project. What are these? And have they become more complicated in the age of Covid-19 and uncertainties about travel?

***Maiani*:** The IHEP has a very good record in assembling and running complex experiments carried out by international collaborations. Experiments like BESIII work with the same kind of rules as CERN experiments, albeit on a smaller scale. Just as at CERN, Covid-19 is creating difficulties for on-site collaborations. But external groups currently confined to their own countries can still contribute to some degree, for example with data analysis, conducting simulations of device performance, and so on. Even a partial resumption of international travel, as is now happening at CERN, would be of great help.

***NSR*:** How, if at all, does research in this field differ in China compared to, say, the US, Europe and Japan? Does each region have its own unique 'flavor'?

***Maiani*:** Over the last four years, I spent a good part of my time working in Beijing (Institute of High Energy Physics—IHEP) and Shanghai (Shanghai Jiao Tong University). Except for obvious (and sometimes exciting) differences in lifestyle, food and so on, I can see that science is really universal in scope, method and sources of inspiration.

***NSR*:** How can researchers, especially young researchers, hope to make their mark in projects that require such huge teams? Is a different ethos required, in which scientific understanding is seen to be the product of selfless teamwork as opposed to the individualistic approach often seen in other fields?

***Maiani*:** One has to see a large collaboration such as BESIII as a 'laboratory' of its own, which offers to small teams different fields of research (instrumentation, precision measurements, data analysis, phenomenology and so on). Inside each team, individual talent, skill and ingenuity can shine and be appreciated. A young post-doc can show to senior old hands the way to solve their current problem. In this way, like in the old times, a young person may acquire a reputation that will bring her or him to larger responsibilities inside the 'laboratory' and beyond. This is the path by which Fabiola Gianotti and Yifang Wang have become the directors of CERN and IHEP.

Philip Ball writes for NSR from London.

NSR National Science Review | OPEN ACCESS

- National Science Review Editorial Office
  Science China Press, No. 16, Donghuangchenggen
  North Street, Beijing 100717, China
- **T** 86(10) 6403 7232 **E** nsr@scichina.org **W** academic.oup.com/